Venomic Ecology in Cubozoans (Box Jellyfish)

Submitted by:
Emily O'Hara
In fulfilment of the requirements for the degree of Doctor of Philosophy

College of Public Health Medicine and Veterinary Science
James Cook University

August, 2024

Supervisors:
Professor Jamie Seymour
Dr David Wilson
Dr Jen Whan

Acknowledgements

First and foremost, my eternal thanks go to my parents. Mum and Dad, none of this would have been possible without your unending support, which never falters, even from half a world away. Thank you for encouraging me to pursue my passions from such a bizarrely young age, I can't imagine many parents rolling with a 4/5 year-old declaring they want to be a marine biologist, but you took it in your stride and I'm where I am today because of you. I am forever grateful. To my Great Auntie Marjorie, you started this journey with me but were unable see me cross the finish line. I made it. I will always remember you and am forever grateful for your enthusiastic and unwavering support, thank you. And to Rio, my loveable little menace, my faithful friend and constant companion throughout this PhD journey. With your constant cuddles, destruction of any work you deemed sub-par and general embodiment of chaos at my workstation, I wouldn't have wished it any other way. You kept me sane my fluffy little friend.

To my supervisors: Jamie Seymour, the jellyfish man himself, you are the reason I'm in Australia today working with these incredible animals. Your passion for science and wild enthusiasm is truly inspirational and the confidence with which you present your craft is infectious, I am so grateful to have been a part of your team, thank you for taking a chance on me. To my secondary supervisors, I'm so grateful for your mentoring and advice. Dave, your never-ending patience trying to explain chemistry to my brain that simply did not want to compute is so much appreciated, I'm sure you won't miss that confused look on my face. Jen, you have been a true role model of a fierce woman in science I can only hope to emulate, thank you, and for introducing me to the wonderful world of microscopy, I think my career trajectory may have taken a hard turn towards microscopes thanks to you. I'm down the rabbit hole now…

Libby and Sally, you two became so much more than teammates, thank you for adopting me into your jellyfish family. Two of the strongest women I know, you inspire me every day with your confidence and passion for the geekier side of life, your friendship means the world to me. Sal, there is no one I'd rather have by my side in the lab/aquarium, thank you for your tireless efforts teaching me all things jellyfish. The movie nights, sushi & beach dates and pirating kept me saner thank you'll ever know. I'm proud to have lived our origin stories together, the world will quake the day we embrace our supervillain eras. Lib, you are the Yang to my Yin. I was the friend you never wanted, but we're stuck together now. 5 years later were' still obsessing over plants, crying and/or laughing over endless video chats and keeping science cool. You are the voice in my head when I need to be strong. I can't imagine my life without you two ladies in it, no matter how far apart our adventures take us, thank you for your constant support throughout this PhD.

All the members of the TASRU team, you have been a lifeline throughout this PhD journey and a wonderful little community I feel privileged to be a part of. Most especially, Rob, you were steadfastly there for every up and down (quite literally for some of those stormy nights at sea), thank you for being my human shield and I'm so grateful to have had your support throughout. Danica, we've been cheerleading for each other for so long, thank you – and for taking me fishing for the first time ever, if we learnt anything from that day, its that all you need is determination and will power to catch the best fish (and maybe some pretty lights on the rod). We've got this.

Estelle, the mermaid that just appeared out of nowhere. Thank you for your unwavering support and enthusiasm throughout this PhD. Throughout all the pirate adventures (both real and imagined) all that glitters is no gold, thank you for your friendship, that's the real treasure.

To the team at the University of Sydney, who tirelessly persevered with me and my difficult requests, most especially Gerry and Richard, you have my most sincere thanks. Together we took a very challenging concept and made it a reality.

And finally, a huge thanks to the funding bodies who generously contributed to this research: The James Cook University Postgraduate Scholarship, The Far North Queensland Hospital Foundation; The American Microscopical Society Microscopy Training Fellowship; The Australian Lions Foundation for Scientific and Medical Research on Marine Species Dangerous to Humans; The ER walker bequest bursary, and; The JCU CPHMVS Higher Degree Research Enhancement Scheme.

Statement of contribution of others

The primary author of this thesis Emily O'Hara was extensively involved in all aspects of this work, with the following support and advice greatly appreciated:

Nature of assistance	Contribution	Name	Affiliation
Conceptual and intellectual support	Experimental design	Professor Jamie Seymour Dr Minh Huynh	James Cook University University of Sydney
	Statistical analysis	Professor Jamie Seymour	James Cook University
	Editing of chapters/manuscripts	Professor Jamie Seymour Dr David Wilson Dr Jen Whan	James Cook University James Cook University James Cook University
	Results interpretation/discussion advice	Professor Jamie Seymour Professor Anders Garm Professor Carina Östman Dr David Wilson	James Cook University University of Copenhagen Uppsala University James Cook University
Data collection	Medusa collection	Dr Robert Courtney Professor Jamie Seymour Ms Sally Turner Cairns Surf Life Savers	James Cook University James Cook University James Cook University
	Light experiment set up/conduction	Dr Robert Courtney Ms Sally Turner Mr Tai Tai Inoue	James Cook University James Cook University BioPixel
	Polyp husbandry	Ms Sally Turner	James Cook University
	Assistance from technical staff	Dr Kevin Blake Dr Minh Huynh Dr Shane Askew	James Cook University University of Sydney James Cook University
	Experimental method training and advice	Dr Jen Whan Dr David Wilson	James Cook University James Cook University
External sample processing	uHPLC MS analysis	Dr Alun Jones	University of Queensland
	SBF-SEM analysis and data generation	Dr Gerald Shami Dr Richard Harwood	University of Sydney University of Sydney

Nature of assistance	Contribution	Award/funding body
Financial support	Scholarship award	James Cook University Postgraduate Scholarship
	Funding for scientific studies	Far North Queensland Hospital Foundation American Microscopical Society Microscopy Training Fellowship Australian Lions Foundation for Scientific and Medical Research on Marine Species Dangerous to Humans ER walker bequest bursary JCU College of Public Health, Medical and Veterinary Sciences Higher Degree Research Enhancement Scheme

Thesis abstract

This thesis explores the venom ecology of the highly venomous cubozoan *Carukia barnesi* (the Irukandji jellyfish). I initially present a review of the current literature in regards to the venom ecology of cnidarians, in which the influence of ecological factors such as environmental temperature, salinity, ontogeny, geographic location and diet are examined. Venom research is often focussed on medical relevance, novel compounds and venom evolution, whilst studying the relationship between a venom and its environment – venom ecology - has been conducted to a lesser extent. Given the projected environmental changes envisioned to occur with global warming, it is pertinent now more than ever, to highlight this topic. This review provides an exclusive focus on the cnidarian phylum and encompasses all available published, peer-reviewed literature to our knowledge regarding the ecological factors influencing venom. I find a startling lack of research into the effects of both environmental and biological factors on venoms, with very few to no studies available per category. Importantly, research does exist that suggests these ecological processes may influence other marine or terrestrial venoms, thus highlighting key knowledge gaps this thesis aims to address with *C. barnesi.*

Next, a reliable supply of *C. barnesi* jellyfish was required to conduct experiments with, so a method to induce metamorphosis was developed. I trialled a range of chemical reagents including indole compounds, 9-cis-retinoic acid and Lugol's solution to induce metamorphosis between the polyp and medusa life stages. An optimum method was determined resulting in a 90% metamorphosis rate to healthy medusa by exposing the polyps to 1 µM of 5-methoxy-2-methylindole for 24 hours. Of note is that chemical exposure time significantly impacts health and metamorphosis rates in this species.

Thus, *C. barnesi* jellyfish were now available for research, however they proved difficult to hold in aquaria due to feeding issues. Light has previously been shown to directly influence the feeding ecology of some cnidarians by controlling nematocyst discharge and some cubozoans display marked behavioral reactions to individual light colours. The intention of the next chapter was to determine if light has any effect on the feeding behaviour and frequency of the highly venomous cubozoan *C. barnesi*, with the ultimate goal being to induce feeding in newly detached medusa as this a species currently unable to be reared in aquaria due to feeding difficulties. Here I exposed *C. barnesi* medusa to a range of coloured light regimes and monitored pulse rate and feeding responses. Overall, I found *C. barnesi* displayed higher feeding frequencies in the light compared to in the dark, but frequency varied greatly between individual light colours.

Included next is a divergent piece of research that directly links to the visual side of *C. barnesi's* feeding ecology. Pupillary response under varying conditions of bright light and darkness was compared in three species of Cubozoa with differing ecologies. Maximal and minimal pupil area in relation to total eye area was measured and the rate of change recorded. In *Carukia barnesi*, the rate of pupil constriction was faster and final constriction greater than in Chironex fleckeri, which itself showed faster and greater constriction than in *Chiropsella b*ronzie. Isuggest this allows for differing degrees of visual acuity between the species. I propose that these differences are correlated with variations in the environment which each of these species inhabit, with *C. barnesi* found fishing for larval fish in and around waters of structurally complex coral reefs, *C. fleckeri* regularly found acquiring fish in similarly complex mangrove habitats, while *C. bronzie* spends the majority of its time in the comparably less complex but more turbid environments of shallow sandy beaches where their food source of small shrimps is highly aggregated and less mobile.

Having established a method to supply *C. barnesi* jellyfish for experimental work and attempted to prolong their lifespan using vision to influence their feeding ecology, the remaining chapters focused exclusively on the venom ecology of *C. barnesi*, through direct and indirect experimental analysis. *C. barnesi* is one of the smallest, yet most venomous jellyfish in the world, however current understanding of its venom and venom injecting organelles (nematocysts) is very limited. Conflicting nematocyst identifications in the literature and lack of research from different life stages hinders understanding of this animal's venom ecology. Next, I used a combination of light, electron and fluorescent microscopy to conclusively identify the nematocysts across three ontogenetic stages of *C. barnesi*: polyp, newly detached medusa and adult medusa. Nematocysts from one rarer, older specimen are also included however further research is needed in this life stage. Three confirmed nematocyst types were found in total across the four life stages: Homotrichous Tumiteles, Holotrichous O-Isorhizas and Atrichous or Holotrichous B-Mastigophores, with two other potential nematocyst types discussed. Confirmed nematocyst types were found to significantly change between ontogenetic stages in both proportion and size, evidencing the venom ecology of this animal changes significantly between life stages. Additionally, I present evidence supporting the identification of nematocysts previously found in unsolved human envenomation cases as potentially originating from *C. barnesi*, based on the findings of this research.

Continuing the research trajectory established from the nematocyst identifications, I then strove to further elucidate the ultrastructure of nematocysts in *Carukia barnesi*. Focussing solely on the adult medusa life stage, I develop and optimise a method for creating biologically accurate 3D

models of both the discharged and undischarged states of these microscopic organelles. Through a process known as volume imaging, I used Serial Block Face Scanning Electron Microscopy to create both virtual and physical nematocyst models, to facilitate a deeper understanding of the ultrastructure, which will contribute to future ecological and venom injection research.

And finally, the direct analysis of venom variation is explored in the final data chapter. Venom ecology is a relatively new area of research not well explored within cnidarians, although some venom shifts with environmental temperature, life stage and geography have been documented in a limited number of species. Here I take the highly venomous Irukandji jellyfish *Carukia barnesi* and use Ultra High Performance Liquid Chromatography Mass Spectrometry to assess the venom for compositional differences across three environmental temperatures: 27°C, 29°C and 31°C, and two life stages: polyp and newly detached medusa. Here I find molecular venom variations with both temperature and life stage, suggesting the animals venom is directly linked to those ecological factors. Possible impacts of these venom variations may include sting severity shifts with global warming, major ecological shifts between life stages and potential links to the known variations in symptom onset from Irukandji syndrome.

Table of contents

List of tables

List of figures

List of supplementary information

Supplementary information 1: A log of environmental temperatures within the experimental tanks (BiOrbs) containing *Carukia barnesi* polyps, over the course of the temperature experiments, collected with Ibuttons.

Video 1: A volume image animation of an undischarged Tumitele nematocyst from a *Carukia barnesi* adult medusa tentacle

Video 2: A volume image animation of a close-up cropped tubule from an undischarged Tumitele nematocyst from a *Carukia barnesi* adult medusa tentacle

Video 3: A volume image animation of a discharged Tumitele nematocyst from a *Carukia barnesi* adult medusa tentacle

Video 4: A volume image animation of a discharged Tumitele nematocyst from a *Carukia barnesi* adult medusa tentacle – situating the virtual volume within the raw SBF-SEM image slices.

Video 5: A volume image animation of an undischarged Mastigophore nematocyst from a *Carukia barnesi* older adult medusa tentacle

Video 6: A volume image animation of a close-up cropped tubule from an undischarged Mastigophore nematocyst from a *Carukia barnesi* older adult medusa tentacle

Chapter 1 . An introduction to the life history and venom ecology of the cubozoan *Carukia barnesi*- "the Irukandji jellyfish"

1.1 Class Cubozoa

1.1.1 Biology

Cubozoa are a class of jellyfish commonly known for their distinct box or "cube" shaped bells, earning them the common name of "box jellyfish". Their taxonomic rank is as follows: Kingdom: Animalia: Phylum: Cnidaria; Sub-Phylum: Medusozoa; Class: Cubozoa. Jellyfish , which are the free swimming stage of some cnidarians - are typically associated with two particular classes of cnidarians, the scyphozoa which are the true jellyfish, and the cubozoa which are the box jellyfish, with the cubozoans possessing unique characteristics such as complex eyes (Coates et al., 2006; Garm, Coates, et al., 2007; Garm et al., 2016; O'Connor et al., 2010), strong swimming/orientation ability (Garm, O'Connor, et al., 2007; Kingsford & Mooney, 2014) and potent venoms (Bailey et al., 2005; Endean, 1988; Endean et al., 1969; Kingsford & Mooney, 2014; Kintner et al., 2005; Little et al., 2020; Pereira et al., 2010; Pereira & Seymour, 2013; Ramasamy et al., 2005; Seymour et al., 2020; Winkel et al., 2005)(Kingsford & Mooney, 2014) not found in their scyphozoan relatives.

The majority of jellyfish have a polymorphic life history, typically encapsulating two morphologically distinct life stages - the polyp and the medusa (Aria, 1997; T. Carrette et al., 2014; Courtney et al., 2016; Gurska & Garm, 2014; Hartwick, 1991; Straehler-Pohl & Jarms, 2011; Toshino et al., 2015; Toshino, Miyake, & Shibata, 2018; Underwood et al., 2018). The polyp is a sedentary stage with a stalked body and a mouth surrounded by a ring of tentacles on the apex. The medusa is a free-swimming stage that has a bell-shaped body with protruding tentacles. During its life history the polyp will transition into a medusa. In scyphozoans this is achieved via the process of strobilation, whereby the polyp body is split into segments by transverse division, which develop into separate ephyra (young medusa). The medusa are typically liberated from the polyp as they develop and the polyp body remains intact (Aria, 1997). In contrast, cubozoans typically undergo complete metamorphosis whereby a single polyp will transform completely into a single medusa, with no polyp remaining post metamorphosis (Hartwick, 1991; Kingsford & Mooney, 2014; Toshino, Miyake, & Shibata, 2018; Werner, 1975), although some instances of the polyp regenerating have also been documented (Courtney et al., 2016; Toshino et al., 2015).

The class Cubozoa contains two monophyletic orders, Chirodropida and Carybdeida (Bentlage et al., 2010; Bentlage & Lewis, 2012; Collins, 2009). While both exhibit the characteristic cubozoan

tenacles attached to each corner of their cuboid bell by a pedalium, the Chirodropids possess multiple tentacles originating from each corner, whilst the Carybdeids possess only a single tentacle at each corner (Acevedo et al. 2019;Gershwin, 2006b).

1.1.2 Nematocysts

Cubozoan venom is produced, stored and ejected by microscopic stinging organelles called cnidae. Cnidae are explosive capsules containing venom that is delivered through an eversible tubule. A diagnostic feature of the phylum Cnidaria (named from the Greek root word "cnid", meaning stinging nettle), this microscopic stinging apparatus is present in all cnidarians and comprise a cnidocyte cell containing one giant secretory organelle called the cnidocyst (cnida/cnidae). Cnidocysts are then divided into three categories; spirocysts, used to entangle prey and stick to surfaces, but do not contain venom; ptychocysts, which produce a glue like substance to hold onto prey or create tubes (in burrowing sea anemones); and nematocysts, harpoon-like structures that can penetrate prey with venom and also entangle. These cnidocyst organelles sit in the tissues of the jellyfish and discharge by ejecting and everting a coiled tubule outwards. Some, like the nematocysts, have spines and a tubule that can penetrate prey to inject venom (Hessinger & Lenhoff, 1988; Östman, 2000). Nematocysts are considered the only type of cnidocyst able to deliver venom due to their penetrative nature, arguably making them the single most important structure in the study of cnidarian venoms. These explosive microscopic organelles are characterized in two states: undischarged, where a coiled tubule resides within a capsule containing venom; and discharged, where the tubule everts out of the capsule and toxin is ejected through the tubule. There are over 30 different types of nematocysts (Östman, 2000), each traditionally assumed to contain a unique toxin and it is the ultrastructure of both the undischarged and discharged capsules that is used in identification. Each species of cnidarian typically possesses a unique collection of the various nematocyst types, termed the cnidome and are likely to possess unique toxins characteristic of the species. Ultimately, the cnidocysts, particularly the venom wielding nematocysts, could be argued to play the defining roles in the ecology of these animals, as every major ecological function including feeding, offence, defence, substrate adhesion and competition, traces back to them, the venom they contain and their functional role within the animal.

1.1.3 Venom ecology

Ecology is, broadly speaking, the branch of biology that deals with the relationships between living organisms and their environment (also: the relationships themselves, especially those of a specified organism) (Oxford English Dictionary). The defining characteristics of a venom have undergone much discussion within the literature with the following definition proposed: "a

secretion, produced in a specialised gland in one organism, and delivered to a target organism through the infliction of a wound (regardless of how tiny it is); a venom must further contain molecules that disrupt normal physiological or biochemical processes so as to facilitate feeding or defence by the producing animal" (Fry et al., 2009). Venom has been described as an intrinsically relational trait, its definition founded upon the venomous-envenomed relationship and, therefore, the venom itself is "ecological" by definition (Jackson et al., 2019). Venom ecology is a further term that could seemingly describe a host of venom relationships/characteristics relating to both the venom itself and other ecological concepts, including, but not limited to, venom evolution and venom plasticity (the ability of a venom to change).

Cubozoans are the most dangerous class of jellyfish and are known for their powerful venoms, responsible for hundreds (possibly thousands) of deaths worldwide (Fenner 2005). Consequently, medical research often takes precedence over ecological studies. Some such studies identifying toxins from cubozoan species include Nagai et al (2000), Nagai *et al* (2000b), Nagai et al (2002) and Nagai (2003). However, some recent insights into cubozoan venom ecology have emerged from studies focussed on venom plasticity, the ability of a venom to change compositionally or bioactively with changing biological and/or environmental factors. Venom of the Australian big box jellyfish, *Chironex fleckeri*, displays both pharmacological and biochemical variation with geography (Winter et al., 2010). Ontogeny can also influence the venom composition and activity in *C. fleckeri* (McClounan & Seymour, 2012) and the Irukandji jellyfish, *Carukia barnesi* (Underwood & Seymour, 2007). Any variation in venom will not only directly impact the ecology of the animal, but it can also influence the severity of human envenomation. The study of venom ecology has been highlighted as an important, yet understudied, area within snake venoms (Jackson et al., 2019), and likewise to the study of cubozoan venoms with only three known works currently available for the latter (McClounan & Seymour, 2012; Underwood & Seymour, 2007; Winter et al., 2010).

1.2 *Carukia barnesi*

As early as 1922, in the coastal waters of Queensland, Australia, an unknown marine envenomation was associated with numerous human victims presenting a range of distressing symptoms (Barnes, 1964). In 1945, Dr. Hugo Flecker described the symptoms as ranging from a local sensation at the sting sight absent of pain, progressing to a prostrated body with intense back, stomach and body aches accompanied by retching and vomiting, necessitating the use of opiates, with patients exhibiting serious illness for multiple days before recovery (Flecker, 1945). Flecker would later term the sting symptoms as "Irukandji syndrome", named after the traditional aboriginal tribe who previously inhabited the area (Flecker, 1952). It wasn't until 1964 the

causative organism was confirmed by Dr. Jack Barnes, who confirmed through voluntary human envenomations that a sting from a small cubozoan medusa elicited the described Irukandji syndrome in victims. He also showed there is a latent period between sting and symptom onset, averaging a 26 minute delay (but ranged between 5 and 120 minutes) (Barnes, 1964). The adult stage of the culpable cubozoan was fully described, with both morphological and nematocyst descriptions by Southcott (1967), and given the name *Carukia barnesi. C. barnesi* is uniquely identifiable by the "neckerchief" shaped bands on its tenacles. Since the original syndrome description, symptoms have been updated to include: life-threatening hypertension, pulmonary oedema and toxic global heart dilatation (Fenner & Hadok, 2002; Fenner et al., 1986). *C. barnesi* has also further been attributed to a fatality induced by intracerebral hemorrhage (Carrette et al., 2012; Pereira et al., 2010).

C. barnesi is part of the order Carybdeida, possessing only a single tentacle originating from each of the four corners of its bell. Previously categorized in the family Tamoyidae, Carukiidae is now a separate family, (Bentlage et al., 2010; Bentlage & Lewis, 2012) that includes *C. barnesi* (figure 1.1). Analysis of box jellyfish evolution showed, whilst most of the cubozoans possess unique toxins, Irukandji/Irukandji-like syndrome is caused only by Carybdeida, fully encompassing all Tamoyidae and Carukiidae, but not Carybdeidae or Tripedaliidae (Bentlage et al., 2010; Figure 1.1).

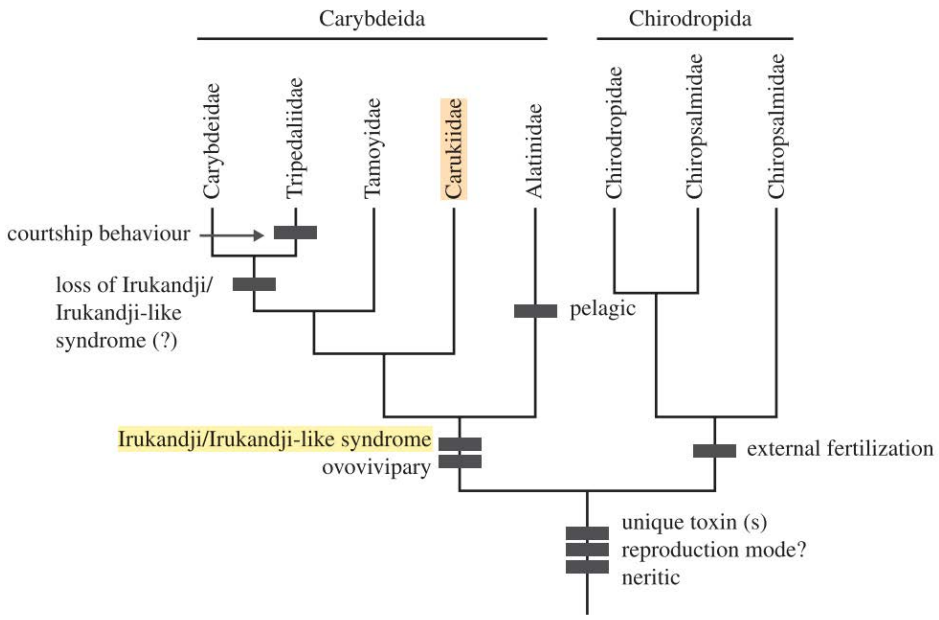

Figure 1.1: Phylogenetic relationships and trends in toxicity and life-history evolution of the Cubozoa, divided into the two orders Carybdeida and Chirodropida.
Figure sourced from Bentlage et al., 2010, with permission from publishing body. Highlights have been added to the original figure by this author (EO) to highlight the relative positioning and attributes of *Carukia barnesi*. Yellow highlight indicates the venom induces Irukandji syndrome; and the orange highlight shows the Carukiidae family.

The early life history of *C. barnesi* has been elucidated (Courtney et al., 2016). Initially, eggs are fertilized and then develop into an encapsulated planula stage, which hatch as a ciliated planula. The ciliated planulae are negatively buoyant and eventually adhere to the substrate and undergo metamorphosis into a primary polyp. The primary polyp develops into a mature polyp, at which point asexual reproduction (cloning) can occur through lateral budding from the polyp stem and produces small swimming polyps, which adhere to the substrate and develop into mature polyps. From the mature polyp stage, the polyp can then transform into a free swimming medusa (Courtney et al., 2016). Some cubozoa have been shown to make this transition via monodisc strobilation, in which the polyp is regenerated after a single medusa detaches (Toshino et al., 2015), and is almost a hybridization of the typical strobilation and metamorphosis most jellyfish undergo. *C. barnesi* is one of the rarer cubozoans that appear to exhibit monodisc strobilation (Courtney et al., 2016). A single newly detached medusa will detach from a polyp, possessing very short tentacles that will grow into a mature adult with a bell height of up to 35 mm and tentacles up to 1.2 m in length (Courtney, 2016; Figure 1.2).

The nematocyst types present in *C. barnesi* have been shown to change between the polyp and newly detached medusa life stages (Courtney et al., 2016) and, whilst nematocyst types from the bell and tentacles of the newly detached medusa were not described to differ by Courtney et al., (2016) they have been conclusively shown to differ in the adult medusa. However, there is strong inconsistency in the literature regarding the nematocysts of the adult medusa. The single nematocyst type documented in the bell has been previously identified as anisorhizas haplonemes (possibly homotrichous) (Southcott, 1967), spherical isorhizas (Gershwin, 2006), homotrichous microbasic rhopaloids and homotrichous haplonemes (Underwood & Seymour, 2007), and spherical anisorhizas (Ávila-Soria, 2009). The single nematocyst type present in the tentacles has been identified as tumiteles (Southcott, 1967), lemon shaped tumiteles (Gershwin, 2006), homotrichous microbasic rhopaloids and homotrichous haplonemes (Underwood & Seymour, 2007) and microbasic mastigophores (Ávila-Soria, 2009). This great disparity in identifications makes it difficult to draw definitive conclusions regarding the nematocysts of *C. barnesi* and the venom they contain.

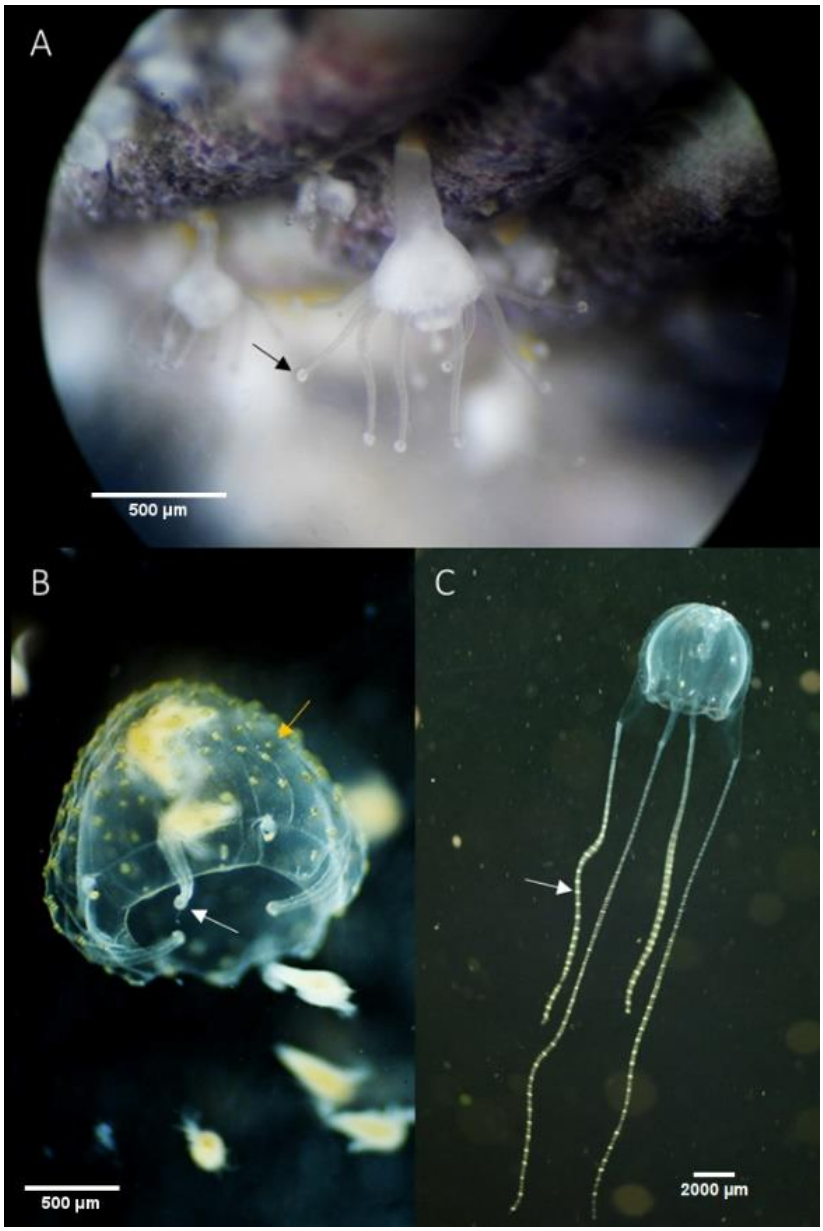

Figure 1.2: Three life stages of the Irukandji jellyfish *Carukia barnesi*.

A: Mature polyp, pictured adhered to a snail shell. The bulbous tentacle tips (black arrow) contain the mature nematocysts. B: The newly detached/juvenile medusa, pictured ingesting *Artemia sp*. The bulbous tentacle tips (white arrow) and bell warts (or mammilations or exumbrellar nematocyst warts) (yellow arrow) contain the mature nematocysts. C: Adult medusa. Tentacular bands/neckerchiefs (white arrow) and bell warts (not indicated) contain the mature nematocysts. Photo credit A/B: Emily O'Hara (author), C: Prof. Jamie Seymour. Figure originally created and used in chapter six, see fig 6.1

The highly dangerous nature of *C. barnesi* has fostered a large research focus on the pharmacological and toxicological aspects of the venom. Medical studies have begun to elucidate the toxic attributes of the venom (Little et al., 2020; Pereira et al., 2010; Pereira & Seymour, 2013; Ramasamy et al., 2005; Seymour et al., 2020; Winkel et al., 2005), although still relatively little is understood, with the venom ecology of the animal studied to an even lesser extent. Only one study has truly examined venom ecology of *C. barnesi.* Underwood and Seymour (2007) described changes in the venom of *C. barnesi* with ontogeny. Compositional differences in the venom between immature and mature medusa were evident and attributed to a change from invertebrate to vertebrate prey with age (Underwood and Seymour, 2007), which is unusual given the nematocyst types present do not change as the venom changes (Underwood and Seymour, 2007). This challenged the common supposition that venom is nematocyst specific and it is possible that venom ontogeny may occur throughout all life stages of the jellyfish regardless of the stable cnidome in the early life stages. Ultimately, the lack of research into the venom ecology of this animal hinders our understanding of the how the venom of this highly dangerous jellyfish can be influenced by both biological and environmental factors.

1.3 Thesis rationale/chapter outline

It is evident that both the venom and ecology of the highly venomous Irukandji jellyfish, *C. barnesi*, are understudied and challenging to interpret from the current literature. The intention of this thesis is to elucidate more of the poorly understood venom ecology of *C. barnesi*.

1.3.1 Chapter two

Chapter two is a comprehensive review of the literature, collating evidence to support the notion that ecological factors such as biology and environment might influence cnidarian venoms. The review does not focus solely on cubozoans but encompasses the whole phylum of cnidaria due to sparsity of literature, from which further knowledge gaps are identified. Key ecological factors such as environmental temperature and animal ontogeny can influence cnidarian venom, but minimal literature showing this in cubozoans and/or the jellyfish *C. barnesi*. Therefore, temperature and ontogeny were chosen as key factors to explore in my research. This chapter is now published as a review article, see appendix A.

1.3.2 Walk through of data chapters

C. barnesi is a seasonal jellyfish, meaning the adults only inhabit the coastal waters of Far North Queensland during the wet season (colloquially known as stinger season) from approximately November – May. Field collection of the adult medusa for research and/or venom extraction is limited. In addition, *C. barnesi* is a logistically difficult species (Rowley, 2021) to field sample, which further limits the venom supply through large catch variability and no guarantee of sample sizes. Captured individual medusa, even at adult maturity, typically measure less than 20 mm in interpedalial distance, and are impossible to rear in aquaria for sustained periods, resulting in extremely low venom yields. Combined, these factors ensure the process of venom acquisition from *C. barnesi* is extremely expensive and logistically difficult. With such a limited supply of adult animals and venom, research is ultimately finite and very costly. Furthermore, the polyp and newly detached medusa life stages have never been found in the wild.

The ultimate research goal of this thesis was to raise *C. barnesi* at varying environmental temperatures and life stages, to analyse venom composition across temperature and ontogeny. Given the low yield and sporadic sampling success of wild caught adults, it was considered unrealistic to endeavour to run the environmental temperature and life stage experiments using field sampled jellyfish. To facilitate the research goal, it was imperative to have a reliable supply of animals in sufficient quantities to run rigorous, well-replicated experiments on demand. Thus, chapters three, four (and to some extend chapter five) are dedicated to creating a supply of *C. barnesi* for the ultimate and penultimate chapters analysing their venom ecology. Chapter three develops a method for inducing metamorphosis in high yields, on demand, from the polyp to the medusa stage. Chapter four explores the manipulation of the medusas visual ecology to induce the jellyfish to eat (to advance aquarium rearing), and chapter five is a tangential chapter to this, exploring the visual acuity of *C. barnesi* in comparison to other cubozoan species. Chapter six aligns to the core research goal, analysing venom ecology indirectly through the identification of the venom wielding nematocysts over different life stages (as facilitated by chapter 2), and chapter seven is another tangential chapter further exploring the nematocyst ultrastructure initiated in chapter six. Chapter eight also directly aligns to the core research goal, by directly analysing extracted venom for compositional differences across environmental temperate and life stage (again facilitated by earlier chapters). See fig 1.3 for a summary of data chapter organisation.

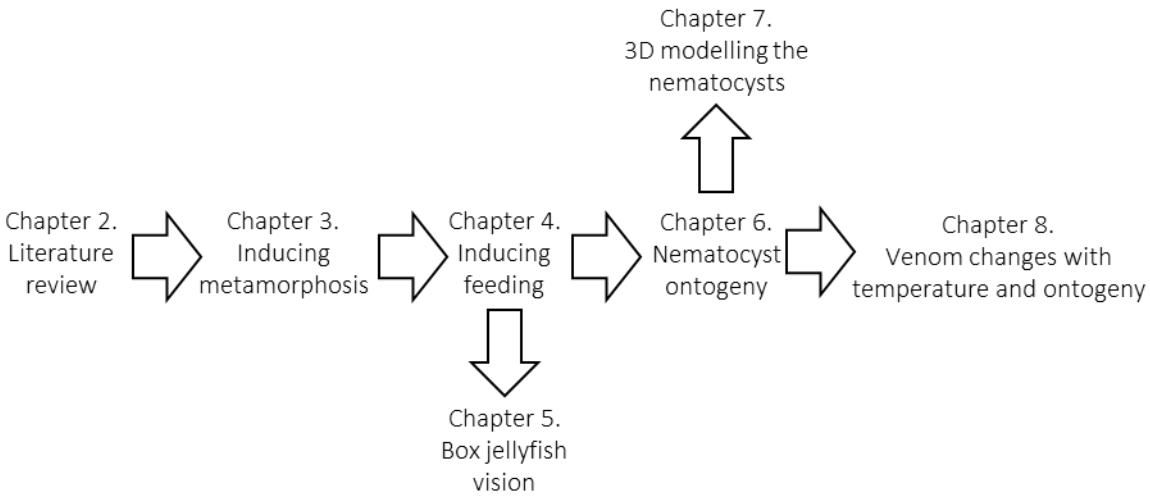

Figure 1.3: Organisation of thesis data chapters and their main aim.

Horizontal flows represent key chapters relevant to the main thesis storyline. Vertical flows represent relevant research that is tangential, but still relevant to the main storyline.

1.3.3 Chapter three

Whilst the polyp stage of *C. barnesi* has never been located in the wild, artificial fertilization from wild caught adults has produced a sustained population of cultured polyps at the James Cook University aquarium, Cairns (Courtney et al., 2016). In chapter three polyps were taken from the established culture and a method developed to induce metamorphosis from the polyp to the medusa life stage. Previous work attempted to induce metamorphosis in *C. barnesi* polyps using natural cues, such as feeding frequency, and thermal and osmotic parameters, but efforts proved unsuccessful (Courtney, 2016). Previously identified artificial methods to induce metamorphosis/strobilation in jellyfish polyps include chemical induction with a range of compounds (Berking et al., 2005; Green et al., 2018; Helm & Dunn, 2017; Muller, 1984; Spangenberg, 1967; Yamamori et al., 2017) .This chapter focused on trialing a range of chemical compounds to induce metamorphosis in *C. barnesi* and further optimizing a method for optimum survival and yield, ultimately enabling a supply of medusa for all subsequent research in this thesis. This chapter is now published (see appendix A).

1.3.4 Chapter four

Newly detached *C. barnesi* medusa and adult medusa have never successfully been reared long-term in aquaria due to their propensity to stop eating after roughly one to two weeks. Chapter four focusses on exploring ways to promote feeding, to facilitate extended rearing in aquaria, with the ultimate hopes of rearing the jellyfish long term for subsequent experiments. Consistent

with most box jellyfish, *C. barnesi* possess highly sophisticated vision and light has been shown to play a key role in prey capture within other cnidarian species by regulating the discharge of the venom injection organelles, the nematocysts (Jindrich, 2012; Plachetzki et al., 2012). Other cubozoa (*Tripedalia cystophora)* have also been shown to use vision to locate prey congregations (Bielecki & Garm, 2018). In this chapter I explored the effect of varying light wavelengths on the feeding ecology and behaviour of newly detached *C. barnesi* to incite the animal to feed.

1.3.5 Chapter five

Chapter five is a published manuscript and is included as a chapter of divergent research, but still relevant to the main thesis. We explored the visual acuity of *C. barnesi*, as alluded to in chapter four, and compared this with the vision of other cubozoan species. This work was done early on in the thesis to again, hopefully aid in keeping the animals alive in aquaria. Similar to the theme of chapter four, we discussed the visual acuity of *C. barnesi* is linked to prey capture and environment.

1.3.6 Chapter six

Chapter six is the first of two chapters to fully explore the core research goal of the thesis, the venom ecology of *C. barnesi*. One overarching complication in the study of cnidarian nematocysts is that the microscopic size of these organelles and their even smaller associated armature means that traditional light microscopy is typically unsuitable to fully visualize these fine structures. All prior research involving the nematocysts of *C. barnesi* has only employed light microscopy and has yielded inconsistent identification in the literature. Here, I used Scanning Electron Microscopy to conclusively identify and describe the venom wielding nematocysts of *C. barnesi* across three life stages (life stages enabled by earlier chapters), increasing the knowledge of the venom ontogeny of *C. barnesi*.

1.3.7 Chapter seven

In chapter seven, the nematocyst identification work of chapter six was advanced to fully elucidate the ultrastructure of *C. barnesi* nematocysts. 3D modelling of nematocysts or nematocyst-like organelles has been only done twice before and here, along with the collaborative efforts of the Australian Centre for Microscopy and Analysis (Sydney University) staff, we employed the novel method of Serial Block Face Scanning Electron Microscopy (SBF-SEM) to image and generate biologically accurate 3D models of *C. barnesi* nematocysts for the first time.

1.3.8 Chapter eight

Chapter eight is the culmination of the data chapters and fully encompasses the core research theme of venom ecology. Here, the polyp and medusa stages of *C. barnesi* were raised at varying environmental temperatures and their venom extracted and analysed for compositional differences to understand the venom ecology of the animals in response to environmental temperature. Venom analysis of the polyp and newly detached medusa life stage has never been directly analysed before as; 1) the small size of the organisms made sufficient venom extraction near impossible in available numbers; 2) the newly detected medusa have never been available in the wild nor aquaria before. Here, information gleaned from earlier chapters enabled the generation of large quantities of *C. barnesi* polyps and medusa, sufficient to extract and conduct venom analysis for the first time using the highly sensitive technique of ultra-high performance liquid chromatography mass spectrometry.

1.3.9 Chapter nine

Chapter nine is a general discussion of the significance of the whole thesis, situating the research presented here in context with current literature. The direction future work needs to take to progress the work of this thesis is discussed.

1.3.10 Thesis aims

Cnidarians are unique in that their venom is produced, contained and stored in thousands to millions of nematocysts dispersed throughout their tentacles (and often other body parts), unlike most venomous animals where venom is usually contained to a single venom gland source or originating organ. This means that cnidarian venom can be researched both indirectly, via analysis of the nematocysts, or directly via venom extraction. The overarching research goal of this thesis was to explore venom ecology of the Irukandji jellyfish, *C. barnesi.* Here I aimed to do so with both direct and indirect methods, with the key aims being:

i) To identify and classify the types of nematocysts present within *C. barnesi* over three key life stages; the polyp, newly detached medusa and adult medusa.

ii) To determine the effects of environmental temperature on the venom composition of *C. barnesi* polyps and medusa.

iii) To identify any difference in venom composition between the polyp and medusa life stages of *C. barnesi.*

To achieve these core research aims, preliminary work was required to facilitate these experiments. Thus, the below aims were also required for this thesis:

iv) To develop and optimise a method to induce *C. barnesi* polyps to metamorphose into medusa.

v) To explore the role of vision in *C. barnesi* medusa in relation to their feeding ecology.

1.4 References

Aria, M. . (1997). *A functional biology of Scyphozoa*. Springer science & budiness media.

Acevedo, M. J., Straehler-Pohl, I., Morandini, A. C., Stampar, S. N., Bentlage, B., Matsumoto, G. I., Fuentes, V. L. (2019). Revision of the genus Carybdea (Cnidaria: Cubozoa: Carybdeidae): clarifying the identity of its type species Carybdea marsupialis. *Zootaxa*, *4543*(4), 515-548.

Ávila-Soria, G. (2009). *Molecular characterization of Carukia barnesi and Malo kingi, Cnidaria; Cubozoa; Carybdeidae.* James Cook University.

Bailey, P. M., Bakker, A. J., Seymour, J. E., & Wilce, J. A. (2005). A functional comparison of the venom of three Australian jellyfish: Chironex fleckeri, Chiropsalmus sp., and Carybdea xaymacana - On cytosolic Ca 2+, haemolysis and Artemia sp. lethality. *Toxicon*, *45*(2), 233–242. https://doi.org/10.1016/j.toxicon.2004.10.013

Barnes, J. H. (1964). Cause and Effect in Irukandji Stingings. *The Medical Journal of Australia*, *1*(24), 897–904. https://doi.org/10.5694/j.1326-5377.1964.tb114424.x

Bentlage, B., Cartwright, P., Yanagihara, A. A., Lewis, C., Richards, G. S., & Collins, A. G. (2010). Evolution of box jellyfish (Cnidaria: Cubozoa), a group of highly toxic invertebrates. *Proceedings of the Royal Society B: Biological Sciences*, *277*(1680), 493–501. https://doi.org/10.1098/rspb.2009.1707

Bentlage, B., & Lewis, C. (2012). An illustrated key and synopsis of the families and genera of carybdeid box jellyfishes (Cnidaria: Cubozoa: Carybdeida), with emphasis on the “Irukandji family” (Carukiidae). *Journal of Natural History*, *46*(41–42), 2595–2620. https://doi.org/10.1080/00222933.2012.717645

Berking, S., Czech, N., Gerharz, M., Herrmann, K., Hoffmann, U., Raifer, H., Sekul, G., Siefker, B., Sommerei, A., & Vedder, F. (2005). A newly discovered oxidant defence system and its involvement in the development of Aurelia aurita (Scyphozoa, Cnidaria): Reactive oxygen species and elemental iodine control medusa formation. *International Journal of Developmental Biology*, *49*(8), 969–976. https://doi.org/10.1387/ijdb.052024sb

Bielecki, J., & Garm, A. (2018). Vision Made Easy: Cubozoans Can Advance Our Understanding of Systems-Level Visual Information Processing. In *Marine organisms as model systems in biology and medicine* (Vol. 65, Issue August, pp. 599–624). https://doi.org/10.1007/978-3-319-92486-1_27

Carrette, T. J., Underwood, A. H., & Seymour, J. E. (2012). Irukandji syndrome: A widely

misunderstood and poorly researched tropical marine envenoming. *Diving and Hyperbaric Medicine*, *42*(3), 214–223.

Carrette, T., Straehler-Pohl, I., & Seymour, J. (2014). Early life history of Alatina cf. moseri populations from Australia and Hawaii with implications for taxonomy (Cubozoa: Carybdeida, Alatinidae). *PLoS ONE*, *9*(1). https://doi.org/10.1371/journal.pone.0084377

Coates, M. M., Garm, A., Theobald, J. C., Thompson, S. H., & Nilsson, D. E. (2006). The spectral sensitivity of the lens eyes of a box jellyfish, Tripedalia cystophora (Conant). *Journal of Experimental Biology*, *209*(19), 3758–3765. https://doi.org/10.1242/jeb.02431

Collins, A. G. (2009). Recent Insights into Cnidarian Phylogeny. *Smithsonian*, *000*(August 2008), 139–149. http://www.si.edu/marinescience/pdf/SCMS_Collins.pdf

Courtney, R. (2016). Life cycle, prey capture ecology, and physiological tolerances of Medusae and polyps of the "Irukandji" jellyfish: Carukia barnesi. In *PhD Thesis, James Cook University*. https://researchonline.jcu.edu.au/49935/

Courtney, R., Browning, S., & Seymour, J. (2016). Early life history of the "irukandji" jellyfish *Carukia barnesi*. *PLoS ONE*, *11*(3). https://doi.org/10.1371/journal.pone.0151197

Endean, R. (1988). Venom of Chironex, the world's most venomous animal. In J. Pearn & J. Covacevich (Eds.), *Venoms and Victims, Queensland Museum, South Brisbane* (pp. 15–24).

Endean, R., Duchemin, C., McColm, D., & Fraser, E. H. (1969). A study of the biological activity of toxic material derived from nematocysts of the cubomedusan Chironex fleckeri. *Toxicon*, *6*(3). https://doi.org/10.1016/0041-0101(69)90118-4

Fenner, P., & Hadok, J. (2002). Fatal envenomation by jellyfish causing Irukandji syndrome. *Medical Journal of Australia*, *177*(7), 362–363.

Fenner, P. J. (2005). Venomous jellyfish of the world. *South Pacific Underwater Medicine Society Journal*, *35*(3), 131–138.

Fenner, P. J., Williamson, J., Callanan, V. I., & Audley, I. (1986). Further understanding of, and a new treatment for, "Irukandji" (Carukia barnesi) stings. *Medical Journal of Australia*, *145*(11–12), 569–574. https://doi.org/10.5694/j.1326-5377.1986.tb139500.x

Flecker, H. (1945). Injuries By Unknown Agents To Bathers in North Queensland. *Medical Journal of Australia*, *1*(4), 98–98. https://doi.org/10.5694/j.1326-5377.1945.tb54481.x

Flecker, H. (1952). Irukandji sting to North Queensland bathers without production of weals but

with severe general symptoms. *The Medical Journal of Australia*, *2*(3), 89–91. https://doi.org/10.5694/j.1326-5377.1952.tb100081.x

Fry, B. G., Roelants, K., Champagne, D. E., Scheib, H., Tyndall, J. D. A., King, G. F., Nevalainen, T. J., Norman, J. A., Lewis, R. J., Norton, R. S., Renjifo, C., & de la Vega, R. C. R. (2009). The Toxicogenomic Multiverse: Convergent Recruitment of Proteins Into Animal Venoms. *Annual Review of Genomics and Human Genetics*, *10*(1), 483–511. https://doi.org/10.1146/annurev.genom.9.081307.164356

Garm, A., Bielecki, J., Petie, R., & Nilsson, D. E. (2016). Hunting in bioluminescent light: Vision in the nocturnal box jellyfish Copula sivickisi. *Frontiers in Physiology*, *7*(MAR), 1–9. https://doi.org/10.3389/fphys.2016.00099

Garm, A., Coates, M. M., Gad, R., Seymour, J., & Nilsson, D. E. (2007). The lens eyes of the box jellyfish Tripedalia cystophora and Chiropsalmus sp. are slow and color-blind. *Journal of Comparative Physiology A: Neuroethology, Sensory, Neural, and Behavioral Physiology*, *193*(5), 547–557. https://doi.org/10.1007/S00359-007-0211-4

Garm, A., O'Connor, M., Parkefelt, L., & Nilsson, D. E. (2007). Visually guided obstacle avoidance in the box jellyfish Tripedalia cystophora and Chiropsella bronzie. *Journal of Experimental Biology*, *210*(20), 3616–3623. https://doi.org/10.1242/JEB.004044

Gershwin, L. A. (2006). Nematocysts of the Cubozoa. *Zootaxa*, *57*(1232), 1–57. https://doi.org/10.11646/zootaxa.1232.1.1

Gershwin, L. (2006b). Comments on Chiropsalmus (Cnidaria: Cubozoa: Chirodropida): a preliminary revision of the Chiropsalmidae, with descriptions of two new genera and two new species. *Zootaxa*, *1231*(1), 1-42.

Green, T. J., Wolfenden, D. C. C., & Sneddon, L. U. (2018). An investigation on the impact of substrate type, temperature, and iodine on moon jellyfish production. *Zoo Biology*, *37*(6), 434–439. https://doi.org/10.1002/zoo.21454

Gurska, D., & Garm, A. (2014). Cell proliferation in cubozoan jellyfish tripedalia cystophora and alatina moseri. *PLoS ONE*, *9*(7). https://doi.org/10.1371/journal.pone.0102628

Hartwick, R. F. (1991). Observations on the anatomy, behaviour, reproduction and life cycle of the cubozoan Carybdea sivickisi. *Hydrobiologia*, *216–217*(1), 171–179. https://doi.org/10.1007/BF00026459

Helm, R. R., & Dunn, C. W. (2017). Indoles induce metamorphosis in a broad diversity of jellyfish,

but not in a crown jelly (Coronatae). *PLoS ONE*, *12*(12), 1–13. https://doi.org/10.1371/journal.pone.0188601

Hessinger, D. A., & Lenhoff, H. M. (1988). *The Biology of Nematocysts* (D. A. Hessinger & H. M. Lenhoff (eds.)). Academic Press, Inc.

Jackson, T. N. W., Jouanne, H., & Vidal, N. (2019). Snake Venom in Context: Neglected Clades and Concepts. *Frontiers in Ecology and Evolution*, *7*(September), 1–9. https://doi.org/10.3389/fevo.2019.00332

Jindrich, K. (2012). *Light influence on nematocyst firing in the sea anemone Haliplanella luciae*. Lund University.

Kingsford, M., & Mooney, C. (2014). The ecology of box jellyfishes (cubozoa). In *Jellyfish Blooms* (pp. 267–302). https://doi.org/10.1007/978-94-007-7015-7

Kintner, A. H., Seymour, J. E., & Edwards, S. L. (2005). Variation in lethality and effects of two Australian chirodropid jellyfish venoms in fish. *Toxicon*, *46*(6), 699–708. https://doi.org/10.1016/j.toxicon.2005.07.015

Little, M., Pereira, P., & Seymour, J. (2020). Differences in Cardiac Effects of Venoms from Tentacles and the Bell of Live Carukia barnesi: Using Non-Invasive Pulse Wave Doppler. *Toxins 2021, Vol. 13, Page 19*, *13*(1), 19. https://doi.org/10.3390/TOXINS13010019

McClounan, S., & Seymour, J. (2012). Venom and cnidome ontogeny of the cubomedusae *Chironex fleckeri*. *Toxicon*, *60*(8), 1335–1341. https://doi.org/10.1016/j.toxicon.2012.08.020

Muller, W. A. (1984). Retinoids and pattern formation in a hydroid. *Journal of Embryology and Experimental Morphology*, *81*, 253–271.

Nagai, H., Takuwa, K., Nakao, M., Ito, E., Miyake, M., Noda, M., & Nakajima, T. (2000). Novel proteinaceous toxins from the box jellyfish (sea wasp) Carybdea rastoni. *Biochemical and Biophysical Research Communications*, *275*(2), 582-588.

Nagai, H., Takuwa, K., Nakao, M., Sakamoto, B., Crow, G. L., & Nakajima, T. (2000b). Isolation and characterization of a novel protein toxin from the Hawaiian box jellyfish (sea wasp) Carybdea alata. *Biochemical and biophysical research communications*, *275*(2), 589-594.

Nagai, H., Takuwa-Kuroda, K., Nakao, M., Oshiro, N., Iwanaga, S., & Nakajima, T. (2002). A novel protein toxin from the deadly box jellyfish (sea wasp, Habu-kurage) Chiropsalmus

quadrigatus. *Bioscience, biotechnology, and biochemistry*, *66*(1), 97-102.

Nagai, H. (2003). Recent progress in jellyfish toxin study. *Journal of Health Science*, *49*(5), 337-340

O'Connor, M., Garm, A., Marshall, J. N., Hart, N. S., Ekström, P., Skogh, C., & Nilsson, D. E. (2010). Visual pigment in the lens eyes of the box ra jellyfish Chiropsella bronzie. *Proceedings of the Royal Society B: Biological Sciences*, *277*(1689), 1843–1848. https://doi.org/10.1098/rspb.2009.2248

Östman, C. (2000). A guideline to nematocyst nomenclature and classification, and some notes on the systematic value of nematocysts. *Scientia Marina*, *64*(SUPPLEMENT 1), 31–46. https://doi.org/10.3989/scimar.2000.64s131

Pereira, P., Barry, J., Corkeron, M., Keir, P., Little, M., & Seymour, J. (2010). Intracerebral hemorrhage and death after envenoming by the jellyfish *Carukia barnesi*. *Clinical Toxicology*, *48*, 390–392. https://doi.org/10.3109/15563651003662675

Pereira, P., & Seymour, J. E. (2013). In vitro effects on human heart and skeletal cells of the venom from two cubozoans, Chironex fleckeri and Carukia barnesi. *Toxicon*, *76*, 310–315. https://doi.org/10.1016/j.toxicon.2013.10.023

Plachetzki, D. C., Fong, C. R., & Oakley, T. H. (2012). Cnidocyte discharge is regulated by light and opsin-mediated phototransduction. *BMC Biology*, *10*. https://doi.org/10.1186/1741-7007-10-17

Ramasamy, S., Isbister, G. K., Seymour, J. E., & Hodgson, W. C. (2005). The in vivo cardiovascular effects of the Irukandji jellyfish (Carukia barnesi) nematocyst venom and a tentacle extract in rats. *Toxicology Letters*, *155*(1), 135–141. https://doi.org/10.1016/j.toxlet.2004.09.004

Rowley, O. (2021). *Rethinking biological tools for logistically difficult species: a case study - the Irukandji (Carukia barnesi) and Box Jellyfish (Chironex fleckeri).* [James Cook University]. https://doi.org/https://doi.org/10.25903/jx3e%2D5w21

Seymour, J., Saggiomo, S., Lam, W., Pereira, P., & Little, M. (2020). Non-invasive assessment of the cardiac effects of Chironex fleckeri and Carukia barnesi venoms in mice, using pulse wave doppler. *Toxicon*, *185*(April), 15–25. https://doi.org/10.1016/j.toxicon.2020.06.018

Southcott, R. V. (1967). Revision of some Carybdeidae (scyphozoa: cubomedusae), including a description of the jellyfish responsible for the "irukandji syndrome." *Australian Journal Of Zoology*, *15*, 651–671. https://www.mendeley.com/viewer/?fileId=2fa0eb3f-b65a-d78b-0aab-8d1da93fdb17&documentId=f0d95e7c-a226-37e1-ba96-636d97beaa71

Spangenberg, D. B. (1967). Iodine induction of metamorphosis in Aurelia. *Journal of Experimental Zoology*, *165*(3), 441–449. https://doi.org/10.1002/jez.1401650312

Straehler-Pohl, I., & Jarms, G. (2011). Morphology and life cycle of Carybdea morandinii, sp. nov. (Cnidaria), a cubo-zoan with zooxanthellae and peculiar polyp anatomy. *Zootaxa*, *2755*, 36–56. https://doi.org/10.11646/zootaxa.2755.1.2

Toshino, S., Miyake, H., & Haruka, S. (2018). Development of Carybdea brevipedalia Kishinouye, 1891 (Cnidaria: Cubozoa: Carybdeida: Carybdeidae) collected from northern Japan. *Plankton and Benthos Research*, *13*(3), 116–128.

Toshino, S., Miyake, H., Ohtsuka, S., Adachi, A., Kondo, Y., Okada, S., Hirabayashi, T., & Hiratsuka, T. (2015). Monodisc strobilation in Japanese giant box jellyfish Morbakka virulenta (Kishinouye, 1910): a strong implication of phylogenetic similarity between Cubozoa and Scyphozoa. *Evolution & Development*, *17*(4), 231–239. https://doi.org/10.1111/EDE.12127

Toshino, S., Miyake, H., & Shibata, H. (2018). Development of carybdea brevipedalia Kishinouye, 1891 (Cnidaria: Cubozoa: Carybdeida: Carybdeidae) collected from northern Japan. *Plankton and Benthos Research*, *13*(3), 116–128. https://doi.org/10.3800/pbr.13.116

Underwood, A. H., & Seymour, J. E. (2007). Venom ontogeny, diet and morphology in *Carukia barnesi*, a species of Australian box jellyfish that causes Irukandji syndrome. *Toxicon*, *49*(8), 1073–1082. https://doi.org/10.1016/j.toxicon.2007.01.014

Underwood, A. H., Straehler-Pohl, I., Carrette, T. J., Sleeman, J., & Seymour, J. E. (2018). Early life history and metamorphosis in Malo maxima Gershwin, 2005 (Carukiidae, Cubozoa, Cnidaria). *Plankton and Benthos Research*, *13*(4), 143–153. https://doi.org/10.3800/PBR.13.143

Werner, B. (1975). Bau und Lebensgeschichte des Polypen von Tripedalia cystophora (Cubozoa, class, nov., Carybdeidae) und seine Bedeutung fiir die Evolution der Cnidaria. *Helgol~inder Wiss. Meeresunters*, *27*, 461–504. http://species-identification.org/species.php?species_group=zsao&id=2412

Winkel, K. D., Tibballs, J., Molenaar, P., Lambert, G., Coles, P., Ross-Smith, M., Wiltshire, C., Fenner, P. J., Gershwin, L. A., Hawdon, G. M., Wright, C. E., & Angus, J. A. (2005). Cardiovascular actions of the venom from the Irukandji (*Carukia barnesi*) jellyfish: Effects in human, rat and guinea-pig tissues in vitro and in pigs in vivo. *Clinical and Experimental Pharmacology and Physiology*, *32*(9), 777–788. https://doi.org/10.1111/j.1440-

1681.2005.04258.x

Winter, K. L., Isbister, G. K., McGowan, S., Konstantakopoulos, N., Seymour, J. E., & Hodgson, W. C. (2010). A pharmacological and biochemical examination of the geographical variation of Chironex fleckeri venom. *Toxicology Letters*, *192*(3), 419–424. https://doi.org/10.1016/j.toxlet.2009.11.019

Yamamori, L., Okuizumi, K., Sato, C., Ikeda, S., & Toyohara, H. (2017). Comparison of the Inducing Effect of Indole Compounds on Medusa Formation in Different Classes of Medusozoa. *Zoological Science*, *34*(3), 173–178. https://doi.org/10.2108/zs160161

Chapter 2 . The influence of ecological factors on cnidarian venoms – a literature review

This chapter is a published manuscript: O'Hara, E. P., Wilson, D., & Seymour, J. E. (2021). The influence of ecological factors on cnidarian venoms. *Toxicon: X*, *9*, 100067. See appendix A.

2.1 Abstract

Venom research is often focussed on medical relevance, novel compounds and venom evolution, whilst studying the relationship between a venom and its environment – venom ecology - has been conducted to a lesser extent. Given the projected environmental changes envisioned to occur with global warming, it is pertinent now more than ever, to highlight this topic. Here we review literature examining the influence of ecological factors such as environmental temperature, salinity, ontogeny, geographic location and diet on cnidarian venoms. This review provides an exclusive focus on the cnidarian phylum and encompasses all available published, peer-reviewed literature to our knowledge regarding the ecological factors influencing venom. We find a startling lack of research into the effects of both environmental and biological factors on venoms, with very few to no studies available per category. Importantly, research does exist that suggest these ecological processes may influence other marine or terrestrial venoms, thus we recommend future research is needed to explore this concept in cnidarians.

2.2 Introduction

Venomous species occur throughout many phyla in the animal kingdom, and some such as the Cnidaria (sea anemones, corals, jellyfish and hydrozoans) are solely composed of venomous animals (Goyffon, 2002). The defining characteristics of a venom have undergone much discussion within the literature and have been thoroughly reviewed with the following definition proposed: "a secretion, produced in a specialized gland in one organism, and delivered to a target organism through the infliction of a wound (regardless of how tiny it is); a venom must further contain molecules that disrupt normal physiological or biochemical processes so as to facilitate feeding or defence by the producing animal"(Fry et al., 2009). Venomous organisms are considered to be "active" when a toxin is produced in a gland or specialised tissue and then injected, whereas "passive" routes of exposure such as excretion are not truly venomous, although some overlap does occur (Goyffon, 2002).

The phylum Cnidaria boasts some of the most venomous animals in the marine environment, with the big box jellyfish *Chironex fleckeri* often revered as the most venomous animal on the planet (Endean, 1988). Unique to the cnidarians, specialised cells called cnidocytes contain stinging organelles called cnidae, characterised as either nematocysts, spirocysts, or ptychocysts (Hessinger & Lenhoff, 1988). The nematocysts are the only type that delivers venom.

The molecular composition forms part of the very definition of a venom (Fry et al., 2009), which highlights its importance as a research topic. How a venom effects its target – and incidentally humans – is determined by the molecules within the venom, and cnidarian venoms can have an array of effects. For example, the venom of the rhizostome jellyfish *Nemopilema nomurai* (initially misidentified as *Stomolophus meleagris*) has been shown to contain over 200 different toxins, with distinct functions such as potassium channel inhibitors, protease inhibitors, metalloproteases and hemolysins, among others (Li et al., 2014). Therefore, understanding the complexity that is venom composition is critical to understanding the venom as a functional whole. Whilst we understand the mechanisms of cnidarian venom delivery (Hessinger & Lenhoff, 1988; Nüchter et al., 2006; Schlesinger et al., 2009), there is a distinct lack of knowledge on how ecological factors – both biological and environmental – can influence the venom profile of these animals. For example, in *C. fleckeri* it has been shown that ontogeny and spatial distribution can affect variation in the venom, and it is further postulated that gender and/or environmental variations could be present (Winter et al., 2010). It could also be argued there is a distinct lack of knowledge of the comprehensive venom compositions. Some toxins have been identified, but the majority remain uncharacterised.

It is easy to assume an individual species will produce an individual venom, however here we present evidence that ecological factors can have a profound influence on intra-species venom variation. These variations will likely have ramifications for the ecology of the individual animal, the development of species-specific anti-venoms and searches for novel compounds. The importance of ecological influences on venom have been highlighted in two previous reviews. Geographic, ontogenetic and prey-associated venom variation within cnidarians has been highlighted (Ashwood et al., 2020), and venom evolution and gland morphology has been discussed in relation to ontogeny across terrestrial animals and cnidarians – with a primary focus on the sea anemone *Nematostella vectensis* (Surm & Moran, 2021). In this review we further expand and build upon these works to encompass more ecological factors, exclusively focusing on cnidarians but exploring a broader species diversity. The literature here is reviewed not from an evolutionary standpoint, but with a focus on plasticity within species venom composition and variation. Here the biological factors of diet and ontogeny, along with the environmental factors of salinity, environmental temperature and geographic location, are reviewed to determine their effects on cnidarian venoms. Appraisal of the knowledge gaps are highlighted, with specific note that some factors such as temperature and salinity are known to influence non-animal toxin production, but little to no research exists examining the influence of these environmental parameters on cnidarian venoms.

2.3 Biological factors

2.3.1 Ontogeny

There is a large amount of developmental diversity amongst cnidarians, which has been concisely summarised by Jouiaei et al., (2015). However, the available literature relating to venom ontogeny is dominated by sea anemones and jellyfish, of which the sexual reproduction involves the maturation of a gastrula to a planula in the development of cnidarians, which is then followed by two distinct stages: a sessile polyp and mobile medusa (both stages are not present in all cnidaria). When the available literature is combined, ontogenetic shifts in venom have been described spanning the entire cnidarian life cycle, albeit from a variety of species.

Venom analysis of the sea anemone *Nematostella vectensis* from gastrula to primary polyp found dramatic differences in toxin expression and nematocysts, between the gastrula, early planula, late planula, metamorphosing planula and primary polyp (Columbus-Shenkar et al., 2018). Behavioural predator-prey assays were also conducted to determine the ecological role of the observed changes in venom, evidencing that the venom of the planula repels larval fish upon ingestion, and can also paralyse *Artemia* nauplii. Molecular techniques were employed to visualise the expression of toxin genes throughout the life stages and have the potential to be

applied to other venomous cnidarians (Columbus-Shenkar et al., 2018). Further to this work, additional toxin paralogs from *Nematostella vectensis* have more recently been shown to be present only in the early life stages, which themselves vary in toxicity to both fish larvae and arthropods (Sachkova et al., 2019).

Different types of nematocysts have been described in cnidarians and the presence and ratios of these different nematocysts have been shown to change during animal growth. Nematocysts are inherently linked to the production and injection of a cnidarian's venom, with differing types having been described to contain different venom (Carrette et al., 2002; Glasser et al., 2014; McClounan & Seymour, 2012; Wiebring et al., 2010), thus by analysing the occurrence of nematocyst types (the cnidome), changes in venom can be presumed. If we were to assume venom variation using nematocyst composition as proxy, the upside down jellyfish *Cassiopea xamachana* may display venom ontogeny. The proportions of nematocyst type vary within different life stages and the nematocyst bearing structures such as mucus and cassiosomes are life stage specific (Ames et al., 2020). The entire life cycle of the Irukandji jellyfish *C. barnesi* has been examined and shows new nematocyst types are added as the animal grows (Courtney et al., 2016). This variation in nematocyst presence is likely to result in variation in the venom composition of the animal's arsenal. The hatching planula contain one type (Courtney et al., 2016), primary polyps, immature medusa and mature medusa contain two types (Underwood & Seymour, 2007), and very large medusa contain three types (Pereira et al., 2010). These studies also highlight a common problem within nematocyst nomenclature. The two main types of nematocysts are called tumiteles and isorhizas (Courtney et al., 2016), or holotrichous microbasic rhopaloids and homotrichous haplonemes (Underwood & Seymour, 2007), and are actually identical nematocyst types classified differently by different authors.

Ontogenetic shifts in venom composition between immature and mature medusa of *C. barnesi* are evident (Underwood & Seymour, 2007), which is unusual as the nematocyst types present within the animal do not change as the venom changes (Underwood & Seymour, 2007). This challenges the common supposition that venom is nematocyst specific, indeed toxin variation within the same nematocyst type has been previously documented in a sea anemone (Columbus-Shenkar et al., 2018). Whilst nematocyst-specific venom has been documented in big box jellyfish (*C. fleckeri)* nematocysts (Carrette et al., 2002; McClounan & Seymour, 2012), it has previously been highlighted that scant data exist to support these assumptions in other species of cnidarians (McClounan & Seymour, 2012). Therefore, it remains possible that, regardless of a stable cnidome in the early life stages (polyps and immature medusa) of *C .barnesi*, venom ontogeny may well still occur as seen in the later life stages. Further to this, very large mature medusa have been

caught on occasion possessing an additional nematocyst type: the microbasic mastigophore (Pereira et al., 2010). There have been two confirmed deaths from an Irukandji sting (Fenner & Hadok, 2002) and skin scrapings from one of these victims (data not available for the second case) detailed nematocysts consistent with that found only in the larger medusa (Pereira et al., 2010). Whilst the venom from this new nematocyst has not been analysed, it is tempting to postulate it may contain more lethal toxins, hence the associated fatality. However, without comparable data from the only other mortality, the evidence to support this theory is anecdotal at best and would require further research to validate. Although, it would certainly be possible to screen large medusa specimens for this type of nematocyst and compare the venom.

Later life stages in the big box jellyfish (*C. fleckeri)* also present changes in venom with ontogeny. In direct comparison to the aforementioned *C. barnesi*, the switch in venom in this animal coincides with a change in cnidome at the 7-10 tentacles stage in the animal's life (McClounan & Seymour, 2012). This shift in venom was theorised to correlate with *C. fleckeri's* known feeding ecology, as the animal grows and begins targeting vertebrate rather than invertebrate prey (Carrette et al., 2002).

Whilst there is some documentation of cubozoan nematocysts in the very early life stages (Courtney et al., 2016), currently there is no literature examining the actual venom. Therefore, the stinging ability and/or potency of these early stages remains an unknown, presenting an opportunity for further investigation, especially concerning the more medically important species.

2.3.2 Diet

Research into the effect of diet on cnidarian venom is completely absent for early life stages and has only been described for two cubozoan species in the later life stages. However, venomous feeding structures in siphonophores have been described to change between species in relation to diet (Damian-Serrano et al., 2021).

Venom, cnidome and venom toxicity have been described to correlate to the feeding ecology of the big box jellyfish (*C. fleckeri)*, with toxicity changes corresponding to the increased need to capture vertebrate prey. In the study, dietary information from the literature was connected to the results observed for changes in the jellyfish's diet (McClounan & Seymour, 2012). Diet data has been collected from animals from multiple locations around Northern Australia (Darwin, Mission Beach and Townsville), which would indicate *C. fleckeri* as a species has a consistent diet at different locales within its distribution range (Carrette et al., 2002). However, no direct diet

data, such as gut contents, was used to support conclusions on venom ontogeny (McClounan & Seymour, 2012).

Changes in venom composition of the jellyfish *C. barnesi* have also been linked to changes in the diet, with suggestion that compositional differences between immature and mature venom is due to the animal shifting from catching invertebrate to vertebrate prey (Underwood & Seymour, 2007). Again, no actual diet data is presented in support of this.

Diet specific venom has been evidenced and well-reviewed in numerous terrestrial animals, with implications that this could be a major driver in evolving venom composition (Casewell et al., 2013). It remains unclear why this field has been neglected in not only cnidarians, but the greater context of marine venoms. An obvious limitation of much of the available literature is the apparent reliance on literature sourced dietary data. With Lewis Ames and Macrander (2016) also emphasising that there are very limited accounts of cubozoan prey capture documented in natural settings. Whilst the studies presented here use the feeding ecology of the animals to rationalize results of venom differences, they are *not* inherently designing or analysing dietary experiments, i.e. not trialling different diets then analysing venom content, thus there is no control for confounding factors. It has previously been cautioned that captivity can influence venom quantity and quality, however, perhaps captive experiments may be the only way to control and test the effects of diet, as current in situ literature remains ambiguous (Kirchhoff et al., 2014; Modahl et al., 2010).

2.3.3 Environmental factors

Whilst biological influences on venom have been covered to some extent within the literature, research into the influence of environmental factors such as geography, salinity and temperature is sorely lacking. What is currently known on the influence of environmental factors is reviewed here.

2.3.4 Geographic location

Venom variation in cnidarian specimens over small-scale geographic distances has been explored, whereby the venom of the cubozoan *C. fleckeri* was found not to vary between regional geographic locations (less than 70km distance) (McClounan & Seymour, 2012). Marine venoms from other sources, such as the cone snail *Conus vexillum*, do vary between geographic locations of comparable distances (Abdel-Rahman et al., 2011). Whilst no variation was seen over small distances, the composition of *C. fleckeri* venom does differ between larger national geographic locations with differences observed in animals from an estimated range of over 500 km across Northern Australia (Winter et al., 2010).

Similar geographic distances have been explored in regard to the venom composition and toxicity of the giant jellyfish *Nemopilema nomurai,* which has been analysed for animals caught at multiple locations throughout the Yellow Sea (Yue et al., 2019). No effects of geographic location could be established, however dramatic venom variation was found between individuals. Whilst the authors describe compositional and toxicity differences between the venom of two animals caught at the same location, the cause of these variances remained inconclusive. The sampled locations spanned approximately 800 km, but the giant jellyfish has been described to be widely distributed in the Yellow Sea due to currents and the swimming ability of the animals (Yue et al., 2019). These results may potentially reflect an overlap in the ranges of these animals, and the described differences between animals from the same location could be attributed to such an overlap spanning sample locations.

Additionally, toxin gene expression within the sea anemone *Nematostella vectensis* has been examined between animal populations >900km (estimated) apart. This is the only evidence of a controlled environment study, whereby the separate populations were raised in identical conditions, in which toxin gene expression from each population was measured in response to heat shock and salinity. It has been described that *N. vectensis* animals from North Carolina express toxin genes differently in response to heat stress than those from Massachusetts (Sachkova et al., 2020). Whilst not a comparison of standard venom content across location, the authors describe that populations from different climatic conditions respond differently to heat stress (Sachkova et al., 2020), thus evidencing the ecological significance of cnidarian venom plasticity.

Lastly, geographical venom differentiation has been identified at very large-scale distances in one species of sea anemone, *Bunodosoma caissarum* (Orts et al., 2013). Two "geographically distant" populations were analysed, from the south coast of Brazil and an archipelago separated by over 3000 km. Reversed-phase high performance liquid chromatography (rp-HPLC) analysis showed similar venom profiles between both locations, however, only two toxins have currently been characterised for this species, one of which was absent from the archipelago venom profile, evidencing there are distinct differences in the venom between these locations. This work specifically notes that ecological and genetic factors could not be controlled, but venom collection and animal size was standardised. Previous work with *C. fleckeri* (Winter et al., 2010) discusses the possible impacts of having analysed jellyfish of different sizes (due to size varying with location), but as evidenced here with *B. caissarum* (Orts et al., 2013) it could be that even if size was standardised, location related differences in the venom would still have been found. Whilst

C. fleckeri are known to change venom with age (McClounan & Seymour, 2012) the fact that their size is location related suggests they are still reaching peak maturity, they are just smaller.

Little to no literature exists pertaining to hydrozoans, with only an incidental mention in otherwise focussed research in which hydrocorals have been described to maintain similar toxic effects regardless of location (García-Arredondo et al., 2015). However, this appears to be in reference to multiple papers (Middlebrook et al., 1971; Wittle et al., 1971, 1974) that describe the general mode of toxic effects of *Millepora species, with each study sampling at a different location and/or contrasting different species, rather than comparing the venom of a single species across location.*

Geographic venom variation in true anthozoan corals – rather than the hydrocorals – has been studied to a slightly greater extent, though research is still lacking. Indeed true venom analysis is rarer still, with most available literature examining whole body extracts in lieu of specific venom extraction. The global proteome (the total complement of proteins in the venom) from the heterotrophic coral *Tubastraea coccinea* has been shown to change over time, if a population is transplanted from one geographic location to another (separated on a small regional scale ~40km). However, the actual composition of *toxic* venom components remained identical in all populations, thus evidencing no change (Kitahara et al., 2020), interesting as the authors specifically note very different environmental conditions between the two sites. This lack of venom change is consistent with the findings of McClounan and Seymour (2012) in the analysis of the previously mentioned *C. fleckeri* venom over small geographic scales. This however cannot be interpreted as a cnidarian specific pattern across small distances, as local (Harvell et al., 1993) and even intracolonial (Gunthorpe & Cameron, 1990) toxin variation has been described in other corals. In the West Indian gorgonian coral *Briareum asbestinum* the overall defensive chemistry – rather than venom only extract – differs not only substantially between Bahamian colonies and US Virgin islands colonies, but also between individual Bahamian colonies (Harvell et al., 1993). A range of scleractinian corals (*Lobophyllia corymbosa, Favites abdita, Favia matthaü, Favia stelligera, Platygyra daedalea, Leptoria phrygia, Cyphastrea serailia, Hydnophora exesa* and *Astreopora myriophthalma*) further demonstrate intracolonial toxin variation over time, with successive extracts of each colony displaying different toxic activity profiles (Gunthorpe & Cameron, 1990). The latter of which should actually serve as a cautionary note when interpreting the plasticity of toxic activity in cnidarians, given this temporal propensity to change after sampling.

Geographic locations are inferred very differently within the literature, with analysis conducted on a broad diversity of scales which needs to be considered when interpreting the

presence/absence of venom variation. At greater distances it may logically be expected to see differences, as populations are more separate. However, none of the research presented here actually controls for influencing factors to just analyse geography, e.g. collecting animals from separate locations, raising them in identical conditions to determine if the geographic location is solely responsible rather than the changing environment that comes with changing location. Only one study acknowledged that ecological and genetic factors could not be standardised (Orts et al., 2013), although similar research with cone snails (Duda & Lee, 2009) did analyse the mitochondrial locus of animals to determine that genetic differentiation was not responsible for the observed venom differences, suggesting that the environmental conditions may be responsible rather than genetic drift between separate locations. Geographical distance, especially at the smaller regional scale, appears not to be a reliable indicator for predicting geographical venom differentiation. Whilst the literature showed venom differences between all largely separate areas (thousands of km), cnidarian venom does not seem to be influenced on a smaller scale. However, this conclusion should be interpreted cautiously, given the small amount of research available.

2.3.5 Salinity

All marine organisms are exposed to the differences salinity induces on ecosystems, but literature regarding the effect on venom/toxins is only available for the non-animal toxins. Whilst the primary focus of this review is on actively venomous cnidarians, some inclusion of other passive forms (e.g. toxic dinoflagellates) was deemed necessary where literature was completely absent for true venoms, but existed for passive toxins. Cnidarians have an intrinsic link with algal and dinoflagellate species, as numerous cnidarians host these as symbionts. Whilst these symbionts are located in the very tissue of cnidarians, they are still exposed and respond to varying changes in salinity, as evidenced by salinity induced bleaching (Kerswell & Jones, 2003). Whilst this is no means an ideal proxy, we do know algae and dinoflagellates within cnidarian tissue can be physically influenced by salinity, therefore the toxins contained within these same invertebrate tissues, and indeed the invertebrates themselves (which ultimately control the production of toxins), have the same potential to react to salinity. As such, non-animal non-cnidarian toxins are briefly discussed here.

Salinity affects toxins in various ways, sometimes specific to species, sometimes to individual strains, with no one prevailing trend. Multiple studies found that salinity affects the toxins of the dinoflagellate *Alexandrium minitum,* with toxicity and toxin content increasing with salinity (Grzebyk et al., 2003; Hwang & Lu, 2000; Lim & Ogata, 2005), yet a later study contrastingly reported no effect of salinity in the same species (Lim et al., 2011). Similarly, within the

cyanobacterium *Nodularia spumigena,* whilst literature determines that salinity does effect toxins, each available study describes a different effect (Blackburn et al., 1996; Hobson & Fallowfield, 2003; Mazur-Marzec et al., 2005). Whilst the multitudes of contrasting results may initially seem unhelpful, they actually serve to highlight the point that salinity is affecting these toxin-producing organisms in very diverse ways, suggesting that the ecology of the organism is being influenced right down to a strain specific level.

The salinity/toxin relationship can also provide further insights into the ecology of an organism. The toxin content of *A. minitum* was much higher in offshore seawater and was all but zero in estuarine seawater, however, as *A. minitum* grew well in both salinities, the authors hypothesised that "toxin biosynthesis was greatly weakened due to the lack of amino acid precursors in prey material" (Grzebyk et al., 2003). This theory could also be applicable to animal venoms.

It has been suggested that research in this field is inherently flawed as cell size would naturally vary with physical environmental changes and thus toxin content would change with cell size (Granéli & Flynn, 2006), an argument also relevant to animal venoms/toxins. However, multiple studies have considered this and present results that contradict the criticism, evidencing that cellular toxin quota was not affected by salinity-dependent growth rate, nor did toxin profiles change with salinity (Lim et al., 2011). Indeed, the toxin content of some species can peak at sub-optimal growth salinity(Lim & Ogata, 2005). Additionally, in the dinoflagellate *A. fundyense*, there is no relationship between photosynthesis or growth with toxicity, and the authors ultimately hypothesized that toxicity is at least partly driven directly by environmental conditions (Etheridge & Roesler, 2005). This hypothesis should be emphasized across all toxicity studies and should be used to explore the knowledge gap concerning other toxin and/or venom wielding marine organisms.

Research into the effect of salinity on the venom/toxins of not only cnidarians, but marine animals as a whole is scarce. Only one study could be found examining this in zootoxins, in which toxin gene expression was analysed in the sea anemone *Nematostella vectensis* (Sachkova et al., 2020). Although this was analysed in relation to population specific adaptations to salinity stress, rather than a salinity oriented study, it demonstrated that reduced salinity stress causes varying levels of toxin gene expression in a number of geographically separated sea anemone populations, suggesting salinity is a contributing ecological factor in venom/toxin production.

The evidence of salinity as an influencing factor to algal toxicity is vast, so why this has not been explored further within animal toxins/venom is perplexing. Indeed, multiple studies control for

salinity when analysing venom (Dutertre et al., 2010; Hoepner et al., 2019; Sivan et al., 2010), presumably to mitigate its influence, yet there is very little research into its effect.

2.3.6 Temperature

Variation in toxin/venoms with environmental temperature is all but unheard of within zootoxins, although some research has been conducted with snake venoms (Yin et al., 2020), but has been better documented within non-animal toxins (Band-Schmidt et al., 2014; Gedaria et al., 2007; Lim et al., 2006), posing a compelling argument that similar effects could be seen in animal venoms and warrants further investigation.

Only two studies could be found that analyse the influence of environmental temperature on cnidarian toxins. Firstly, toxins in the sea anemone *Actinia equina* have been analysed using Reverse Transcription quantitative Polymerase Chain reaction (RT-qPCR), to quantify the expression of toxin genes over different temperatures (O'Hara et al., 2018). The study aimed to assess long-term temperature change to reflect projected temperature changes with global warming. The anemones were held for five months at experimental temperatures to negate the possibility of results relating to thermal shock response. The expression of two toxin genes, equinatoxin and equistatin, were observed to change at 10 °C and 22 °C compared to a 16 °C control, although only the colder temperature was reported as significant downregulation in both genes. Whilst not statistically significant, it is interesting to note the two toxin genes displayed opposite trends in relation to the warm treatment, suggesting the ecological response of the anemones to environmental temperature change is toxin specific (O'Hara et al., 2018). This evidenced for the first time that environmental temperature does influence toxin production in cnidarians. *A. equina* is a common and relatively harmless cnidarian, but provides a foundation to continue work with species that pose a threat to human health.

Secondly, toxin gene expression in the sea anemone *N. vectensis* was analysed in response to short-term (24hr) environmental heat stress (Sachkova et al., 2020). As also noted in the geographic location and salinity sections of this review, it has been described that sea anemone populations from different climatic conditions respond differently to heat stress in relation to venom production. Strong evidence highlights that the thermal ecology of the animal plays a role in toxin gene expression, as the thermal regimes differ between *N. vectensis* habitats, and those populations not naturally exposed to higher temperatures respond differently in their toxin gene expression (Sachkova et al., 2020).

We can therefore conclude that environmental temperature can impact cnidarian venom toxins in both short term (Sachkova et al., 2020) and long term (O'Hara et al., 2018) instances. Whilst

the gene analysis of the two studies was quantitative, changes in the venom toxicity were not analysed, so it remains unknown what precise ecological impacts the changes in the toxins have. However, the study on *N. vectensis* (Sachkova et al., 2020) did include at least some proteomic analysis by LC-MS/MS that showed very similar trends to the transcriptomic analyses.

Overall, we highlight the knowledge gap for venom/toxin work in relation to environmental temperature, most especially in medically socio-economically important cnidarian species, given evidence from less potent species suggests temperature does affect venom composition.

2.4 Conclusion

Whilst the literature is scattered across taxa, often with each species only receiving sparse dedicated analysis, it is evident that ecological parameters do affect cnidarian venom composition, albeit in very different and often unpredicted ways. The challenge now is to use this knowledge to advance the field of venom research and tease out the effects these parameters may have on venom profiles.

There is large amount of evidence detailing that environmental temperature and salinity can influence toxins in non-animal organisms such as dinoflagellates, whereas no comparable research exists for zootoxins. Given sea surface temperature and salinity are parameters predicted to change with global warming forecasts, it would seem these are the urgent areas required to be explored in the animal venoms if we are to stand a chance at predicting changing venom ecology. It is interesting that environmental temperature has not previously been analysed along with venom, as venomous animals have been noted to predominantly reside in intertropical areas of the world (Goyffon, 2002) suggesting an innate or even evolutionary relationship between venom and temperature.

The value of ecology is largely overlooked in medical research, however as evidenced here it has the ability to drastically influence the venom of some of the most dangerous cnidarians on the planet. One clear example is the urging conclusion within a medical research journal for the need to conduct venom studies on Irukandji jellyfish in order to develop preventive strategies and effective treatments (Fenner & Hadok, 2002). Venom studies alone will not be sufficient. The ecology and toxicology must unite, the understanding of how venom changes with ecology must come first, as medical treatments cannot advance if we do not acknowledge the two are inherently linked. The two fields need to coalesce, as working separately has led to drastic gaps in our understanding, leaving us unprepared to predict how a changing environment will affect the severity of human envenomations by dangerous cnidarians.

Through the compilation of literature presented here, we see there is a very real link between a cnidarian's venom and its ecology. The plasticity of these venoms across both biological and environmental factors is astounding, especially given the very simple nature of the organism themselves. This is a concept that will affect not only our understanding of medical treatments, but also our knowledge of the fundamental ecology of the animals themselves. A rather daunting prospect is that if venoms can indeed change with changing environments, we may well begin to see heretofore relatively harmless cnidarians begin to exhibit more hazardous traits as the world changes around them.

2.5 References

Abdel-Rahman, M. A., Abdel-Nabi, I. M., El-Naggar, M. S., Abbas, O. A., & Strong, P. N. (2011). Intraspecific variation in the venom of the vermivorous cone snail Conus vexillum. *Comparative Biochemistry and Physiology - C Toxicology and Pharmacology*, *154*(4), 318–325. https://doi.org/10.1016/j.cbpc.2011.06.019

Ames, C. L., Klompen, A. M. L., Badhiwala, K., Muffett, K., Reft, A. J., Kumar, M., Janssen, J. D., Schultzhaus, J. N., Field, L. D., Muroski, M. E., Bezio, N., Robinson, J. T., Leary, D. H., Cartwright, P., Collins, A. G., & Vora, G. J. (2020). Cassiosomes are stinging-cell structures in the mucus of the upside-down jellyfish *Cassiopea xamachana*. *Communications Biology*, *3*(1), 1–15. https://doi.org/10.1038/s42003-020-0777-8

Ashwood, L. M., Norton, R. S., Undheim, E. A. B., Hurwood, D. A., & Prentis, P. J. (2020). Characterising Functional Venom Profiles of Anthozoans and Medusozoans within Their Ecological Context. *Marine Drugs*, *18*(202). https://doi.org/10.3390/md18040202

Band-Schmidt, C. J., Bustillos-Guzmán, J. J., Hernández-Sandoval, F. E., Núñez-Vázquez, E. J., & López-Cortés, D. J. (2014). Effect of temperature on growth and paralytic toxin profiles in isolates of Gymnodinium catenatum (Dinophyceae) from the Pacific coast of Mexico. *Toxicon*, *90*, 199–212. https://doi.org/10.1016/j.toxicon.2014.08.002

Blackburn, S. I., Mccausland, M. A., Bolch, C. J. S., Newman, S. J., & Jones, G. J. (1996). Effect of salinity on growth and toxin production in cultures of the bloom-forming cyanobacterium Nodularia spumigena from Australian waters. *Phycologia*, *35*(6), 511–522. https://doi.org/10.2216/i0031-8884-35-6-511.1

Carrette, T., Alderslade, P., & Seymour, J. (2002). Nematocyst ratio and prey in two Australian cubomedusans, Chironex fleckeri and Chiropsalmus sp. *Toxicon*, *40*, 1547–1551. www.elsevier.com/locate/toxicon

Casewell, N. R., Wüster, W., Vonk, F. J., Harrison, R. A., & Fry, B. G. (2013). Complex cocktails: The evolutionary novelty of venoms. In *Trends in Ecology and Evolution* (Vol. 28, Issue 4, pp. 219–229). https://doi.org/10.1016/j.tree.2012.10.020

Columbus-Shenkar, Y. Y., Sachkova, M. Y., Macrander, J., Fridrich, A., Modepalli, V., Reitzel, A. M., Sunagar, K., & Moran, Y. (2018). Dynamics of venom composition across a complex life cycle. *ELife*, *7:e35014*. https://doi.org/https://doi.org/10.7554/eLife.35014

Courtney, R., Browning, S., & Seymour, J. (2016). Early life history of the “irukandji” jellyfish

Carukia barnesi. *PLoS ONE*, *11*(3). https://doi.org/10.1371/journal.pone.0151197

Damian-Serrano, A., Haddock, S. H. D., & Dunn, C. W. (2021). The evolution of siphonophore tentilla for specialized prey capture in the open ocean. *National Acad Sciences*, *118*(8), 2021. https://doi.org/10.1073/pnas.2005063118/-/DCSupplemental

Duda, T. F., & Lee, T. (2009). Ecological release and venom evolution of a predatory marine snail at Easter Island. *PLoS ONE*, *4*(5). https://doi.org/10.1371/journal.pone.0005558

Dutertre, S., Biass, D., Stöcklin, R., & Favreau, P. (2010). Dramatic intraspecimen variations within the injected venom of Conus consors: An unsuspected contribution to venom diversity. *Toxicon*, *55*(8), 1453–1462. https://doi.org/10.1016/j.toxicon.2010.02.025

Etheridge, S. M., & Roesler, C. S. (2005). Effects of temperature, irradiance, and salinity on photosynthesis, growth rates, total toxicity, and toxin composition for Alexandrium fundyense isolates from the Gulf of Maine and Bay of Fundy. *Deep-Sea Research Part II: Topical Studies in Oceanography*, *52*(19-21 SPEC. ISS.), 2491–2500. https://doi.org/10.1016/j.dsr2.2005.06.026

Fenner, P., & Hadok, J. (2002). Fatal envenomation by jellyfish causing Irukandji syndrome. *Medical Journal of Australia*, *177*(7), 362–363.

Fry, B. G., Roelants, K., Champagne, D. E., Scheib, H., Tyndall, J. D. A., King, G. F., Nevalainen, T. J., Norman, J. A., Lewis, R. J., Norton, R. S., Renjifo, C., & de la Vega, R. C. R. (2009). The Toxicogenomic Multiverse: Convergent Recruitment of Proteins Into Animal Venoms. *Annual Review of Genomics and Human Genetics*, *10*(1), 483–511. https://doi.org/10.1146/annurev.genom.9.081307.164356

García-Arredondo, A., Rojas-Molina, A., Bah, M., Ibarra-Alvarado, C., Gallegos-Corona, M. A., & García-Servín, M. (2015). Systemic toxic effects induced by the aqueous extract of the fire coral Millepora complanata and partial purification of thermostable neurotoxins with lethal effects in mice. *Comparative Biochemistry and Physiology Part - C: Toxicology and Pharmacology*, *169*, 55–64. https://doi.org/10.1016/j.cbpc.2014.12.004

Gedaria, A. I., Luckas, B., Reinhardt, K., & Azanza, R. V. (2007). Growth response and toxin concentration of cultured Pyrodinium bahamense var. compressum to varying salinity and temperature conditions. *Toxicon*, *50*(4), 518–529. https://doi.org/10.1016/j.toxicon.2007.04.021

Glasser, E., Rachamim, T., Aharonovich, D., & Sher, D. (2014). Hydra actinoporin-like toxin-1, an

unusual hemolysin from the nematocyst venom of Hydra magnipapillata which belongs to an extended gene family. *Toxicon*, *91*, 103–113. https://doi.org/10.1016/j.toxicon.2014.04.004

Goyffon, M. (2002). The venomous function. In A. Ménez (Ed.), *Perspectives in Molecular Toxinology* (p. 423). John Wiley & Sons, Ltd.

Granéli, E., & Flynn, K. (2006). Chemical and Physical Factors Influencing Toxin Content. In E. Granéli, Turner, & T. Jefferson (Eds.), *Ecological Studies,Vol. 189. Ecology of Harmful Algae* (pp. 229–241). Springer-Verlag .

Grzebyk, D., Béchemin, C., Ward, C. J., Vérité, C., Codd, G. A., & Maestrini, S. Y. (2003). Effects of salinity and two coastal waters on the growth and toxin content of the dinoflagellate Alexandrium minutum. *Journal of Plankton Research*, *25*(10), 1185–1199. https://doi.org/10.1093/plankt/fbg088

Gunthorpe, L., & Cameron, A. M. (1990). Intracolonial variation in toxicity in scleractinian corals. *Toxicon*, *28*(10), 1221–1227. https://doi.org/10.1016/0041-0101(90)90121-M

Harvell, C. D., Fenical, W., Roussis, V., Ruesink, J. L., Griggs, C. C., & Greene, C. H. (1993). Local and geographic variation in the defensive chemistry of a West Indian gorgonian coral (Briareum asbestinum). *Marine Ecology Progress Series*, *93*(1–2), 165–173. https://doi.org/10.3354/meps093165

Hessinger, D. A., & Lenhoff, H. M. (1988). *The Biology of Nematocysts* (D. A. Hessinger & H. M. Lenhoff (eds.)). Academic Press, Inc.

Hobson, P., & Fallowfield, H. J. (2003). Effect of irradiance, temperature and salinity on growth and toxin production by Nodularia spumigena. In *Hydrobiologia* (Vol. 493).

Hoepner, C. M., Abbott, C. A., & da Silva, K. B. (2019). The ecological importance of toxicity: Sea anemones maintain toxic defence when bleached. *Toxins*, *11*(5). https://doi.org/10.3390/toxins11050266

Hwang, F. D., & Lu, H. Y. (2000). Influence of environmental and nutritional factors on growth, toxicity, and toxin profile of dinoflagellate Alexandrium minutum. *Toxicon*, *38*, 1491–1503. www.elsevier.com/locate/toxicon

Jouiaei, M., Yanagihara, A. A., Madio, B., Nevalainen, T. J., Alewood, P. F., & Fry, B. G. (2015). Ancient venom systems: A review on cnidaria toxins. *Toxins*, *7*(6), 2251–2271. https://doi.org/10.3390/toxins7062251

Kerswell, A. P., & Jones, R. J. (2003). *Effects of hypo-osmosis on the coral* Stylophora pistillata *: nature and cause of 'low-salinity bleaching.' 253*, 145–154.

Kirchhoff, K. N., Klingelhöfer, I., Dahse, H. M., Morlock, G., & Wilke, T. (2014). Maturity-related changes in venom toxicity of the freshwater stingray Potamotrygon leopoldi. *Toxicon*, *92*, 97–101. https://doi.org/10.1016/j.toxicon.2014.10.011

Kitahara, M. V., Jaimes-Becerra, A., Gamero-Mora, E., Padilla, G., Doonan, L. B., Ward, M., Marques, A. C., Morandini, A. C., & Long, P. F. (2020). Reciprocal transplantation of the heterotrophic coral *Tubastraea coccinea* (Scleractinia: Dendrophylliidae) between distinct habitats did not alter its venom toxin composition. *Ecology and Evolution*, *10*(4), 1794–1803. https://doi.org/10.1002/ece3.5959

Lewis Ames, C., & Macrander, J. (2016). Evidence for an Alternative Mechanism of Toxin Production in the Box Jellyfish Alatina alata. *Integrative and Comparative Biology*, *56*(5), 973–988. https://doi.org/10.1093/icb/icw113

Li, R., Yu, H., Xue, W., Yue, Y., Liu, S., Xing, R., & Li, P. (2014). Jellyfish venomics and venom gland transcriptomics analysis of Stomolophus meleagris to reveal the toxins associated with sting. *Journal of Proteomics*, *106*, 17–29. https://doi.org/10.1016/j.jprot.2014.04.011

Lim, P. T., Leaw, C. P., Sato, S., van Thuoc, C., Kobiyama, A., & Ogata, T. (2011). Effect of salinity on growth and toxin production of Alexandrium minutum isolated from a shrimp culture pond in northern Vietnam. *Journal of Applied Phycology*, *23*(5), 857–864. https://doi.org/10.1007/s10811-010-9593-8

Lim, P. T., Leaw, C. P., Usup, G., Kobiyama, A., Koike, K., & Ogata, T. (2006). Effects of light and temperature on growth, nitrate uptake, and toxin production of two tropical dinoflagellates: Alexandrium tamiyavanichii and Alexandrium minutum (Dinophyceae). *Journal of Phycology*, *42*(4), 786–799. https://doi.org/10.1111/j.1529-8817.2006.00249.x

Lim, P. T., & Ogata, T. (2005). Salinity effect on growth and toxin production of four tropical Alexandrium species (Dinophyceae). *Toxicon*, *45*(6), 699–710. https://doi.org/10.1016/j.toxicon.2005.01.007

Mazur-Marzec, H., Żeglińska, L., & Pliński, M. (2005). The effect of salinity on the growth, toxin production, and morphology of Nodularia spumigena isolated from the Gulf of Gdańsk, southern Baltic Sea. *Journal of Applied Phycology*, *17*(2), 171–179. https://doi.org/10.1007/s10811-005-5767-1

McClounan, S., & Seymour, J. (2012). Venom and cnidome ontogeny of the cubomedusae *Chironex fleckeri*. *Toxicon*, *60*(8), 1335–1341. https://doi.org/10.1016/j.toxicon.2012.08.020

Middlebrook, R. E., Wittle, L. W., Scura, E. D., & Lane, C. E. (1971). Isolation and purification of a toxin from Millepora dichotoma. *Toxicon*, *9*(4). https://doi.org/10.1016/0041-0101(71)90130-9

Modahl, C. M., Doley, R., & Kini, R. M. (2010). Venom analysis of long-term captive Pakistan cobra (Naja naja) populations. *Toxicon*, *55*(2–3), 612–618. https://doi.org/10.1016/j.toxicon.2009.10.018

Nüchter, T., Benoit, M., Engel, U., Özbek, S., Biology, T. H.-C., & 2006, undefined. (2006). Nanosecond-scale kinetics of nematocyst discharge. *Current Biology*, *16*(9). www.current-biology.com/cgi/content/

O'Hara, E. P., Caldwell, G. S., & Bythell, J. (2018). Equistatin and equinatoxin gene expression is influenced by environmental temperature in the sea anemone Actinia equina. *Toxicon*, *153*, 12–16. https://doi.org/10.1016/j.toxicon.2018.08.004

Orts, D. J. B., Peigneur, S., Madio, B., Cassoli, J. S., Montandon, G. G., Pimenta, A. M. C., Bicudo, J. E. P. W., Freitas, J. C., Zaharenko, A. J., & Tytgat, J. (2013). Biochemical and electrophysiological characterization of two sea anemone type 1 potassium toxins from a geographically distant population of bunodosoma caissarum. *Marine Drugs*, *11*(3), 655–679. https://doi.org/10.3390/md11030655

Pereira, P., Barry, J., Corkeron, M., Keir, P., Little, M., & Seymour, J. (2010). Intracerebral hemorrhage and death after envenoming by the jellyfish *Carukia barnesi*. *Clinical Toxicology*, *48*, 390–392. https://doi.org/10.3109/15563651003662675

Sachkova, M. Y., Macrander, J., Surm, J. M., Aharoni, R., Menard-Harvey, S. S., Klock, A., Leach, W. B., Reitzel, A. M., & Moran, Y. (2020). Some like it hot: Population-specific adaptations in venom production to abiotic stressors in a widely distributed cnidarian. *BMC Biology*, *18*(1), 121. https://doi.org/10.1186/s12915-020-00855-8

Sachkova, M. Y., Singer, S. A., Macrander, J., Reitzel, A. M., Peigneur, S., Tytgat, J., & Moran, Y. (2019). The Birth and Death of Toxins with Distinct Functions: A Case Study in the Sea Anemone Nematostella. *Molecular Biology and Evolution*, *36*(9), 2001–2012. https://doi.org/10.1093/molbev/msz132

Schlesinger, A., Zlotkin, E., Kramarsky-Winter, E., & Loya, Y. (2009). Cnidarian internal stinging mechanism. *Proceedings of the Royal Society B: Biological Sciences*, *276*(1659), 1063–1067. https://doi.org/10.1098/rspb.2008.1586

Sivan, G., Venketasvaran, K., & Radhakrishnan, C. K. (2010). Characterization of biological activity of Scatophagus argus venom. *Toxicon*, *56*(6), 914–925. https://doi.org/10.1016/j.toxicon.2010.06.014

Surm, J. M., & Moran, Y. (2021). Insights into how development and life-history dynamics shape the evolution of venom. In *EvoDevo* (Vol. 12, Issue 1, p. 1). BioMed Central Ltd. https://doi.org/10.1186/s13227-020-00171-w

Underwood, A. H., & Seymour, J. E. (2007). Venom ontogeny, diet and morphology in *Carukia barnesi*, a species of Australian box jellyfish that causes Irukandji syndrome. *Toxicon*, *49*(8), 1073–1082. https://doi.org/10.1016/j.toxicon.2007.01.014

Wiebring, A., Helmholz, H., Sötje, I., Lassen, S., Prange, A., & Tiemann, H. (2010). A New Method for the Separation of Different Types of Nematocysts from Scyphozoa and Investigation of Proteinaceous Toxins Utilizing Laser Catapulting and Subsequent Mass Spectrometry. *Marine Biotechnology*, *12*(3), 308–317. https://doi.org/10.1007/s10126-010-9261-7

Winter, K. L., Isbister, G. K., McGowan, S., Konstantakopoulos, N., Seymour, J. E., & Hodgson, W. C. (2010). A pharmacological and biochemical examination of the geographical variation of Chironex fleckeri venom. *Toxicology Letters*, *192*(3), 419–424. https://doi.org/10.1016/j.toxlet.2009.11.019

Wittle, L. W., Middlebrook, R. E., & Lane, C. E. (1971). Isolation and partial purification of a toxin from Millepora alcicornis. *Toxicon*, *9*(4). https://doi.org/10.1016/0041-0101(71)90129-2

Wittle, L. W., Scura, E. D., & Middlebrook, R. E. (1974). Stinging coral (Millepora tenera) toxin: A comparison of crude extracts with isolated nematocyst extracts. *Toxicon*, *12*(5), 481–482. https://doi.org/10.1016/0041-0101(74)90037-3

Yin, X., Guo, S., Gao, J., Luo, L., Liao, X., Li, M., Su, H., Huang, Z., Xu, J., Pei, J., & Chen, S. (2020). Kinetic analysis of effects of temperature and time on the regulation of venom expression in Bungarus multicinctus. *Scientific Reports*, *10*(1). https://doi.org/10.1038/s41598-020-70565-2

Yue, Y., Yu, H., Li, R., Liu, S., Xing, R., & Li, P. (2019). Insights into individual variations in nematocyst venoms from the giant jellyfish Nemopilema nomurai in the Yellow Sea. *Scientific Reports*,

9(1). https://doi.org/10.1038/s41598-019-40109-4

Chapter 3 . Inducing metamorphosis in the Irukandji jellyfish *Carukia barnesi*

This chapter is a is a published manuscript: O'Hara, E., & Seymour, J. (2022). Inducing metamorphosis in the irukandji jellyfish *Carukia barnesi*. *Scientific Reports*, *12*(1), 9052. See appendix A.

3.1 Abstract

Here we utilize chemical ecology as a tool to manipulate the biological system of a small, but highly venomous to humans, cubozoan jellyfish, *Carukia barnesi.* We trialled a range of chemical reagents including indole compounds, 9-cis-retinoic acid and Lugol's solution to induce metamorphosis between the polyp and medusa life stages. An optimum method was determined resulting in a 90% metamorphosis rate to healthy medusa by exposing the polyps to 1 µM of 5-methoxy-2-methylindole for 24 hours. Of note is that chemical exposure time significantly impacts health and metamorphosis rates in this species. We also present a theoretical mechanism for the chemical/biological interactions occurring during metamorphosis. This is a significant methodological advancement which now enables rearing of this animal *en mass* in aquaria - a world first for this species - which will subsequently supply and facilitate venom research into this understudied jellyfish.

3.2 Introduction

Irukandji syndrome is the complex and excruciatingly painful condition resulting from a sting from a range of small, almost invisible box jellyfish species. The species most commonly associated with Irukandji syndrome from Northern Australia is *Carukia barnesi* (Barnes, 1964; Southcott, 1967), which is known to cause a range of symptoms from extreme muscle pains, nausea and vomiting, to instances which induce intracerebral haemorrhage and death (Fenner & Hadok, 2002; Pereira et al., 2010). Whilst often revered in the media as one of the most venomous jellyfish in the world (Crew, 2013), the venom of this animal remains poorly understood, which poses a major detriment to human health and tourism.

The supply of venom may be considered the biggest hindrance to advancing research on this dangerous jellyfish. Current venom collection from this species is reliant on extraction from wild caught adult medusa, collection of which is restricted to what is colloquially termed "stinger season": the months of approximately November to May when the medusae are present in the wild. *Carukia barnesi* is a logistically difficult species to field sample which further limits the venom supply through large catch variability and no guarantee of sample sizes. Captured individual medusa, even at adult maturity, typical measure less than 12mm in interpedalial distance, resulting in extremely low venom yield per jellyfish. These factors combined ensure the process of venom acquisition from *C. barnesi* is extremely expensive and logistically difficult. With such a limited supply of venom, research is ultimately finite and very costly, posing a major problem for such a medically important species.

The resolution to this quandary may be to circumvent the use of wild caught medusa entirely and rear these medusa to adulthood *en mass* in aquaria. Mass culture of this venomous jellyfish may be the starting point to facilitating further venom research, an important step towards advancing biomedical, biotechnology and bioprospecting sectors. However, this firstly requires us to step back through the life stages to better grasp how to control them. Three out of the four classes of cnidaria transition from a sessile polyp into a free swimming medusa as part of their life cycle. Each class typically changes in one of three ways as defined by Holstein and Laudet (Holstein & Laudet, 2014): polyps may undergo strobilation – this occurs in scyphozoans (true jellyfish) in which transverse fissions transform the entire polyp into multiple disc-like young medusa. polyps may complete metamorphosis, this can occur in cubozoans (box jellyfish) in which the polyps metamorphose into a single medusa, or the polyps may generate medusa though lateral budding (Holstein & Laudet, 2014) which occurs in hydrozoans. However, some cubozoa have been shown to transition via monodisc strobilation, almost a hybridization of strobilation and metamorphosis in which the polyp is regenerated before a single medusa detaches (Toshino et al., 2015), which

has previously been observed in *C. barnesi* (Courtney et al., 2016). All venom and sting research on *C. barnesi* to date has been derived from the larger adult or sub-adult medusae (Pereira & Seymour, 2013; Ramasamy et al., 2005; Seymour et al., 2020; Underwood & Seymour, 2007; Wiltshire et al., 2000; Winkel et al., 2005), with no venom analysis conducted on the polyp stages or smaller (<8mm (Underwood & Seymour, 2007)) medusas, so it remains a mystery if these very early life stages are as lethal as their adult counterparts. This knowledge gap is predominantly due to difficulties in acquiring these early stages in the wild and extracting sufficient quantities of venom.

Methods to induce metamorphosis/strobilation in jellyfish polyps have been described for multiple species, however the majority of literature is based on scyphozoans, with very little analysis of cubozoans (Helm & Dunn, 2017; Yamamori et al., 2017). Promising reagents that have successfully been used to induce metamorphosis in other cubozoan species include a number of indole containing compounds (Helm & Dunn, 2017; Yamamori et al., 2017) which may work as a proxy for a specific peptide sequence upregulated during the metamorphosis process (Fuchs et al., 2014). Lugol's solution (aqueous iodine) can successfully induce strobilation in a range of scyphozoan species (Berking et al., 2005; Green et al., 2018; Spangenberg, 1967) by influencing an oxidant defense system (Berking et al., 2005) and has now been seen to anecdotally produce metamorphosis in cubopolyps (JCU aquarium staff, S. Turner, personal communication, 2020). In addition, retinoids can influence metamorphosis in Hydractinian polyps (Muller, 1984) which may be applicable to cubopolyps as other cubozoan species have been shown to contain a retinoic receptor (Kostrouch et al., 1998).

Populations of *C. barnesi* polyps, created from the in vitro fertilisation of spawning adults, are available in culture (Courtney et al., 2016). Whilst the natural environmental cue to trigger metamorphosis from polyp to medusa in this species remains a mystery, this current work aimed to artificially chemically induce metamorphosis to create a reliable and increased supply of medusa to facilitate an unrestricted and inexpensive yield of venom for future research.

In this study we explore the following hypothesis: In this study, we test the following null hypotheses: H_0 Metamorphosis in *Carukia barnesi* polyps is not induced by: 1) exposure to chemical compounds; 2) the concentration of said chemicals, 3) or by the duration of exposure. Finally, we expect there is not a three-way interaction among those three factors.

Available literature documents a number of known metamorphic responses exhibited by this species, consequently allowing us to choose four key stages of metamorphosis to analyse in

response to chemical, concentration and time. Tentacle migration is one of the first visually obvious stages of metamorphosis in this species (Courtney et al., 2016), so was chosen to indicate the initiation of metamorphosis. The polyp producing a detached medusa is quintessentially the very definition of metamorphosis so was chosen as key metric of complete metamorphosis. We also opted to expand on the latter as the literature suggests some chemical compounds can cause deformed unhealthy medusa when inducing metamorphosis (Helm & Dunn, 2017) and we needed a realistic metric of healthy detached medusa. Similarly, some chemicals are known to inhibit polyp reformation post metamorphosis (Helm & Dunn, 2017), thus, we also chose polyp survival as a metamorphic response to give us an idea of whole colony impact.

3.3 Method

3.3.1 Animal husbandry

Carukia barnesi polyps were available in culture from the James Cook University Aquarium, spawned from medusa originally collected near Double Island, North Queensland, Australia (16°43.5'S, 145°41.0'E) in 2014 and 2015(Courtney et al., 2016). Populations exponentially increase through asexual reproduction (Courtney et al., 2016). Detached buds and swimming polyps were collected from the main culture, and transferred into 6-well tissue culture plates in natural filtered seawater. Plates were maintained in darkness to inhibit algae growth at 27 °C in a constant temperature cabinet. Buds and swimming polyps were left to develop and attach to well bottoms, at which point they were then fed freshly hatched *Artemia* nauplii and water changed 2-3 times per week. Lids remained attached to tissue culture plates to negate water evaporation and maintain a stable salinity. Polyps were maintained in this way for a minimum of 4 months before experiments began, with all individuals matured with the ability to asexually reproduce further buds. To preserve water quality (Helm & Dunn, 2017) polyps were starved for two days prior to experiment start and were not fed for the duration of the trials. One day prior to the experiment start, all immature buds and polyps were removed from wells, leaving approximately 5-10 mature polyps attached to the substrate for analysis.

3.3.2 Preparation of reagents

Reagents:

Six chemicals were trialed in the current study to induce metamorphosis in *C. barnesi* polyps. Four indole containing compounds were chosen that have previously been trialed with other cubozoan species: 5-methoxy-2-methyl-3-indoleacetic acid, 5-methoxyindole-2-carboxylic acid, 2-methylindole (Yamamori et al., 2017) and 5-Methoxy-2-methylindole (Helm & Dunn, 2017; Yamamori et al., 2017). Along with the retinoic X receptor 9-cis-retinoic acid and Lugol's solution.

Indole compound treatments:

Chemical concentrations of indoles documented in the literature were used to conduct preliminary concentration tests. Fifty mM stock solutions were prepared with 100% ethanol, which was diluted with filtered seawater to the desired experimental concentrations: 50 µM (Yamamori et al., 2017), 20 µM and 5 µM (Helm & Dunn, 2017). Due to high fatality rates at all of these concentrations when used in this study on *C. barnesi*, all concentrations were diluted. Fifty mM stock solutions of 5-methoxy-2-methyl-3-indoleacetic acid, 5-methoxyindole-2-carboxylic acid, 2-methylindole and 5-Methoxy-2-methylindole were prepared with 50% ethanol (50% Milli-Q® water) and stored at -20°C. Fifty mM stock solutions were diluted with filtered seawater to the experimental concentrations of 5 µM, 1 µM, 0.5 µM, 0.1 µM and 0.05 µM. The carrier solution of 50% ethanol (50% Milli-Q® water) was diluted to the equivalent of the experimental concentrations listed above for use as a control, and incorporated into data as concentration 0. Seventeen ml of solution was added to polyps to fill each well of a 6-well plate.

Iodine treatment (Lugol's solution):

Aqueous iodine in the form of Lugol's solution (0.37% iodine and 0.74% potassium iodide (sigma product information)) was prepared with equivalent concentrations of moles iodine/iodide: 1.5 µM, 3 µM , 6 µM, 12 µM and 24 µM. Filtered seawater only was used a control for this treatment and incorporated into data as concentration 0. 17 ml of solution was added to polyps to fill each well of a 6-well plate

Retinoid treatment:

To reduce ethanol associated fatality of polyps 0.015% ethanol in Milli-Q® water was used to prepare a 1mM stock solution of 9-*cis*-Retinoic acid. The 1 mM stock solution was diluted with filtered seawater to the experimental concentrations of 5 µM, 1 µM, 0.5 µM, 0.1 µM and 0.05 µM. The carrier solution of 0.015% ethanol (Milli-Q® water) was diluted to the equivalent of the experimental concentrations listed above for use as a control, and incorporated into data as concentration 0. 17 ml of solution was added to polyps to fill each well of a 6-well plate.

3.3.3 Metamorphosis trials

Primary trials:

Experimental concentrations of reagents were added to *C. barnesi* polyps growing in the wells of sterile 6-well tissue culture plates. One plate was used per chemical, per concentration, in which five wells functioned as replicates containing the chemical being trialed, whilst the sixth well

contained only the control medium. Five concentrations were run for each of six chemicals; 30 plates in total.

The filtered seawater the polyps were growing in was exchanged for the experimental chemical on day 0, and was not changed for the duration of the trial. Lids remained attached to tissue culture plates to negate water evaporation and hence salinity changes.

Polyps in each well were photographed each day through a dissection microscope over a period of 34 days. Results were then recorded from the photographs, categorised (fig. 3.1) as the number of polyps which displayed:

Tentacle migration – one of the key signs of metamorphosis in this species, polyp tentacles merge, migrating to form four distinct corners in a square shape (Courtney et al., 2016)

Detached medusa – a medusa formed and detached from the polyp, recorded regardless of health

Mobile detached medusa - a healthy medusa formed and detached from the polyp, with the ability to swim.

Polyp survival – this was then used to calculate the number of polyps which survived the treatment which did not metamorphose.

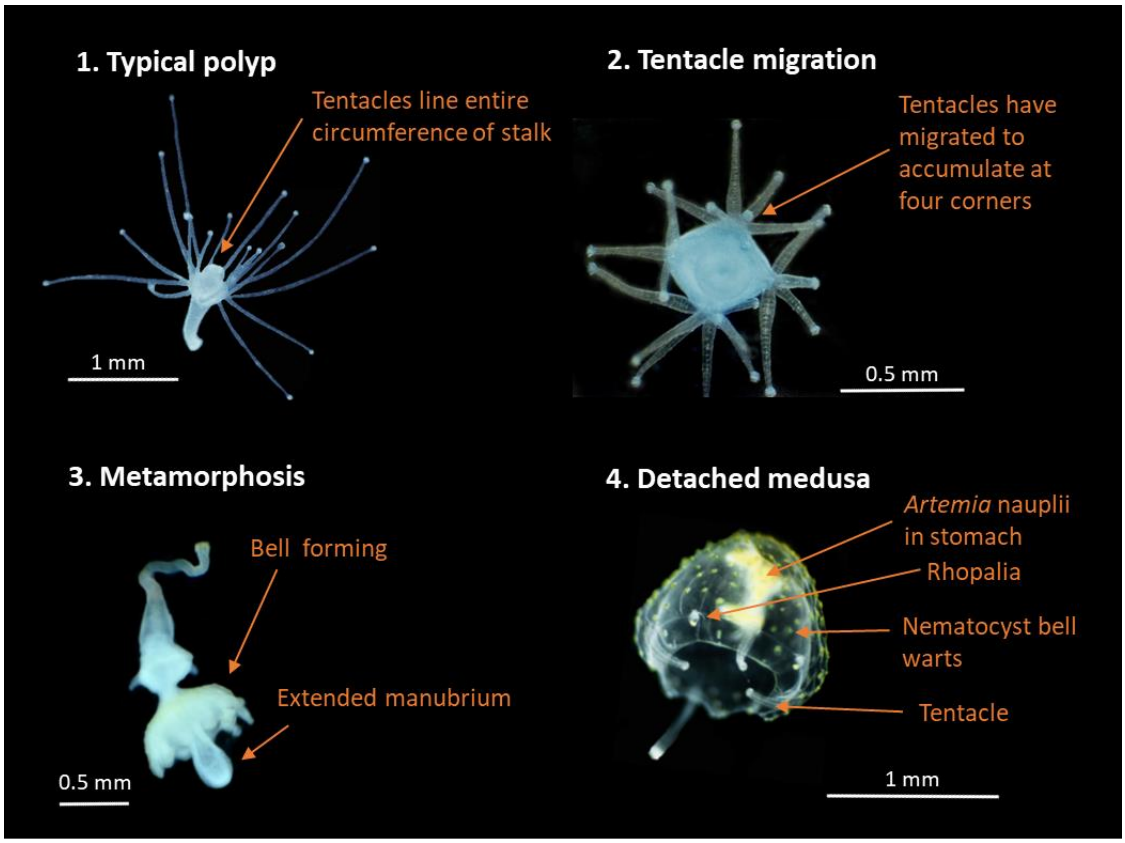

Figure 3.1: Representative stages observed in metamorphosis of *Carukia barnesi* polyps.
1: Typical healthy polyp (side view). 2: Polyp exhibiting the first stage of metamorphosis, tentacle migration (dorsal view). 3: Medusa forming on the end of a polyp during metamorphosis. 4: A medusa detached from polyp following metamorphosis. Note tentacles are not fully formed at this immature stage.

Optimisation trial:

The optimal chemical and concentration was then deduced by choosing the combination that produced the largest percentage of healthy detached medusa, in this case 5-methoxy-2-methylindole at 1 µM. A final trial was then run with this to determine if length of chemical exposure could optimize healthy medusa yield. Three replicates of a minimum of five polyps were used per treatment, in which in 1 µM of 5-methoxy-2-methylindole (in seawater) was added to polyps for 24, 48, 72, 96 and 120 hours, before the solution was changed to fresh seawater. A sea water only control was also run. The total number of healthy detached medusa were recorded each day.

3.3.4 Data analysis

All statistical analysis was conducted in IBM SPSS Statistics Ver28. Graphs were produced in Microsoft Excel 2016 and OriginPro Graphing and Analysis 2021.

Primary trials:

The effect of chemical, concentration and time was analysed using a repeated measures three-way ANOVA for four sets of data gathered during the metamorphosis process: percentage of polyps to display tentacle migration, percentage of polyps to have medusa detach, percentage of polyps to have healthy swimming medusa detach, percentage survival of polyps that did not metamorphose. Percentage data was arcsine square root transformed prior to analysis. Mauchly's Test of Sphericity indicated that the assumption of sphericity had been violated on all four sets of data and therefore, a Greenhouse-Geisser correction was used.

Optimisation trial:

Differences in the mean percentage of healthy medusa produced at different exposure times was analysed using ANOVA. Differences between means were elucidated using a Post hoc Tukey pairwise comparison test (Tukey HSD alpha 0.05).

3.4 Results

3.4.1 Primary trials

Tentacle migration

There was a significant interaction effect of chemical, concentration and time on the mean percentage of polyps displaying tentacle migration (repeated measures three-way ANOVA, $F(59.922,345.152) = 9.431$, $P < 0.001$). The chemicals 5-methoxyindole-2-carboxylic acid and 9-cis-retinoic acid did not induce any tentacle migration regardless of concentration or time of exposure, whereas 5-methoxy-2-methyl-3-indoleacetic acid, 2-methylindole, 5-methoxy-2-methylindole and Lugol's solution all induced tentacle migration at varying levels dependant on concentration and time (fig 3.2). The highest concentrations (5 and 1 µM) of 5-methoxy-2-methyl-3-indoleacetic acid induced the highest levels of migration in less time than medium concentrations (0.5 µM) which induced less migration after a longer time, whilst the lowest concentrations (0.5 µM and control) did not induce any migration regardless of time (fig 3.2). The highest concentrations (5 and 1 µM) of 2-methylindole induces nearly 100% tentacle migration between 3-5 days, however this migration is reversed completely in the highest concentration 5 µM after approx. 10 days, with the 1 µM concentration reverting to ≈40% migration in a similar

time frame. The medium concentration (0.5 µM) begins to induce metamorphosis later at around 9 days, to a much lower percentage, again with the lowest concentrations (0.5 µM and control) never inducing any migration (fig 3.2). 5-methoxy-2-methylindole induced migration at all concentrations, however the higher the quicker migration was induced (fig 3.2). The Lugol's solution however displays no time/concentration relationship, with low amounts of migration induced only at lower concentrations, induced between 6-25 days.

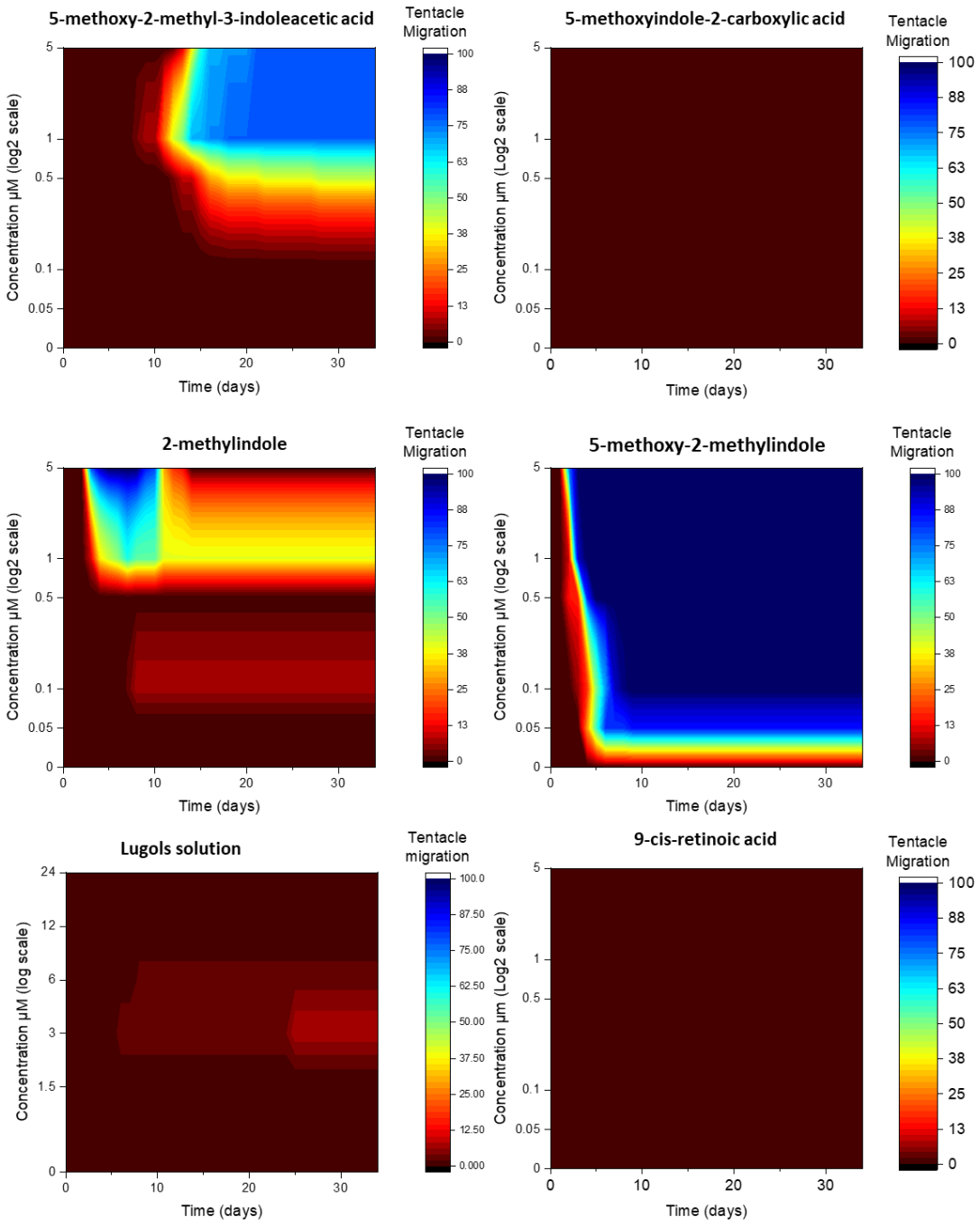

Figure 3.2:The cumulative percentage of *Carukia barnesi* polyps that displayed tentacle migration after exposure to six chemical treatments, over time in response to chemical concentration.

3.4.2 Detached medusa

There was a significant interaction effect of chemical, concentration and time on the mean percentage of polyps that produced detached medusa (repeated measures three-way ANOVA, $F(42.045,242.177) = 10.854$, $P < 0.001$). The chemicals 5-methoxyindole-2-carboxylic acid, 2-methylindole and 9-cis-retinoic acid did not induce any detached medusa regardless of concentration or time of exposure (fig 3.3), despite the fact that 2-methylindole did induce tentacle migration (fig 2.2). Detached medusa were produced in low numbers after exposure to 5-methoxy-2-methyl-3-indoleacetic acid after a long time frame of 20+ days and only at high concentrations, whereas 5-methoxy-2-methylindole produced detached medusas much quicker after only 10+ days with medusa peaking at 1 µM, with fewer to none produced at higher and lower concentrations (fig 3.3). The Lugol's solution displays no time/concentration relationship, with very low amounts of detached medusa induced only at lower concentrations (fig 3.3).

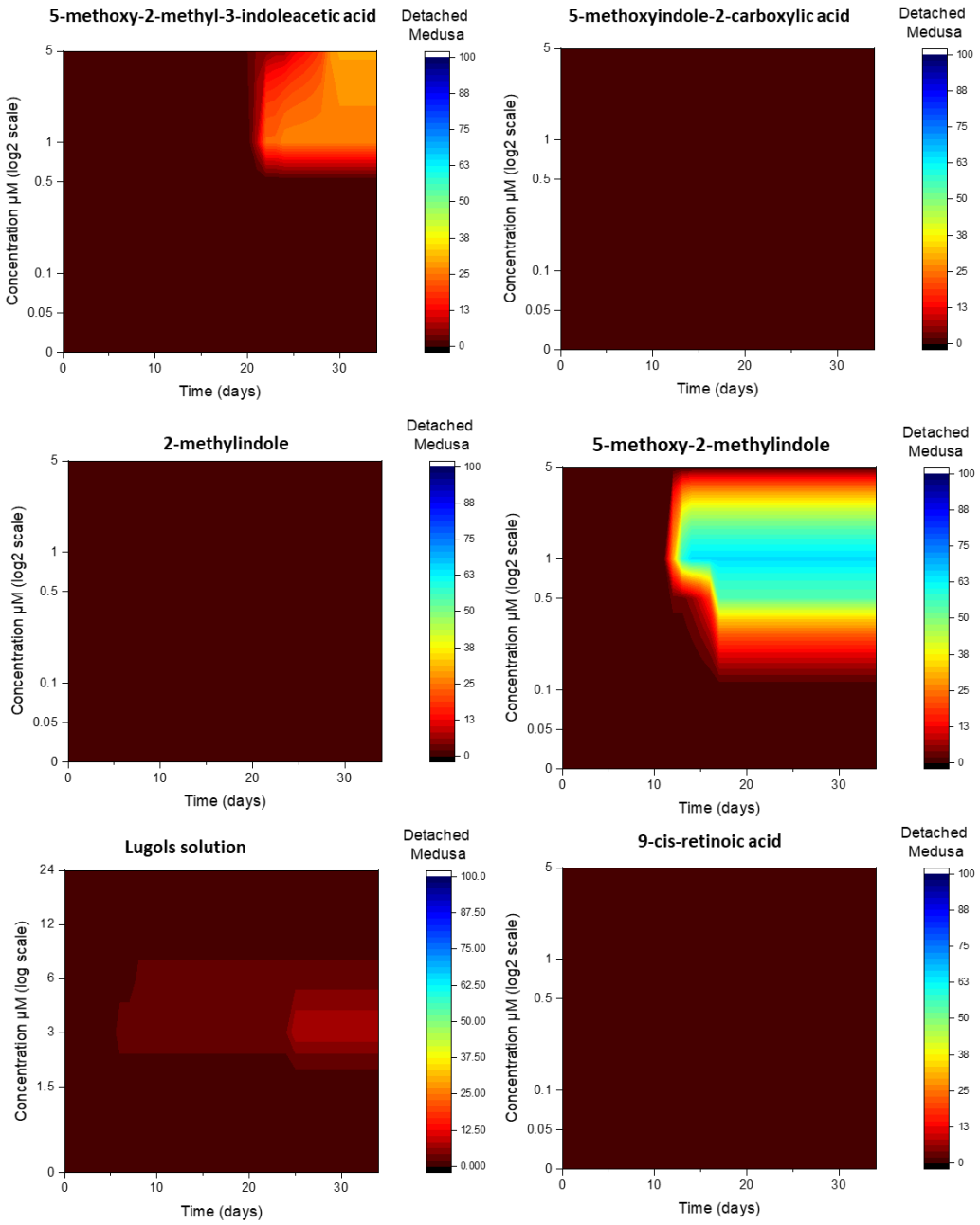

Figure 3.3: The cumulative percentage of detached medusa from *Carukia barnesi* polyps after exposure to six chemical treatments, over time in response to chemical concentration.

3.4.3 Healthy detached medusa

There was a significant interaction effect of chemical, concentration and time on the mean percentage of polyps that produced detached medusa (repeated measures three-way ANOVA, $F(46.944, 270.396) = 3.486$, $P < 0.001$). The chemicals 5-methoxyindole-2-carboxylic acid, 2-methylindole and 9-cis-retinoic acid did not induce any healthy detached medusa regardless of concentration or time of exposure (fig 3.4) which was only to be expected as neither of these produced any detached medusa. Production of healthy detached medusa from 5-methoxy-2-methyl-3-indoleacetic acid was after a long time frame of 20+ days and only at high concentrations (fig 3.4), the same pattern as the production of detached medusa (fig 3.3) except the healthy medusa were at lower quantities (fig 3.4). Again, similar to the production of detached medusa, 5-methoxy-2-methylindole produced healthy detached medusas much quicker after only 10+ days peaking at 1 µM but percentages of healthy medusa were lower than those of just detached medusa (figs 3.3 & 3.4). Lugol's solution produced very low amounts of healthy detached medusa which were induced only at lower concentrations, however unlike all other chemicals, 100% of the detached medusa were also healthy.

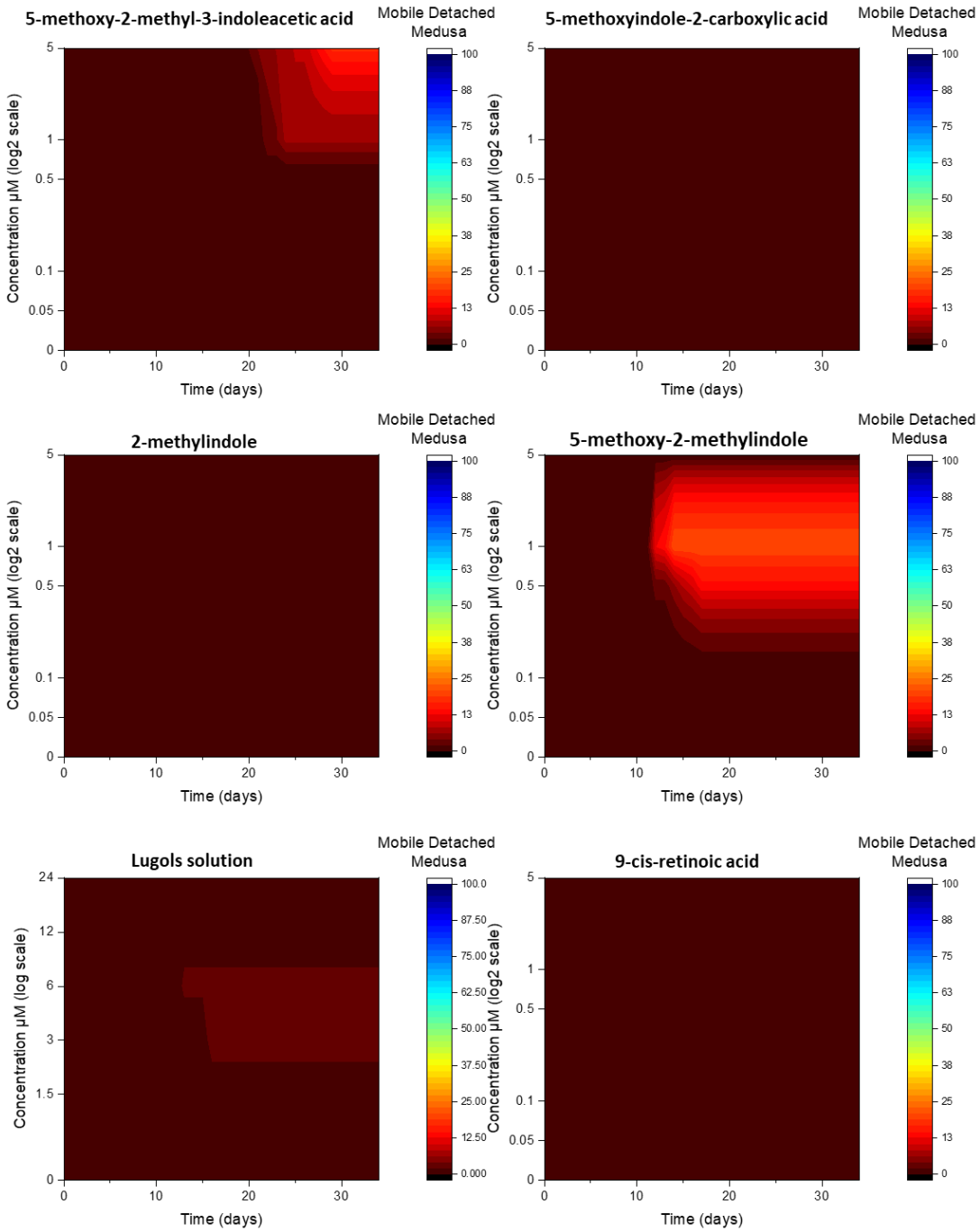

Figure 3.4: The cumulative percentage of *Carukia barnesi* polyps that detached healthy medusa after exposure to six chemical treatments, over time in response to chemical concentration.

3.4.4.Survival of polyps that did not morph

There was a significant interaction effect of chemical, concentration and time on the mean percentage of polyps that produced detached medusa (repeated measures three-way ANOVA, $F(38.857,223.814) = 2.062$, $P < 0.001$). All chemicals caused some polyp mortality, which with the exclusion of 2-methylindole, was concentration dependent. 5-methoxy-2-methyl-indoleacetic acid, Lugol's solution and 9-cis-retinoic acid all had increased polyp mortality at high concentrations typically only towards the end of the 34 day experiment. 5-methoxyindole-2-carboxylic acid also induced mortality towards the end of the experiment time, but had the highest mortality rates at the medium concentration of 0.5 µM (fig 3.5). 2-methyindole was the only chemical to cause a consistent rate polyp mortality (approx. 80% survival) at all concentrations. 5-methoxy-2-methylindole was the only chemical to cause 100% of the polyps that had not morphed to die, a clear concentration/time relationship is evident. The higher the concentration the quicker it causes polyps to die (fig 3.5). Note, low levels of mortality are evident in some of the controls (concentration 0), suggesting there is some low level natural mortality in these experimental conditions.

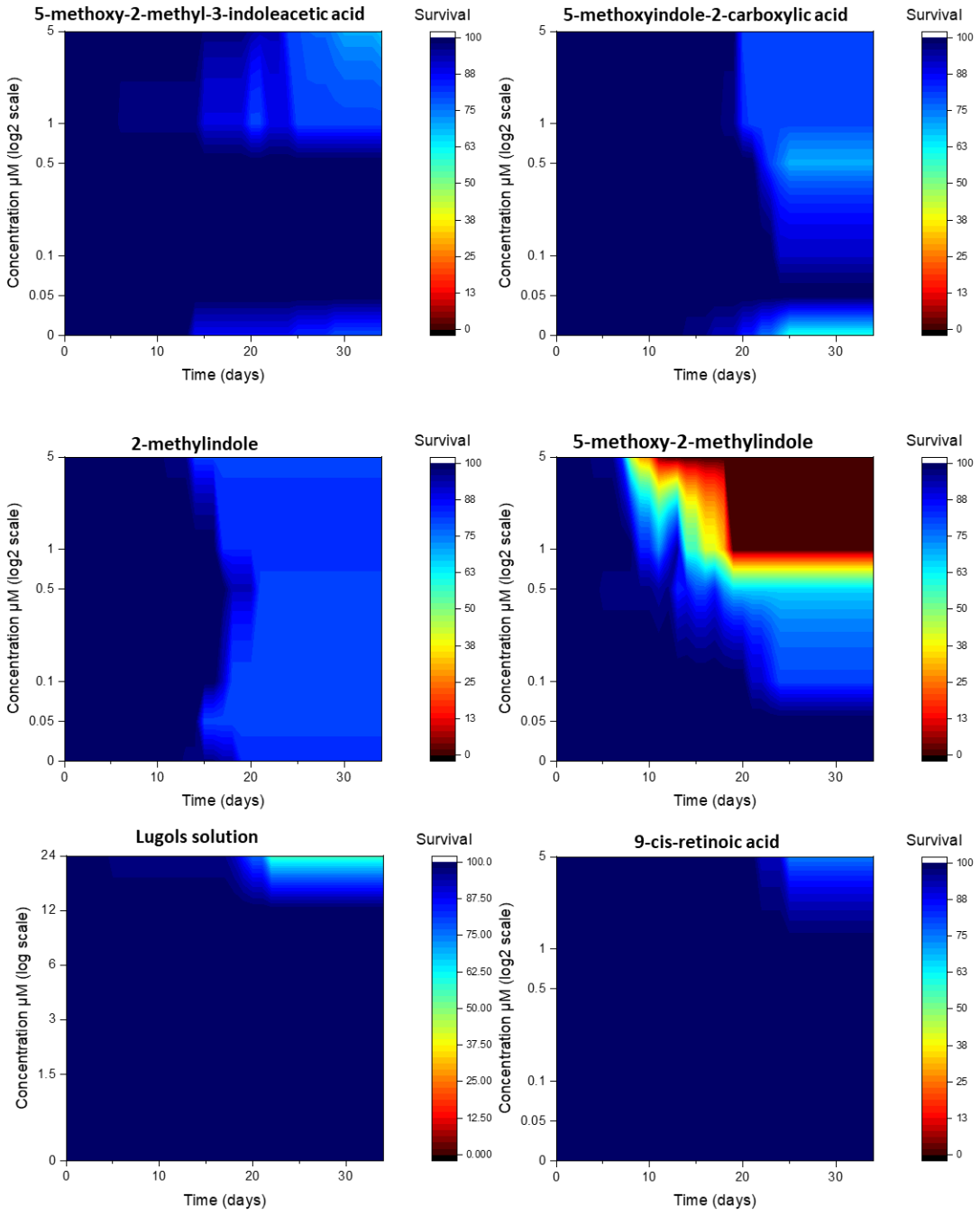

Figure 3.5: The cumulative percentage of *Carukia barnesi* polyps that survived (that did not morph) after exposure to six chemical treatments, over time in response to chemical concentration.

3.4.5 Optimisation trial

5-methoxy-2-methylindole at 1 µM was the peak chemical and concentration deduced from primary trials, resulting in around 20% healthy detached medusa and thus was chosen as the sole chemical for use in the optimisation trial. There was a statistically significant difference in the mean percentage of healthy medusas produced by polyps at different exposure times to 5-methoxy-2-methylindole at 1 µM (ANOVA, $F = 12.631$, $df = 5,12$, $P < 0.05$) (Fig. 3.6A). Post hoc Tukey pairwise comparison ($P = 0.05$) showed that there was no significant difference between 24 hour (mean =91.7 ± 14.4 %) and 48 hour treatments (mean = 87.1 ± 14.5 % S.D). There was no significance difference between 72 hour (mean = 33.3 ± 29.7 % S.D) , 96 hour (mean = 13.3 ± 23 % S.D), 120 hour (mean = 19.2 ± 18.8 % S.D) and control (mean =91.7 ± 14.4 %) treatments.

There was however overall a significant negative effect of exposure time and the percentage of healthy medusa produced. Percentage of healthy medusa detached was highest for 24 and 48 hours, which were both significantly higher than the 72, 96, 120 hour treatments and the control.

The optimisation trial resulted in a peak of 90% healthy detached medusa, when the polyps are exposed to 5-methoxy-2-methylindole at 1 µM for 24 hours, then changed to fresh seawater (Fig 3.6A). Over 21 days of observations post exposure, the 24 and 48 hour treatments produced the largest percentages of healthy detached medusa in the quickest time frames, with the longer the exposure times taking longer to produce less medusa (Fig. 3.6B).

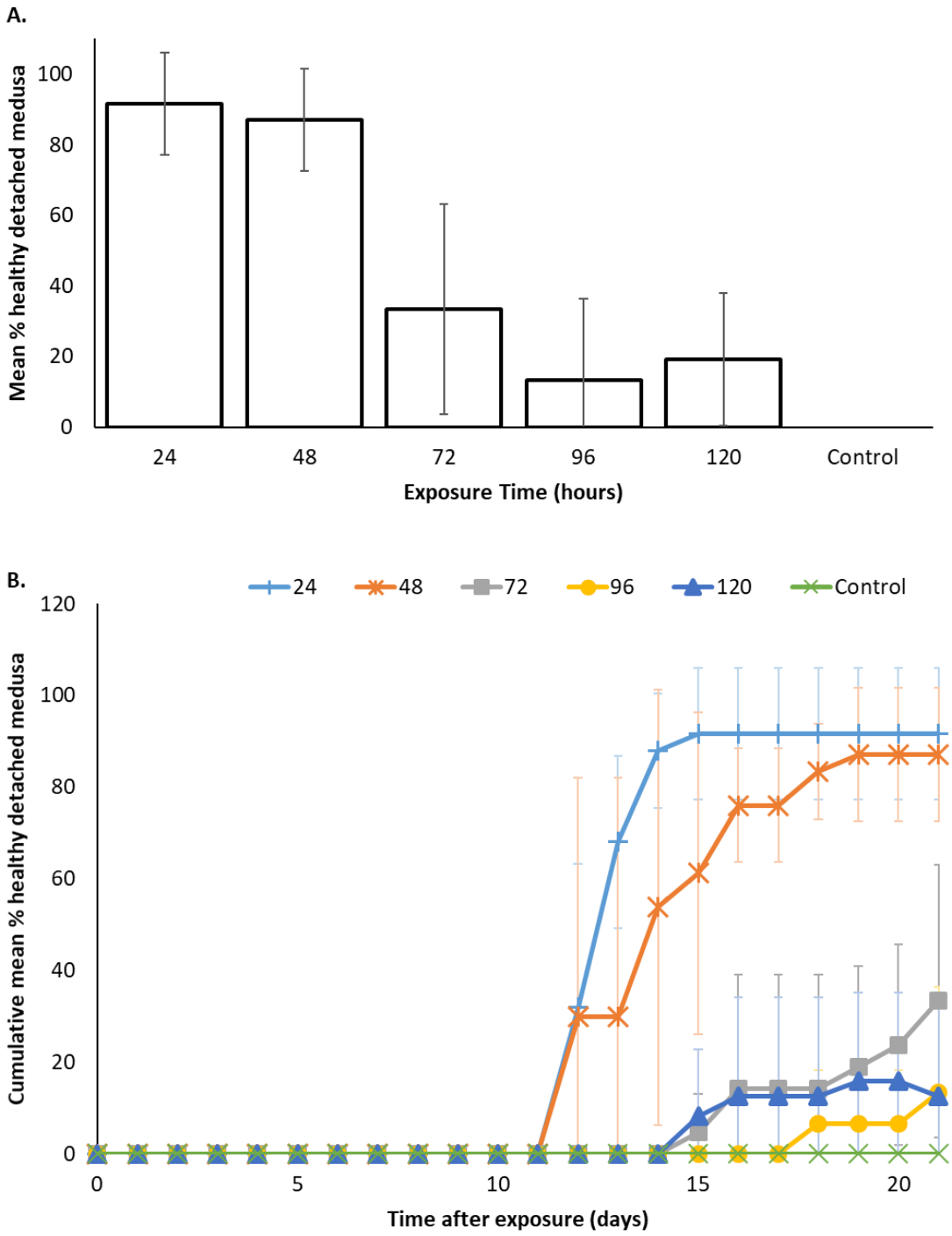

Figure 3.6:Optimisation trial results.

A: Total Mean percentage (± SD error bars) after 21 days of healthy medusas produced by *Carukia barnesi* polyps exposed to 5-methoxy-2-methylindole at 1 µM for different time periods. Exposure time (hours) before solution was changed out to seawater only. Control is seawater only. 6B: Cumulative mean percentage (± SD error bars) of detached healthy medusas over a 21 day period following exposure to 5-methoxy-2-methylindole at 1 µM.

3.5 Discussion

This study aimed to ascertain an efficient method to artificially induce metamorphosis from polyp to medusa in the cubozoan *Carukia barnesi*. The intention was to verify a chemical and concentration combination that had the capacity to produce the highest quantities of healthy medusa, to facilitate a plentiful supply of medusa for venom collection and further research. Indoles have been successfully used to induce metamorphosis in a small number of cubozoan species (Helm & Dunn, 2017; Yamamori et al., 2017); however high concentrations have been reported to cause severe deformities and inconsistent metamorphosis (Helm & Dunn, 2017). As such, we placed an emphasis on quantifying both the total of detached medusas and the further subset of those that were healthy, fully formed and actively mobile, as that was the most useful metric to enable subsequent rearing of the medusae to adults. Both 5-methoxy-2-methyl-3-indoleacetic acid and 5-methoxy-2-methylindole induced medusa formation and detachment, with the amount of healthy medusa produced much lower than the total number detached. Those that were not healthy presented deformities previously noted in the literature (Helm & Dunn, 2017) including shriveled bells and the inability to swim, rendering them unsuitable for further rearing. Lugol's solution was the only chemical in which all medusa that formed and detached were healthy, though induction of metamorphosis was much more inconsistent and at lower quantities than the two successful indoles.

Previous assays of indoles on the cubozoan *Carybdea* sp. documented severe medusa and phenotypic deformities theorised to be toxicity associated when dosed at high concentrations (50 and 20 µM)(Helm & Dunn, 2017). From preliminary trials we deduced that the indole concentrations employed in the literature (Helm & Dunn, 2017; Yamamori et al., 2017) that induce metamorphosis in other cubozoan species were completely unsuitable for our species *Carukia barnesi.* 5-methoxy-2-methylindole caused total mortality of *C. barnesi* polyps within 2-3 days, when added at 50 µM (Helm & Dunn, 2017; Yamamori et al., 2017) and 20 µM(Helm & Dunn, 2017), thus, our experimental range was reduced to 0.05 – 5 µM to negate this toxicity effect. However, we did still note higher mortality rates in higher concentrations. 100% ethanol was used to dissolve the indoles into solution, before being diluted to experimental concentrations with sea water as per the literature; where this seems suitable for other cubozoan species (Helm & Dunn, 2017; Yamamori et al., 2017), our carrier solution (100% ethanol) controls also caused mortality at higher concentrations in preliminary tests – suggesting *C. barnesi* species has high chemical sensitivity in comparison to other species. As such, we reduced the concentration of ethanol to 50% to reduce toxicity of the carrier solution whilst still maintaining its efficiency as a solvent. Some natural variability in survival was evident, as slight mortality was

observed in some controls. This could be natural, or could be a result of experimental caveats such as small water volumes.

Of the six chemicals tested three successfully induced metamorphosis in *C. barnesi* with varying efficacy: 5-methoxy-2-methylindole, 5-methoxy-2-methyl-3-indoleacetic acid and Lugol's solution (from highest to lowest percentage of metamorphosis). With the two indoles, a correlation is evident in that the most successful chemical/concentration combination for metamorphosis also presents the highest levels of polyp mortality (fig. 3.5), suggesting that they may act to induce metamorphosis by stressing polyps and simultaneously are toxic to the polyps. Potentially an extension of this toxicity, it has previously been noted that indoles can inhibit polyp reformation after medusa production(Helm & Dunn, 2017), thus we elected to measure survival of polyps that did not metamorphose. *C. barnesi* does usually leave a polyp remaining after producing a single medusa (Courtney et al., 2016), arguably more similar to monodisc strobilation observed in scyphozoans than the complete metamorphosis of one whole polyp into one single medusa which is described in cubozoans. In a most unusual occurrence, 5-methoxy-2-methylindole not only induced metamorphosis in the adult polyp, but also in any lateral buds growing from the adult polyp. This documents, to our knowledge, the first incidence of a single cubozoan polyp undergoing multiple metamorphoses. This is of course assumed to be a forced measure from artificial stimulation and not propounded to be an *in situ* characteristic of this species.

The chemicals explored in this work were intended to be used as a tool to induce metamorphosis and do not illustrate natural triggers. Some *Aurelia* jellyfish upregulate a specific peptide during strobilation, which contains indole rings of two tryptophans (Fuchs et al., 2014), thus indoles are theorised to essentially shortcut the natural environmental trigger and act internally by replicating a key part of this peptide to artificially induce metamorphosis in other species. Indoleamines have also been linked to endocrine-like signalling and metamorphosis in Cnidarians (Tarrant, 2005). Of specific interest, when added exogenously the indoleamine melatonin (a derivative of tryptophan) can initiate expansion of the oral disk and protrusion of the actinopharynx in sea anemones (Tarrant, 2005; Tsang et al., 1997), similar to our observation with *C. barnesi* medusa production, in which one of the first changes (subsequent to tentacle migration) was protrusion of the mouth (Fig. 3.1). Iodine has long been known to induce strobilation in *Aurelia* jellyfish (Spangenberg, 1967), with Berking et al.(Berking et al., 2005) succinctly linking previous works by Paspalev (Paspaleff, 1938) and Riley and Chester(Riley & Chester, 1971) to highlight that in sea water containing below average trace amounts of iodine *Aurelia* strobilation is inhibited, suggesting it plays a key role in strobilation. Whilst the iodine and

indoles may initially appear to act on polyps in very different ways, there is some crossover in their activity which may speculatively rationalize the capability of two very different chemicals to induce metamorphosis. Iodine induces metamorphosis in *Aurelia aurita* (scyphozoa, Cnidaria) by functioning as an oxidative defence system, in which iodine initially reacts with tyrosine, which subsequently reduces tyrosine levels (Berking et al., 2005). Indoleamines such as L-Tryptophan, L-5-hydroxytryptophan and serotonin have been shown to increase tyrosine aminotransferase activity in mice (Deguchi & Barchas, 1971), and whilst tyrosine aminotransferase is usually found in the liver, genes encoding for this have been found in *Aiptasia* (Anthozoa, Cnidaria)(Lenhert, 2013). Tyrosine aminotransferase is an enzyme which catalyses tyrosine to 4-hydroxyphenylpyruvate, thus tyrosine levels would drop as the indoleamines increase enzyme activity. Serotonin (an indoleamine) has further been demonstrated to influence metamorphosis in other cnidarian species (McCauley, 1997). Thus, we suggest that there is a theoretical mechanism of action in which both indoles and iodine induce metamorphosis in cnidarian polyps by altering levels of tyrosine.

Using the peak chemical and concentration from the primary (trials 5-methoxy-2-methylindole at 1 µM), we ran a final optimisation trial to deduce if we could reduce the toxicity effect by decreasing the length of exposure time and potentially increase healthy medusa yield. Length of exposure had a significant effect on the quantity of healthy medusa produced by *C. barnesi* polyps, with results peaking at a mean of 90% healthy medusa production when the indole solution was exchanged for seawater after 24 hours. Healthy medusa production decreased the longer the polyps were exposed to the solution, with longest exposure levels (96 and 120 hours) producing quantities of medusa in line with the quantities seen in the preliminary trials for 5-methoxy-2-methylindole at 1 µM, in which the polyps were exposed to the indole solution for the entire experimental period. For the optimization trials, healthy detached medusa was the only metric collected and analysed, as it is the most valuable measure for the experimental aim. Polyp survival was not measured because as previously noted, we observed the indoles inhibited polyp reformation in line with the observations of Helm & Dunn (Helm & Dunn, 2017).

The significant increase in healthy medusa production at 24 and 48 hours of exposure alludes to the idea that too much chemical is overwhelming the polyp. In line with the toxicity noted with increased concentration in the preliminary trial, the longer exposure times in the optimization trials saw the polyps take longer to produce less medusa (Fig. 3.6B). In this artificial set up, the levels of indole in the polyp are being increased exogenously, whereas naturally it is an internally regulated event. From our results, the prime exposure time is 48 hours or less, suggesting the internal mechanism that initiates metamorphosis is naturally only switched on for a very short

amount of time, as we see longer exposure times or greater concentration is detrimental to the medusae wellbeing. In the wider search for the natural environmental cue, it would then seem prudent to investigate short term events that occur during the stinger season such as marine spawning events, photoperiod and/or wet season pulses such as monsoonal downpours, all of which could physically influence the chemical biology of these polyps.

The implications of this work will enable mass production of *C. barnesi* medusa, which will facilitate a supply of medusae and therefore venom, as and when necessary. For the first time, venom analysis of this newly detached medusa (<1mm) may be conducted to elucidate ontogenetic differences, as presently all venom research in this species has been conducted on the larger adult or sub-adult medusas (>8mm). Up until now, medusa collection was restricted to labour intensive and expensive field sampling, confined to the stinger season (November – May) which is also accompanied by the bad weather and poor field conditions of the monsoon season. The loss of polyps due to the indoles propensity to inhibit polyp reformation is negligible, as polyp cultures exponentially asexually reproduce, populations should be easily replaced. We have determined an optimum method for inducing metamorphosis in the Irukandji jellyfish *Carukia barnesi,* resulting in a 90% metamorphosis rate to healthy medusa by exposing the polyps to 1 µM of 5-methoxy-2-methylindole for 24 hours. These medusa are fit enough to be further reared in aquaria and we hope this increased supply can further research into the venomous nature of this animal.

3.6 References

Barnes, J. H. (1964). Cause and Effect in Irukandji Stingings. *The Medical Journal of Australia*, *1*(24), 897–904. https://doi.org/10.5694/j.1326-5377.1964.tb114424.x

Berking, S., Czech, N., Gerharz, M., Herrmann, K., Hoffmann, U., Raifer, H., Sekul, G., Siefker, B., Sommerei, A., & Vedder, F. (2005). A newly discovered oxidant defence system and its involvement in the development of Aurelia aurita (Scyphozoa, Cnidaria): Reactive oxygen species and elemental iodine control medusa formation. *International Journal of Developmental Biology*, *49*(8), 969–976. https://doi.org/10.1387/ijdb.052024sb

Courtney, R., Browning, S., & Seymour, J. (2016). Early life history of the "irukandji" jellyfish *Carukia barnesi*. *PLoS ONE*, *11*(3). https://doi.org/10.1371/journal.pone.0151197

Crew, B. (2013). *The Smallest and Deadliest Kingslayer in the World - Scientific American Blog Network*. https://blogs.scientificamerican.com/running-ponies/the-smallest-and-deadliest-kingslayer-in-the-world/

Deguchi, T., & Barchas, J. (1971). Induction of hepatic tyrosine aminotransferase by indole amines. *Journal of Biological Chemistry*, *246*(23), 7217–7222. https://doi.org/10.1016/s0021-9258(19)45875-4

Fenner, P., & Hadok, J. (2002). Fatal envenomation by jellyfish causing Irukandji syndrome. *Medical Journal of Australia*, *177*(7), 362–363.

Fuchs, B., Wang, W., Graspeuntner, S., Li, Y., Insua, S., Herbst, E. M., Dirksen, P., Böhm, A. M., Hemmrich, G., Sommer, F., Domazet-Lošo, T., Klostermeier, U. C., Anton-Erxleben, F., Rosenstiel, P., Bosch, T. C. G., & Khalturin, K. (2014). Regulation of polyp-to-jellyfish transition in Aurelia aurita. *Current Biology*, *24*(3), 263–273. https://doi.org/10.1016/j.cub.2013.12.003

Green, T. J., Wolfenden, D. C. C., & Sneddon, L. U. (2018). An investigation on the impact of substrate type, temperature, and iodine on moon jellyfish production. *Zoo Biology*, *37*(6), 434–439. https://doi.org/10.1002/zoo.21454

Helm, R. R., & Dunn, C. W. (2017). Indoles induce metamorphosis in a broad diversity of jellyfish, but not in a crown jelly (Coronatae). *PLoS ONE*, *12*(12), 1–13. https://doi.org/10.1371/journal.pone.0188601

Holstein, T. W., & Laudet, V. (2014). Life-History Evolution: At the Origins of Metamorphosis. *Current Biology*, *24*(4), R159–R161. https://doi.org/10.1016/J.CUB.2014.01.003

Kostrouch, Z., Kostrouchova, M., Love, W., Jannini, E., Piatigorsky, J., & Rall, J. E. (1998). Retinoic acid X receptor in the diploblast, Tripedalia cystophora. *Proceedings of the National Academy of Sciences of the United States of America*, *95*(23), 13442–13447. https://doi.org/10.1073/pnas.95.23.13442

Lenhert, E. M. (2013). *Developing the anemone aiptasia as a tractable model for cnidarian-dinoflagellate symbiosis: generating transcriptomic resources and profiling gene expression* (Issue August) [STANFORD UNIVERSITY]. https://stacks.stanford.edu/file/druid:bv901hc0997/MasterThesis-augmented.pdf

McCauley, D. W. (1997). Serotonin plays an early role in the metamorphosis of the hydrozoan Phialidium gregarium. *Developmental Biology*, *190*, 229–240. https://doi.org/10.1006/dbio.1997.8698

Muller, W. A. (1984). Retinoids and pattern formation in a hydroid. *Journal of Embryology and Experimental Morphology*, *81*, 253–271.

Paspaleff, B. W. (1938). Über die Entwicklung von Rhizostoma pulmo Agass. *Varna, Arb. Biol. Meeresst*, *7*, 1–17.

Pereira, P., Barry, J., Corkeron, M., Keir, P., Little, M., & Seymour, J. (2010). Intracerebral hemorrhage and death after envenoming by the jellyfish *Carukia barnesi*. *Clinical Toxicology*, *48*, 390–392. https://doi.org/10.3109/15563651003662675

Pereira, P., & Seymour, J. E. (2013). In vitro effects on human heart and skeletal cells of the venom from two cubozoans, Chironex fleckeri and Carukia barnesi. *Toxicon*, *76*, 310–315. https://doi.org/10.1016/j.toxicon.2013.10.023

Ramasamy, S., Isbister, G. K., Seymour, J. E., & Hodgson, W. C. (2005). The in vivo cardiovascular effects of the Irukandji jellyfish (Carukia barnesi) nematocyst venom and a tentacle extract in rats. *Toxicology Letters*, *155*(1), 135–141. https://doi.org/10.1016/j.toxlet.2004.09.004

Riley, J. P., & Chester, R. (1971). *Introduction to marine chemistry*. Academic Press New York.

Seymour, J., Saggiomo, S., Lam, W., Pereira, P., & Little, M. (2020). Non-invasive assessment of the cardiac effects of Chironex fleckeri and Carukia barnesi venoms in mice, using pulse wave doppler. *Toxicon*, *185*(April), 15–25. https://doi.org/10.1016/j.toxicon.2020.06.018

Southcott, R. V. (1967). Revision of some Carybdeidae (scyphozoa: cubomedusae), including a description of the jellyfish responsible for the “irukandji syndrome.” *Australian Journal Of Zoology*, *15*, 651–671. https://www.mendeley.com/viewer/?fileId=2fa0eb3f-b65a-d78b-

0aab-8d1da93fdb17&documentId=f0d95e7c-a226-37e1-ba96-636d97beaa71

Spangenberg, D. B. (1967). Iodine induction of metamorphosis in Aurelia. *Journal of Experimental Zoology*, *165*(3), 441–449. https://doi.org/10.1002/jez.1401650312

Tarrant, A. M. (2005). Endocrine-like Signaling in Cnidarians : Current Understanding and Implications. *Hormones*, *45*(1), 201–214.

Toshino, S., Miyake, H., Ohtsuka, S., Adachi, A., Kondo, Y., Okada, S., Hirabayashi, T., & Hiratsuka, T. (2015). Monodisc strobilation in Japanese giant box jellyfish Morbakka virulenta (Kishinouye, 1910): a strong implication of phylogenetic similarity between Cubozoa and Scyphozoa. *Evolution & Development*, *17*(4), 231–239. https://doi.org/10.1111/EDE.12127

Tsang, W., McGAUGHEY, N., Wong, Y., & Wong, J. (1997). Melatonin and 5-Methoxytryptamine Induced Muscular Contraction in Sea Anemones. *THE JOURNAL OF EXPERIMENTAL ZOOLOGY*, *279*(3), 201–207. https://doi.org/10.1002/(SICI)1097-010X(19971015)279:3

Underwood, A. H., & Seymour, J. E. (2007). Venom ontogeny, diet and morphology in *Carukia barnesi*, a species of Australian box jellyfish that causes Irukandji syndrome. *Toxicon*, *49*(8), 1073–1082. https://doi.org/10.1016/j.toxicon.2007.01.014

Wiltshire, C. J., Sutherland, S. K., Fenner, P. J., & Young, A. R. (2000). Optimization and preliminary characterization of venom isolated from 3 medically important jellyfish: The box (Chironex fleckeri), irukandji (Carukia barnesi), and blubber (Catostylus mosaicus) jellyfish. *Wilderness and Environmental Medicine*, *11*(4), 241–250. https://doi.org/10.1580/1080-6032(2000)011[0241:OAPCOV]2.3.CO;2

Winkel, K. D., Tibballs, J., Molenaar, P., Lambert, G., Coles, P., Ross-Smith, M., Wiltshire, C., Fenner, P. J., Gershwin, L. A., Hawdon, G. M., Wright, C. E., & Angus, J. A. (2005). Cardiovascular actions of the venom from the Irukandji (*Carukia barnesi*) jellyfish: Effects in human, rat and guinea-pig tissues in vitro and in pigs in vivo. *Clinical and Experimental Pharmacology and Physiology*, *32*(9), 777–788. https://doi.org/10.1111/j.1440-1681.2005.04258.x

Yamamori, L., Okuizumi, K., Sato, C., Ikeda, S., & Toyohara, H. (2017). Comparison of the Inducing Effect of Indole Compounds on Medusa Formation in Different Classes of Medusozoa. *Zoological Science*, *34*(3), 173–178. https://doi.org/10.2108/zs160161

Chapter 4 . The Influence of Light Wavelength on the Feeding Ecology and Behaviour of the Irukandji Jellyfish *Carukia Barnesi*

4.1 Abstract

Light has previously been shown to directly influence the feeding ecology of some cnidarians by controlling nematocyst discharge and some cubozoans display marked behavioural reactions to individual light colours. The intention of this study was to determine if light has any effect on the feeding behaviour and frequency of the highly venomous cubozoan *Carukia barnesi*, with the ultimate goal being to induce feeding in newly detached medusa as this a species currently unable to be reared in aquaria due to feeding difficulties. Here we exposed *C. barnesi* medusa to a range of coloured light regimes and monitored pulse rate and feeding responses. Overall, we found *C. barnesi* displayed higher feeding frequencies in the light compared to in the dark, but frequency varied greatly between individual light colours. In contrast to previous studies with adult *C. barnesi* medusa, the newly detached medusa showed highest pulse rates in darkness, and slowed down in the lights, which again varied greatly between individual light colours. No correlation between pulse rate and feeding frequency was observed. We also discuss the unexpected possibility that *C. barnesi*, unlike most cubozoans, may be able to perceive UV light and a further may perceive multiple colours.

4.2 Introduction

Carukia barnesi is a small species of cubozoan (box jellyfish), whose sting can induce Irukandji syndrome in human victims (Barnes, 1964). The syndrome presents as an extremely painful range of symptoms including severe back ache and vomiting (Barnes, 1964), an impending sense of doom, and in rare instances intracerebral haemorrhages resulting in death (Pereira et al., 2010). Due to the severity of this animal's sting, research is often focussed on its venom and potential medical implications. *Carukia barnesi* is classed as a logistically difficult species (Rowley, 2021); the animal's small size and elusive nature make field collection difficult and research into this animal's ecology is therefore challenging.

However, insights into its prey capture ecology have been documented by Courtney et al. 2015, who showed that adult *C. barnesi* medusa exhibit a condition-specific behavioural response, which is mediated by the diurnal light-dark cycle. The medusa extend their tentacles during light conditions and actively attract prey by twitching there tentacular bands as lures for larval fish, a fishing behaviour not observed during dark conditions. This suggests that adult medusa of *C. barnesi* are not opportunistically grazing in the water column, but are instead actively fishing for prey – a behaviour mediated by environmental light conditions. Consistent with most box jellyfish, *C. barnesi* possesses highly sophisticated vision, with each medusa containing four sets of rhopalia, within each are two compound eyes, two cup-shaped ocelli and two slit-shaped ocelli, totalling 24 eyes per medusa (Seymour & O'Hara, 2020). When exposed to direct sunlight, the pupils of *C. barnesi* have been shown to contract more rapidly that other cubozoan eyes (Seymour & O'Hara, 2020), which is consistent with the concept of *C. barnesi* being a light driven predator, as proposed by (Courtney et al., 2015).

Light has also been shown to play a key role in prey capture within the anthozoan *Haliplanella luciae* and the hydrozoan *Hydra magnipapillata*, by regulating the discharge of the venom injection organelles – the nematocysts (Jindrich, 2012; Plachetzki et al., 2012). Jindrich 2012 postulated that it is likely that light modulates nematocyst discharge for all classes of Cnidaria. It has also been speculated it might be possible that box jellyfish extract colour information from their surroundings (O'Connor et al., 2010). In most cases, light has been analysed as present/absent or shades in between, such as bright/dim, although the effects of individual colour spectra have been specifically analysed on one species of cubozoan, *Chironex fleckeri* (Gershwin & Dawes, 2008). The animals were shown to exhibit positive phototaxis to all colours presented, although the authors noted a possible feeding behaviour only displayed during blue light exposure.

To date, adult specimens have been the focus of all aforementioned light research. Recent findings into the metamorphosis triggers for *C. barnesi* (O'Hara & Seymour, 2022) now allow us to produce newly detached medusa in large numbers within aquaria. However, one consistent obstacle in rearing these medusa in aquaria is feeding – they will not readily or regularly ingest food for prolonged periods of time, so cannot be sustained beyond a few weeks. To better understand the role of light in the prey capture ecology of this jellyfish, with the intention of applying this to promoting feeding in the newly detached medusa of this species, the current study explores the influence of differing light spectra. Here we expose the animals to a multitude of light colours to analyse both behavioural and feeding responses.

4.3 Methods

4.3.1 Experimental set up

Jellyfish medusa were housed in 25 L ©Exotic Aquaculture Ephyrae Holding Aquariums, constructed from transparent material allowing full light penetration, for the duration of the light trials. Three aquariums were run simultaneously as three experimental replicates, each connected to an air supply creating a laminar circular water current, which prevented medusa from becoming stuck to the tank walls. Air supply and current flow was standardized across all replicates. Each aquarium was fitted with a transparent lid, on which two light sources were mounted: an AquaIllumination LED Hydra aquarium light for visible and UV light and an InfraRed light to enable video capture in the dark. The set up is detailed in fig 4-1. Water and aquaria were maintained at constant room temperature for the duration of the experiments.

For feeding experiments, nauplii of *Artemia sp.* were added to the aquarium water prior to medusa in a standardised concentration of two nauplii per ml of water. *Artemia sp.* were fully changed out and replaced with newly hatched nauplii every 3 hours to prevent moulting to next life stage.

4.3.2 Jellyfish medusa

Carukia barnesi polyps in culture at James Cook University, Cairns (Courtney et al., 2016), were induced to metamorphose into medusa using 5-methoxy-2-methylindole as per O'Hara & Seymour, (2022). The age of all medusa used in this study was standardised to three days old, defined as three days post medusa detachment. At this age the jellyfish were physically capable of capturing and consuming prey *Artemia sp*. and possess rhopalia containing at least four developed eyes (fig 4-2).

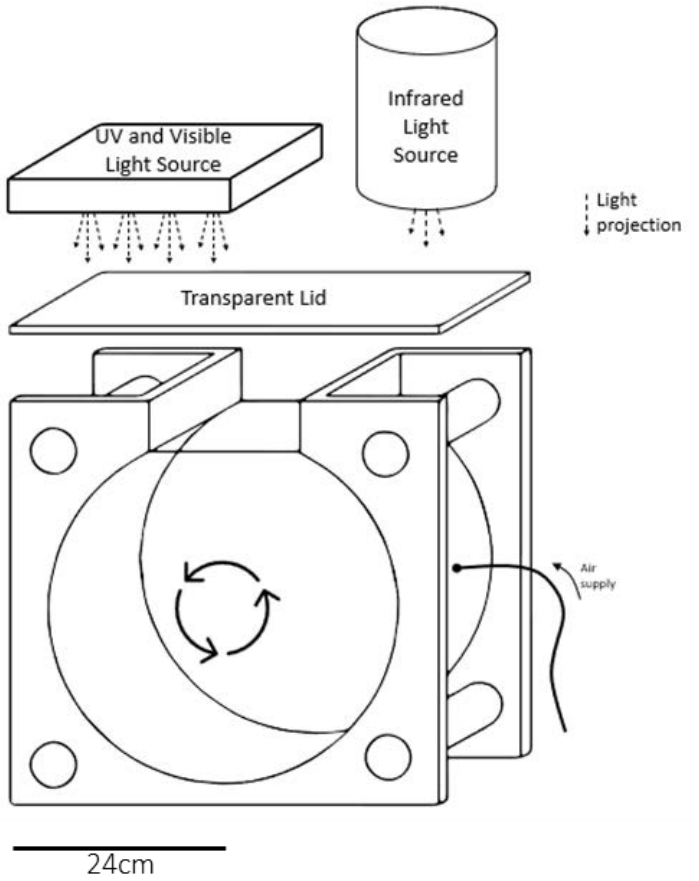

Figure 4.1: Exploded view drawing of experimental set up. Showing one out of three replicate tanks. Scale bar is approximate.

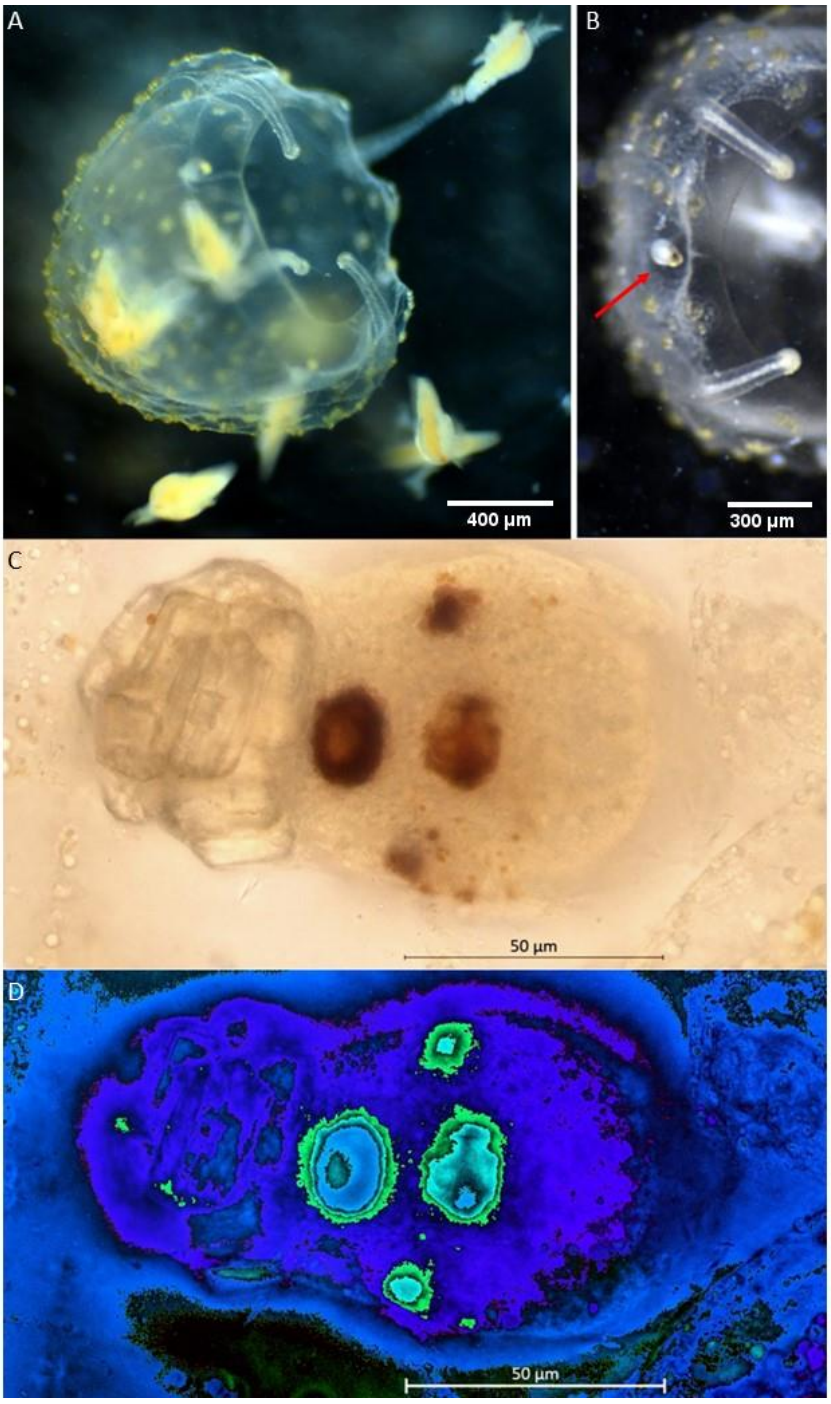

Figure 4.2: A three day old *C. barnesi* medusa, with a single Artemia sp. captured on one extended tentacle, multiple Artemia sp. are also visible ingested within the stomach and manubrium. B: Rhopalium (red arrow) situated between two tentacles, not surrounded by a rhopalial niche at this age as in the adults, but here protrudes out from the bell tissue. C/D: A focus stacked light microscopy image of a rhopalium. Four out of the six eyes present in adulthood are developed at this age. Two large lens eyes visible in the centre, with two smaller eyes (most likely slit eyes) present on the periphery. C: Crystals of the developing statolith are also visible. D: Image filtered through a colour look up table better highlights the structure of the lens eyes in the centre.

4.3.3 Experimental design

Medusa were exposed to ten combinations of light in total:

1) Dark → UV
2) Dark → Red
3) Dark → Blue
4) Dark → White
5) Dark → UV → Red
6) Dark → UV → Blue
7) Dark → Red → Blue
8) Dark → Red → UV
9) Dark → Blue → Red
10) Dark → Blue → UV

Approximate wavelengths for the LEDs used were: UV:380-420nm; Blue: 430-520nm; Red:625-780nm; White:430-700nm.

For every light combination 30 medusa were added to each of three aquariums (fig 4-1) running simultaneously, with new medusa used for each new light combination. Every light combination began with the medusa present in a dark control period. Medusa were exposed to each dark/light colour in the combination for a total of 15 minutes, the first five minutes of each was a designated adjustment period for the animals where no filming/data collection took place. Following this, the medusa were filmed using a camera capable of recording in both visible and InfraRed light, for a further ten minutes in each of the dark and/or colour exposures.

4.3.4 Pulse rate

Thirty medusa were added at the start of each light combination. No *Artemia sp.* were present in the water used in the pulse rate experiments. Data was collected in post by analysing the video footage. Within the 10 minutes of filming per light, ten medusa were picked at random and the pulse rate (the continuous pulse visible by the relaxing and contracting of the medusa's bell) was counted for each over a period of 30 seconds. Data were recorded and analysed as pulse rate per 30 seconds.

4.3.5 Feeding

Thirty medusa were added to tanks containing *Artemia sp*. at the start of each light combination. At the end of each individual light treatment ten medusa were removed from each tank and fixed in 4% formaldehyde. Light experiments then continued with the remaining number of medusa.

Data were collected in post by counting how many fixed medusa had captured artemia present in their gastrovascular cavity. Data were recorded as percentage of medusa with prey.

4.3.6 Light intensity

The Hydra AI light settings were set to 90% for each available colour setting. Light intensity was measured for each light colour using solarmeters (320-400nm mW/cm^2 and 400-1100nm W/m^2) and did not show any correlation to observed pulse rate or prey ingestion patterns.

4.3.7 Statistical analysis

All data were calculated as the difference between the dark treatment and the light colour, so we could analyse the effect of changing from a dark control period to a light colour. For the two-light combination experiments, we needed to prevent second light data from skewing results of the final light, i.e. if animals ingested prey in the first light colour but not the second, to prevent a false positive result for the second light, we calculated the data as ((2^{nd} light colour – 1^{st} light colour) – dark). All data analysis was conducted in IMB SPSS Statistics version 28.0.0.0(142) using normality tests (Shapiro-Wilk, P= 0.05), 1-sample T-tests (2-sided P= 0.05) and 1-way-ANOVA (P= 0.05) with *Post hoc* Tukey pairwise comparisons (P =0.05).

4.4 Results

4.4.1 Pulse rate/feeding

No relationship between feeding (*Artemia sp*. ingestion) and pulse rate was observed (fig 4.3), suggesting the two responses are completely decoupled.

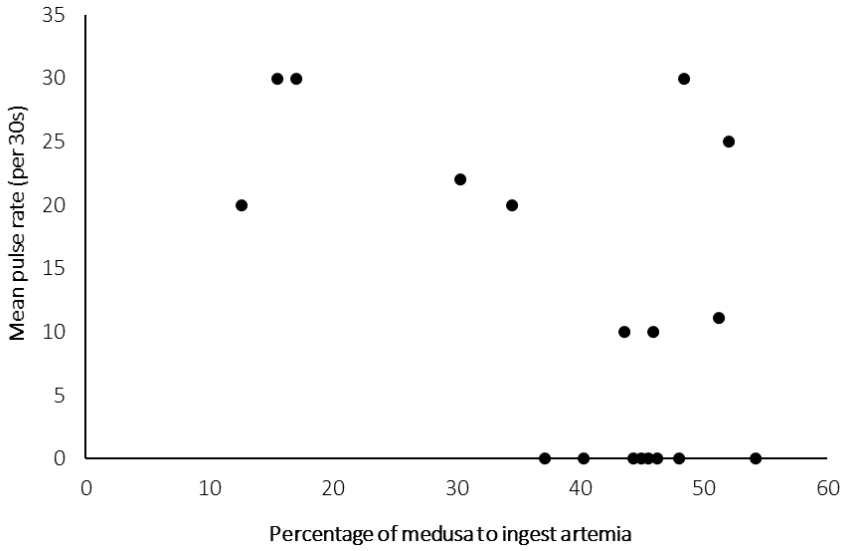

Figure 4.3: Scatter plot showing a non-linear relationship (no relationship) between mean pulse rate and the *Artemia* sp ingestion in newly detached Carukia barnesi medusa. Date for each point gathered from an individual tank replicate (fig 4.1) of ten medusa in an individual light treatment. Data shown is pooled from dark, UV, red and blue colour exposures.

4.4.2 Pulse rate response to light

Individual lights:

All data conformed to a normal distribution (Shapiro-Wilk, $P > 0.05$). The mean difference in pulse rate for each light exposure compared to dark (dark calculated as 0) was statistically significant (1-sample T-tests, 2-sided $P=0.05$) in UV ($t(2) = -16.025$, $P = 0.004$) and white light ($t(2) = -17.543$, $P = 0.003$) but not in blue ($t(2) = -3.8$, $P = 0.062$) or red ($t(2) = 0.294$, $P = 0.797$.)(fig.4.4). This indicates that in all light except red, jellyfish pulse rate slowed down significantly compared to in the dark. There was also a statistically significant difference between lights (1-way-ANOVA, $F = 38.119$, df $= 3$, $P < 0.01$), indicating that pulse rate is influenced and is different in the individual light colours. *Post hoc* Tukey pairwise comparison ($P = 0.05$) results are displayed in Fig.4.4, where all light colours are significantly different from each other, with the exception of blue and white light, which show no significant difference.

Two-light combinations:

All data conformed to a normal distribution (Shapiro-Wilk, $P > 0.05$). The mean difference in pulse rate for each light exposure combination compared to dark (dark calculated as 0) was statistically significant (1-sample T-tests, 2-sided *P=0.05*) for all colour combinations blue→red ($t(2) = -15.594$, *P =0.004*), blue→UV ($t(2) = -86.058$, *P =<0.001*), red→blue ($t(2) = -80.484$, *P =<0.001*), red→UV ($t(2) = -28.424$, *P =0.001*), UV→blue ($t(2) = -7.698$, *P =0.016*) except UV→red ($t(2) = -1.326$, *P =0.316*)(Fig 4.5). This indicates that in all light combinations except UV→red, jellyfish pulse rate slowed down significantly compared to in the dark. There was also a statistically significant difference between lights combinations (1-way-ANOVA, $F = 110.173$, df $= 3$, $P < 0.01$), indicating that pulse rate changes speed based on the light combination the jellyfish are exposed to. *Post hoc* Tukey pairwise comparison ($P = 0.05$) results are displayed in Fig 4-4, where all light colour combinations are significantly different from each other, with the exception of blue→red^{c} and UV→blue^{c}, and blue→ UV^{b} and red →blue^{b}, which show no significant difference to each other.

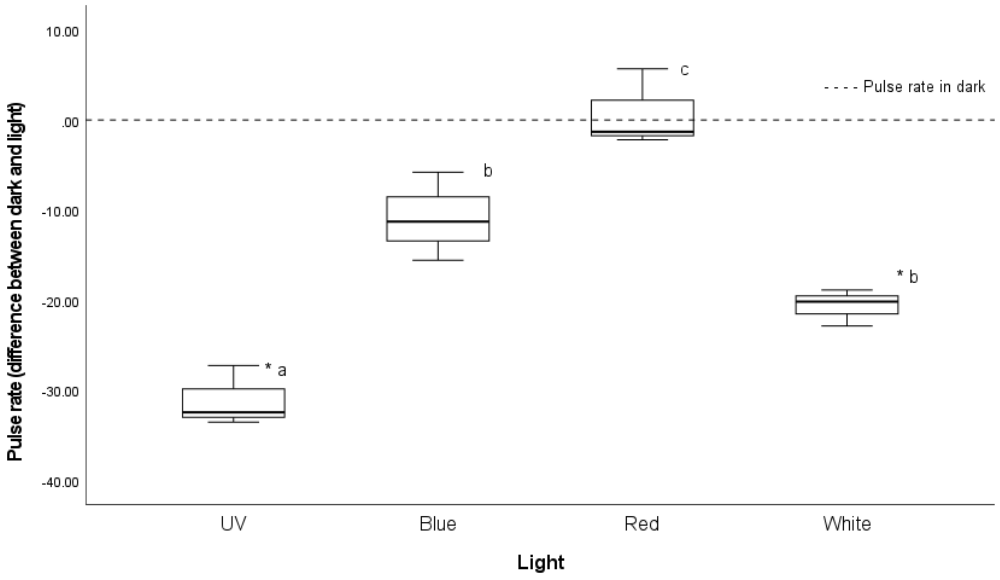

Figure 4.4: Difference in *Carukia barnesi* medusa pulse rate (per 30s) between dark and one light colour exposure. * indicates statistically significant differences than in the dark (1-sample T-test per individual light exposure). [a,b,c] indicates statistically significant differences between light exposure (1-way ANOVA, post hoc Tukey HSD). Box and whisker plots with 95% confidence intervals.

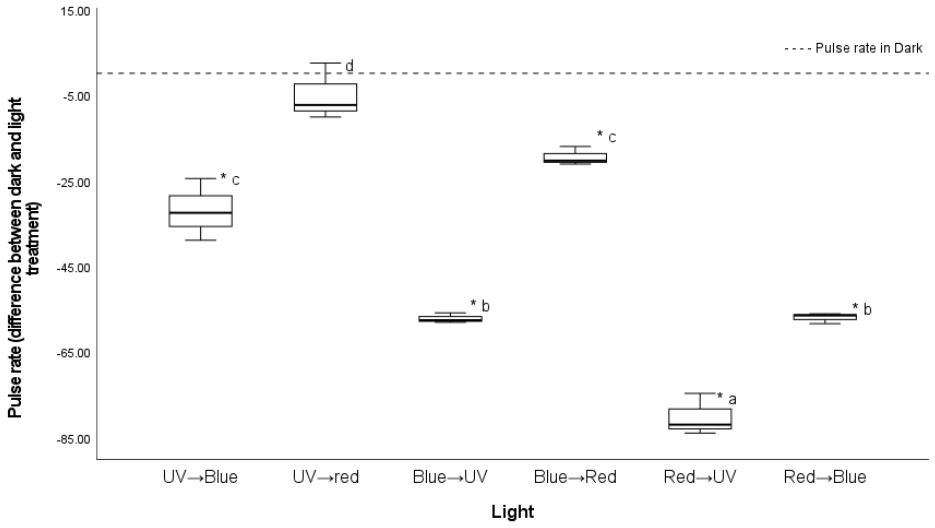

Figure 4.5: Difference in *Carukia barnesi* medusa pulse rate (per 30s) between dark and two-light colour exposures. * indicates statistically significant differences than in the dark (1-sample T-test per individual light treatment). [a,b,c] indicates statistically significant differences between light treatments (1-way ANOVA, post hoc Tukeys HSD). Box and whisker plots with 95% confidence intervals.

4.4.3 Feeding response to light

Individual lights:

All data conformed to a normal distribution (Shapiro-Wilk, $P > 0.05$). The mean difference in the percentage of medusa to ingest prey for each light exposure compared to dark (dark calculated as 0) was statistically significant (1-sample T-tests) in blue ($t(2)=4.330$, 2-sided $P=0.049$) and UV light ($t(2)=15.88$, 2-sided $P=0.004$), but not in Red ($t(2)=3.185$, 2-sided $P=0.086$) or White light ($t(2)=0.171$, 2-sided $P=0.880$)(fig 4.6). This indicates that the number of jellyfish ingesting prey was significantly more in blue and UV lights in the dark, but not in red and white lights. There was no statistically significant difference between lights colours (1-way-ANOVA, $F=0.843$, df =3, $P=0.508$).

Two-light combinations:

All data conformed to normal distribution (Shapiro-Wilk, $P > 0.05$). The mean difference in pulse rate for each light exposure combination compared to dark (dark calculated as 0) was not statistically significant (1-sample T-tests, $P=0.05$) for any of the combinations of light. This indicates that exposing jellyfish to a combination of light colours did not significantly influence how many ingested prey compared to in the dark. There was also no statistically significant difference between light colour combinations (1-way-ANOVA, $F=0.463$, df =5, $P=0.796$) (fig 4.7).

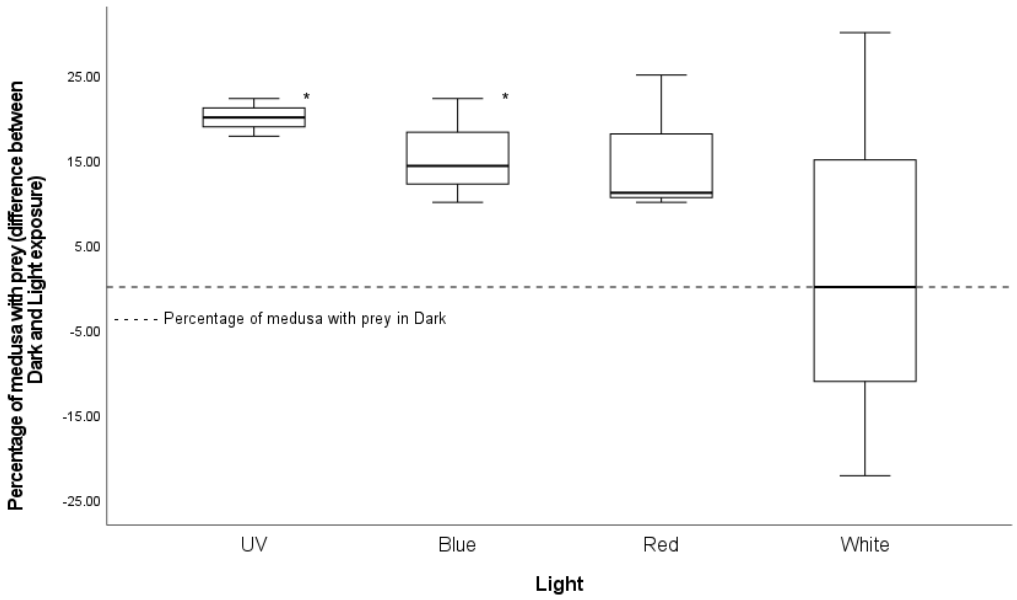

Figure 4.6: Difference in the percentage of *Carukia barnesi* medusa that ingested prey between dark and one light colour exposure. * indicates statistically significant differences than in the dark (1-sample T-test per individual light exposure). Box and whisker plots with 95% confidence intervals.

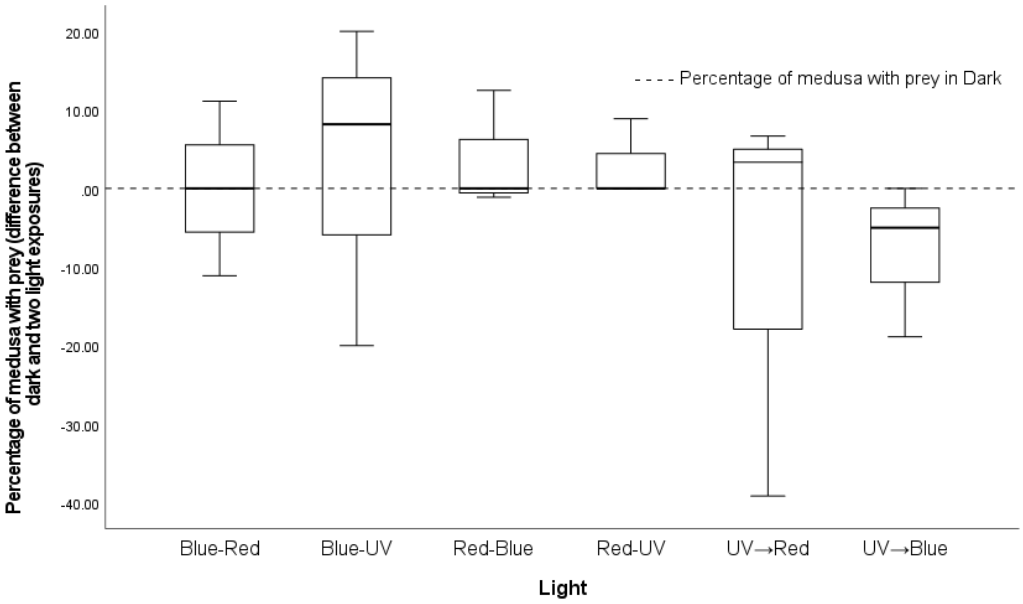

Figure 4.7: Difference in the percentage of *Carukia barnesi* medusa that ingested prey between dark and two-light colour exposure. Box and whisker plots with 95% confidence intervals.

4.5 Discussion

The intention of this study was to determine if light had any effect on feeding behaviour with the ultimate goal to induce feeding in newly detached *Carukia barnesi* medusa. Whilst no one light colour was determined to induce greater feeding, we confirmed that any light will incite a higher feeding response than darkness. We also uncovered a range of behavioral responses demonstrating that light exposure is a key component to the integrated behavior of this animal, although the results are non-linear and the ecological relevance is not presently elucidated.

Prey ingestion results did not provide any similarities or any obvious correlations to the pulse rate results (fig 4.3), suggesting the two are completely unassociated. Whilst this is consistent with previous studies noting no links between feeding and pulse rate in scyphozoan jellyfish (Titelman et al., 2007; Titelman & Hansson, 2006), cubozoan jellyfish often slow their pulse rate as they stop swimming to swallow (Personal communication, A Garm, Unpublished data on *Copula, Tripedalia* and *Chiropsalmus sp*.) so a correlation was expected, but not found (fig 4.3).

When exposed to a single red light, *C. barnesi* (Figs. 4.4 and 4.6) show no statistically significant difference from the dark treatment in either pulse rate or prey ingestion response, indicating the animals are either non-reactive to red light or most likely are unable to perceive it. This is consistent with finding from other cubozoan species (*Tripedelia cystophora* and *Chiropsalmus sp*.), which have been shown to possess colour-blind eyes, with their spectral sensitivity peaking in the blue-green region (Coates et al., 2006; Garm et al., 2007). Although *Tripedelia cystophora* demonstrated a mild reaction to UV in its large lens eye, the authors Garm et al. (2007) ultimately determined that the animal was blind to both UV and red light. We are now likely seeing a similar instance of cubozoan eyes blind to red light with *C. barnesi* in the present study.

We do find one significantly different attribute to that of Garm et al. (2007) in that *C. barnesi* displays significant reactions to UV light[1]. When exposed to two combinations of light colour, *C. barnesi*'s pulse rate changes the least when exposed to UV→ red, then changed the most when exposed to red→UV (Fig.4.5). This drastic change in pulse rates evidences the animal is perceiving and reacting to at least one of the two colours, UV or red. As the data for two-light combinations was calculated to represent the effect of the final colour, we can assume that it is the final colour in the combination the animals are reacting to; least reaction to red, and most reaction to UV.

[1] The UV LED does also emit some light above 400nm, thus within the UV treatment the jellyfish are exposed to some visible light also which must be considered during interpretation.

This is corroborated by the pulse rate response to individual light colours, where we observed no change in pulse rate to red light alone, but see the most significant change out of all the colours when exposed to UV alone (Fig 4.4). Similarly, with the prey ingestion response to individual light exposures, red light instigates no statistically significant change from dark, whereas UV incites the largest change in prey ingestion out of all colours (Fig 4.6). Logically, we conclude that *C. barnesi,* in difference to other previously studied cubozoan species, can perceive and react to UV light. Adult cubozoan rhopalia are situated in niches within the surface of the bell margin and it has been suggested that the bell tissue may absorb UV light explaining the UV blind eyes of *Tripedelia cystophora* (Coates et al., 2006). However, at the young age of medusa used in the present study, *C. barnesi* rhopalia are not situated in niches, but rather sit atop the bell surface, similar to the tentacle (fig 4.2B), and UV absorption from the tissue would not be applicable. From an ecological standpoint, blindness to red light but not UV in an aquatic environment at first seems confusing as UV and red light typically penetrate to similar depths meaning there would not be an environmental instance one could envision where one colour was present but not the other. *C. barnesi* does significantly change both pulse rate and prey ingestion (separately – the two are not linked) when exposed to certain lights compared to in the dark (Figs. 4.4 and 4.6), demonstrating an awareness of the difference between light and dark. One possibility to explain UV perception but not red light is that at night, starlight exhibits strong peaks in the red spectrum (Johnsen et al., 2006; Kelber et al., 2017), accordingly red blindness may be a way for the animal to differentiate night from day, even given the presence of red light at night. Another, simpler and more likely scenario is the animals are controlling their diurnal rhythm by measuring intensity, i.e. there is useful information in the UV light but not in the red, since UV intensity increases fast as you approach the water surface this could dictate the animals' relative distance to the surface.

Metabolic rate experiments in adult *C. barnesi* have evidenced that even when consistently exposed to artificial white light, oxygen consumption is significantly reduced during nighttime hours as opposed to during the daytime (Courtney, 2016), suggesting adult *C. barnesi* jellyfish possess the ability to perceive the time of day regardless of light exposure. Adult *C. barnesi* also display very distinct physiological diurnal/nocturnal reactions: during light/daytime they relax their tentacles to fish and perform a twitching behavior as a lure, the reverse of which is observed during darkness/nighttime where they contract their tentacles and do not twitch (Courtney et al., 2015). Whilst the newly detached *C. barnesi* used in the present study do not possess tentacles long enough to relax/contract (Fig 4.2), they are still displaying marked differences in pulse rate and prey ingestion between light and dark treatments. If we were to assume a red colour blindness, the animals significantly slow down their pulse rate in all light colours they appear to

perceive (Fig 4.4 (individual colours) and 4.5 (re. final colour in combination)) compared to in the dark/red where they pulse significantly faster. Their prey ingestion is also increased in blue and UV light compared to dark and red (Fig 4.6). We know at least one species of cubozoans need to "sleep" at night (Seymour et al., 2004) and that the adults of this species do not target prey at night (Courtney et al., 2015), so the increase in pulse rate in the dark here is difficult to explain. Perhaps the newly detached medusa are able to perceive day/night regardless of light as the adults can, and the increase in dark pulse rate we are observing (fig 4.4) is a reaction to being in the dark during the day and attempting to move out of this environment into the light which better facilitates prey capture (Fig 4.6). Alternatively, it could be that the newly detached medusa need to pulse in the dark to stay in the water column.

Interestingly, the pulse rate of newly detached *C. barnesi* is reacting to individual colours, but the pulse rate response to the broad white light was varied and not significantly different from the dark treatment. Whereas prey ingestion does not display this variation in the broad white light, we observed a unique defined response to white light, similar to the other individual colours. This suggests any visible light in general incites specific responses in pulse rate, whereas prey ingestion is specifically influenced by individual colours. Aside from the UV→red, the combination of light colours also significantly affects pulse rate, and the combination data differs from the individual light data. These responses could be tenuously attribute to time of day i.e. the natural sequence of peak wavelengths in the daylight spectrum over time. However, this would require further data collection, including geographically accurate spectrographic measurements over the course of the day, which is beyond the scope of this study.

Whilst we have assumed a red colour blindness for most of this discussion, as is the norm with cubozoans, that is not strictly in line with what our data is showing us if we look further than the strict lines of statistical significance. When exposed singularly to red light, pulse rate does not change from the dark which suggest red colorblindness. Also their feeding response showed no statistical difference from that observed to occur in darkness. But consider here p=0.086 (very close to the significance cut off) and from fig 4.6 we can see there is still a strong response to red light. Additionally in the two-colour treatment there is a lowered pulse rate between blue→ red light. Thus, whilst a red colour blindness may be the simpler, more convenient option, we do not believe it should be assumed here. Newly detached *C. barnesi* did exhibit some responses to red light, which requires consideration of the opsins within their eyes. If they are colourblind, they will have a single opsin. Under the assumption that *C. barnesi* are colourblind and have only blue photoreceptors peaking at 460nm (which would make most sense in clear ocean waters), then blue light would be perceived as the brightest to the jellyfish, followed by the white and then the

UV, with red not visible at all (fig 4.8A). If they only have a UV receptor peaking at 395nm, then UV light would be the brightest but the blue would still be brighter than the white light (fig 4.8B). The challenge to interpreting our results is, no matter which single opsin they were to use, there would be a non-linear response with the results, which is perplexing. Perhaps the only option not yet explored is the possibility these jellyfish possess multiple opsins, have colour vision and are truly reacting to each colour individually. Colour vision is currently unheard of within jellyfish, and the ecological reasoning as to why this one species would posses it whilst no others are known to is unknown. Nevertheless, based on the results presented in the current study, it should be postulated that we could be observing the behavioral responses of a jellyfish that may possess colour vision, which has previously been considered possibility in cubozoans but never proven (O'Connor et al., 2010).

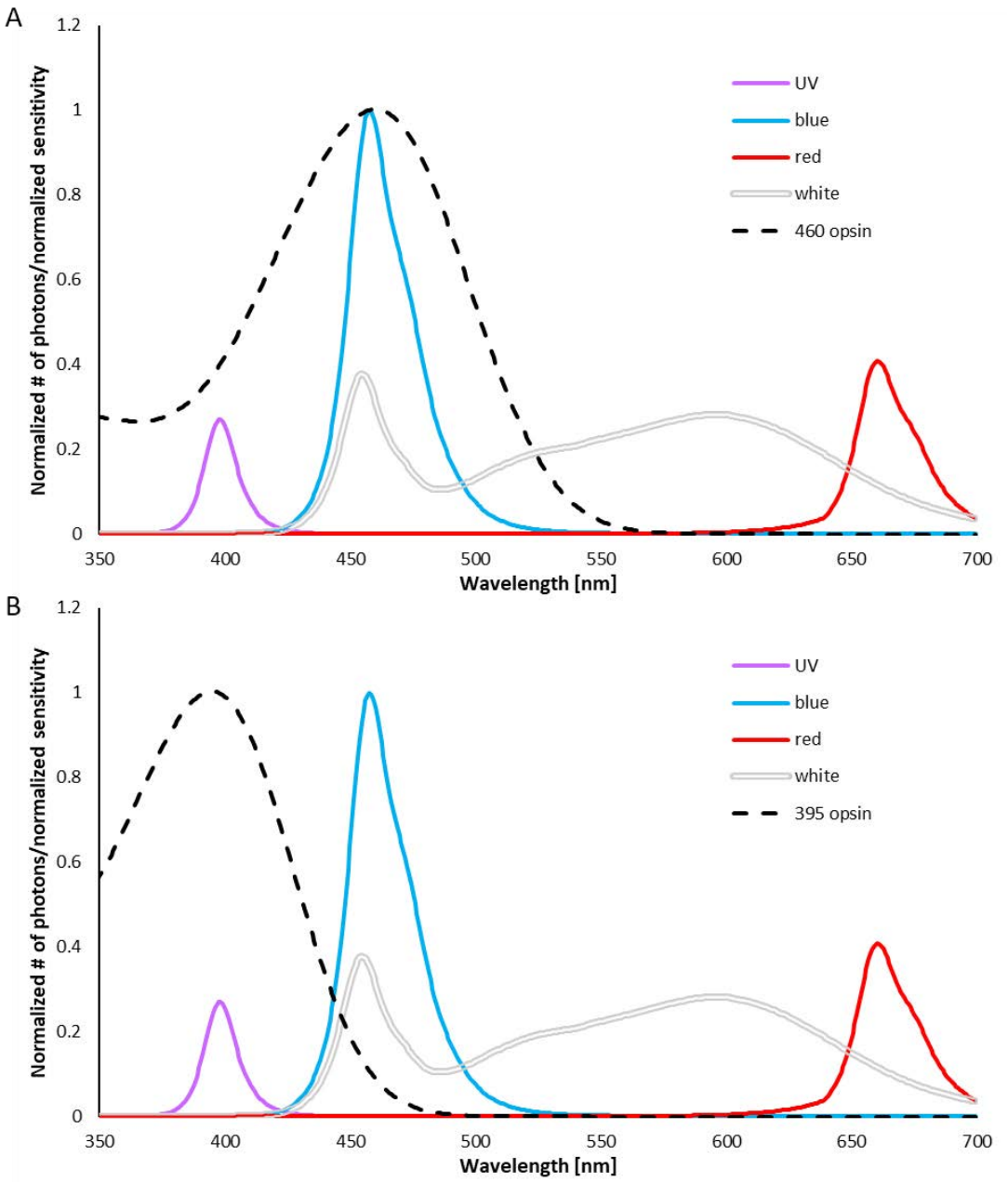

Figure 4.8: LED spectra (adjusted from intensity measurements recorded within the light trials) displayed alongside a single opsin (calculated and produced by Prof. A Garm, cnidarian vision expert, personal communication 2024). Jellyfish possessing a single opsin may perceive only the colours present beneath the opsins curve. The relative brightness a colour is perceived is calculated as the area beneath the colour's curve (within the opsins peak). A: 460nm opsin. B: 395nm opsin.

These experiments have highlighted that light has an effects (separately) on the pulse rates and feeding frequency of *C. barnesi* newly detached medusa, but fails to fully explain the process behind these interactions. What is required to progress these ideas is greater understanding of the visual system of this animal as well as more sophisticated and higher resolution light and feeding experiments. Only then will the intricacies of the feeding ecology and light of these animals be elucidated.

4.6 References

Barnes, J. H. (1964). CAUSE AND EFFECT IN IRUKANDJI STINGINGS. *Medical Journal of Australia*, *1*(24), 897–904. https://doi.org/10.5694/j.1326-5377.1964.tb114424.x

Coates, M. M., Garm, A., Theobald, J. C., Thompson, S. H., & Nilsson, D. E. (2006). The spectral sensitivity of the lens eyes of a box jellyfish, Tripedalia cystophora (Conant). *Journal of Experimental Biology*, *209*(19), 3758–3765. https://doi.org/10.1242/jeb.02431

Courtney, R. (2016). Life cycle, prey capture ecology, and physiological tolerances of Medusae and polyps of the "Irukandji" jellyfish: Carukia barnesi. In *PhD Thesis, James Cook University*. https://researchonline.jcu.edu.au/49935/

Courtney, R., Browning, S., & Seymour, J. (2016). Early life history of the "irukandji" jellyfish *Carukia barnesi*. *PLoS ONE*, *11*(3). https://doi.org/10.1371/journal.pone.0151197

Courtney, R., Sachlikidis, N., Jones, R., & Seymour, J. (2015). Prey capture ecology of the cubozoan Carukia barnesi. *PLoS ONE*, *10*(5), 1–12. https://doi.org/10.1371/journal.pone.0124256

Garm, A., Coates, M. M., Gad, R., Seymour, J., & Nilsson, D. E. (2007). The lens eyes of the box jellyfish Tripedalia cystophora and Chiropsalmus sp. are slow and color-blind. *Journal of Comparative Physiology A: Neuroethology, Sensory, Neural, and Behavioral Physiology*, *193*(5), 547–557. https://doi.org/10.1007/S00359-007-0211-4

Gershwin, L. A., & Dawes, P. (2008). Preliminary observations on the response of Chironex fleckeri (Cnidaria: Cubozoa: Chirodropida) to different colors of light. *Biological Bulletin*, *215*(1), 57–62. https://doi.org/10.2307/25470683

Jindrich, K. (2012). *Light influence on nematocyst firing in the sea anemone Haliplanella luciae*. Lund University.

Johnsen, S., Kelber, A., Warrant, E., Sweeney, A. M., Widder, E. A., Lee, R. L., & Hernández-Andrés, J. (2006). Crepuscular and nocturnal illumination and its effects on color perception by the nocturnal hawkmoth Deilephila elpenor. *Journal of Experimental Biology*, *209*(5), 789–800. https://doi.org/10.1242/jeb.02053

Kelber, A., Yovanovich, C., & Olsson, P. (2017). Thresholds and noise limitations of colour vision in dim light. *Philosophical Transactions of the Royal Society B: Biological Sciences*, *372*(1717). https://doi.org/10.1098/rstb.2016.0065

O'Connor, M., Garm, A., Marshall, J. N., Hart, N. S., Ekström, P., Skogh, C., & Nilsson, D. E. (2010). Visual pigment in the lens eyes of the box ra jellyfish Chiropsella bronzie. *Proceedings of the Royal Society B: Biological Sciences*, *277*(1689), 1843–1848.

https://doi.org/10.1098/rspb.2009.2248

O'Hara, E., & Seymour, J. (2022). Inducing metamorphosis in the irukandji jellyfish Carukia barnesi. *Scientific Reports 2022 12:1*, *12*(1), 1–12. https://doi.org/10.1038/s41598-022-12812-2

Pereira, P., Barry, J., Corkeron, M., Keir, P., Little, M., & Seymour, J. (2010). Intracerebral hemorrhage and death after envenoming by the jellyfish *Carukia barnesi*. *Clinical Toxicology*, *48*, 390–392. https://doi.org/10.3109/15563651003662675

Plachetzki, D. C., Fong, C. R., & Oakley, T. H. (2012). Cnidocyte discharge is regulated by light and opsin-mediated phototransduction. *BMC Biology*, *10*. https://doi.org/10.1186/1741-7007-10-17

Rowley, O. (2021). *Rethinking biological tools for logistically difficult species: a case study - the Irukandji (Carukia barnesi) and Box Jellyfish (Chironex fleckeri).* [James Cook University]. https://doi.org/https://doi.org/10.25903/jx3e%2D5w21

Seymour, J. E., Carrette, T. J., & Sutherland, P. A. (2004). Do box jellyfish sleep at night? *Medical Journal of Australia*, *181*(11–12), 707. https://doi.org/10.5694/j.1326-5377.2004.tb06529.x

Seymour, J. E., & O'Hara, E. P. (2020). Pupillary response to light in three species of cubozoa (Box jellyfish). *Plankton and Benthos Research*, *15*(2), 73–77. https://doi.org/10.3800/pbr.15.73

Titelman, J., Gandon, L., Goarant, A., & Nilsen, T. (2007). Intraguild predatory interactions between the jellyfish Cyanea capillata and Aurelia aurita. *Marine Biology*, *152*(4), 745–756. https://doi.org/10.1007/s00227-007-0721-1

Titelman, J., & Hansson, L. J. (2006). Feeding rates of the jellyfish Aurelia aurita on fish larvae. *Marine Biology*, *149*(2), 297–306. https://doi.org/10.1007/s00227-005-0200-5

Chapter 5 . In the blink of an eye: Pupillary response to light in three species of Cubozoa (box jellyfish)

This chapter is a published manuscript: Seymour, J. E., & O'Hara, E. P. (2020). Pupillary response to light in three species of Cubozoa (box jellyfish). *Plankton and Benthos Research*, *15*(2), 73-77. See appendix A.

5.1 Abstract

Pupillary response under varying conditions of bright light and darkness was compared in three species of Cubozoa with differing ecologies. Maximal and minimal pupil area in relation to total eye area was measured and the rate of change recorded. In *Carukia barnesi*, the rate of pupil constriction was faster and final constriction greater than in *Chironex fleckeri*, which itself showed faster and greater constriction than in *Chiropsella bronzie*. We suggest this allows for differing degrees of visual acuity between the species. We propose that these differences are correlated with variations in the environment which each of these species inhabit, with *C. barnesi* found fishing for larval fish in and around waters of structurally complex coral reefs, *C. fleckeri* regularly found acquiring fish in similarly complex mangrove habitats, while *C. bronzie* spends the majority of its time in the comparably less complex but more turbid environments of shallow sandy beaches where their food source of small shrimps is highly aggregated and less mobile.

5.2 Introduction

The primary function of pupil constriction and dilation in complex eyes is to enable light regulation on the retina which serves to increase sensitivity and acuity (Erichsen et al. 2000, Douglas et al. 2005). Comparative studies on visual systems in vertebrate fauna have shown that differences in this basic pupillary movement can dictate the visual awareness capabilities required to cope with the lifestyle demands of a particular species within the ecological niche in which they operate, for example vertebrates operating in complex environments and variable light intensity show more rapid and greater pupil constriction resulting in better control over visual acuity than those with restricted pupil responses (Arrese 2002, Litherland et al. 2009).

Within the invertebrate fauna, complex eyes are relatively uncommon and are currently known from only two phyla: Mollusca and Cnidaria. Research into the visual systems of these invertebrates has mainly focused on the structure and optics and particulary in regards to their evolutionary development (O'Connor et al. 2009). Although limited studies have investigated pupillary movement of invertebrates (Douglas et al. 2005, O'Connor et al. 2009), none exist directly comparing pupillary movement between species in relation to their habitat and lifestyle.

Members of the Phylum Cnidaria have developed a variety of visual systems ranging from simple eye spots to pigment cup ocelli (Yamasu & Yoshida 1973, Yamasu & Yoshida 1976, Singla 1974, Blumer et al. 1995, Nordström et al. 2003) to advanced complex eyes similar to those found in vertebrates and potentially derived by convergent evolution (Nilsson et al. 2005). These complex camera-type eyes belong to the medusa stage of the cubozoans (box jellyfish) (Berger 1898, Pearse & Pearse 1978, Martin 2002, Nilsson et al. 2005). Research into cubozoan visual systems has noted that the medusa of all species studied possess four sensory clubs or 'rhopalia,' each housing a pair of simple light sensitive pigment cups, a pair of light sensitive pigment slits, and a pair of complex eyes (O'Connor et al. 2010, Garm et al. 2011). Both complex eyes have a cornea, a lens, a pigment layer, an iris and a retina (Piatigorsky et al. 1989, Hamner et al. 1995, Martin 2002, Nilsson et al. 2005, O'Connor et al. 2009) with the lower of the two complex eyes displaying pupil movement (Nilsson et al. 2005, O'Connor et al. 2009). However, studies have demonstrated the inability of these complex visual structures to focus sharply questioning what level and type of image these animals are able to produce (Nilsson et al. 2005, O'Connor et al. 2009).

To examine whether invertebrate fauna possessing complex eyes demonstrate a similar relationship between changes in pupil size and habitat as observed in vertebrate fauna, we investigated differences in the rate and extent of pupil movement in the lateral complex eye of three species of cubozoan found in Tropical North Queensland, *Chiropsella bronzie, Carukia*

barnesi and *Chironex fleckeri*. These three species show a distinct difference in their feeding ecologies. Mature medusae of *C. fleckeri* actively hunt (Kinsey 1986) and feed on fish (Kinsey 1986, Carrette et al. 2002), *C. bronzie* passively captures its prey, the small marine shrimp *Acetes australis*, by swimming through bait balls (Carrette et al. 2002), and *C. barnesi* actively lures and feeds on larval planktonic fish (Underwood & Seymour 2007, Courtney et al. 2015). The environment in which each of these species are commonly found also varies; *C. bronzie* inhabits the shallow waters of sandy foreshores (Barnes 1961, Gordon et al. 2004) where their prey is located in generally slightly turbid waters (Kinsey 1986); *C. fleckeri* is more often found in the complex environments of the mangroves roots along river banks (Kinsey 1986, Hartwick 1991, Gordon & Seymour 2012); *C. barnesi*, a reportedly offshore medusae (Southcott 1967, Kinsey 1986, Williamson et al. 1996, Kingsford et al. 2012), is regularly found in coral-lined bays of offshore islands (Kingsford et al. 2012). If light regulation in complex eyes of invertebrate species operates according to environmental niche requirements as has been shown for vertebrates, the contrasts in habitat and feeding ecologies displayed by these three species of box jellyfish should be reflected by differences in the functional capacities of their pupils. This study elaborates on the previous research documenting pupil constriction in the cubozoans, *Tripedalia cystophora* (Nilsson et al. 2005) and *C. bronzie* (O'Connor et al. 2009) and presents these findings in relation to the ecological niche in which each species operates.

5.3 Methods

Live medusae were caught at Mission Beach, 17.8694° S, 146.1069° E (*Chironex fleckeri*), Port Douglas, 16.4836° S, 145.4653° E (*Chiropsella bronzie*) and Double Island near Cairns, 16.7259° S, 145.6839° E (*Carukia barnesi*). Animals were transported directly to an aquarium facility and eyes used in this experiment were excised within 12 hours of capture. Entire rhopalia were detached from live animals at the top of the rhopalial stalk as per O'Connor et al. (2009). No more than two rhopalia were used from any individual animal with a single excised rhopalium used only once in any experiment. Each rhopalium was embedded in a wax cup containing seawater (at the same salinity and temperature at which the animals were collected) on a mounting slide with the lateral compound eye facing upwards. The slide was then placed under a dissecting microscope (SZ-ST, Olympus, Japan) and covered in darkness for 30 minutes to ensure maximum pupil dilation and adjustment. The lateral compound eyes of *C. bronzie* were subjected to three different light intensities. The highest (2000 µmol photons s−1 m−2) represented a high light intensity the organism would normally not encounter. The lowest (600 µmol photons s−1 m−2) represented the light intensity at 1 m depth in the field. These intensities were achieved by shining a variable cold light source (halogen globe, 3200°K) directly onto the eye. The medium intensity (1400 µmol

photons s−1 m−2) which is full sunlight, was obtained by placing the excised rhopalia in direct sunlight. Light intensities were measured by placing the photoreceptive end of a light meter (LuxFc, N19Q1367, Dicksmith Electronics, Australia) at the same distance from the cold light source or direct sunlight as the excised rhopalia. Using a series of digital photographs taken at 60 second intervals for the first 10 minutes and then every 5 minutes thereafter for a total of 20 minutes, the total surface area of the eye was measured followed by the total pupil area (represented by a dark area in the centre of the eye) (Fig. 5.1). These measurements were converted to a percentage of the maximum pupil opening (100%) as determined from the photograph taken immediately after the initial 30 minutes of dark adaptation for each trial.

For experiments carried out on all three species in direct sunlight (1400 µmol photons s−1 m−2,) a total of seven eyes from four mature *C. fleckeri* medusae, five eyes from three mature *C. bronzie* medusae, and eight eyes from four mature *C. barnesi* medusae were tested. Pupil dilation was measured in the same manner as outlined above.

Data analysis was performed using SPSS version 14. Differences between the pupil dilation of the three species and time in direct sunlight where investigated using general linear model analysis.

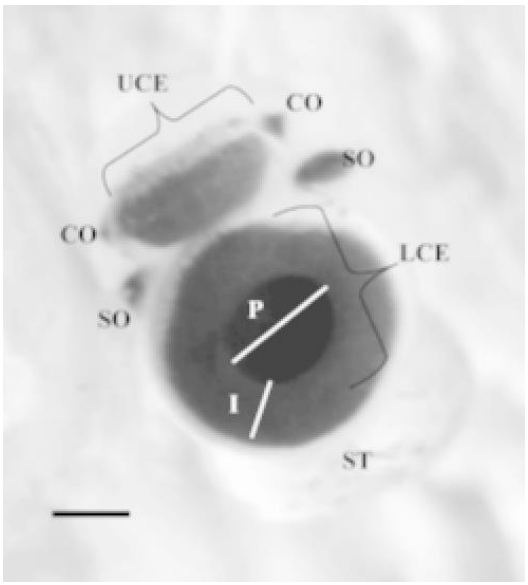

Figure 5.1: Single rhopalium of *Chironex fleckeri* showing four types of visual structures.
UCE, upper compound eye (with fixed pupil); CO, cup-shaped occelli; SO, slit-shaped occelli; LCE, lateral compound eye (with moveable pupil); ST, statolith; P, pupil opening; I, iris. Scale bar represents 0.5 mm

5.4 Results

The pupils in the lateral compound eye of *Chiropsella bronzie* responded differently under the three alternate light intensities to which these eyes were exposed. Time to maximal pupil contraction was fastest at 15 minutes in 2000 µmol photons s−1 m−2 with a maximum pupil contraction to 48% of maxium dilation (Fig 5.2).

When the eyes of all three species where exposed to direct sunlight, the pupils of *Carukia barnesi* contracted more rapidly and to a greater extent than did *Chironex fleckeri* which likewise contracted more rapidly and to greater extent than *C. bronzie* pupils (F= 3.51, 22*136 d.f, p <0.001) (Fig 5.3). Maximal pupil contraction in all three species occurred at approximately 10 minutes. Under sustained exposure to each light intensity, the pupils of all three species were not able to maintain the fully contracted state presumably due to muscle fatigue.

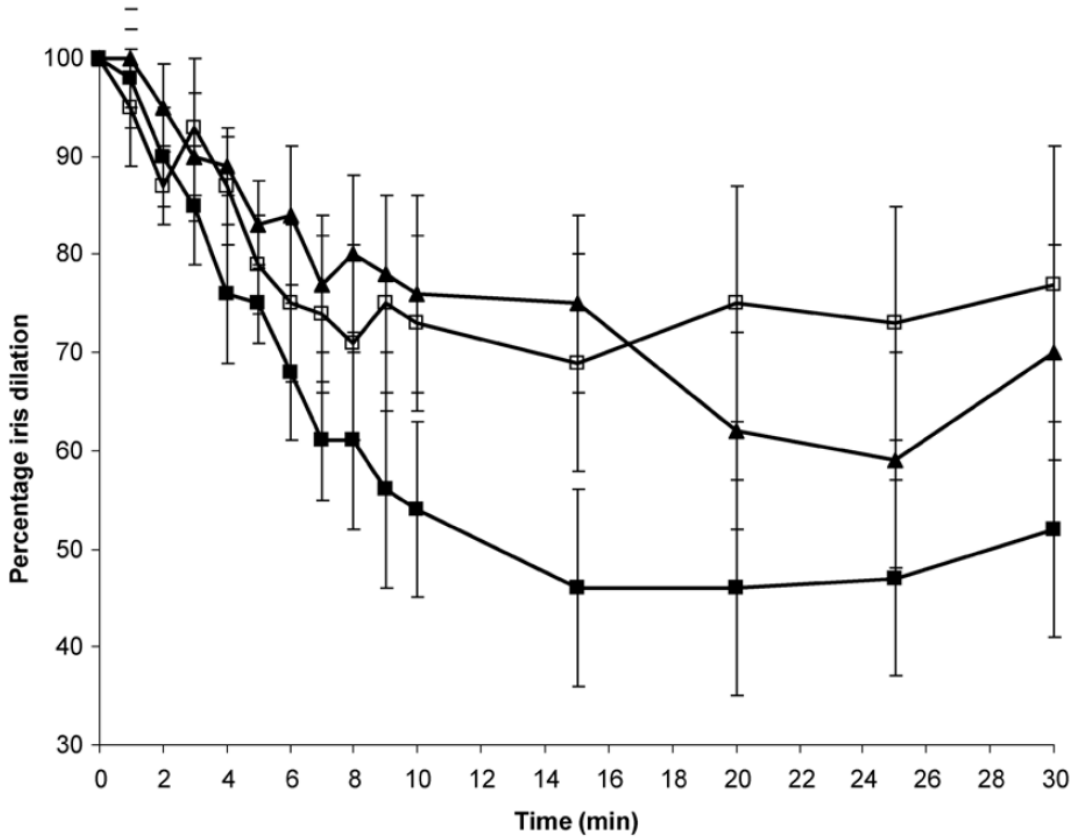

Figure 5.2:Percentage iris dilation at three different light intensities for *Chiropsella bronzie* (■=2000 µmol photons/s/m2, □=1400 µmol photons/s/m2, ▲= 600 µmol photons/s/m2)

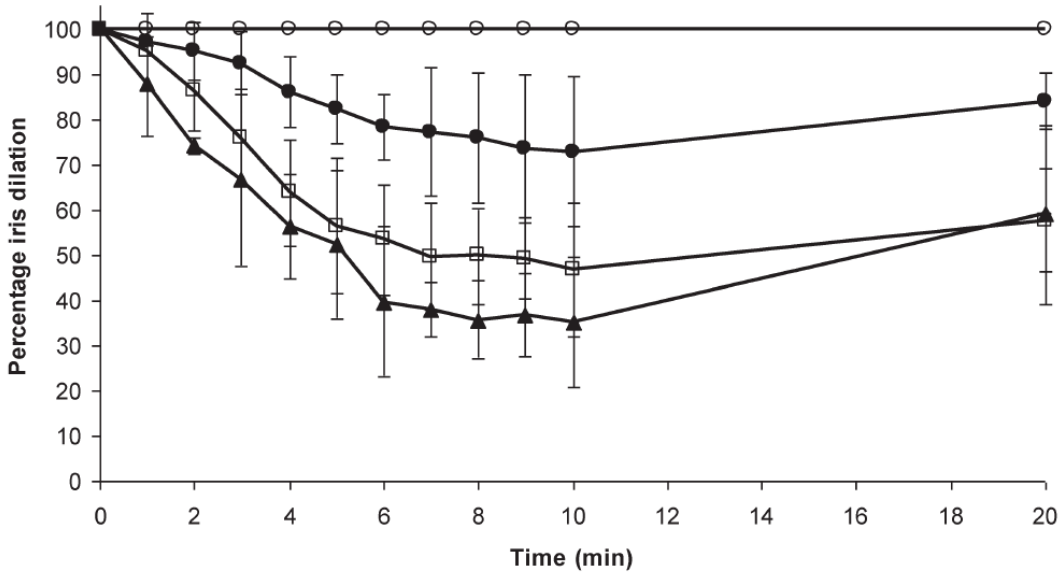

Figure 5.3: Percentage iris dilation for *Chiropsella bronzie* (•), *Chironexfleckeri* (▫) and *Carukia barnesi* (▲) under direct sunlight (1400 μmol photons/s/m$_2$) and for all species in complete darkness (○)

5.5 Discussion

As with vertebrates, pupillary movement in invertebrate cubozoans appears to vary with the ecological niche occupied by different species. *Carukia barnesi* has a faster pupil reaction time and greater constriction capabilities than *Chironex fleckeri*, which has faster and greater pupillary movement than *Chiropsella bronzie*. We believe these differences in eye function are related to the particular ecological niche exploited by these three cubozoan species. For *C. bronzie*, a medusae regularly found on calm shallow beach fronts (Kinsey 1986, Gordon et al. 2004) in low visibility water, visual acuity would not be of prime importance and would therefore not confer any major visual advantage. The diet of these medusae consists solely of *Acetes* sibogae *australis* (Carrette et al. 2002), which are commonly found in aggregations of thousands m2 in the waters of sandy foreshores (Omundsen et al. 2000). These marine shrimp prefer water with low visibility resulting from the presence of their main food source of organic material in the water column (Omundsen et al. 2000). Ch. bronzie appears to randomly swim through these dense prey schools catching the shrimp on their tentacles (Kinsey 1986) and as such, a tightly contracting pupil affords no real advantage. Poor vision has similarly been linked to feeding ecology in the nocturnal box jellyfish *Copula sivickis*i which possesses underfocused eyes with very low temporal resolution (Garm et al. 2016). The bioluminescence of their dinoflagellate prey can be detected with low intensity vision, however individual prey items cannot be observed due to low spatial

resolution. Although, a peak spectral sensitivity of 460 nm enhances the contrast of the coral structures needed for shelter at dawn, demonstrating a compromise between prey capture and habitat detection.

The comparative lack of obstacles in the environment where *C. bronzie* are found, compared to those of *C. fleckeri* and *C. barnesi*, reduces the need for increased visual acuity. In the cases of *C. barnesi* and *C. fleckeri*, medusae of these species are known to inhabit the more structurally complex three dimensional environments of mangroves (*C. fleckeri*, Gordon & Seymour 2012) and coral reefs (*C barnesi*, Kingsford et al. 2012). These medusae have to contend not only with numerous physical structures such as tree roots or coral branches, but also low level fluctuations in light as well as fast moving vertebrate prey. Under laboratory conditions, *C. fleckeri* have been shown to use vision in obstacle avoidance (Hamner et al. 1995), whereas *C. bronzie* displayed very poor obstacle avoidance capabilities in a similar experiment (Garm et al. 2007b). As a result, the visual acuity of *C. fleckeri* compared to that seen in *C. bronzie* would presumably have a positive selection pressure. Similarly, increased visual acuity brought about by a greater depth of field as a result of the smaller pupil openings in *C. fleckeri* and *C. barnesi*, would assist these animals in better negotiating their environment.

These results support and elaborate on a study (O'Connor et al. 2009) that linked variation in eye structure and optics of *C. bronzie* and *Tripedalia cystophora*, with distinct ecological habitats of each species. O'Connor et al. (2009) noted a ten-fold faster reaction time to maximum pupil dilation in *T. cystophora* (1 minute to max. dilation) under high intensity light compared to the maximum contraction times recorded for the three species of this study. However, this may also be a factor of differences in the habitat and behaviour of *T. cystophora* which swims in and out of light shafts in short periods of time (Garm et al. 2007a) and uses vision for prey capture (Buskey 2003) and orientation to specific habitat features in their mangrove habitats (Garm et al. 2011). *T. cystophora* and *C. fleckeri* both inhabit mangrove roots at lagoon edges. Nilsson et al. (2005) determined that although the compound eyes of *T. cystophora* have the potential for sharp image focus, the ray paths in *T. cystophora* result in the eyes being severely underfocused. This was deduced to remove high spatial frequencies allowing the animal to visualise the large mangrove structures in its environment, but not small floating particles. However, if the animals' prey source is considered, and compared with the visual sensitivity now demonstrated in *C. fleckeri*, this could perhaps be interpreted as a trade-off between prey detection and obstacle avoidance. Both *T. cystophora* and *C. fleckeri* must be able to visualise the large mangrove structures dominating their environment, however whilst *C. fleckeri* also requires sharp image focus to locate fast agile prey fish, T. cystophora feeds on dense copepod swarms (Buskey 2003) similar to *C. bronzie*,

negating the need of both species to visualise fine details. This demonstrates an important relationship between visual acuity and feeding ecology. Studies on marine vertebrates have also shown vast differences in the operational speed of pupil movement which they suggest may be correlated to the ecological niche each species operates in (Douglas et al. 1998, Douglas et al. 2002).

Cubozoans are an appropriate taxon for further studies of visual ecology in invertebrates due to the similarities in morphology of their visual systems but differences in ecological niches. To further this hypothesis of the relationship between pupil movement and environmental requirements, additional studies are needed before any constructive conclusions can be made regarding the advantages (or disadvantages) offered to cubozoan medusae by varying rates of contraction. These findings should be linked with studies on how, if at all, these medusae are able to process images collected by their relatively complex visual system.

5.5 References

Arrese, C. (2002). Pupillary mobility in four species of marsupials with differing lifestyles. *Journal of Zoology*, *256*(2), 191-197.

Barnes, J. H. (1966). Studies on three venomous cubomedusae. In *Symp. Zool. Soc. Lond* (Vol. 16, pp. 307-332).

Berger, E. W. (1898). The histological structure of the eyes of cubomedusae. *Journal of Comparative Neurology*, *8*(3), 223-230.

Blumer, M. J., Salvini-Plawen, L. V., Kikinger, R., & Büchinger, T. (1995). Ocelli in a Cnidaria polyp: the ultrastructure of the pigment spots in Stylocoronella riedli (Scyphozoa, Stauromedusae). *Zoomorphology*, *115*, 221-227.

Buskey, E. (2003). Behavioral adaptations of the cubozoan medusa Tripedalia cystophora for feeding on copepod (Dioithona oculata) swarms. *Marine Biology*, *142*, 225-232.

Carrette, T., Alderslade, P., & Seymour, J. (2002). Nematocyst ratio and prey in two Australian cubomedusans, Chironex fleckeri and Chiropsalmus sp. *Toxicon*, *40*(11), 1547-1551.

Courtney, R., Sachlikidis, N., Jones, R., & Seymour, J. (2015). Prey capture ecology of the cubozoan Carukia barnesi. *PLoS One*, *10*(5), e0124256.

Douglas, R. H., Collin, S. P., & Corrigan, J. (2002). The eyes of suckermouth armoured catfish (Loricariidae, subfamily Hypostomus): pupil response, lenticular longitudinal spherical aberration and retinal topography. *Journal of Experimental Biology*, *205*(22), 3425-3433.

Douglas, R. H., Harper, R. D., & Case, J. F. (1998). The pupil response of a teleost fish, Porichthys notatus: description and comparison to other species. *Vision research*, *38*(18), 2697-2710.

Douglas, R. H., Williamson, R., & Wagner, H. J. (2005). The pupillary response of cephalopods. *Journal of Experimental Biology*, *208*(2), 261-265.

Erichsen, J. T., Hodos, W., & Evinger, C. (2000). The pupillary light reflex, accommodation and convergence: Comparative considerations. In *Accommodation and vergence mechanisms in the visual system* (pp. 31-42). Birkhäuser Basel.

Garm, A., Bielecki, J., Petie, R., & Nilsson, D. E. (2016). Hunting in bioluminescent light: vision in the nocturnal box jellyfish Copula sivickisi. *Frontiers in Physiology*, *7*, 99.

Garm, A., Coates, M. M., Gad, R., Seymour, J., & Nilsson, D. E. (2007). The lens eyes of the box jellyfish Tripedalia cystophora and Chiropsalmus sp. are slow and color-blind. *Journal of Comparative Physiology A*, *193*, 547-557.

Garm, A., O'Connor, M., Parkefelt, L., & Nilsson, D. E. (2007). Visually guided obstacle avoidance in the box jellyfish Tripedalia cystophora and Chiropsella bronzie. *Journal of Experimental Biology*, *210*(20), 3616-3623.

Garm, A., Oskarsson, M., & Nilsson, D. E. (2011). Box jellyfish use terrestrial visual cues for navigation. *Current Biology*, *21*(9), 798-803.

Gordon, M., Hatcher, C., & Seymour, J. (2004). Growth and age determination of the tropical Australian cubozoan Chiropsalmus sp. *Hydrobiologia*, *530*, 339-345.

Gordon, M., & Seymour, J. (2012). Growth, development and temporal variation in the onset of six Chironex fleckeri medusae seasons: a contribution to understanding jellyfish ecology. *PloS one*, *7*(2), e31277.

Hamner, W. M., Jones, M. S., & Hamner, P. P. (1995). Swimming, feeding, circulation and vision in the Australian box jellyfish, Chironex fleckeri (Cnidaria: Cubozoa). *Marine and Freshwater Research*, *46*(7), 985-990.

Hartwick, R. F. (1991). Distributional ecology and behaviour of the early life stages of the box-jellyfish Chironex fleckeri. In *Coelenterate Biology: Recent Research on Cnidaria and Ctenophora: Proceedings of the Fifth International Conference on Coelenterate Biology, 1989* (pp. 181-188). Springer Netherlands.

Kingsford, M. J., Seymour, J. E., & O'Callaghan, M. D. (2012). Abundance patterns of cubozoans on and near the Great Barrier Reef. *Jellyfish Blooms IV: Interactions with humans and fisheries*, 257-268.

Kinsey BE (1986) Barnes on Box Jellyfish. Sir George Fisher Centre for Tropical Marine Studies. James Cook University of

North Queensland, Townsville, 160 pp.

Litherland, L., Collin, S. P., & Fritsches, K. A. (2009). Visual optics and ecomorphology of the growing shark eye: a comparison between deep and shallow water species. *Journal of Experimental Biology*, *212*(21), 3583-3594.

Martin, V. J. (2002). Photoreceptors of cnidarians. *Canadian Journal of Zoology*, *80*(10), 1703-1722.

Nilsson, D. E., Gislén, L., Coates, M. M., Skogh, C., & Garm, A. (2005). Advanced optics in a jellyfish eye. *Nature*, *435*(7039), 201-205.

Nordström, K., Wallén, Seymour, J., & Nilsson, D. (2003). A simple visual system without neurons in jellyfish larvae. *Proceedings of the Royal Society of London. Series B: Biological Sciences*, *270*(1531), 2349-2354.

O'Connor, M., Garm, A., & Nilsson, D. E. (2009). Structure and optics of the eyes of the box jellyfish Chiropsella bronzie. *Journal of Comparative Physiology A*, *195*, 557-569.

O'Connor, M., Nilsson, D. E., & Garm, A. (2010). Temporal properties of the lens eyes of the box jellyfish Tripedalia cystophora. *Journal of Comparative Physiology A*, *196*, 213-220.

Omundsen, S. L., Sheaves, M. J., & Molony, B. W. (2000). Temporal population dynamics of the swarming shrimp, Acetes sibogae australis, in a tropical near-shore system. *Marine and Freshwater Research*, *51*(3), 249-254.

Pearse, J. S., & Pearse, V. B. (1978). Vision of cubomedusan jellyfishes. *Science*, *199*(4327), 458-458.

Piatigorsky, J., Horwitz, J., Kuwabara, T., & Cutress, C. E. (1989). The cellular eye lens and crystallins of cubomedusan jellyfish. *Journal of Comparative Physiology A*, *164*, 577-587.

Singla, C. L. (1974). Ocelli of hydromedusae. *Cell and Tissue Research*, *149*, 413-429.

Southcott, R. V. (1967). Revision of some Carybdeidae (Scuphozoa: Cubomedusae) including a description of the jellyfish responsible for the'Irukandji syndrome'. *Australian Journal of Zoology*, *15*(3), 651-671.

Underwood, A. H., & Seymour, J. E. (2007). Venom ontogeny, diet and morphology in Carukia barnesi, a species of Australian box jellyfish that causes Irukandji syndrome. *Toxicon*, *49*(8), 1073-1082.

Burnett, J. W. (1996). *Venomous and poisonous marine animals: a medical and biological handbook*. UNSW Press.

Yamasu, T., & Yoshida, M. (1973). Electron microscopy on the photoreceptors of an anthomedusa and a scyphomedusa. *Publications of the Seto Marine Biological Laboratory*, *20*, 757-778.

Yamasu, T., & Yoshida, M. (1976). Fine structure of complex ocelli of a cubomedusan, Tamoya bursaria Haeckel. *Cell and Tissue Research*, *170*, 325-339.

Chapter 6 . Too Much of a Good Sting: Nematocyst Identification and Classification in the Irukandji Jellyfish *Carukia barnesi*

6.1 Abstract

Carukia barnesi is one of the smallest, yet most venomous jellyfish in the world, however current understanding of its venom and venom injecting organelles (nematocysts) is very limited. Conflicting nematocyst identifications in the literature and lack of research from different life stages hinders understanding of this animal's venom ecology. Here, I use a combination of light, electron and fluorescent microscopy to conclusively identify the nematocysts across three ontogenetic stages of *C. barnesi*: polyp, newly detached medusa and adult medusa. Nematocysts from one rarer, older specimen are also included however further research is needed in this life stage. Three confirmed nematocyst types were found in total across the four life stages, homotrichous tumiteles, holotrichous O-isorhizas and atrichous or holotrichous B-mastigophores, with two other potential nematocyst types discussed. Confirmed nematocyst types were found to significantly change between ontogenetic stages in both proportion and size, evidencing the venom ecology of this animal changes significantly between life stages. Additionally, we present evidence supporting the identification of nematocysts previously found in unsolved human envenomation cases as potentially originating from *C. barnesi*, based on the findings of this research.

6.2 Introduction

All cnidarians - coral, sea anemones, hydrozoans and jellyfish – possess specialised cells called cnidocytes. These cnidocytes contain secretory stinging organelles called cnidae (or cnidocysts), which are usually characterised as either nematocysts, spirocysts, or ptychocysts (Hessinger & Lenhoff, 1988). Nematocysts are considered the only type able to deliver venom due to their penetrative nature, arguably making them the single most important entities in the study of cnidarian venoms. These explosive microscopic organelles are characterised in two states: undischarged – a coiled tubule resides within a capsule containing venom, and discharged – the tubule everts out of the capsule and toxin is ejected through this tubule. There are over 30 different types of nematocysts (Östman, 2000), each traditionally assumed to contain a unique toxin and it is the ultrastructure of both the undischarged and discharged capsules that is used in identification. Each species of cnidarian typically possesses a unique collection of the various nematocyst types, termed the cnidome and, as such, will possess unique toxins characteristic of the species.

Carukia barnesi is a small, almost invisible cubozoan (box jellyfish) possessing one of the most potent venoms on the planet. *C. barnesi* is native to North Queensland (Barnes, 1964) and is one of the most commonly encountered and vilified species of Irukandji jellyfish. A sting will almost certainly induce Irukandji syndrome - a complex and excruciatingly painful condition invariably requiring hospital treatment. The syndrome elicits a range of symptoms from extreme muscle pains, nausea and vomiting to instances of induced intracerebral haemorrhage and death (Pereira et al., 2010), resulting in hundreds of emergency hospitalisations a year throughout Queensland. Unfortunately, for such a medically important species, *C. barnesi's* venom is still poorly understood and the literature available analysing the nematocysts is conflicting. All current literature (to the best of the author's knowledge) presenting nematocyst identification in *C. barnesi* is displayed in Table 6.1 and discrepancies are immediately obvious. Whilst Weill (Weill, 1934) is regarded as the father of cnidocyst identification, producing a thorough classification method, this keystone work has since been adapted and modernised by a multitude of authors. As such, the conflicting identifications illustrated in Table 6.1 could be due to a multitude of factors not necessarily rooted in misidentification, such as differing classification method, updated terminology, level of classification, etc.

Table 6.1: Literature in which nematocysts types are identified in Carukia barnesi, across three life stages (polyp, newly detached medusa and adult medusa) and two body parts (bell and tentacles). Cases which present named identifications only are listed – instances presenting only images were omitted.

	Polyp	Newly detached medusa		Adult medusa	
Reference	Tentacles	Bell	Tentacles	Bell	Tentacles
Southcott, 1967	-	-	-	▪anisorhizas haplonemes (possibly homotrichous)	▪tumitiles
Gershwin, 2006	-	-	-	▪spherical isorhizas	▪lemon-shaped tumitiles
Underwood & Seymour, 2007	-	-	-	▪homotrichous microbasic rhopaloids ▪homotrichous haplonemes	▪homotrichous microbasic rhopaloids ▪homotrichous haplonemes
`Ávila-Soria, 2009	-	-	-	▪spherical anisorhizas	▪microbasic mastigophores
Courtney et al., 2016	▪tumiteles ▪isorhizas	▪tumiteles ▪isorhizas		-	-

As the nematocysts play the defining roles in venom ecology, this lack of cohesion in the literature is difficult to build venom research upon. Instances where nematocyst identification can provide medically important information, such as helping to identify the species responsible for hospitalization from a jellyfish sting (Huynh et al., 2003), rely on accurate and complete cnidome identifications. For example, doctors have described serious sting victims with symptoms consistent with *C. barnesi* envenomation, but skin scrapings have produced nematocysts which appear not to originate from *C. barnesi*.

One overarching complication in attaining true nematocyst identifications is that the microscopic size of these organelles and their even smaller associated armature means that traditional light microscopy is typically unsuitable to visualize these fine structures. This has long been an acknowledged limitation in the literature, thus higher resolution microscopy such as electron microscopy should be included to visualise and conclusively characterise nematocyst types (Östman, 2000). All the previous research involving *C. barnesi* nematocysts (Table 6.1) has employed only light microscopy techniques, which may be a contributing factor to the discrepancies in identification.

This current research addresses the uncertainty surrounding the cnidome of *C. barnesi* by using scanning electron microscopy to visualize the full range of nematocysts within the jellyfish, using ultrastructural detail to conclusively identify the nematocyst types following Östman's (2000) classification system.

Additionally, most nematocyst analysis in *C. barnesi* has been conducted only in the adult medusa (Table 6.1), as traditionally wild caught adults were the only specimens available to sample. Whilst the *in situ* ecology of the younger polyp stage remains a mystery, specimens are now available in laboratory culture (Courtney et al., 2016) and recent work has now enabled researchers to induce metamorphosis of *C. barnesi* polyps to its free-swimming medusa stage (chapter three; O'Hara & Seymour, 2022). The current project additionally aimed to conclusively characterize the nematocysts from various ontogenetic stages spanning both its polyp and medusa body form. Unlike with adult medusa, venom from the polyp and newly detached medusa stages has not yet been analysed, but nematocyst identification is the first step into understanding the venom of these younger life stages.

Along with qualitative results classifying the nematocyst types present in *C. barnesi*, quantitative results will be presented to explore the following null hypotheses:

H_{0a}: The range of nematocyst types (cnidome) does not change between ontogenetic stages in the jellyfish *C. barnesi*.

H_{0b}: The absolute size of nematocysts does not change between ontogenetic stages in the jellyfish *C. barnesi*.

H_{0c}: The range of nematocyst types (cnidome) does not change between body parts (bell or tentacle) in the jellyfish *C. barnesi*.

H_{0d}: The absolute size of nematocysts does not change between body parts (bell or tentacle) in the jellyfish *C. barnesi*.

6.3 Methods

6.3.1 Jellyfish collection

C. barnesi samples were collected over three ontogenetic stages: polyp, newly detached medusa and adult medusa (fig 6.1). Polyps were bred in culture at James Cook University, Cairns in BiOrb tanks. Polyps adhered to tank walls and substrate and were collected by gently detaching the polyp base with a plastic transfer pipette. Polyps were induced to metamorphose into medusa with 1 µM of 5-methoxy-2-methylindole for 24 hours (chapter three; O'Hara & Seymour, 2022). Newly detached medusa were collected with a plastic transfer pipette. Adult medusa were wild caught, collected from water surrounding Double Island and Haycock Island, North Queensland, Australia, during the wet seasons of 2019-2024. Sample collection occurred after sunset, whereby adult medusa were attracted to waterproof LED lights suspended in the water from a boat. Medusa were collected from the water with a net, then transferred into individual specimen containers.

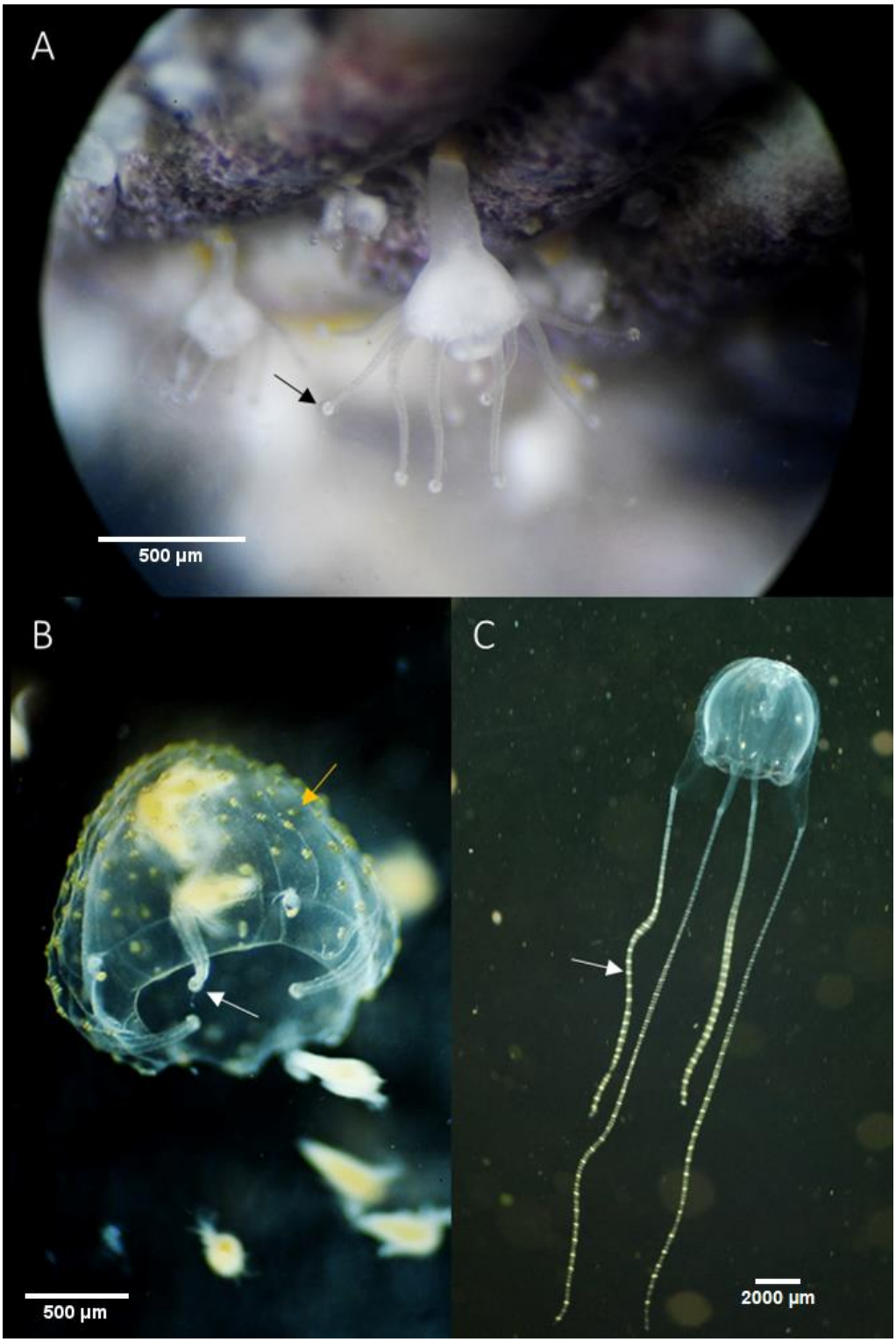

Figure 6.1: Three life stages of the Irukandji jellyfish *Carukia barnesi*. A: Mature polyp, pictured adhered to a snail shell. The bulbous tentacle tips (black arrow) contain the mature nematocysts. B: The newly detached/juvenile medusa, pictured ingesting Artemia sp. The bulbous tentacle tips (white arrow) and bell warts (or mammilations)(yellow arrow) contain the mature nematocysts. C: Adult medusa. Tentacular bands/neckerchiefs (white arrow) and bell warts (not indicated) contain the mature nematocysts. Photo credit A/B: Emily O'Hara (author), C: Prof. Jamie Seymour.

6.3.2 SEM Sample fixation

Samples for scanning electron microscopy (SEM) were either prepared attached to coverslips or in solution. A minimum of 40 polyp specimens, 40 newly detached medusa and ten adult medusa were analysed with SEM. Thermanox coverslips culture treated on one side for enhanced cell attachment were used to ensure continued adhesion of nematocysts during sample preparation. Most samples were processed from fresh specimens (as above), however one adult medusa was processed from frozen at -80 °C. Live specimens were relaxed in a 0.36M $MgCl_2$ solution in RO water, to a final 1:1 $MgCl_2$ solution:seawater. Specimens were then rinsed with autoclaved natural seawater (not freshwater – this caused tissue contraction from osmotic stress) filtered through a 0.22 µm syringe filter to ensure they were as clean as possible.

For fixing on coverslips: Whole polyps and newly discharged medusa were pipetted onto the coverslips. Adult medusa were dissected into bell and tentacles which were further dissected into smaller sections, before being placed onto Thermanox coverslips. All liquid was removed from the coverslip and briefly left to evaporate in a fumehood. 100% ethanol was then pipetted onto samples to discharge the nematocysts within the tissue, this was allowed to briefly evaporate and repeated 2-3 times. Nematocyst discharged from within the tissues could be seen under a light microscope with tubules adhered to the cover slip surface. Some tentacle samples were gently probed with forceps as the slight movement can cause the nematocyst capsule to detach from the tissue and be fully visible on cover slip. The entire coverslip was then fixed in glutaraldehyde solution (3% glutaraldehyde in Sorensen's phosphate buffer, pH 7.2) and kept refrigerated at 4 °C until further processing.

For in-solution fixing: Whole polyps and newly discharged medusa were placed either individually or in small aggregations in 2 mL Eppendorf tubes. Adult medusa were dissected into bell and tentacles which were further dissected into smaller sections, and similarly placed either individually or in small aggregations in 2 mL Eppendorf tubes. As much liquid as possible was removed from tubes using a micropipette and 100% ethanol was added to fully immerse samples to discharge nematocysts. Samples were split either individually or into small aggregations prior to addition of the ethanol to avoid the nematocysts attaching to each other and neighbouring biological tissue upon discharge. . Ethanol was removed with a micropipette and samples fixed in glutaraldehyde solution (3% glutaraldehyde in Sorensen's phosphate buffer, pH 7.2) and kept refrigerated at 4 °C until further processing.

6.3.3 SEM preparation

For both coverslip and samples in solution, the fixative was removed and samples washed in 0.1M cacodylate buffer three times for five minutes. A 1% osmium tetroxide solution was added to samples and left at room temperature for one hour, then washed in milliQ water three times for five minutes. Samples were then dehydrated with a graded ethanol series: 30% and 50% for 15 minutes at each concentration then left in 70% overnight. The next day a further graded ethanol series of 80% and 90% for 15 minutes each was applied. 100% ethanol was then added and exchanged three times for 15 minutes each.

Samples were then either critical point dried using a coverslip holder and/or individual baskets, or treated further to dry in HMDS as follows: 2:1 solution of ethanol:HMDS for 15 minutes, then exchanged for a 1:1 solution of ethanol:HMDS for 15 minutes, then exchanged for a 2:1 solution of HMDS:ethanol for 15 minutes, then exchanged to a final concentration of 100% HMDS for 15 minutes repeated three times, finally leaving samples overnight for HMDS to evaporate.

6.3.4 SEM processing

Samples were sputter coated with platinum, then imaged using scanning electron microscopy with a Hitachi SU5000 FE-SEM (field emission) at 5kV accelerating voltage. Acquired images were saved as TIFF files with scale bars automatically embedded onto the images.

6.3.5 Post SEM processing

SEM image acquisition is only available in black/white/greyscale. However, studies herald the idea that the addition of colour often results in a differentiation between subject and background which aids in the illustration of a specimen, and many of the aesthetic qualities of a photograph taken with visible light are possible by applying colour (Antonovsky, 1984). The background visuals in our nematocyst images are often turbulent due to the nature of imaging from biological tissue samples and not purified extracts as possible in some other fields. In this work false colour was added to some SEM TIFFs to distinguish prominent nematocysts and/or identifying features from other visuals in the image. False colour was added in post-production to SEM TIFF files in Adobe Photoshop (2022 23.2.2 release) via a combination of 1) manipulating the colour balance options, and 2) manually assigning colour to image regions with the “colorize” neural filter.

6.3.6 Light Microscopy sample preparation

Light microscopy is a necessary addition to SEM to fully identify nematocysts, especially for visualising the internal structures of undischarged capsules. Whilst SEM can visualise structures to a higher resolution and magnification, it only images the surface of a sample. Nematocyst

identifications require accompanying light microscope to visualise the internal features of undischarged capsules, that cannot be seen with SEM. Most samples were prepared from freshly harvested tissue; however, some samples were fixed due to specimen availability.

Fresh discharged nematocysts: Whole polyps, newly detached medusa and adult medusa were relaxed in a 0.36M $MgCl_2$ solution in RO water, to a final 1:1 $MgCl_2$ solution:seawater ratio. Two methods were used to induce nematocyst discharge: 1) a squash preparation was made by sandwiching the tissue between a glass microscope slide and cover slip, and exerting pressure by hand to squash the tissue. This is a common method in nematocysts preparation, the physical pressure discharges the nematocysts and also results in an even thin layer of tissue for good microscope optics (Note this method does not work with nematocysts in the adult medusa bell tissue); 2) 100% ethanol was added directly to tissue samples, causing mass nematocyst discharge. Preparations discharged by both methods were used to visualise discharged nematocysts for ID purposes only. Nematocyst capsules are known to change size slightly upon discharge, so no discharged capsules were used for measurement data collection.

Fresh undischarged nematocysts: Whole polyps, newly detached medusa and adult medusa were relaxed in a 0.36M $MgCl_2$ solution in RO water, to a final 1:1 $MgCl_2$ solution:seawater ratio. Polyps and newly detached medusa were used whole, adult medusa were dissected into bells and tentacles, then further into smaller tissues pieces for ease of handling (tentacles) and to flatten out curved body parts (bell). All samples were placed on a glass microscope slide with a coverslip. These undischarged samples would be used to obtain count, measurement and identification data.

Fixed undischarged nematocysts: Adult *C. barnesi* medusa were not available at all times throughout the year and preserved specimens from the Seymour Lab collection at James Cook University, Cairns (collected between 03/02/2016 – 07/02/2016 from Double Island, Cairns, Australia) were used when required. Medusa had been preserved first in 4% formalin, then transitioned to permanent storage in 100% ethanol. Five biological replicates of these fixed specimens were used, sized between 5.6 - 10.8 mm interpedalial distance (IPD) and 7.1 - 17.7 mm bell height. Note, some IPD sizes from preserved samples may be slightly (<2 mm) smaller than biological actuality due to tissue contraction during fixation. The preservation process unfortunately causes jellyfish tissue to become opaque and can make for challenging optics in microscopy and these samples were not used for nematocyst identification imaging purposes (it was not possible to visualise the finer ultrastructure) but were still used for count and measurement data. All samples were placed on a glass microscope slide with a coverslip.

6.3.7 Light microscopy processing

All light microscopy was conducted using a Zeiss Axioimager, with image capture and analysis using the software Zen (blue edition) by Zeiss, Version: 3.5.093.00002. Nematocyst counts, along with capsule length and width was measured in Zen directly from captured images. Ten polyp replicates were used, with 50 nematocysts catalogued from each. Ten newly detached medusa replicates were used, with 50 bell nematocysts and 50 tentacle nematocysts catalogued from each. Five adult medusa replicates (fixed) were used due to both the opaque nature of fixed tissue and the relative lack of bell nematocysts present in the adults, all (between 40-200) visible bell nematocysts were catalogued for each replicate; and 50 tentacle nematocysts were catalogued from each replicate.

6.3.8 Qualitative data

Nematocyst identification: Nematocyst identification was conducted primarily using the nomenclature and classification system by Östman (2000), in conjunction with personal communication to said author (CO). This author (EO) transcribed the Östman classification system published in paragraph form (Östman, 2000) into a flow chart for ease of use in the identification process (fig 6.2). Identifications were made based on organelle ultrastructure visualised from both light and scanning electron micrographs, of both discharged and undischarged cnidae. Fig 6.3 illustrates some of the finer identifying features used in the identification process.

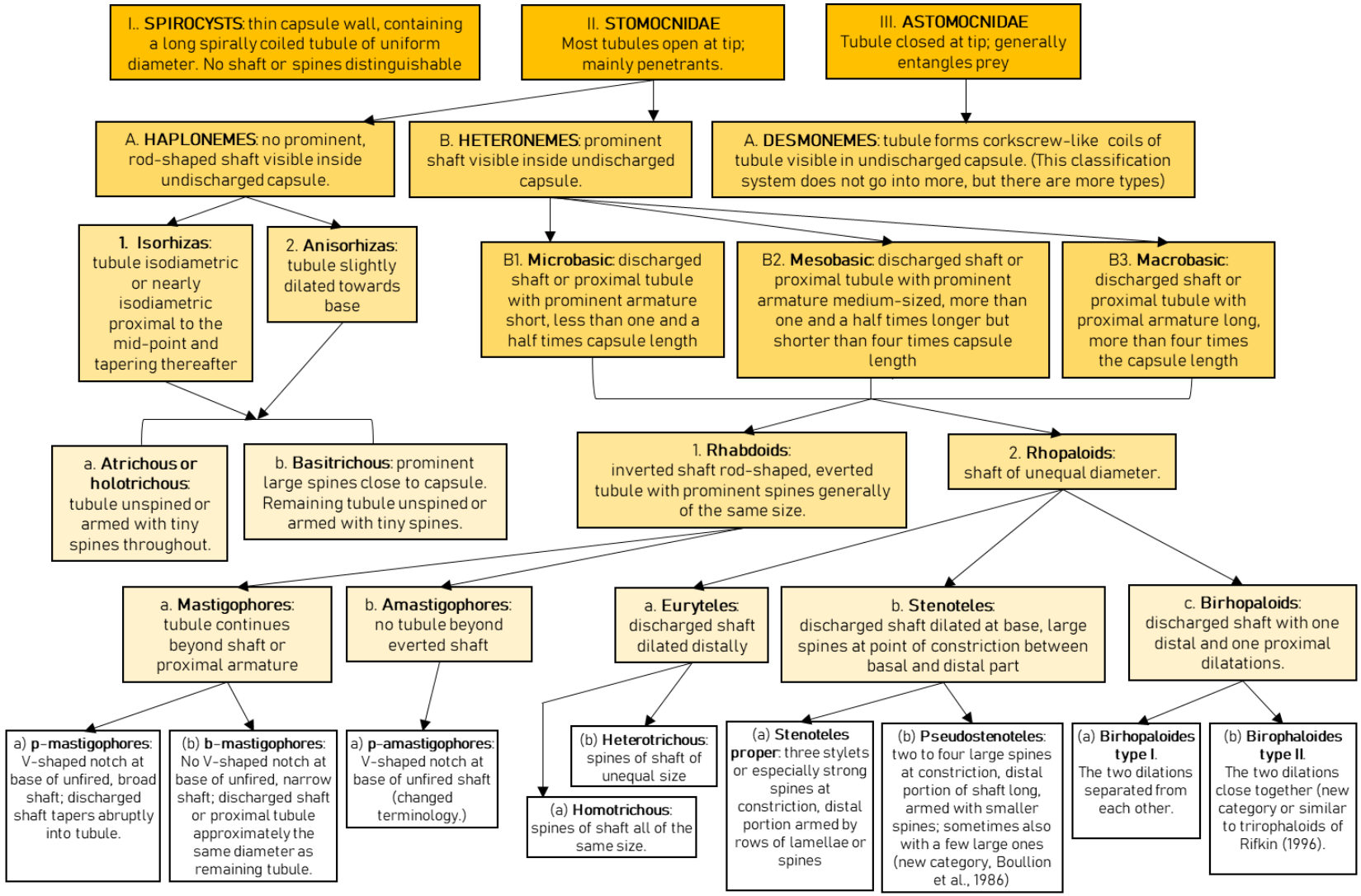

Figure 6.2: Nematocyst identification system. Classification system developed and presented in paragraph form by Östman (2000) transcribed into a flowchart form by this author (EO) for ease of use.

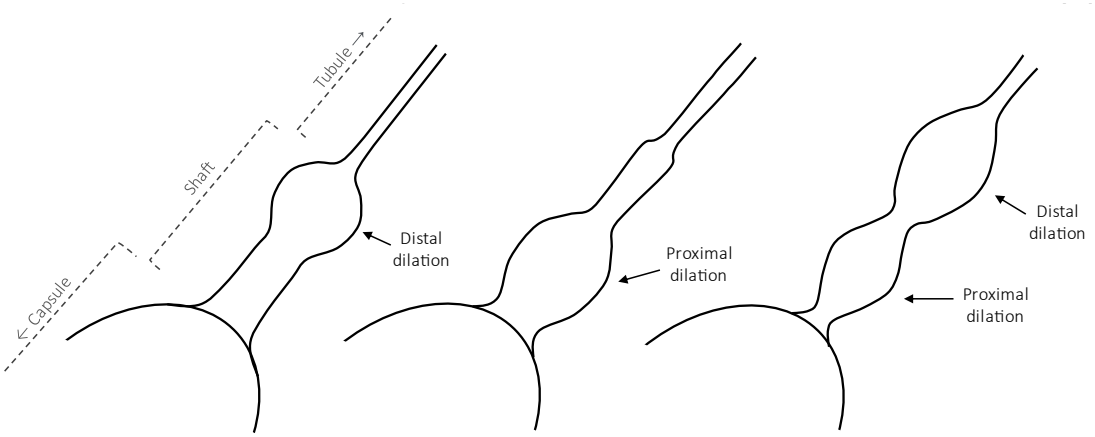

Figure 6.3: Illustration of ultrastructural dilations of cnidae shafts. Dilations being points of enlargement, expansion, or widening. Proximal (dilation) meaning closer to the shaft origin – the capsule; distal (dilation) meaning further away from the shaft origin – the capsule. Diagram created by the author (EO) from nomenclature used in Östman's (2000) cnidae classification system. Note: any shaft and/or tubule spines were omitted from illustrations for diagram clarity.

6.3.9 Quantitative data

Nematocyst sizes and proportions: Size measurements and nematocyst type counts were taken from light microscopy images (see above) analysed in the Zen software (blue edition) by Zeiss, Version: 3.5.093.00002. All quantitative data analsysis was conducted using the IMB SPSS Statistics, Version: 28.01.0 (142) software. Nematocyst volume was chosen over the traditional length/width measurements which are often included in nematocyst data, as capsule volume presents more ecological relevance in the form of a value for maximum venom content. The below formulas were used to calculate nematocyst volume.

For spherical capsules:

$$V = \frac{\left(\frac{4}{3}\pi * r^3\right)}{10^9}$$

Where *V* is Volume (µL) and *r* is radius (µm)

For ellipsoid capsules:

$$V = \left(\frac{\left(\frac{4}{3}\pi\right) * \left(\frac{l}{2}\right) * \left(\frac{w}{2}\right) * \left(\frac{w}{2}\right)}{10^9} \right)$$

Where *V* is Volume (µL), *l* is length (µm) and *w* is width (µm)

Size data: Not all of the nematocyst volume data (per body part, per life stage) was normally distributed (Kolmogorov-Smirnov P <0.05), therefore non-parametric tests were used for the statistical analysis. The Kruskal Wallis test was used to compare >2 sets of data and the Mann Whitney U-test was used where there were only 2 sets of data to compare.

Count/proportion data: To analyze the proportions of nematocyst types Pearson's chi-square tests were used to test for association between nematocyst type and life stage and/or body parts.

Fluorescence intensity: Newly detached medusa exhibited some undischarged cnidae that were too small for visualisation of the internal structures with light microscopy and did not discharge in squash preparations, nor with the application of ethanol, and were unable to be identified by ultrastructure. Alegaldine A is a pH dependent fluorescent stain, which can be used to determine the relative maturity of cnidae as their pH changes as they mature (Obermann et al., 2012). Ageladine A was used to determine, via relative fluorescence intensity, if the small cnidae were a different type to the larger cnidae observed, or if they were simply immature versions of the same type (the latter was suspected given the lack of discharge with ethanol). Newly detached medusa were added to 1 M Sodium Citrate solution for 15 mins-1 hour at room temperature, before being gently pipetted up and down with a 3 mL transfer pipette to encourage cnidae dissociation from the tissue and was then strained through a 70 µm cell strainer. The strained solution was briefly spun in a benchtop centrifuge at 12500 g to form a pellet of nematocysts and the supernatant discarded. As per (Obermann et al., 2012) we added a 1 mM stock solution of Ageladine A to seawater at a 1:100 ratio, so 12.5 µL:1250 µL. The nematocyst pellet was then resuspended in this solution and left in the dark for 60 mins. The solution was again centrifuged to form a pellet and the supernatant discarded, and the nematocysts resuspended in clean seawater. This nematocyst solution was then imaged on a Zeiss Axioimager using the DAPI filter cube. Ageladine A fluorescence specifications were parameters which can be visualised using the DAPI filter cube : excitation 325 – 415nm, maximum at 370nm; emission 415 – 500nm, maximum at 415nm. Using the software Zen (blue edition) by Zeiss, Version: 3.5.093.00002 fluorescent intensity was collected for spherical/elliptical areas on each image, which the software computes as a mean value termed “intensity mean value”, a unitless number. Eight image replicates were analysed

and intensity values were collected for at least ten background areas and all visible in focus cnidae per image (fig 6.4). The average value was then calculated from the 10 background 'intensity mean values' taken, and this was subtracted from each individual nematocyst 'intensity mean value' per image to calculate the final fluorescence intensity for each nematocyst. The fluoresce intensity data was normally distributed (Kolmogorov-Smirnov *P* >0.05); however, due to differing sample sizes between replicates equal variances were not assumed (Levene's test for equal variance *P* <0.05), and the Welch's *t*-Test (also known as the Unequal Variance *t*-Test) was used to analyse fluorescence intensity data. Statistical data analysis was conducted using the software IMB SPSS Statistics, Version: 28.01.0 (142).

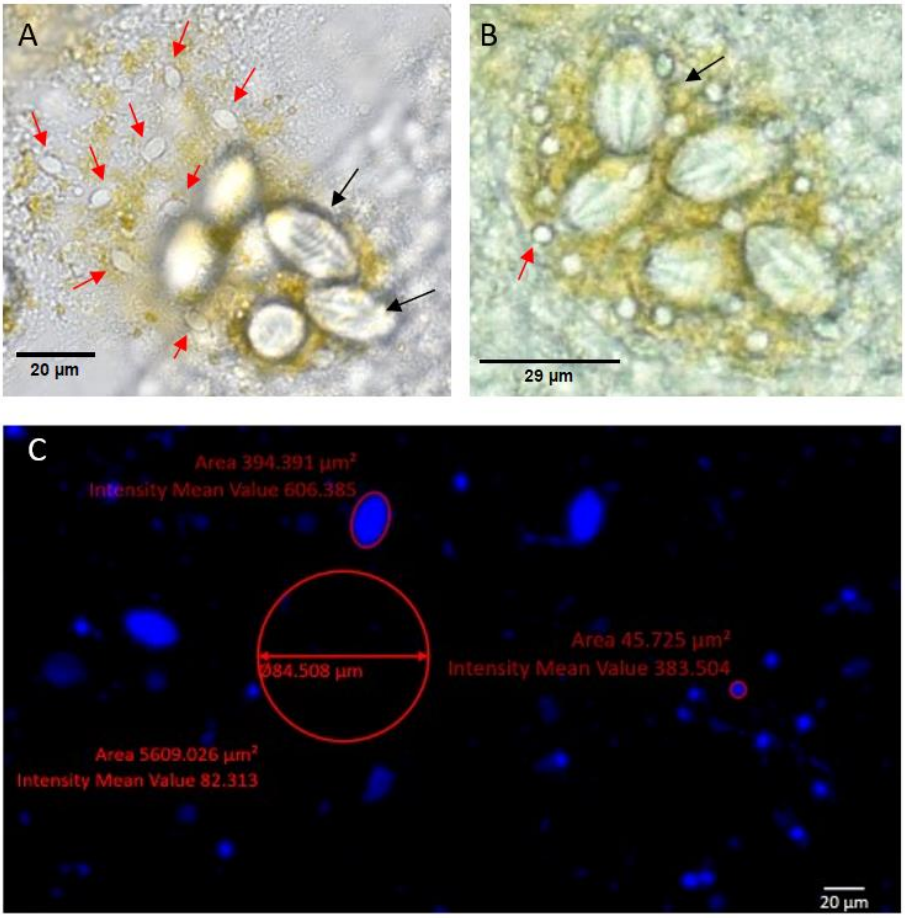

Figure 6.4: Example data collection using Ageladine A fluorescent stain. A/B: Small cnidae (red arrows) and larger cnidae (black arrows). C: Small and large cnidae stained with Ageladine A, fluorescing blue when imaged with a DAPI filter cube. Example data collection in red, depicting florescence intensity mean value for both large and small cnidae and areas of background.

6.4 Results

6.4.1 Qualitative analysis from light microscopy and scanning electron microscopy data

All the microscopy images of nematocysts exhibiting ultrastructural features used in nematocyst type identification are presented. The following identifications were made for the cnidome of *Carukia barnesi* over 4 different life stages (polyp, newly detached medusa, adult medusa and one rarer specimen of an older adult medusa) and two body parts (tentacle and bell (where applicable)).

Confirmed cnidae:

Type 1: stomocnidae→ heteronemes →microbasic → rhopaloids →tumitele→homotrichous

Classification description: Most tubules open at the tip → prominent shaft visible inside undischarged capsule → discharged shaft or proximal tubule with short prominent armature short, less than one and a half times capsule length → inverted shaft of unequal diameter → "tumitele" being a newer class of Rhopaloids described by Southcott (1967), currently only observed in the Carybdeidae. This is a microbasic rhopaloid which fits into neither of the usual classes (eurytele, stenotele or birhopaloids (Östman, 2000)), with a discharged shaft singularly dilated neither distally nor proximally, only in its middle→ The dilation of the shaft bears a collection of uniform spines all the same size

These were found in the polyp tentacles (figs 6.5,6.6,6.7), newly detached medusa tentacles (figs 6.8,6.9) and bell (fig 6.11) and the adult medusa tentacles (6.13,6.14), and very rarely but still present in the adult bell (fig 6.15).

Type 2: stomocnidae →haplonemes →O-isorhizas→holotrichous

Classification description: Most tubules open at the tip→no prominent, rod-shaped shaft visible inside undischarged capsule→O-refers to the spherical shape of capsule, isorhizas- tubule isodiametric or nearly isodiametric tubule armed with spines throughout.

These were found in the newly detached medusa bell (fig 6.10) and the adult medusa bell (fig 6.16).

Type 3: stomocnidae →heteronemes* →microbasic →rhabdoids→mastigophores→b-mastigophores**→ atrichous or holotrichous.

Classification description: Most tubules open at the tip → prominent shaft visible inside undischarged capsule →Discharged shaft or proximal tubule with prominent armature short, less than one and a half times capsule length inverted shaft rod-shaped**, everted tubule with

prominent spines generally of the same size→tubule continues beyond shaft or proximal armature→No v-shaped notch at base of unfired narrow shaft**;discharged shaft proximal tubule approximately the same diameter as remaining tubule tubule unspined or armed with tiny spines throughout. These nematocysts are almost certainly the latter, however debris present on the SEM prepared tubules prevents a conclusive identification.

* indicates where the whole definition for that classification level refers to undischarged capsules visualised with light microscopy, which was not possible with this single specimen. This classification level is assumed as we can confidently assign lower classification levels which follow on from this.

** indicates where part of the definition for that classification level refers to undischarged capsules visualised with light microscopy which was not possible with this single specimen. We have confidently assigned this classification based on the identifying features of the discharged capsules which make up half of this classification definition, in addition to our samples possessing features which do not fit into any remaining categories.

These were found in one rarer specimen of an older adult medusa (figs 6.18 and 6.20)

Potential/Unconfirmed cnidae:

Type 4: stomocnidae →haplonemes → isorhizas (ellipsoid)→atrichous

Classification description: Most tubules open at the tip→ prominent, rod-shaped shaft visible inside undischarged capsule→tubule isodiametric or nearly isodiametric (capsule ellipsoid in shape) tubule unspined.

These were found in the adult medusa bell (fig 6.17), and were classified above based on sperate images of discharged tubules and potentially (undischarged cnidae), however their status as true cnidae remains unconfirmed.

Type 5: Small mastigophore or haploneme (elongate)

These may potentially be small versions of Type 3, differing only in that there is no prominent armature visible on the shaft. Although, an inability to confirm the presence of a shaft may suggest these are small haplonemes. These were found in one rarer specimen of an older adult medusa (fig 6.18).

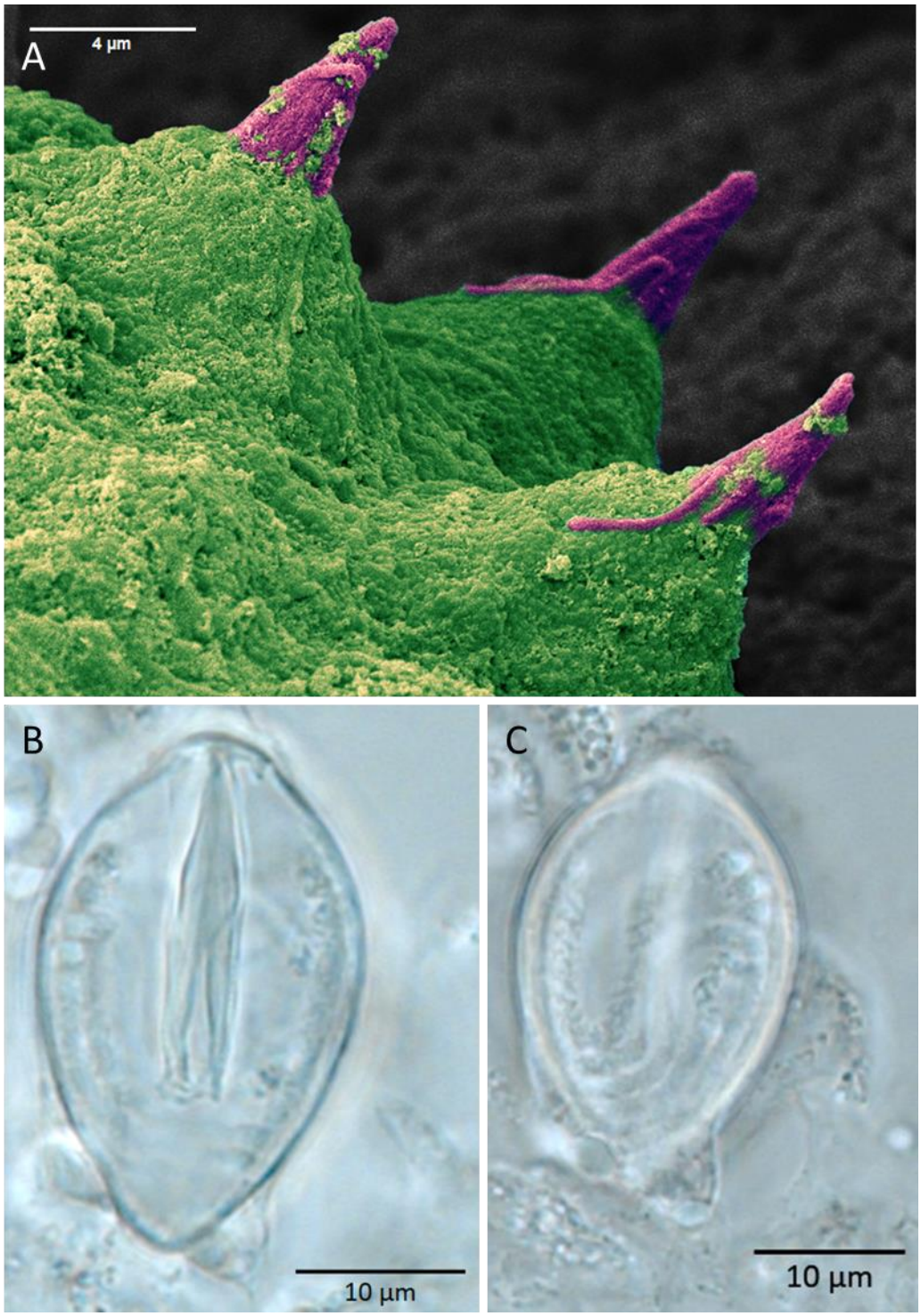

Figure 6.5: Undischarged tumiteles from the tentacles of *Carukia barnesi* polyps.

A: Cnidocils protruding from tentacle tip (False colour SEM). Sterocilia surrounding the cnidocil may be visible. B: Undischarged tumitele (LM), Operculum (lid) is visible at the apex of the capsule, at which the long spines inside the inverted shaft point at. The inverted tubule with tubule coils is faintly visible within the capsule. C: Varying focal depth to B, coiled tubule within capsule is more visible.

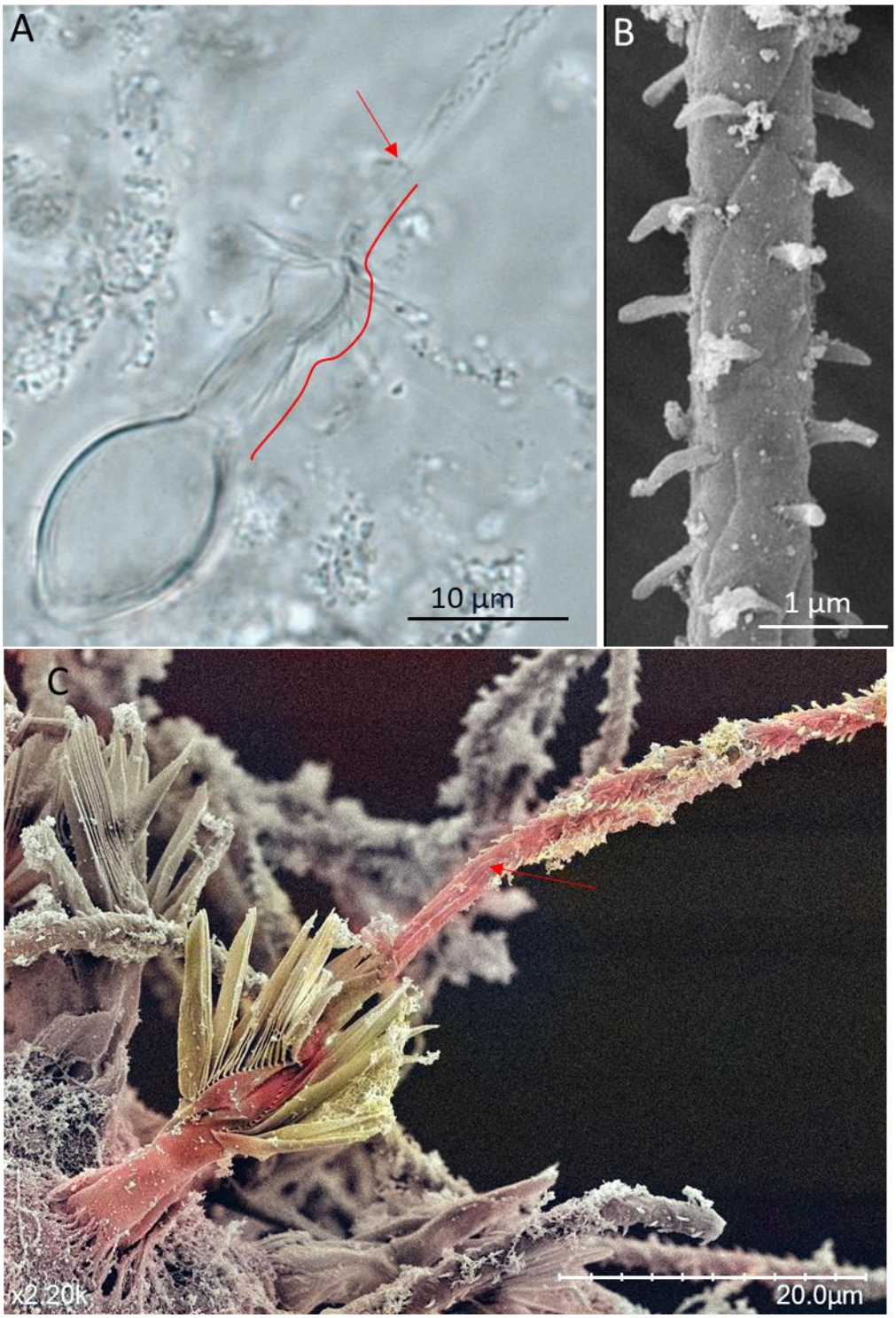

Figure 6.6: Discharged tumiteles from the tentacles of *Carukia barnesi* polyps.

A: Discharged tumiteles (LM). Arrow indicates start of small, triangular-shaped spines on distal tubule. Red line depicts shape of dilations of the shaft. B: Spines helically organized on discharged tumiteles tubule (SEM). C: Discharged tumiteles with large shaft spines (false colour SEM), arrow indicates beginning of spines on distal tubule.

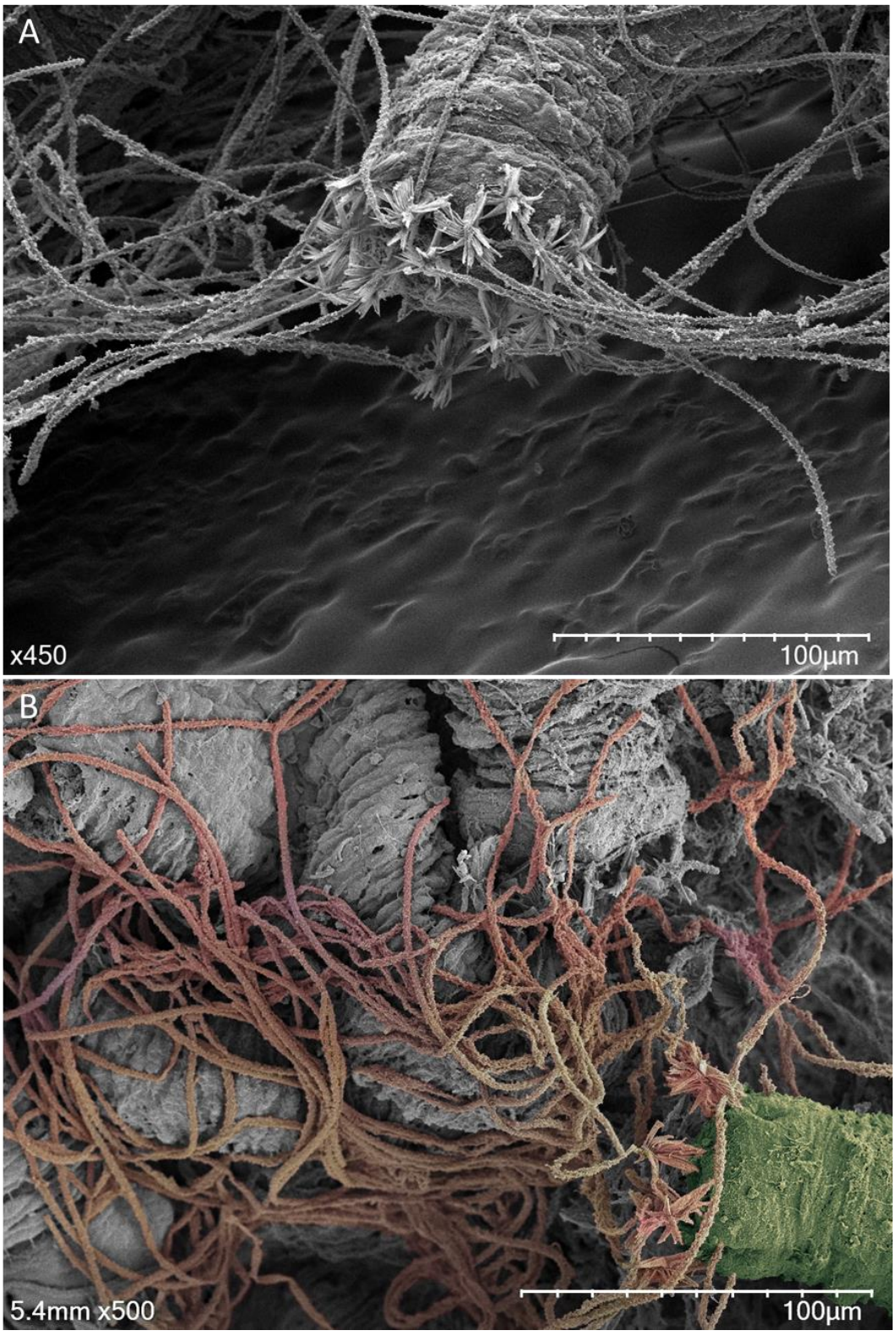

Figure 6.7: Discharged tumiteles from in tentacle tips of *Carukia barnesi* polyps (SEM) showing shafts with large spines and tubule armed with small spines.

A,B: Discharged tubules freely around tentacle tip. B: Cnidae tubules (false colour) attached onto a neighbouring polyp bodies (grayscale) with lots of coiled distal tubules. Some of the large shaft spines are still pointing forwards, suggesting some spines are not fully discharged.

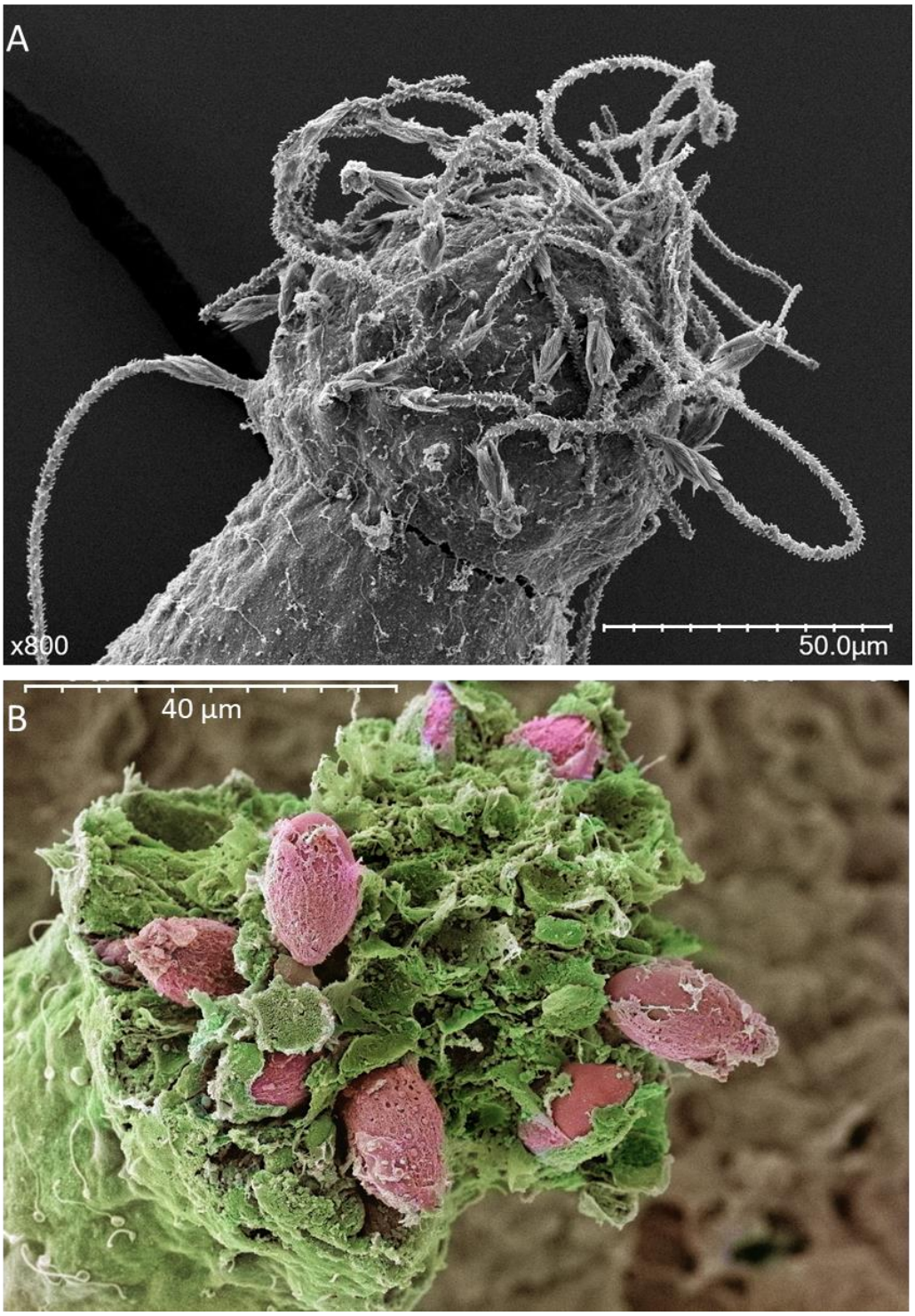

Figure 6.8: Tumiteles from the tentacles of newly detached *Carukia barnesi* medusa (SEM).

A: Discharged tumiteles protruding from tentacle tip. B: Tentacle damaged during SEM preparation reveals undischarged ellipsoid shaped tumiteles situated within the tentacle tip (false colour SEM). The capsule shape - the broad protruding apical capsule and the slightly pointed basal capsule - is the same as that of the Tumitele capsules found in the polyp tentacles.

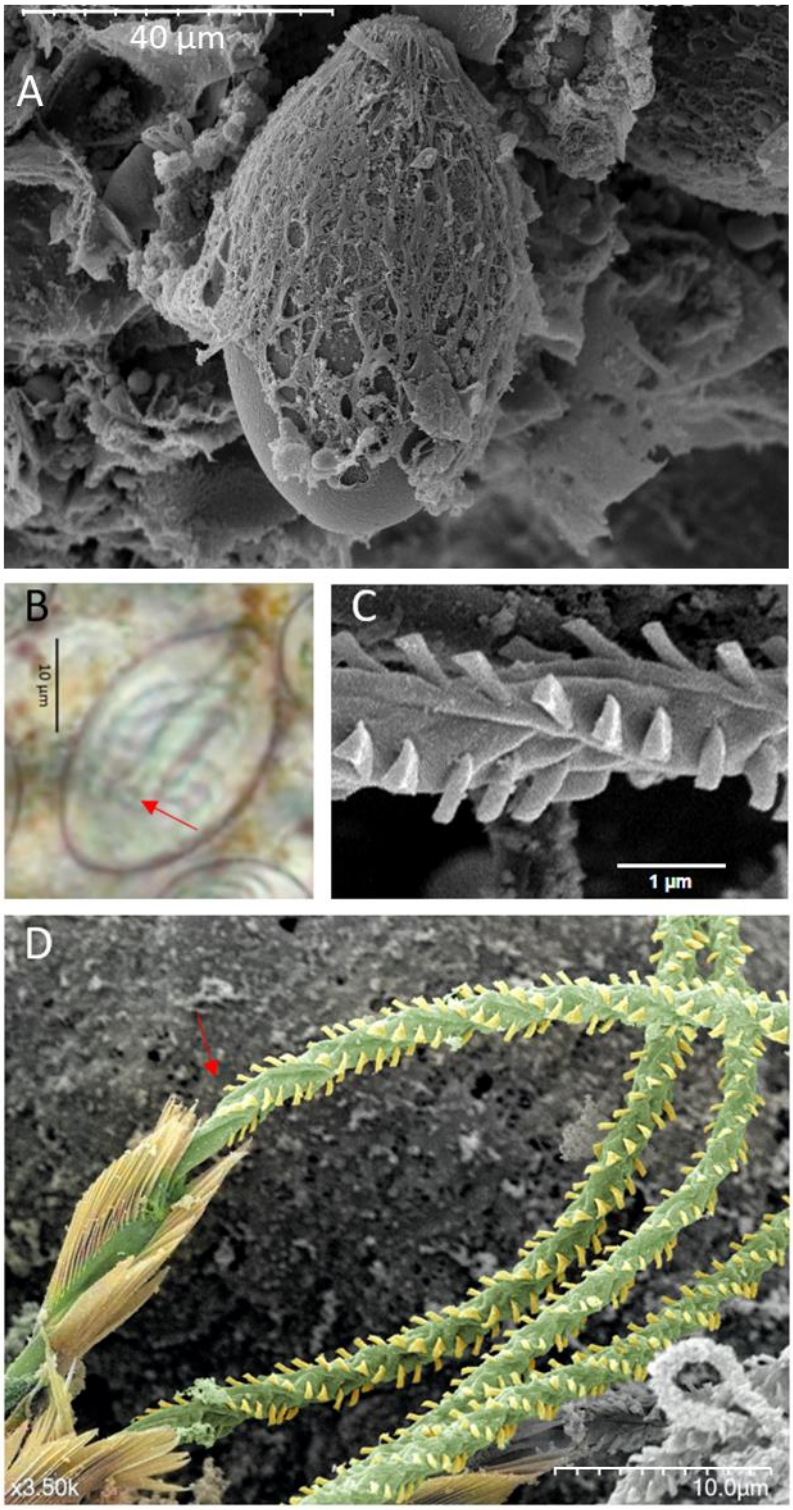

Figure 6.9: Tumiteles from the tentacles of newly detached *Carukia barnesi* medusa.

A: Undischarged ellipsoid shaped tumitele (SEM). B: Undischarged ellipsoid shaped tumitele, coiled tubule and shaft visible within, red arrow indicates V-shaped notch in shaft (LM). C: Spines in helices on discharged distal tubule (SEM). D: Discharged tumitele with large spines on distal shaft (false colour SEM), arrow indicates beginning of barbs on tubule.

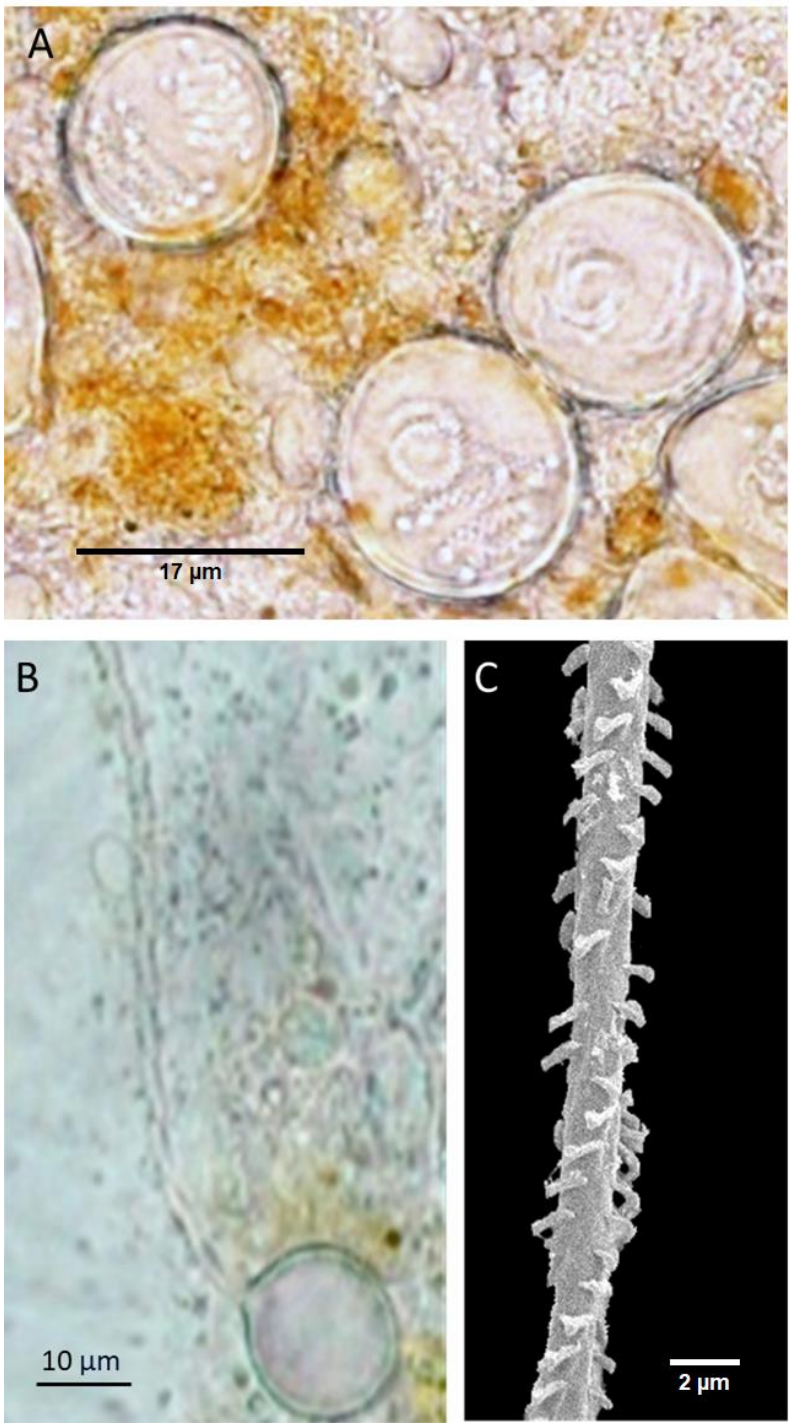

Figure 6.10: Cnidae from the bell of newly detached *Carukia barnesi* medusa

A: Undischarged O-isorhizas and undischarged elliptical tumiteles. The O-isorhiza shows the loosely coiled inverted distal tubule. B: LM of discharged O-isorhizas, showing everted tubule with the typical three helical pattern of the spines. C: SEM of distal tubule of O-isorhizas – no shaft armed with small, broad-based triangular-shaped spines, forming the generally occurring three helices of spines around the tubule. The spines are attached to the distal tubule with its broad base, which form a broad shallow v. Small contamination from the fixation procedure are attached to the tubule and spines.

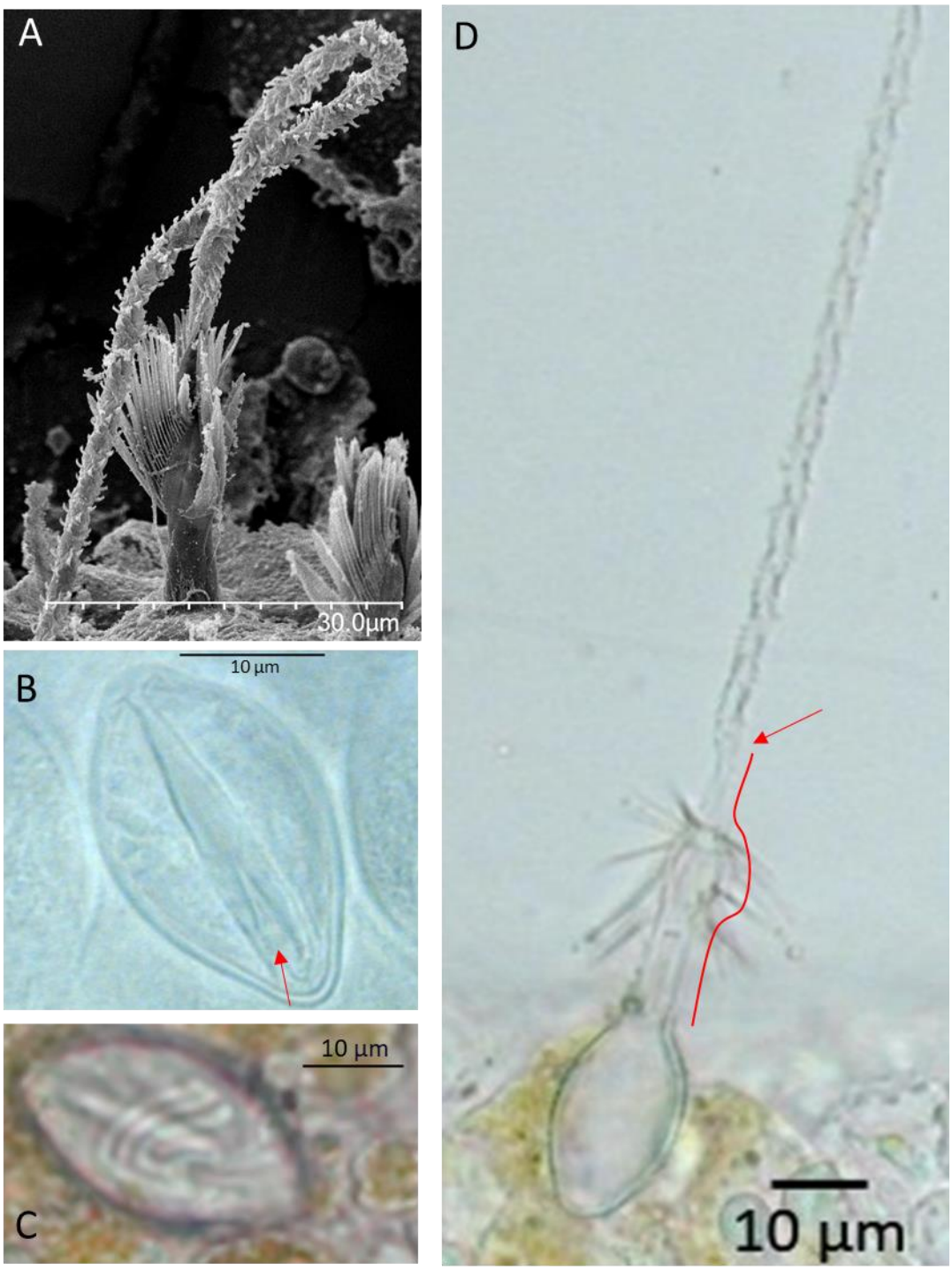

Figure 6.11: Tumiteles from the bell of newly detached *Carukia barnesi* medusa.

A: a discharged Tumitele, 11. seen is a dilation of the shaft armed with large spines still pointing towards tip of distal tubule (SEM). B: Undischarged Tumitele (LM) Arrow indicates v-shaped notch. These elliptical shaped tumiteles show the same capsule shape as the tumiteles in both the polyp and newly detached medusa tentacles. C: Undischarged tumitele (LM), coiled tubule is visible. D: Discharged tumitele, one dilation on shaft. The dilation shape highlighted by red line, arrow indicates the start of small helical spines on the distal tubule.

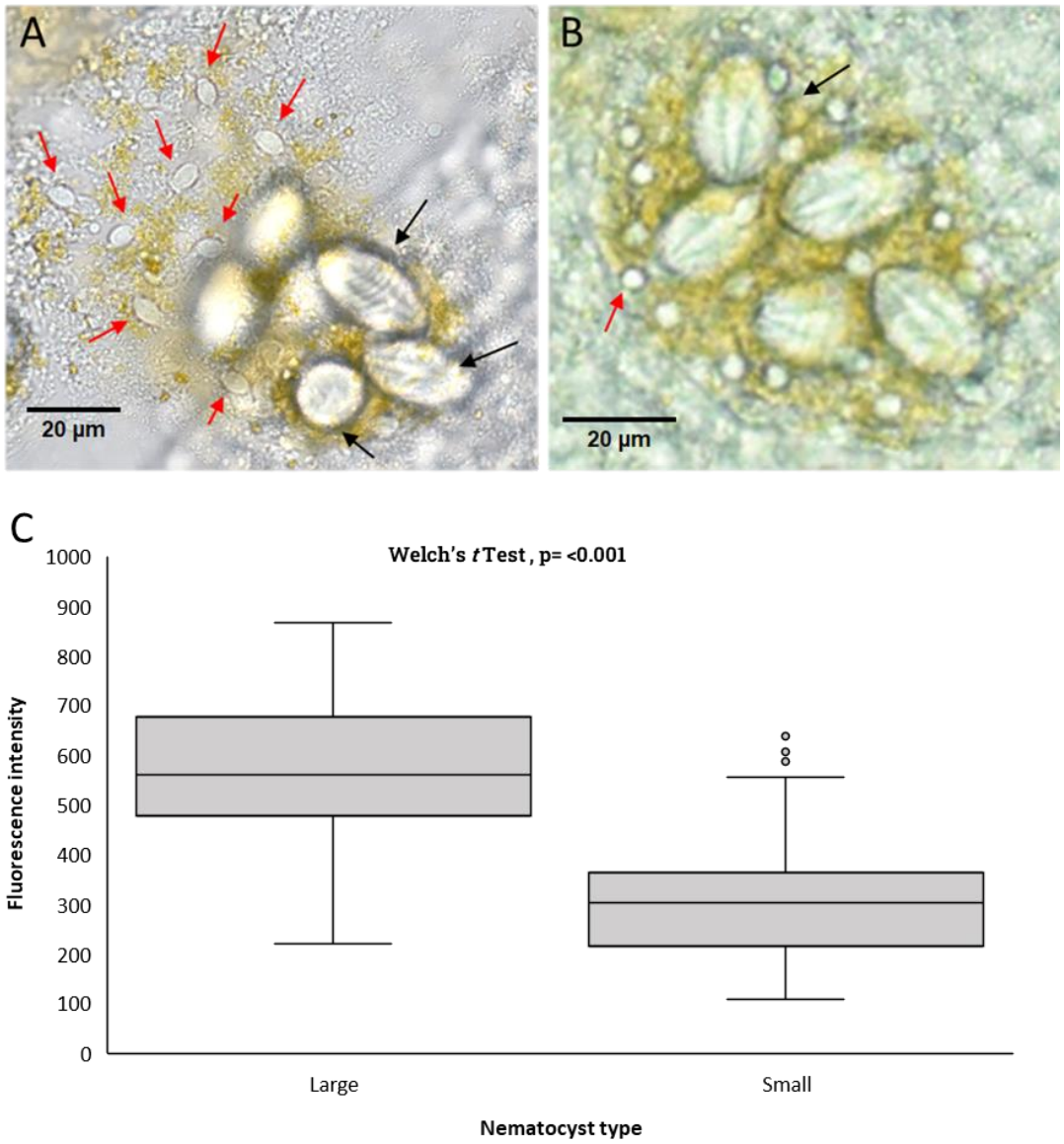

Figure 6.12: Cnidae from the bell of newly detached *Carukia barnesi* medusa.

A,B: Small cnidae (red arrows) are present in the bell warts along with larger cnidae (black arrows). C: Box plot (95% CI) depicting florescence intensity mean value for large and small cnidae when stained with Ageladine-A. Welch's tTest indicates a significant difference between the two fluoresce intensities ($p = <0.001$)

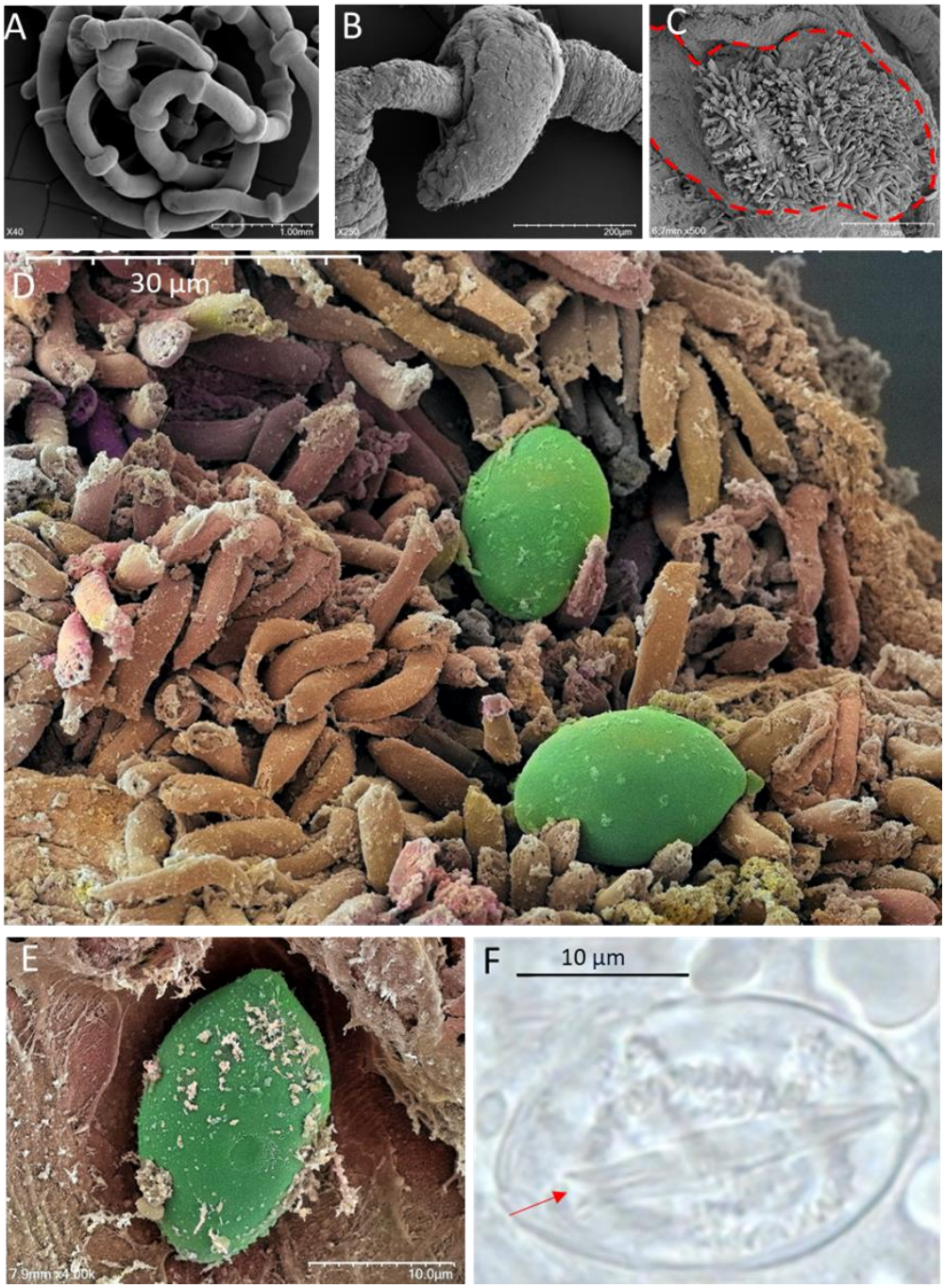

Figure 6.13: Tentacle structure and cnidae from adult *Carukia barnesi* tentacles.

A: Coiled tentacles. Tentacle bands called "neckerchiefs" are interspersed along the length of the tentacles. B,C: Close up of tentacle neckerchief, note flick shape on one side of the band, characteristic of Carukia barnesi. C: Tissue damage (sample was frozen prior to fixation) during SEM preparation has exposed the internal structures of the neckerchief – outlined with red line. Thin elongated structure are presumed to be accessory cells. D: Undischarged tumiteles situated amongst accessory cells, within the tentacle neckerchief. E: Close up of undischarged tumitele, note the broad protruding apical capsule and the slightly pointed basal capsule. F: Undischarged tumitele (LM) red arrow notes V-shaped notch in shaft.

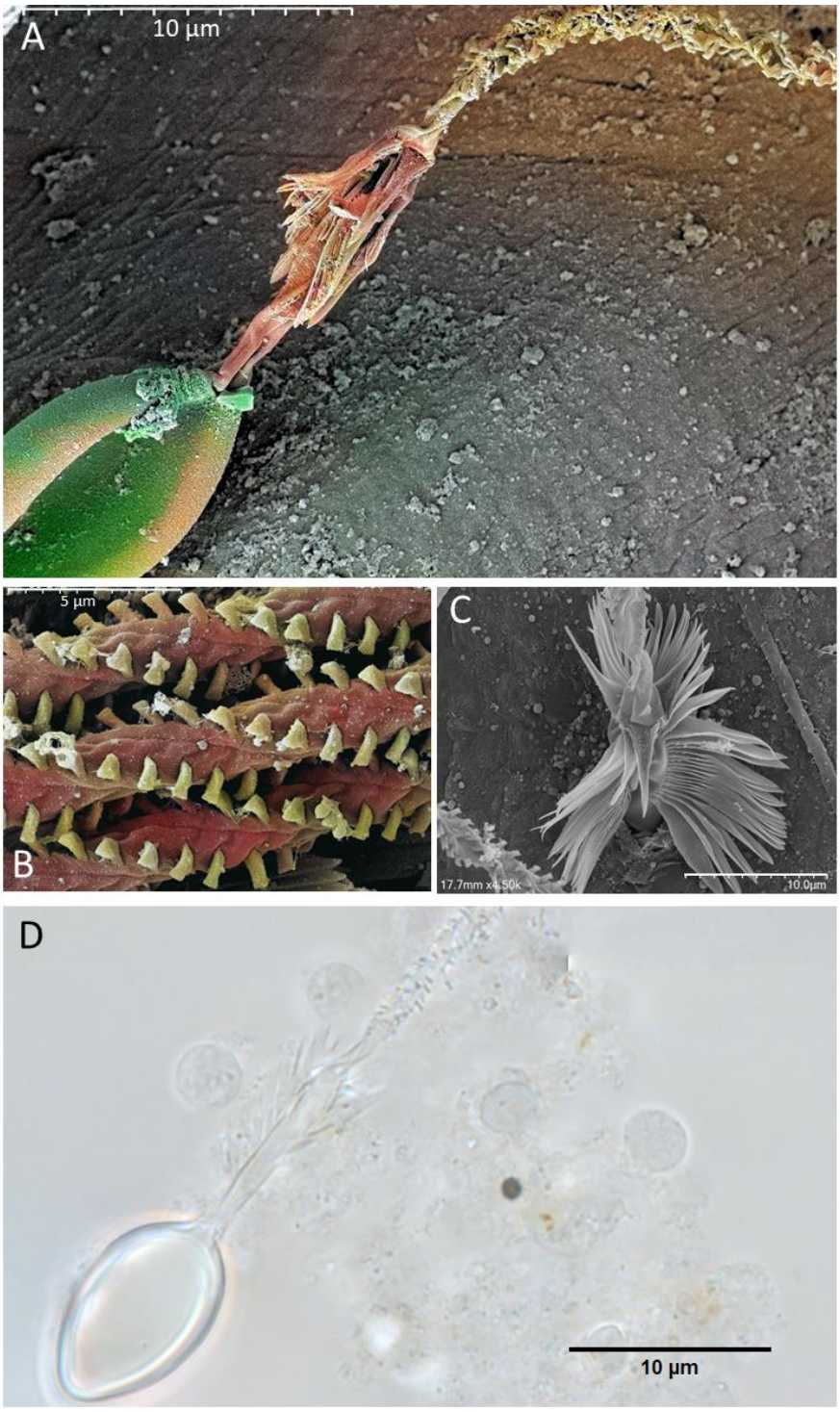

Figure 6.14: Discharged tumiteles in adult *Carukia barnesi.*

A: Discharged tumiteles (SEM) with large homotrich spines on shaft. B: Three discharged distal tubules side by side, armed with small spines in a helical pattern, pointed back towards the capsule. C: Large spines on a discharged shaft, with the capsule still situated within the tentacle tissue. D: LM of discharged Tumitele, the elongate capsules are broader apically compared to the capsule base. Dilation of shaft is less prominent here due to visibility in this focal plane but can be seen in A and C.

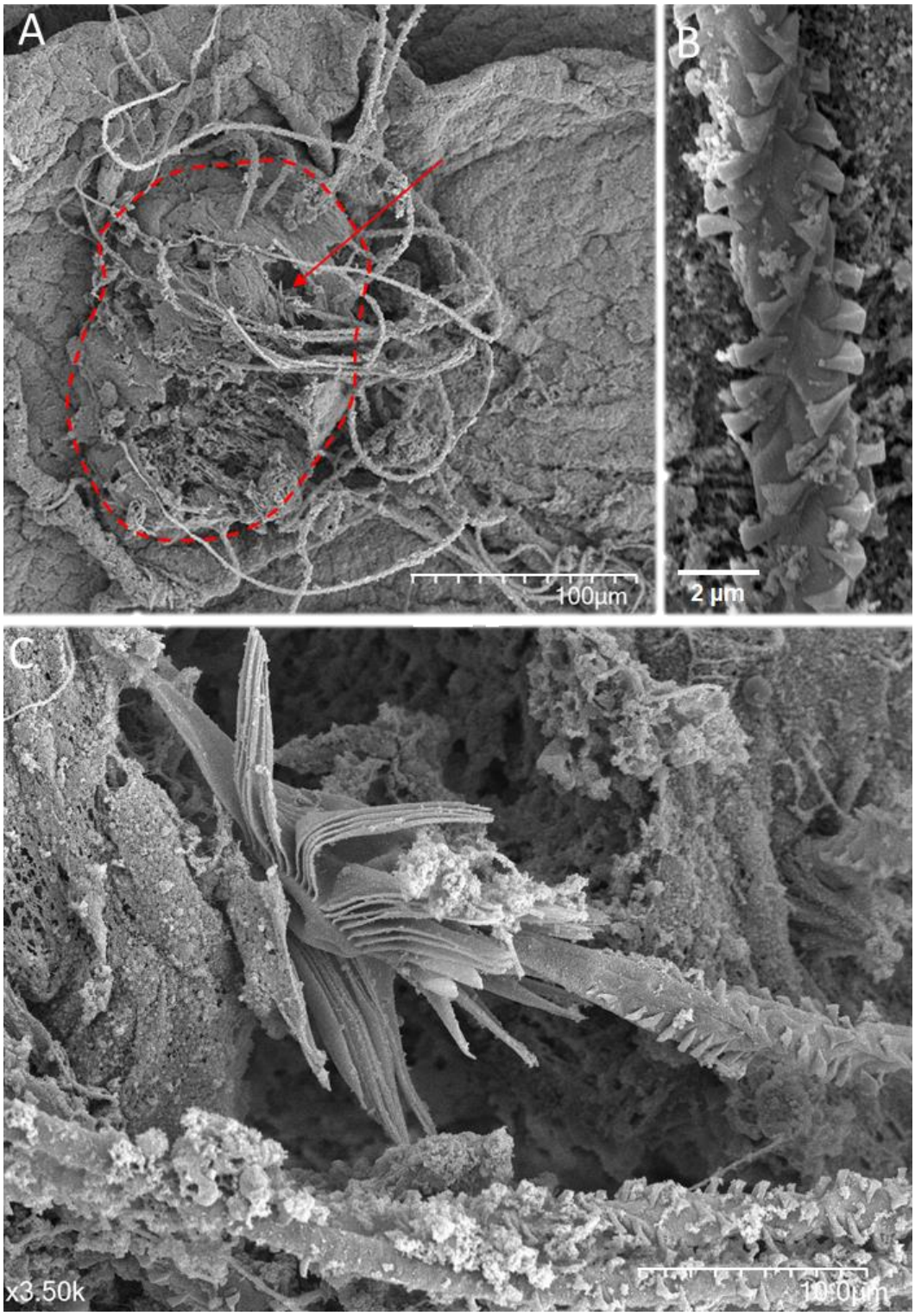

Figure 6.15:Cnidae from the bell of adult *Carukia barnesi* medusa (SEM).

A: bell wart outlined by red dashed line in bell tissue, with discharged tubules. Red arrow indicates the only cnidae present with a shaft with large spines. This is a singular tumitele located within the bell wart. B: Spines and helical structure of discharged Tumitele tubule- as indicated in A. C: SEM of enlarged tumitele indicated in A by arrow, which possesses large broad-based spines on shaft basal to un-spined region of distal tubule.

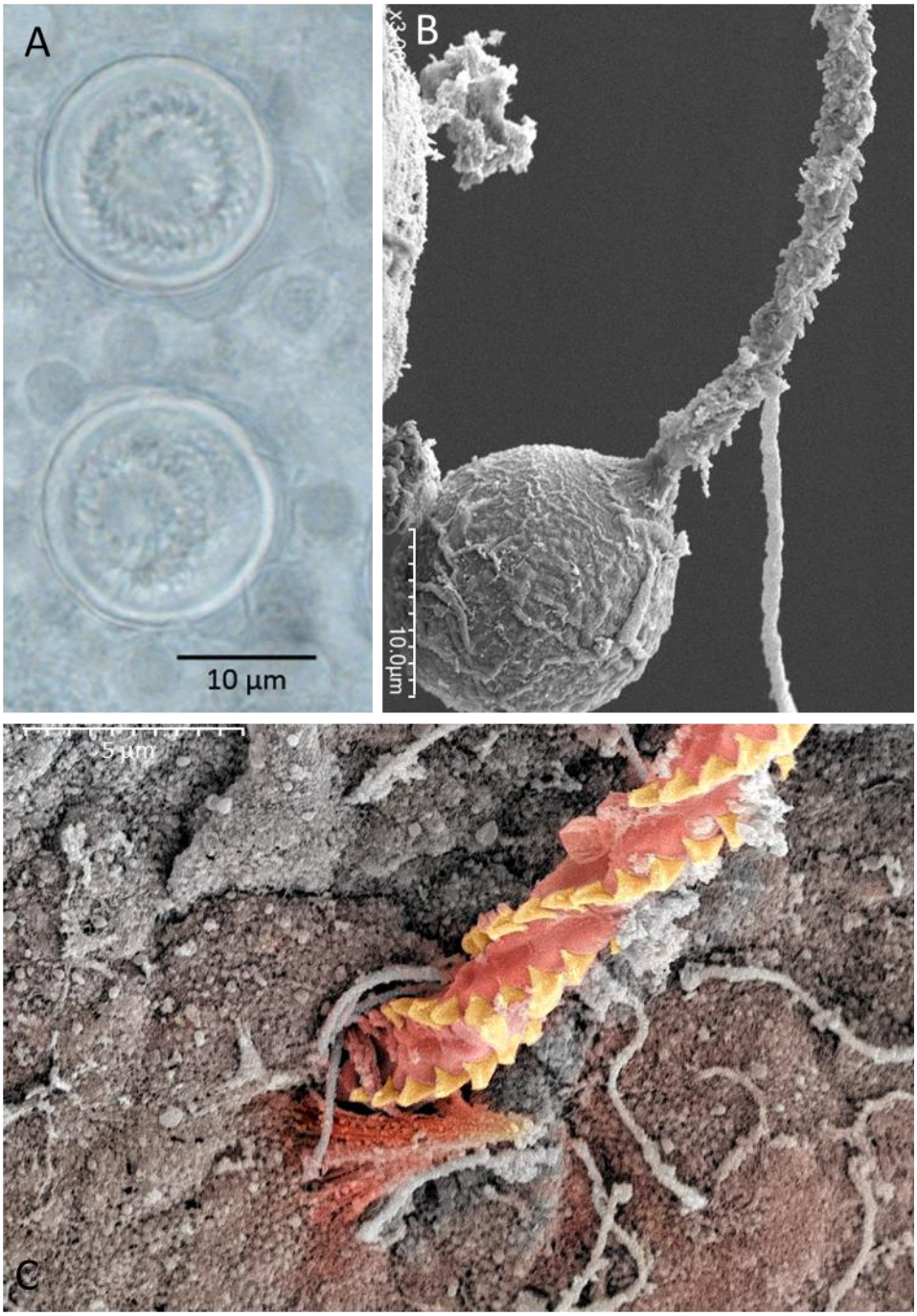

Figure 6.16: O-isorhizas from the bell of adult *Carukia barnesi* medusa.

A: Undischarged spherical O-isorhiza, with inverted, visible coiled tubule (LM). B: Discharged O-isorhiza. Tubule with broad based, triangular, homotrichous spines (SEM). C: Discharged tubule ejected from bell tissue, with helically organized spines (stylet/shaft absent at base). Cnidocil is visible partially surrounding base of tubule (false colour SEM).

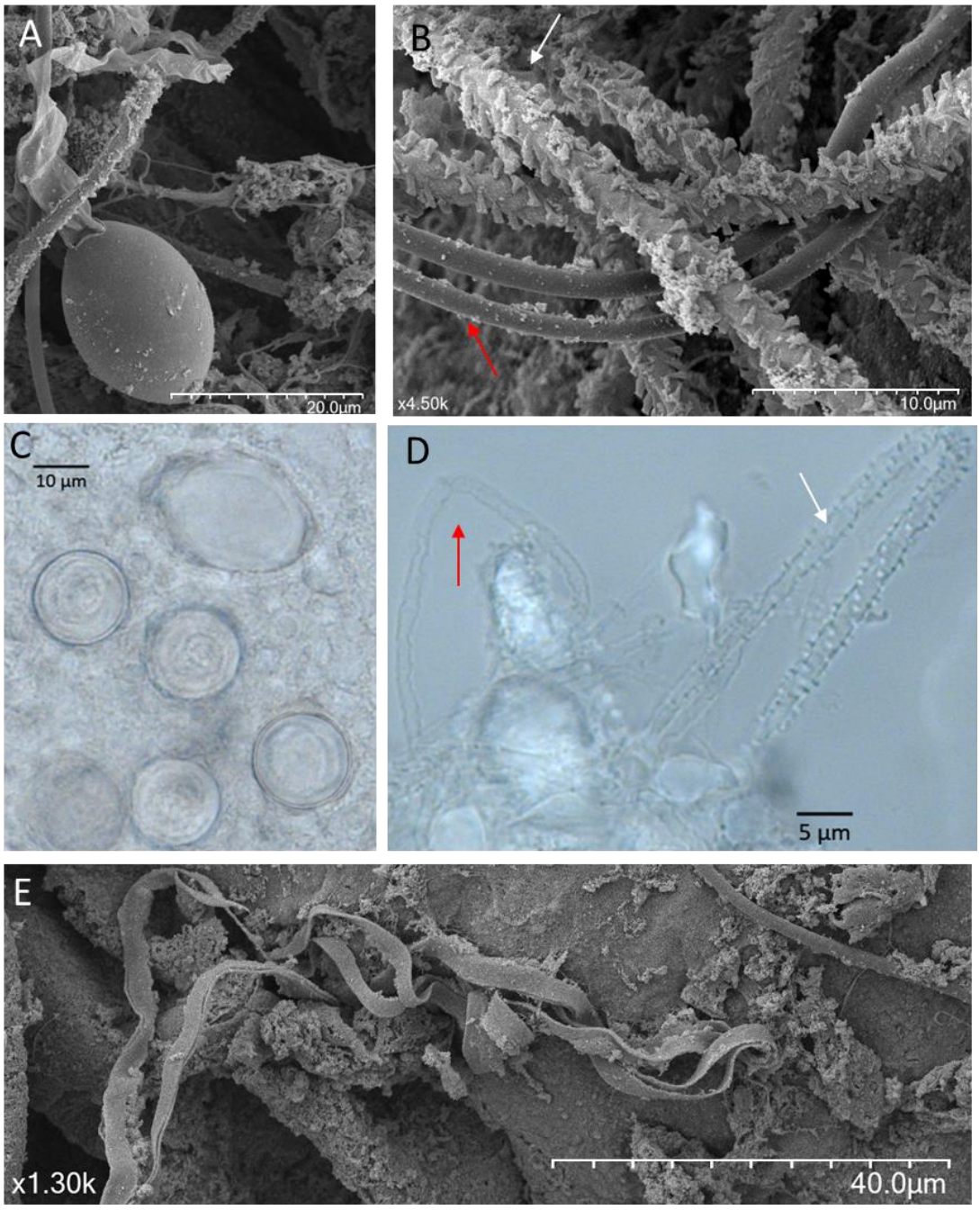

Figure 6.17: Inconclusive cnidae from the bell of adult *Carukia barnesi* medusa.

A: Discharged ellipsoid shaped cnida capsule. The flattened tubule appears to be lacking spines uncertain (SEM). B: Discharged cnidae tubules both with (white arrow) and without (red arrow) small, triangular spines in helices. C: Undischarged spherical cnidae (O-isorhizas) seen in dorsal-ventral view, the coils are perpendicular towards the long axis of the capsule. O-isorhizas are recognized since no shaft is visible in the center of the capsule. Note undischarged, possible ellipsoid cnida with no visible tubule (LM). D: Discharged cnidae tubules both with (white arrow) and without (red arrow) spines in helical structure (LM). E: Discharged cnidae tubule similar to D (red arrow) lacking spines. Tubules appeared flattened (SEM).

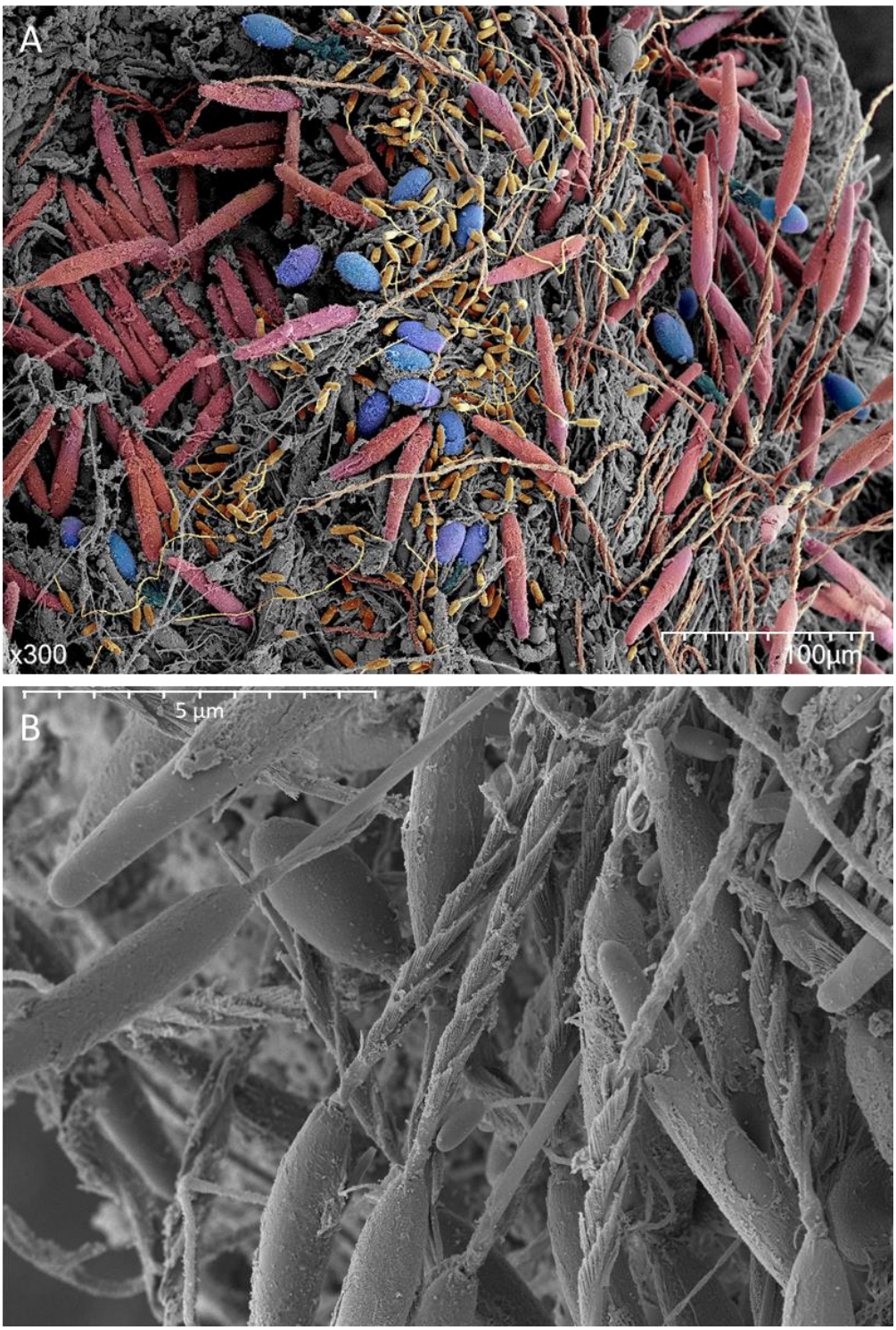

Figure 6.18: Cnidae from the tentacle of adult *Carukia barnesi* medusa (rare older specimen) (SEM).

A: Discharged and undischarged elongate microbasic b-mastigophores (red), discharged and undischarged tumiteles (blue), presumed very small elongate discharged mastigophores (yellow) (False colour SEM). B: microbasic b-mastigophores, on the discharged shafts one to five spine-rows are visible, distal tubule on some b-mastigophores.

Comparison to previously unidentified cnidae:

Two nematocyst types identified in the current study possess characteristics in line with those presented previously by Huynh et al., (2003) from unidentified cnidae, of which there were grounds to suggest *Carukia barnesi* may have been the originating organism. Fig 6.19 presents a visual comparison between an unidentified cnidae from Huynh et al., (2003) and two Tumitele nematocysts identified in the present study. The Tumitele images captured at varying focal planes present similar morphologies to those of the previously unidentified cnidae. Similarly, fig 6.20 shows a second unidentified cnidae from Huynh et al., (2003) in comparison to large Mastigophore nematocysts identified in the present study, which present similar morphologies .

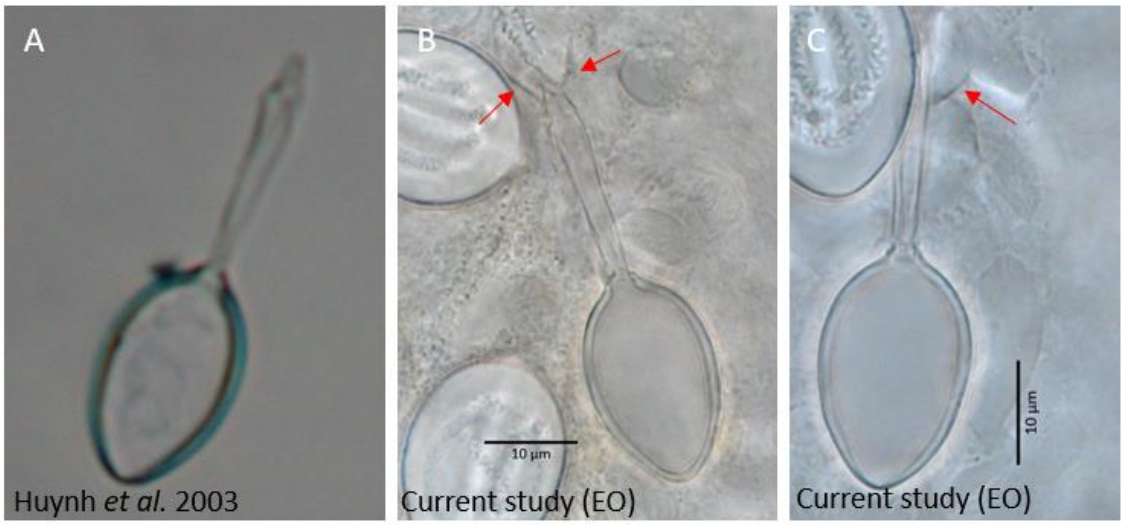

Figure 6.19: A: Nematocyst (damaged- missing distal tubule)) collected via skin scraping from a patient presenting with irukandji syndrome (Huynh et al.,(2003), the nematocyst remained unidentified by the authors, assumed inconsistent with the cnidome of *Carukia barnesi*). B,C:. Nematocysts (Tumitiles) from an adult *Carukia barnesi*, collected in the current study. The large spines on shaft (red arrows) and single shaft dilations are barely visible due to varying focal planes and optics through the tentacle tissue.

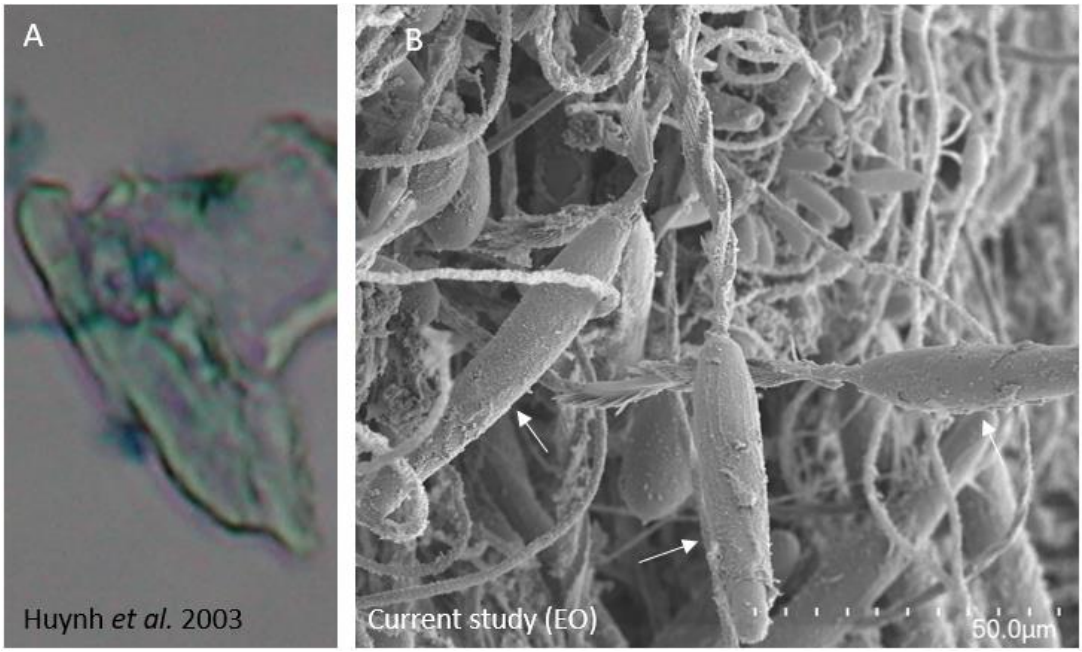

Figure 6.20: A. Cigar-shaped nematocyst collected via skin scraping from a patient fatality who presented with irukandji syndrome (Huynh et al. 2003, the nematocyst remained unidentified by the authors, assumed inconsistent with the cnidome of *Carukia barnesi*). **b** Cigar-shaped nematocysts (mastigophores, see 6.18) from a less common, older specimen of Carukia barnesi, collected in the current study. Three cigar-shaped capsules are in focus in the foreground (white arrows) each with discharged tubules

6.4.2 Quantitative analysis from light microscopy data

Nematocyst types:

Note, data from unconfirmed nematocyst types is not included in the following statistical analysis.

Nematocysts from the tentacles do not change type or proportion with life stage, 100% of nematocysts at each stage are type one nematocysts (fig 6.18). However, nematocysts from the bell do change with life stage (fig 6.21). There was a statistically significant association between nematocyst type and life stage in bell nematocysts (*Chi-square test, c^2 = 538.774, df = 1, P < 0.001).* The polyp stage does not have a bell so is not applicable here, but we see the newly detached medusa have two nematocyst types in their bell, while the adults only have one.

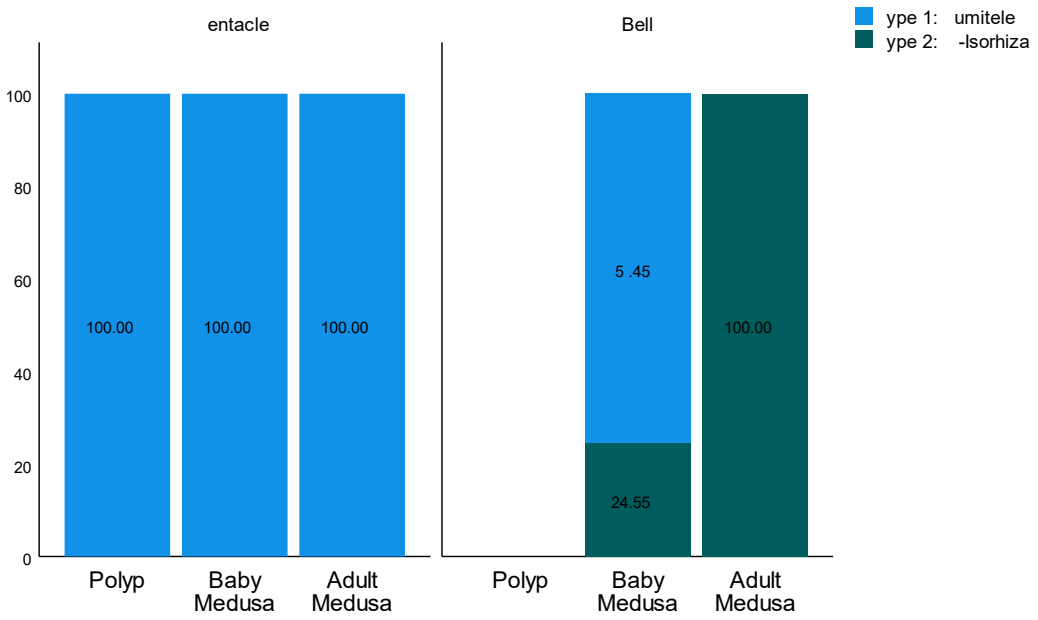

Figure 6.21: Stacked bar chart depicting the proportions (%) of the different types of nematocysts in *Carukia barnesi*. Proportions displayed are total % per variable: body part the nematocysts originate in (horizontal panels), further split by life stage the life stage of the jellyfish (x axis). Note the polyp stage does not have a bell so no data is presented here.

Nematocyst sizes:

The volume of each nematocyst type is influenced by both life stage and body part, we can see that the nematocyst volumes change within the same type across these variables (fig 6.22). Instances where the same nematocyst type is present across different body parts and/or life stages were analysed as follows:

There was a statistically significant difference in the volume of type 1 nematocysts from the tentacle between the life stages, Kruskal-Wallis H = 900.691, p =<0.001 . See figure 6.22, left panel, type 1. With the largest volumes present in the polyp stage and lowest in the newly detached medusa.

There was a statistically significant difference in the volume of type 1 nematocysts between bell and tentacles of newly detached medusa, Mann-Whitney Test U=1205, p =<0.001. See figure 6.22, newly detached medusa, type 1. Type 1 bell nematocysts were significantly larger in volume than those in the tentacles.

There was a statistically significant difference in the volume of type 2 nematocysts in the bells between newly detached medusa and adult medusa, Mann-Whitney Test U=17492.500, p =<0.001. See figure 6.22. type 2, newly detached medusa and adult medusa. The nematocysts were significantly larger in the newly detached medusa than those in the adult medusa.

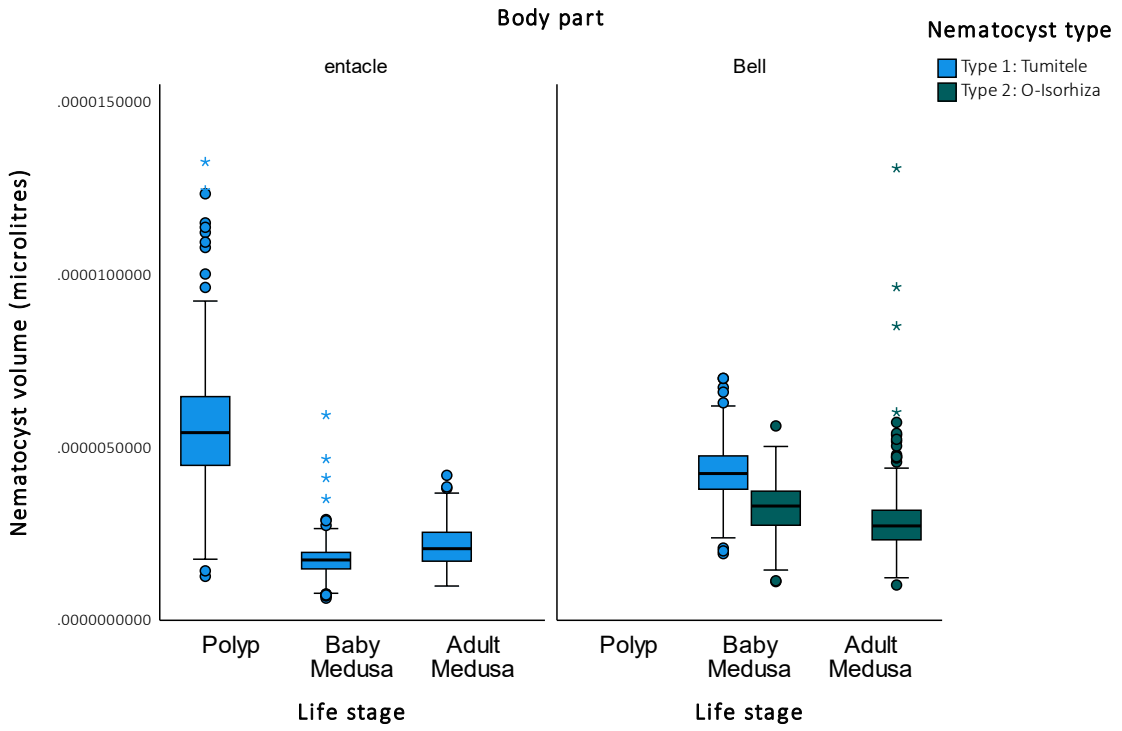

Figure 6.22: Box and whisker plot (95% CIs) depicting the volume (µL) of the different types of nematocysts in *Carukia barnesi*. Results are displayed per variable: body part the nematocysts originate in (horizontal panels), further split by life stage the life stage of the jellyfish (x axis). Note the polyp stage does not have a bell so no data is presented here..

6.5 Discussion

6.5.1 Nematocyst identification

Carukia barnesi is one of the smallest species of cubozoan, yet one of the most venomous to humans. Conflicting nematocyst identifications for this species within the current literature are detrimental to understanding both the ecology of this dangerous animal and providing definitive links to sting victims through nematocyst identification. We have therefore conducted an in depth, thorough examination of the cnidome of *C. barnesi* over three major life stages; the sessile polyp stage, the newly liberated medusa and the adult medusa. We also had the opportunity to examine the tentacular nematocysts of one single, rarer older specimen of *C. barnesi,* albeit less in depth than the latter life stages. To the best of our knowledge, every nematocyst identification previously documented within *C. barnesi* (Table 6.1) has employed only light microscopy analysis. The higher resolution achieved by scanning electron microscopy (SEM) has been documented to reveal errors in the previous interpretations of the fine structures of nematocysts, leading to misclassifications (Östman, 2000). We therefore chose to use SEM techniques to better visualise

these microscopic organelles and their even smaller associated armature, in addition to traditional light microscopy, to attain conclusive nematocyst identifications for this species. Some SEM images were manually false coloured to promote greater visual acuity, delineation and understanding of image components. Notable work has added false colour to enhance SEM images of bloodstains, and emphasizes that other monochromatic or quasi-monochromatic samples are also susceptible of increasing their realistic appearance by colouring them (Hortolà, 2010). Whilst light microscopy can only visualise the finer structures – especially on the discharged tubules – to a substantially lower resolution than SEM, it is still critical to include in this analysis. Many of the nematocyst classification categories rely on visualising the broader shapes and/or presence/absence of the inverted shafts within the undischarged capsules. An act which can only be accomplished with light microscopy whilst the sample remains permeable to light, whereas imaging provides detail only on the external topography and morphology of the sample. It is therefore imperative to combine both SEM and light microscopy to achieve true nematocyst identifications.

In the current study three confirmed types of nematocyst were identified, and two unconfirmed nematocyst types are presented:

Type 1: Homotrichous Tumiteles (confirmed)

Dr Jack Barnes first described *Carukia barnesi* as the cubozoan species responsible for Irukandji syndrome – the plague of excruciating symptoms resulting from contact with an as then unknown unknown marine stinger (Barnes, 1964) and whilst he acknowledged each species of jellyfish possess unique nematocysts, he did not describe nor identify those of *C. barnesi.* It was Southcott (1967) who described the cnidome of *C. barnesi* and who first introduced "Tumitele" as a new classification category within the nematocysts – to better encompass the characteristics of nematocysts found in carybdeidae, proposing it should be added to the established key in Cleland & Southcott (1965). One of the major foundational nematocyst identification systems by Weill (1934) divided the rhopaloids into (1) Euryteles, where the discharged shaft is dilated distally and, (2) Stenoteles, where the discharged shaft is dilated proximally at the base. In more modern systems such as Östman (2000) there is a further category (3) Biropaloids, where the discharged shaft has both one distal and one proximal dilation (see Figure 6.3 for dilation illustrations). Southcott (1967) added "Tumitele, butt swollen in middle, but unexpanded at proximal and distal ends" as a (now) fourth category of Rhopaloids, having derived the name from (tum- = root of swell; telum = weapon, dart,). Figure 6.23C illustrates the shaft dilation for this new class "Tumitele", presented with a Tumitele nematocyst first identified and described by (Southcott,

1967)(fig 6.23A) alongside a Tumitele nematocyst identified and described in the current study (fig 6.23C).

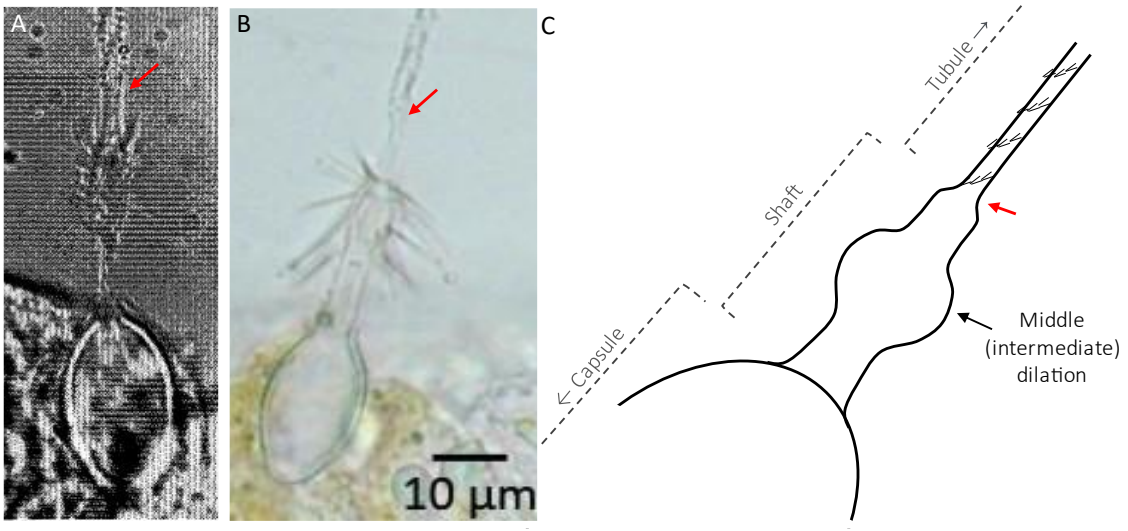

Fig 6.23. Tumitele comparisons.

A: Figure from Southcott 1967, the original nematocyst identified in *Carukia barnesi* tentacles, for which the new terminology "tumitele" was developed. B: Figure from the current study, nematocyst from adult *Carukia barnesi* tentacles, identified as a tumitele. C: Illustration of the identifying features of a "Tumitele", notably the dilation in the middle of the shaft. See figure 6.3 for comparative distal and proximal dilations. Large spines on the shaft dilation have been omitted for diagram clarity. Diagram was created by the current author (EO) based on Southcott's original description and in reference to Östman's (2000) nematocyst classification system.

Issues surrounding the identification of this particular nematocyst, found predominantly in the tentacles of *C. barnesi* (both polyp and medusa) are therefor understandable. Tumitele is not a standard category typically included in modern nematocyst classification systems and the only known instance for its creation specifically relates to nematocysts of the carybdeidae (Southcott, 1967). There appears to be mass acceptance of the class "Tumitele" in most (but not all) of the literature involving *C. barnesi* nematocysts (Table 6.1), with some studies identifying their nematocysts as tumiteles -as seems convention with this species- without accompanying descriptions of said classifying features, leading us to speculate the accuracy of some of the previously published *C. barnesi* nematocyst identifications. Gershwin (2006) presents a most thorough and in-depth publication reviewing nematocysts within the Cubozoa, however their reporting of the tumiteles is confusing, noting separate descriptive features each for euryteles

and tumiteles, but in the same work also states that Tumitele is just another name for a eurytele (Gershwin, 2006), further adding to difficulties in the nomenclature surrounding this nematocyst identification. Issues with classification nomenclature can cause further confusion within the literature, especially in difficult nematocysts such as these tumiteles, for example Underwood and Seymour (2007) identified them as "homotrichous microbasic rhopaloids". At first glance, readers unfamiliar with the intricacies of the classification systems could interpret this as being a completely different nematocyst type to a tumitele, which would be incorrect. Tumitele being a further category of rhopaloids, the authors here simply identified to the lowest possible classification level (here one step above tumitele), but it evidences how varying nomenclature within the literature can be misleading. Unusually, these tentacular nematocysts are identified (Ávila-Soria, 2009) as microbasic mastigophores (table 6.1), which are not a differing level of classification but indeed a different type. The author notes they "confirmed earlier observations of Southcott (1967)" finding microbasic mastigophores in *C. barnesi* tentacles, however confusion arises here as Southcott 1967 specifically states these could no longer be termed mastigophores and thus created the new category of tumitele (as discussed above) specially for these nematocysts. Whilst the current study does also present mastigophores in *C. barnesi*, (as discussed in detail below), these have been rarely documented and only in older rarer specimens and never as the only nematocyst present. Thus, we do not assume these were the same nematocysts reported by Ávila-Soria, no identifying features of said nematocysts were described by Ávila-Soria so we are unable to compare to the current work.

The current study found this particular nematocyst (which ultimately was classified as a Tumitele) to be particularly challenging to identify for a number of reasons. Firstly, there was some difficulty determining the relative position of the dilation of the shaft (figs 6.3 and 6.23). Discrepancies occurred around the "middle", in some instances the dilation could be classed as distal depending on what the observer distinguished as shaft and tubule. The discharged shaft above the dilation can appear narrower than the proximal region of the shaft below the dilation. In fig 6.23B above the dilation is narrower than below, the space above the dilation possesses no spines, which could confuse this area as the start of the tubule and not a continuation of the shaft– so with this interpretation the dilation appears distal on the shaft. These observations are further complicated as we see in fig 6.23A, the proximal shaft is incredibly difficult to visualise in Southcott's original nematocyst image, making comparisons of this key identifying feature very difficult to draw. But, there is a slight point of constriction/a slight narrowing before the helices of spines start on the tubule (fig 6.23B), perhaps the true delineation between the shaft end and the tubule – which

would confirm the dilation is indeed in the middle of the shaft. Thus we confirmed this nematocyst identification as a Tumitele.

Type 2: Holotrichous O-Isorhizas (confirmed)

These nematocysts were altogether much simpler to identify than the tumiteles (above), with their presenting ultrastructure fitting neatly into the categories of Östman's (2000) classification system. These nematocysts – primarily found in the bell of the medusa stages – were originally identified by Southcott (1967) as haplonemes, anisorhizas and possibly homotrichous. Over the course of the literature (Table 1) they are typically identified as isorhizas or anisorhizas, sometimes to one classification level prior as haplonemes. With the distinction between Isorhizas or Anisorhizas, according to Östman's (2000) classification system being the diameter of the tubule, something very difficult to ascertain along the full length of the tubule when observing only undischarged capsules where the tubule remains both inverted and coiled, as was the case in Southcott (1967). Östman's (2000) classification system states anisorhizas have a tubule that is slightly dilated towards the base, which we can see clearly in figures 10B and 16B this not the case for this nematocyst, thus classifying it as an isorhiza, the tubule isodiametric or nearly isodiametric proximal to the midpoint. The "O" in the final description O-Isorhiza refers to the near spherical shape of the capsule, although there is a small eminence at the discharge pole as noted by Southcott (1967).

Type 3: Atrichous or holotrichous b-mastigophores (confirmed)

This is the first instance in which these larger, elongate b-mastigophores have been confirmed in *C. barnesi.* There has been speculation and debate amongst leading scientists regarding these nematocysts in larger and/or older specimens of this animal (discussed in more detail in the below sections) but this discussion has previously remained unpublished/undocumented.

The "Irukandji season" in which *C. barnesi* medusa are present in the wild, was originally described as mid-November to late January (Barnes, 1964), but has changed somewhat in recent years with climate change, as we now do find wild *C. barnesi* into March and April although more infrequently. The single animal in which b-mastigophores were found was collected in April, a uncommon that late in the season and the only animal caught that month and the last caught that season. It was therefore confidently labelled as an older animal given the timing (note size was not used to estimate age due to the propensity of jellyfish to shrink when resources are low, at the culmination of the season size would be a dubious indicator of age). In figure 6.18A we see these larger elongate b-mastigophores present in large numbers in the tentacle neckerchief,

alongside the smaller tumiteles typical of this species. From this single shot there appears an approximate 4:1 ratio of large b-mastigophores: tumiteles.

Type 4: Type 4: *Atrichous isorhizas (ellipsoid)(unconfirmed)*

In both light microscopy and SEM analysis, we found evidence for a potential fifth type of nematocyst present in the bells of adult *C. barnesi* medusa (fig 6.17), however this requires further investigation to confirm. From light microscopy analysis of fixed specimens we found a number of capsules present in the bell warts alongside the holotrichous O-isorhizas. These were mostly ellipsoid in shape, similar to the tumiteles, but were also found in more irregular shapes. This could be due to capsule damage inflicted during fixation, although unlikely as nematocysts tend to be extremely robust – indeed it is often a challenge to break them open for venom collection. The secondary option is that they are not cnidae capsules but some other unknown component of the bell wart. Whilst all the holotrichous O-isorhizas in the fixed samples remained undischarged with the inverted coiled tubules clearly visible within, these unknown capsules appear to lack a visible tubule within. In Southcott's (1967) original description, he notes and evidences the presence of these capsules (Southcott 1967, plate 5, image 3) but identifies them as presumably discharged versions of the isorhizas typically found in the bell. These same capsules can also be seen in the *C. barnesi* paratype described by Gershwin (2006), but the author gives no commentary on them. However, observations from the current study lead us to the conclusion they are in fact either a different type of nematocyst from the holotrichous O-isorhizas (here type 2) or are not a nematocyst at all. All photographic evidence from the aforementioned studies and the current study shows these capsules as not spherical, rather distinctly ellipsoid/lemon shaped, immediately suggesting they are of a different ilk. Exploring the notion they are simply discharged type 2 nematocysts due to the lack of tubule visible within, we observed these capsules through all possible focal distances and orientations and found no evidence of discharge, the capsules appeared sealed all around, with no visible openings or open operculum. From our light microscopy analysis on squash samples of fresh bell tissue, we can see discharged tubules from the bell both spined and unspined (fig 6.17D), indicating two separate types of cnidae present. Unfortunately, due to the nature of the bell tissue which is much thicker and less translucent than tentacle tissue tracing these tangled tubules back to their capsule of origin was impossible. Through SEM analysis we did observe a number of discharged atrichous (unspined) tubules, the majority of which appeared flattened – whether this was a product of dehydration during SEM preparation or a true indication of the tubules nature remains undetermined. Note though that tubules visible in figures 6.17A and E are mostly flattened, but some are fully distended in the same sample, suggesting sample preparation may not be the cause. Figure 6.17A presents the

only observed example of an ellipsoid capsule with an attached atrichous tubule, however given the again flattened tubule it would be remis to conclusively state this is the nematocysts intended form without further replicates, although likely. The very fact the tubules appear atrichous (unspined) may be the reason the inverted tubule is not visible inside these undischarged capsules, coupled with the challenging thickness of the bell tissue, the lack of spines may be enough to lack definition visible at traditional light microscopy resolution. Only one previous study has documented two differing types of nematocyst in the adult bell, with other than the standard isorhizas, homotrichous microbasic rhopaloids were identified by Underwood and Seymour (2007), the same type identified in the tentacles (equivalent to the type 1 tumiteles in the current study). These authors are the first to distinguish a second type of nematocyst in the adult bell, however we would disagree with the identification. Whilst the capsules do have the same ellipsoid shaped capsules as the tumiteles, they lack a spined shaft and tubule. No nematocyst descriptions or images were presented by Underwood and Seymour (2007) so we are unable to compare with the findings of the current study. To conclude, if these capsules are indeed nematocysts, no shaft is visible in the unfired capsule and the discharged tubule is unspined, thus we have termed them atrichous isorhizas (ellipsoid shaped). However, further investigations such as Transmission Electron Microscopy would be required to view the internal undischarged capsules to confirm this, along with clear replicates of intact discharged capsules with the tubule attached. To that end, these unconfirmed cnidae were not included in any quantitative analysis of the cnidome.

Type 5: small mastigophores or elongate haplonemes (unconfirmed)

During SEM image analysis of the rarer, older *C. Barnesi* specimen, small elongate forms were noted in the sample, each with a long thin protruding mass (fig 18). These were initially discounted for in-depth imaging and further analysis, assumed to be bacteria with flagella and irrelevant to nematocyst analysis. Thus, all SEM imaging of this sample focused entirely on elucidating the tumitele and larger b-mastigophore nematocysts in this specimen. However, upon personal communication with Dr. C Östman (nematocyst expert and author of the Östman (2000) nematocyst classification guide) in which consultation was sought to identify the tumitele and large mastigophores obvious in this sample, it was advised that the smaller background forms were actually very small mastigophore nematocysts (fig 6.18). Corroborating this, it has also been suggested that they appear slightly larger at ~10 µm (capsule/body length) than the bacteria at ~2-6µm they were initially assumed to be. Additionally, this is not how filamentous bacteria typically appear, instead here possessing one single defined extrusion (personal communication, Dr. J Whan, senior electron microscopist), suggesting they are unlikely to be bacteria and in fact

possess morphology more consistent with nematocysts. Here they are categorized simply to mastigophore level, as further identification would require more detailed imaging. These nematocysts loosely appear to be smaller versions of the larger confirmed type 3, b-mastigophores, with the long extrusion appearing to be one single diameter. However, from the current images it is difficult to deduce if this is in line with the definition of a b-mastigophore "discharged shaft or proximal tubule approximately the same diameter as the remaining tubule" (Östman, 2000) or it potentially does not posses a shaft at all – in which case it would not even be classed as a mastigophore, but perhaps an haploneme (no prominent, rod-shaped shaft (Östman, 2000)). Another difference to the larger b-mastigophores is the lack of prominent armature/spines on the – possible – shaft. To conclusively identify this a nematocyst and further to the correct type, more detailed SEM imaging would be required, along with LM imaging of the undischarged states. Unfortunately, this specimen was processed in its entirety for the original SEM analysis prior to finding these undocumented nematocysts, thus preventing any supporting LM work. The nature of this being an uncommon specimen that is rarely collected impeded any further exploratory analysis within the current study, however this certainly warrants further investigation from any future research fortunate enough to collect such a specimen.

Ageladine-A fluorescent staining

In both the polyp stage (stalk) and newly detached medusa stage (bell) of *C. barnesi,* very small cnidae were observed. Whilst the cnidae of the polyp has only been documented once before, with two types detailed- tumiteles and isorizas (Courtney et al., 2016), the current study concludes only one type is present in the polyp. We found tumiteles present in the tentacles, consistent with the findings of (Courtney et al., 2016) however the smaller spherical cnidae observed in the stalk did not discharge either with pressure under a squash preparation nor chemically with ethanol suggesting these are small immature forms of the tumiteles, migrating up the stalk to their final destination in the tentacles. No discharged tubules were observed anywhere along the stalk even under high power SEM. Similar very small cnidae observed in the bell warts of the newly detached medusa (fig 6.12) further corroborate this conclusion. It would be inappropriate to judge these immature cnidae solely on their ability to discharge as in the polyps, as these small cnidae were surrounded by numerous large cnidae (fig 6.12), thus any discharged tubules (or lack of) could not accurately be attributed solely to the smaller cnidae. Without confirming with Transmission Electron Microscopy the internal identifying features of such small cnidae capsules were impossible to visualise. Therefore, to clarify the maturity of these smaller cnidae, we employed a method developed by Obermann, Bickmeyer, and Wägele (2012) – cnidae change pH with maturity, which can be measured by the pH sensitive fluorescing alkaloid

Ageladine A. If the larger capsules fluoresced at the same intensity as the smaller ones, they would be the same maturity, then based on their largely different morphologies it would be concluded they were different types of cnidae. However, the smaller cnidae fluoresced at significantly different intensities to the larger cnidae, confirming they are the same cnidae type just at different stages of maturity.

Cnidome overview

Whilst the combined use of LM and SEM is necessary to fully identify the nematocysts, we can see from Table 2 SEM does reveal a slightly more detailed cnidome when employed individually. From the entire quantitative nematocyst counts conducted with LM, Tumitele nematocysts were not observed in the adult medusa bell, but *were* noted very sporadically in SEM analysis. This higher resolution technique does help to differentiate the less common nematocysts from the masses in a sample. Additionally, whilst the tentacle tissue of the older, rarer medusa was not available for LM analysis, the size at ~10 µm of the small unconfirmed mastigophores/haplonemes would not have been accurately visible with traditional LM anyway and likely would have been overlooked. We can therefor conclude that the summary presented from the SEM analysis in Table 6.2, provides the most accurate depiction of *Carukia barnesi*'s cnidome to date.

Table 2. Cnidome overview for three life stages and two body parts of *Carukia barnesi* life as elucidated from light microscopy and scanning electron microscopy. *Tissue not analsyed

Life stage	Body part	Nematocyst type	
		Light Microscopy	Scanning Electron Microscopy
Polyp	Tentacle	Tumiteles	Tumiteles
Newly detached medusa	Tentacle	Tumiteles	Tumiteles
	Bell	Holotrichous O-isorizas	Holotrichous O-isorizas
		Tumiteles	Tumiteles
Adult medusa	Tentacle	Tumiteles	Tumiteles
	Bell	Holotrichous O-isorizas	Holotrichous O-isorizas
		-	Tumiteles
		Atrichous isorizas (uncomfirmed)	Atrichous isorizas (unconfirmed)
Older adult medusa (rare specimen)	Tentacle	N/A*	b-mastigophores -large
		N/A*	Mastigophores/haplonemes -small (unconfirmed)
	Bell	N/A*	N/A*

6.5.2 Comparison to previously unidentified cnidae

Irukandji stings plagued the people of North Queensland long before the associated species was identified by Barnes (1964) as the small and near transparent nature of the animal, coupled with the often 20 minute delay between sting and symptom onset, made locating the offending specimen next to impossible. In this pioneering work Barnes believed scraping the skin of victims for identifying nematocysts could be a method to link the sting victim to the responsible jellyfish species, "these microscopic organoids may be detected in material scraped from sting sites. As nematocysts exhibit a wide variety of form and internal organization, and as these characteristics are constant for each particular species of jellyfish, the method has considerable diagnostic value".

This skin scraping analysis would be later conducted by Huynh et al. (2003) who, amongst multiple successful identifications, presented two unidentified cnidae not consistent with the known cnidome of *C. barnesi* but were collected from patients exhibiting symptoms consistent with the species (figs 6.19A and 6.20A). Here, the current study presents evidence connecting Huynh's (2003) unknown cnidae to those of *C. barnesi.* The first, figure 19, may simply be a damaged Tumitele, known to be present in all life stages – the various physical processes the nematocyst will have endured i.e. initial discharge onto skin, turbulence as the tentacles were pulled from the skin, physically scraped from the skin and applied to microscopy slide for analysis,

are more than enough to damage the discharged tubule. We then present for the first-time that the varying focal planes of Tumiteles with known dilations in the shaft can appear as if no dilation is present, appearing just like that presented by Huynh et al. (2003) if the large shaft spines had also broken off. However, if Huynh's nematocyst (fig 6.19A) is fully intact it would be more consistent with the characteristics of an amastigphore "no tubule beyond everted shaft" (Östman, 2000). With only a single replicate it is not possible to draw a conclusive identification.

Secondly, Huynh et al. (2003) presented a larger unidentified "cigar-shaped" cnidae, collected from a fatality who presented with symptoms consistent with but *not* attributed to *C. barnesi* (fig 6.20A), as this cnidae had not at the time been suggested in this species. In 2010 Pereira et al., published a clinical toxicology study in which there is mention of some cases of larger *C. barnesi* specimens (>20mm body height) being found to contain long mastigophore nematocysts, but no supporting evidence was presented. Here we present for the first-time scanning electron micrographs of large, "cigar-shaped" cnidae (figs 6.18 and 6.20B) present in the tentacles of a rarer, older specimen of *C. barnesi* (specimen age discussed above). Identified as b-mastigophores, evidencing that nematocysts morphologically similar to that found in Huynh et al. (2003), and consistent with the mastigophores described in Pereira et al., (2010) do exist in *C. barnesi* and may therefore be included in future diagnostics to *C. barnesi* stings.

6.5.3 Quantitative analysis

It is evident that the type of bell nematocysts of *C. barnesi* significantly change between life stages (fig 6.21) with the addition of a second type after the polyp stage, however the tentacle nematocysts remain a single type unchanged into adulthood[2].

Although type 1 (tumiteles) are consistently the single type present within the tentacles, the volume of these capsules significantly changes between the three life stages (fig 6.22). Nematocyst volume is an important metric, superior to simple length/width measurements in ecological relevance, as it indicates the maximum venom load capable of being injected from said

[2] Light microscopy analysis and quantitative data was not collected on the rarer, older *C. barnesi* specimen discussed throughout, in which an additional nematocyst type *is* present within the tentacles. Upon collection, this specimen was processed solely for electron microcopy analysis, intended for nematocyst identification purposes only. The observation of the new nematocysts type was fortuitous but unexpected, with the realization occurring only after the animal had been processed in its entirety. Thus, all quantitative data presented is from LM analysis only from the polyp to the typical adult medusa.

capsule[3]. By far the largest volumed tentacle nematocysts (type 1) are within the polyp tentacles, with lower volumes in the adult tentacles, and lower again in the newly detached medusa. This opposition between the polyp and adult medusa nematocysts is ecologically logical, the polyp tentacles are far shorter (<1mm) than the adults (<0.75m) and thus contain substantially less nematocysts. Lower in number, but higher in volume is one way to maintain a similar venom load between life stages. Consider though, *C. barnesi* venom composition has been shown to change with age, even within the same nematocyst type, reflecting the animals ontogenetic shift from invertebrate to vertebrate prey (Underwood & Seymour, 2007). So perhaps this volume change is not purely venom focused, but to facilitate the mechanics of capturing more complex vertebrate prey. The presence of lots more, smaller nematocysts each bearing spined tubules would be more effective at penetrating, entangling and most importantly retaining i.e. a moving larval fish (adult *C. barnesi*'s confirmed prey (Courtney et al., 2015)), than a few single tubules from larger capsules. However, this does not explain why the newly detached medusa tentacle nematocysts have the smallest volumes of the three life stages. The newly detached medusa have even fewer tentacles than the polyps, similar in length if not smaller, thus compared to the polyps they have *lower* numbers of smaller nematocysts. One possible explanation may be this is the only life stage to posses both type 1 and 2 nematocysts in their bell. To date, this species has never been successfully raised in aquaria, persistent feeding problems abound and the animals ultimately starve to death (chapter four). Given the relatively short length of even a fully extended tentacle at this age (fig 6.1B), they do not appear biological engineered for fishing at this length. Perhaps at this newly detached stage the animal is relying more heavily on the bell nematocysts, a logical assumption given it's the only stage to wield both type 1 and 2 nematocysts in its bell, and its otherwise inexplicable possession of relatively few, very small volumed type 1 nematocysts in its tentacles. This explanation is further corroborated as the newly detached medusa possess type 1 nematocysts in both their tentacles and their bell (indeed the only age to possess type 1 in their bell at all), with the bell nematocysts being significantly greater in volume than the tentacle nematocysts (fig 6.22).

The current study documented only type 2 nematocysts in the adult bell, findings that initially seem to conflict with the results of Underwood and Seymour (2007) who documented a distinct proportional split between two types (31%:69%) in the adult bell. However, this reflects the

[3] For the purposes of discussion, this is an informed estimate only. A precise value would require further calculations such as subtraction of the tubule mass, etc. Thus here referred to as the "maximum" possible venom load, the volume capable of being contained within the capsule dimensions.

unconfirmed nematocysts observed in the current study and discussed at length above,, which were not included in the quantitative analysis here as the reality of a second cnidae type in this instance was ambiguous. A predilection for bell nematocysts over their tentacle nematocysts in the newly detached medusa would align with the presence of only a single nematocyst type (type 2) in the adult bells, which are also significantly smaller than those in the newly detached medusa bell. The adults reducing down to a single type and making them smaller, would ecologically suggest less of a reliance on them, especially when at this age they possess orders of magnitude more weaponry in their tentacles.

6.6 References

Antonovsky, A. (1984). The application of colour to sem imaging for increased definition. *Micron And Microscopica Acta*, *15*(2), 77–84. https://doi.org/10.1016/0739-6260(84)90005-4

Ávila-Soria, G. (2009). *Molecular characterization of Carukia barnesi and Malo kingi, Cnidaria; Cubozoa; Carybdeidae.* James Cook University.

Barnes, J. H. (1964). Cause and Effect in Irukandji Stingings. *The Medical Journal of Australia*, *1*(24), 897–904. https://doi.org/10.5694/j.1326-5377.1964.tb114424.x

Clelland, J. ., & Southcott, R. . (1965). *Injuries to Man from Marine Invertebrates in the Australian Region.*

Courtney, R., Browning, S., & Seymour, J. (2016). Early life history of the "irukandji" jellyfish *Carukia barnesi*. *PLoS ONE*, *11*(3). https://doi.org/10.1371/journal.pone.0151197

Courtney, R., Sachlikidis, N., Jones, R., & Seymour, J. (2015). Prey capture ecology of the cubozoan Carukia barnesi. *PLoS ONE*, *10*(5), 1–12. https://doi.org/10.1371/journal.pone.0124256

Gershwin, L. A. (2006). Nematocysts of the Cubozoa. *Zootaxa*, *57*(1232), 1–57. https://doi.org/10.11646/zootaxa.1232.1.1

Hessinger, D. A., & Lenhoff, H. M. (1988). *The Biology of Nematocysts* (D. A. Hessinger & H. M. Lenhoff (eds.)). Academic Press, Inc.

Hortolà, P. (2010). Using digital colour to increase the realistic appearance of SEM micrographs of bloodstains. *Micron*, *41*(7), 904–908. https://doi.org/10.1016/j.micron.2010.06.010

Huynh, T. T., Seymour, J., Pereira, P., Mulcahy, R., Cullen, P., Carrette, T., & Little, M. (2003). Severity of Irukandji syndrome and nematocyst identification from skin scrapings. *Medical Journal of Australia*, *178*(1), 38–41. https://doi.org/10.5694/J.1326-5377.2003.TB05041.X

O'Hara, E., & Seymour, J. (2022). Inducing metamorphosis in the irukandji jellyfish Carukia barnesi. *Scientific Reports 2022 12:1*, *12*(1), 1–12. https://doi.org/10.1038/s41598-022-12812-2

Obermann, D., Bickmeyer, U., & Wägele, H. (2012). Incorporated nematocysts in *Aeolidiella stephanieae* (Gastropoda, Opisthobranchia, Aeolidoidea) mature by acidification shown by the pH sensitive fluorescing alkaloid Ageladine A. *Toxicon*, *60*(6), 1108–1116. https://doi.org/10.1016/j.toxicon.2012.08.003

Östman, C. (2000). A guideline to nematocyst nomenclature and classification, and some notes

on the systematic value of nematocysts. *Scientia Marina*, *64*(SUPPLEMENT 1), 31–46. https://doi.org/10.3989/scimar.2000.64s131

Pereira, P., Barry, J., Corkeron, M., Keir, P., Little, M., & Seymour, J. (2010). Intracerebral hemorrhage and death after envenoming by the jellyfish *Carukia barnesi*. *Clinical Toxicology*, *48*, 390–392. https://doi.org/10.3109/15563651003662675

Southcott, R. V. (1967). Revision of some Carybdeidae (scyphozoa: cubomedusae), including a description of the jellyfish responsible for the "irukandji syndrome." *Australian Journal Of Zoology*, *15*, 651–671. https://www.mendeley.com/viewer/?fileId=2fa0eb3f-b65a-d78b-0aab-8d1da93fdb17&documentId=f0d95e7c-a226-37e1-ba96-636d97beaa71

Underwood, A. H., & Seymour, J. E. (2007). Venom ontogeny, diet and morphology in *Carukia barnesi*, a species of Australian box jellyfish that causes Irukandji syndrome. *Toxicon*, *49*(8), 1073–1082. https://doi.org/10.1016/j.toxicon.2007.01.014

Weill, R. (1934). Contribution à l'étude des cnidaires et de leurs nématocystes. *Laboratoire d'évolution Des Êtres Organisés.*

Chapter 7 . Good Stings Come in Little Packages: 3D Modelling Nematocysts from the Irukandji Jellyfish *Carukia barnesi*

7.1 Abstract

Continuing the research trajectory established in chapter six, here I strive to further elucidate the nematocysts of *Carukia barnesi*. Focussing solely on the adult medusa life stage, we develop and optimise a method for creating biologically accurate 3D models of both the discharged and undischarged states of these microscopic organelles. Through a process known as volume imaging, here we employ Serial Block Face Scanning Electron Microscopy to create both virtual and physical nematocyst models, to facilitate a deeper understanding of the ultrastructure, which will contribute to future ecological and venom injection research.

7.2 Introduction

Irukandji syndrome is the complex and excruciatingly painful condition which results from a sting from a range of small, almost invisible cubozoan (box jellyfish) species. The most commonly encountered species of Irukandji jellyfish in Far North Queensland is *Carukia barnesi,* though their range is speculated to actually extend further along the Northern Australian coastline (Southcott, 1967; Underwood et al., 2018). As the most vilified Irukandji species, *C. barnesi* stings are known to cause a range of symptoms from extreme muscle pains, nausea and vomiting, to instances that induce intracerebral hemorrhage and death (Barnes, 1964; Pereira et al., 2010). The venom ecology of these dangerous animals remains poorly elucidated, with conflicting information in the literature regarding their stinging organelles (chapter 6; table 6.1) hindering further understanding.

All jellyfish possess microscopic stinging apparatus called cnidae: a cnidocyte cell, containing one giant secretory organelle called the cnidocyst. Cnidocysts are then divided into three categories; A) spirocysts are used to entangle prey and stick to surfaces and do not contain venom; B) ptychocysts produce a glue like substance to hold onto prey or create tubes (in burrowing sea anemones); and C) nematocysts, harpoon like in structure, can penetrate prey with venom and also entangle. These cnidocyst organelles sit in the tissues of the jellyfish and discharge by ejecting and everting a coiled tubule outwards. Some, like the nematocysts (see chapter 6), have spines and a tubule, which can penetrate prey to inject venom. The microscopic size of these organelles and their even smaller associated armature means that traditional light microscopy is typically unsuitable to visualise these structures. The only way to conclusively identify these cnidocysts is with electron microscopy, which allows features such as the spines, measuring only nanometres in width, to be visualised with ease. The cnidome, which is the term given to the complement and ratio of the different types of cnidocysts present in an animal, often varies with ontogenetic stage (McClounan & Seymour, 2012; Chapter 6), reflecting the changing ecology of the animals eg. Purely defensive at early stages before a mouth has developed, to more paralytic penetrants as prey capture becomes a priority. Ultimately, the cnidocysts, particularly the venom wielding nematocysts, could be argued to play the defining roles in the ecology of these animals, as every major ecological function feeding, offence, defence, substrate adhesion and competition traces back to the nematocysts, the venom they contain and their functional role within the animal. Therefore, being able to understand these stinging organelles is paramount to unlocking the ecological secrets of these jellyfish.

To fully understand the nematocyst injection mechanics, we must first possess a thorough foundational understanding of their ultrastructure. An in-depth investigation into nematocyst

identification and classification over three key life stages in *C. barnesi* was conducted in chapter 6 and here we build upon that analysis to elucidate the ultrastructure of the tentacular nematocysts of the adult medusa. All human *C. barnesi* envenomations and hospitalisations are assumed to result from the medusa life stage as this has been the confirmed causative organism for Irukandji syndrome (Barnes, 1964) and the polyp stage has never been successfully located in the wild, nor confirmed toxic to humans. Volume imaging is a field of science involving the imaging, generation and analysis of 3D volumetric data, including, but not limited to light, electron and X-ray imaging modalities (*Australian Microscopy and Microanalysis Society, Volume Imaging Australia*, n.d.). Volume imaging with electron microscopy enables imaging and analysis of subcellular structures on the mesoscale (10 nm to 10 µm) (*Karolinska Institute, Volume Imaging*, n.d.) making it an attractive option to elucidate the highly detailed ultrastructure of microscopic nematocysts from *C. barnesi*. Volume imaging has been used only twice before to visualise the ultrastructure of nematocysts (or nematocyst-like organelles). Both studies employed different acquisition methods of serial sectioning with electron microscopy using FIB-SEM (Focussed Ion Beam-Scanning Electron microscopy) (Gavelis et al., 2017) or STEM (Scanning Transmission Electron Microscopy)(Karabulut et al., 2022). The current study adopts a novel approach as we chose to utilize SBF-SEM (Serial Block Face-Scanning Electron Microscopy) to achieve superior ultrastructural resolution, allowing us to volume image and generate detailed 3D renders of multiple nematocysts from the highly venomous and poorly studied *C. barnesi.*

7.3 Methodology

7.3.1 Animal collection

Adult specimens (>8mm interpedalial distance) of *Carukia barnesi* were collected from the sea surrounding Double Island, Cairns, Australia. Methods of collection included attracting the jellyfish to submersible dive lights suspended from the side of a boat at nighttime, hand collection with a net or by way of donation of specimens collected from routine stinger net drags at Palm Cove, Cairns, Australia. All live specimens were transferred to 500 mL containers filled with seawater and stored in the JCU aquarium facility (Cairns) until further processing.

7.3.2 Nematocyst isolation and fixation

Due to their propensity to rapidly degrade in aquaria *C. barnesi* specimens were processed within 48 hours of collection. There is no record to date of this species successfully being reared in aquaria.

Trialed methods:

As a novel sample for SBF-SEM, numerous sample preparations were trialed:

Undischarged nematocysts: Nematocysts were isolated from tentacles by refrigerating (4 °C) dissected tentacles in natural seawater for 5-7 days until the tentacles had degraded, or by placing in 1M sodium citrate 1 hour -1 week (refrigerated at 4 °C) to promote nematocyst expulsion from the tentacle tissue. At 4 °C nematocyst structure is theoretically stable in either seawater or sodium citrate indefinitely, however samples were processed within 1 week. The nematocyst solution was filtered through a 70 µm filter to remove tissue debris. The remaining nematocyst solution was either centrifuged to directly form a pellet, or pelleted and resuspended in agarose to form agarose drops with nematocysts suspended throughout.

Discharged nematocysts: Nematocysts were induced to discharge by either 1) Subjecting the tentacles to electrocution on a glass coverslip, causing the nematocysts to discharge their tubules onto the glass, or, 2) Adding 100% ethanol to a tentacle on a glass coverslip or agarose gel, causing the nematocysts to discharge their tubules onto the glass/agarose surface. The tentacle material was then peeled away from the glass/agarose, dislodging the nematocyst capsules from the tentacles and leaving discharged nematocysts on the glass/agarose surfaces. The agarose drop was processed whole. The coverslip would be later inverted onto a liquid resin block, cured together, then the glass peeled away to leave the discharged nematocysts set into the resin.

None of the above methods ultimately yielded viable results, mainly due to the low densities of nematocysts isolated successfully. Low density samples result in charging during electron microscopy which disrupts image acquisition.

Final method:

The final successful method of sample preparation was to relax freshly excised tentacles in 0.36 M $MgCl_2$ and dissect into small (~3 mm) sections and then process them whole. Tentacles were rinsed three times in autoclaved natural seawater, which was filtered through a 0.22 µm syringe filter. For undischarged nematocysts, these sections were fixed with nematocysts remaining entirely within the tentacle tissue. For discharged nematocysts, discharge was initiated by topically exposing the tentacles to 100% ethanol, whereby the capsule remained situated in the tentacle tissue, with the discharged tubule protruding out from the tissue.

Typical preparation for Serial Block Face Scanning Electron Microscopy (SBF-SEM) would be to fix samples in 2.5% glutaraldehyde in 0.1 M sodium cacodylate buffer pH 7.4 (Australian Centre for Microscopy & Microanalysis (ACMM) Sydney, Adapted from Deerinck et al., 2010). However, marine specimens, particularly jellyfish, are potentially challenging to image due the nature of

their jellylike tissue and salt content from the marine environment. Samples were, therefore, fixed in a solution of 2.5% glutaraldehyde, 2% paraformaldehyde, 3% sucrose in 0.15 M sodium cacodylate buffer and stored at 4 °C as per Garm et al., (2007) in which the authors successfully prepared a similarly small-sized cubozoan jellyfish, *Tripedalia Cystophora*, for Transmission Electron Microscopy (Similar to SBF-SEM).

7.3.3 Sample preparation

Fixed samples were transported on-ice to external collaborators at the University of Sydney, ACMM, for further preparation and imaging. Tissues were washed in 0.1 M sodium cacodylate buffer and post-fixed in 2% osmium tetroxide and 1.5% potassium ferrocyanide for 1 h in darkness. Tissues were then rinsed in ultrapure water and incubated in 1% thiocarbohydrazide for 20 min. Samples were then rinsed in ultrapure water and incubated in 2% aqueous osmium tetroxide for 30 min. Tissues were again rinsed with ultrapure water and stained in 1% uranyl acetate overnight, followed by Walton's lead aspartate at 60 ℃ for 30 min. Samples were dehydrated in graded series of ethanol and acetone, infiltrated and embedded in hard grade Procure 812 resin.

After polymerisation, tissue blocks were trimmed using an ultramicrotome (Leica EM UC7, Leica Microsystems) and mounted onto an aluminium pin using cyanoacrylate glue. Blocks were painted with silver paint and gold-coated to increase sample conductivity.

7.3.4 SBF-SEM

Inverted backscattered electron images (8,192 ´ 8,192) were acquired every 50 nm at 4 keV using a variable pressure field emission scanning electron microscope (Sigma VP, Carl Zeiss) equipped with a Gatan OnPoint BSE detector and 3View 2.XP system. For each sample between 1,000 – 1,400 images/slices were acquired. The pixel size of each image in the stack was 10 nm. The final dataset was anisotropic, with a voxel size of 10 nm(X), 10 nm(Y), 50 nm(Z).

7.3.5 Data processing

SBF-SEM data was returned from external collaborators to the author as image files per slice (TIFF files). The opensource software Microscopy Image Browser was used to both manually and semi-automatically segment nematocyst ultrastructure (Fig 7.1). For whole capsule models, the smaller internal structures were absorbed into the inverted tubule model (Fig 7.1A,B). This was done because 1) the whole capsule model was intended for visualizing the greater overall biological structure, 2) the internal spines of the inverted tubule, even if segmented here would not be visible in the final 3D print, 3) the internal inverted spines required manual segmentation and to

segment these spines for an entire model would increase the processing time for each data set by roughly 4+ months. The decision was made to fully segment the internal spines and hollow areas only on smaller cropped regions of the datasets (fig 7.1C,D).

For regions such as the capsule which possessed a regular spherical shape, manual segmentations could be interpolated between <30 slices at a time. Inverted tubules were highly irregular in shape and were therefor manually segmented for each slice of the dataset. The Frangi filter, which is typically used to detect vessel-like or tube-like structures and fibers in volumetric image data, was used to accurately detect and segment the cross sections of the larger shaft spines present on the discharged nematocyst (fig 7.2).

Early iterations of these segmented models were saved as 3D TIFF files and sent for further processing, optimizing and/or author training to external collaborators at the University of Sydney, ACMM where the segmented model was extracted in FIJI and processed to a volume rendering and animated in AMIRA. Later iterations were processed in house by the author by exporting the segmented models as STL files in Microscopy Image Browser and further rendered and animated in the opensource software Dragonfly.

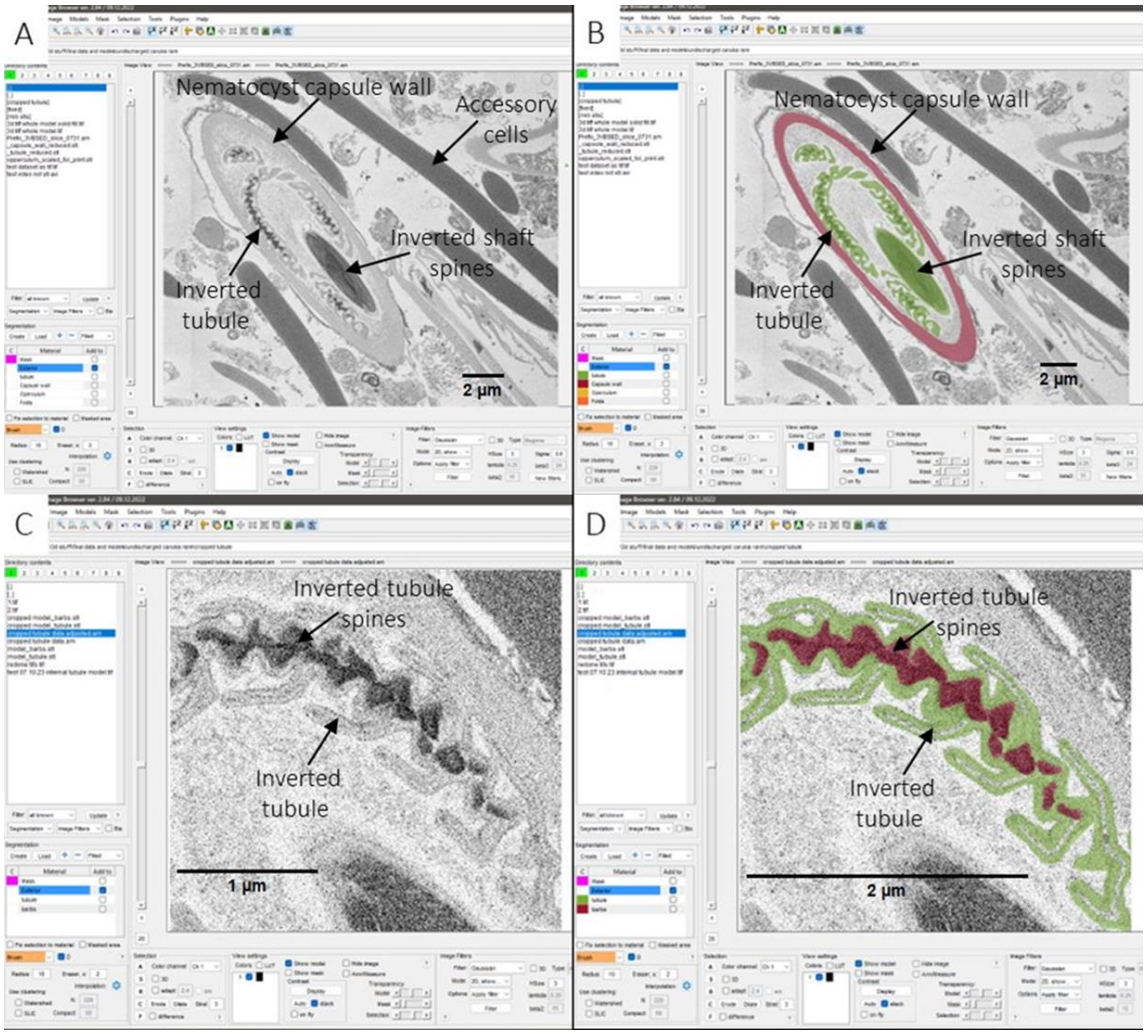

Figure 7.1: Example data segmentation in Microscopy Image Browser of Serial Block Face Scanning Electron Microscopy images of an undischarged nematocyst from an adult Carukia barnesi tentacle. A/B: A single image slice though a whole nematocyst, raw image data (A) and ultrastructures of interest segmented (B) shown is red outer capsule and green inverted tubule. Here the smaller internal spines are not segmented but are absorbed into the tubule model (green). C/D: A cropped region of the inverted tubule, in which more in-depth segmenting is conducted (D), the hollow nature of parts of the tubule is observed (green) and the internal spines previously excluded in B are segmented here.

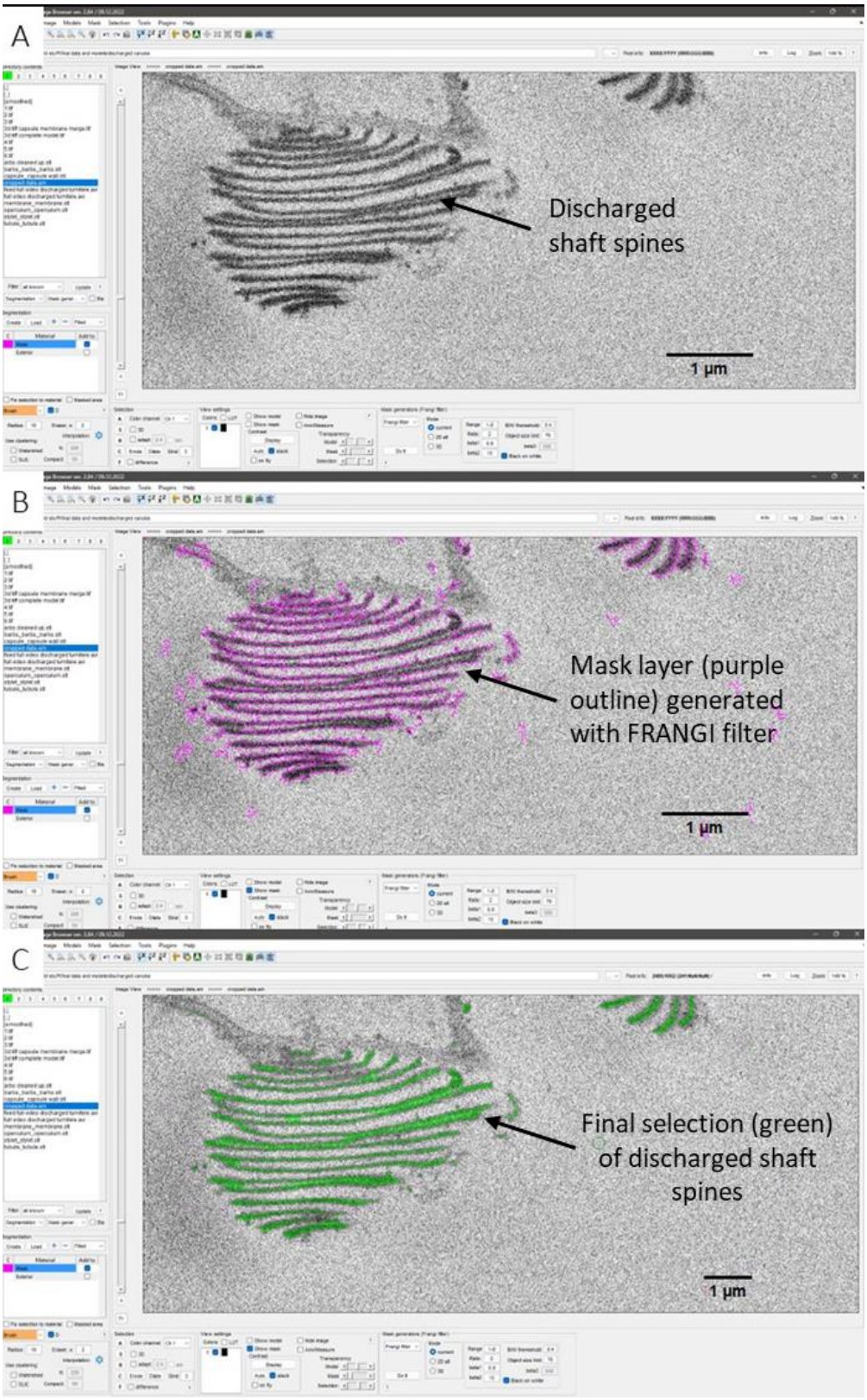

Figure 7.2: Example data segmentation using Frangi filter in Microscopy Image Browser of Serial Block Face Scanning Electron Microscopy images of discharged nematocyst shaft spines from an adult Carukia barnesi tentacle. A: raw image data, B: Mask generated by FRANGI filter (purple outline), C: Segmentation selection generated from mask.

For lack of standard dimensional terminology regarding 3D nematocysts, this author has opted to utilise standard anatomical nomenclature and adapt it as appropriate to nematocyst structure. For descriptive purposes, the dimensional terminology outlined in figure 3 are therefore adopted throughout this work.

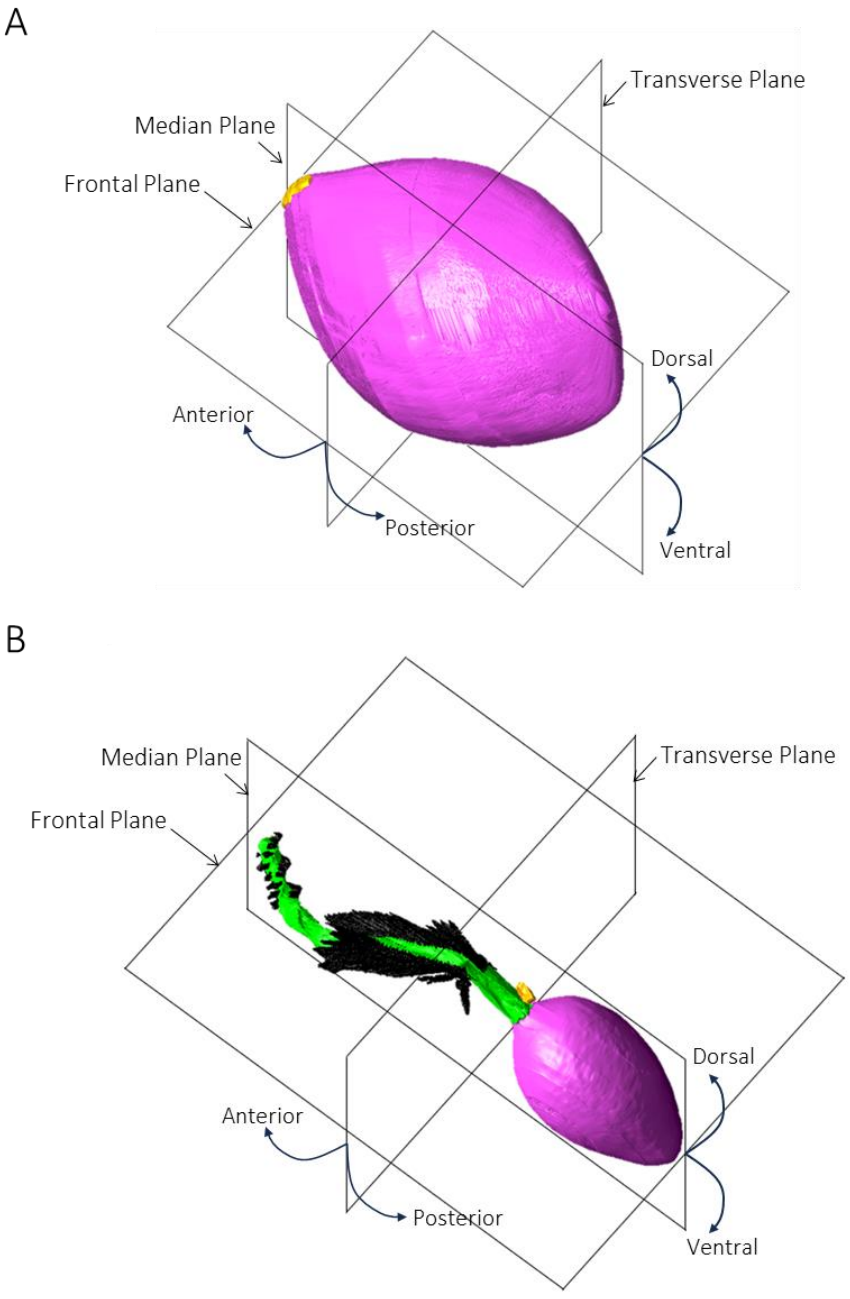

Figure 7.3: Example dimensional terminology for an undischarged nematocyst (A) and a discharged nematocyst (B). Note in the undischarged nematocysts (A) Anterior and Posterior are relative to the middle position of the transverse plane (as pictured), whereas in the discharged

nematocyst (B) Anterior and Posterior are relative to the point of discharge where the everted tubule base is connected to the capsule (as pictured by the transverse plane).

7.3.6 3D printing

For 3D printing, STL files were generated both in house by the author (MIB) and externally at Sydney (FIJI) dependent on the final segmented model file size as larger datasets required a computer with higher processing power. Some STLs were edited to print the model in two parts, i.e., the whole capsules, so the resulting print would be interactive and the internals (inverted tubule) of the model could be added and removed at will for display purposes. Models were 3D printed via stereolithography, a technique superior to standard additive 3D printing as stereolithography can better visualise finer structural details.

7.4 Results

Over 65 nematocysts from adult *C. barnesi* tenacles were captured with Serial Block Face Scanning Electron Microscopy (SBF-SEM), of which three were chosen to fully render as representative 3D models (one undischarged Tumitele, one discharged Tumitele and one undischarged Mastigophore) were rendered firstly to virtual volumes[4] (figs 7.3-7.17), then further as physical 3D printed models (figs 7.19-21).

7.4.1 Undischarged Tumitele – full nematocyst

An ellipsoid, almost lemon shaped capsule (purple) approximately 20 µm in length, with a tripartite occluding operculum (yellow) is visible in figure 7.4A. In figure 7.4B, the same model view is presented but with reduced opacity of the capsule (purple). The inner components of the capsule are visible illustrating the relative positioning and shape of the inverted tubule (green) coiled within. Figure 7.5 highlights the structure of the inverted tubule/shaft (green) coiled within. The relative positioning of the tripartite occluding operculum (yellow) is shown both present (A) and absent (B) situated at the anterior end of the shaft (green). The shaft runs from the anterior capsule tip to the posterior tip, visible in fig 7.6 presenting as a loose helical coil in shape. Views of both the anterior (fig 7.7A) and posterior (fig 7.7B) shaft poles show the shaft is positioned centrally in the transverse plane, with the remaining inverted tubule coiling around this central shaft. The tubule does not fully coil in the transverse plane (i.e., they do not complete a full rotation around the shaft), more the coils occupy a U/horseshoe shape before doubling back (Fig 7.7A). The anterior pole of the shaft is connected to the operculum/capsule opening (figs 7.4 and

[4] The terminology “volume” in this field of work is used to describe 3D volumetric data, i.e. The 3D models presented throughout this work are “volume images”.

7.5), the posterior end is continuously connected to the remaining inverted tubule. The inverted shaft appears straight and rod like due to the large shaft spines (not visible) which are inverted within the tubule. Near the end position of these large spines, we see the inverted tubule become much less rigid, more flexible and tightly coiled. It appears the remaining inverted tubule at the posterior shaft pole is almost entirely doubled back on itself (figure 7.9), due to the transition from large, inverted shaft spines to much smaller spines within the tubule. The SBF-SEM acquisition produces an anisotropic dataset, which results in differences in scan resolution across different regions of the inverted tubule. This is illustrated in figure 7.10 , along with the difference in structural details ultimately produced in the final renders. The full undischarged Tumitele can be viewed from all angles and in closer detail in Video 1, in which the relative positioning of all structures is evident, along with detailed regions of the inverted tubule where the tightly coiled helices are visible, whilst in other tubule regions this patterning is less visible.

7.4.2 Undischarged Tumitele – cropped tubule section

A smaller region of inverted tubule was rendered to display the profoundly coiled helices with as much detail as possible (figure 7.10 and video 2). The small spines are visible in helices on the internals of the inverted tubule. Upon discharge and tubule eversion it is these spines that will line the tubule exterior.

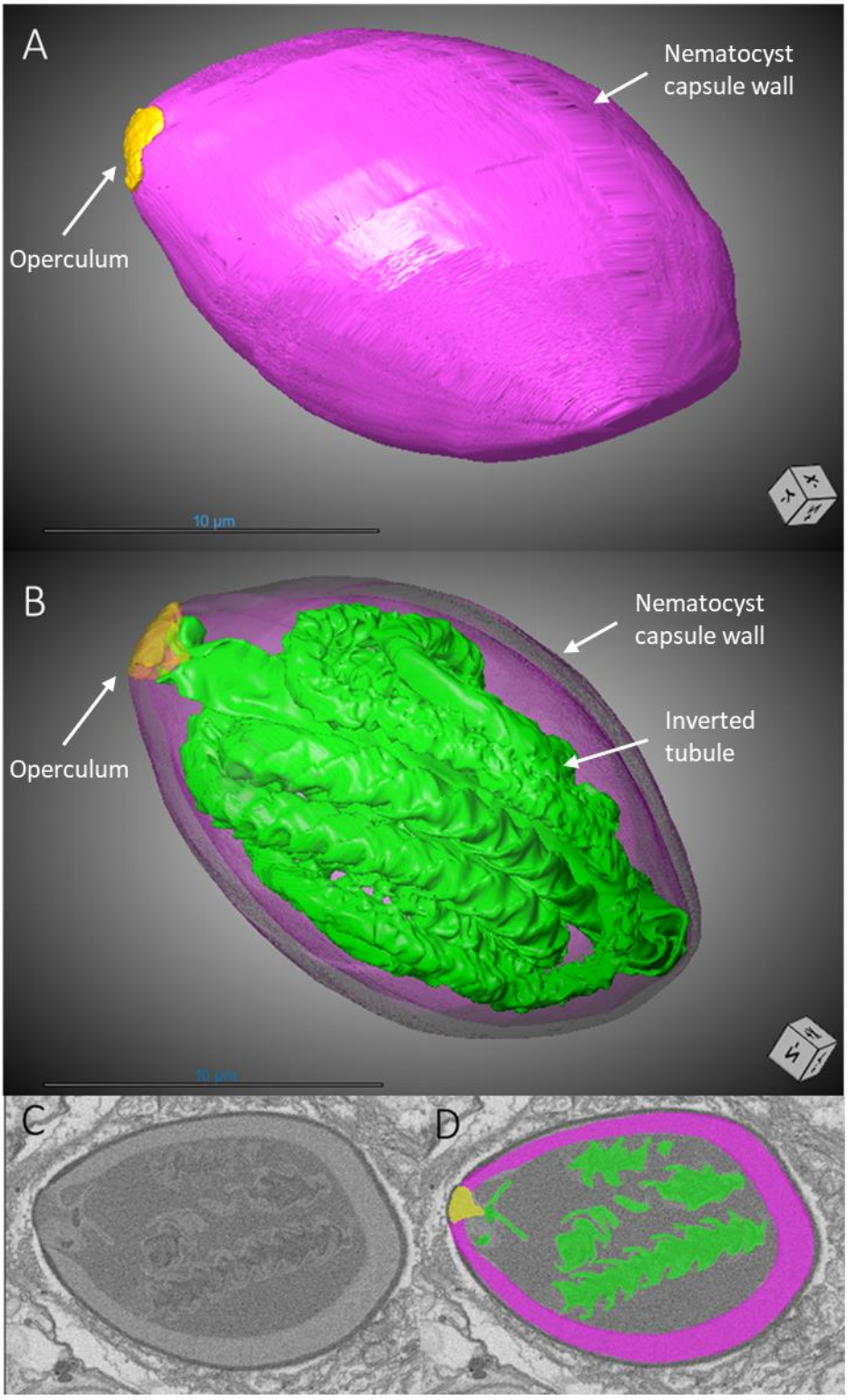

Figure 7.4: 3D model of an undischarged Tumitele nematocyst from the tentacles of an adult Carukia barnesi jellyfish. A: Ellipsoid/lemon shaped capsule (purple) with an occluding tripartite operculum (yellow). B: The same model as in A, but here with the capsule opacity reduced to reveal the relative positioning of the inverted tubule/shaft (green) coiled within. C/D: SBF-SEM slice through the nematocyst, both with (C) and without (D) the segmented regions of interest (purple/yellow/green as in A/B).

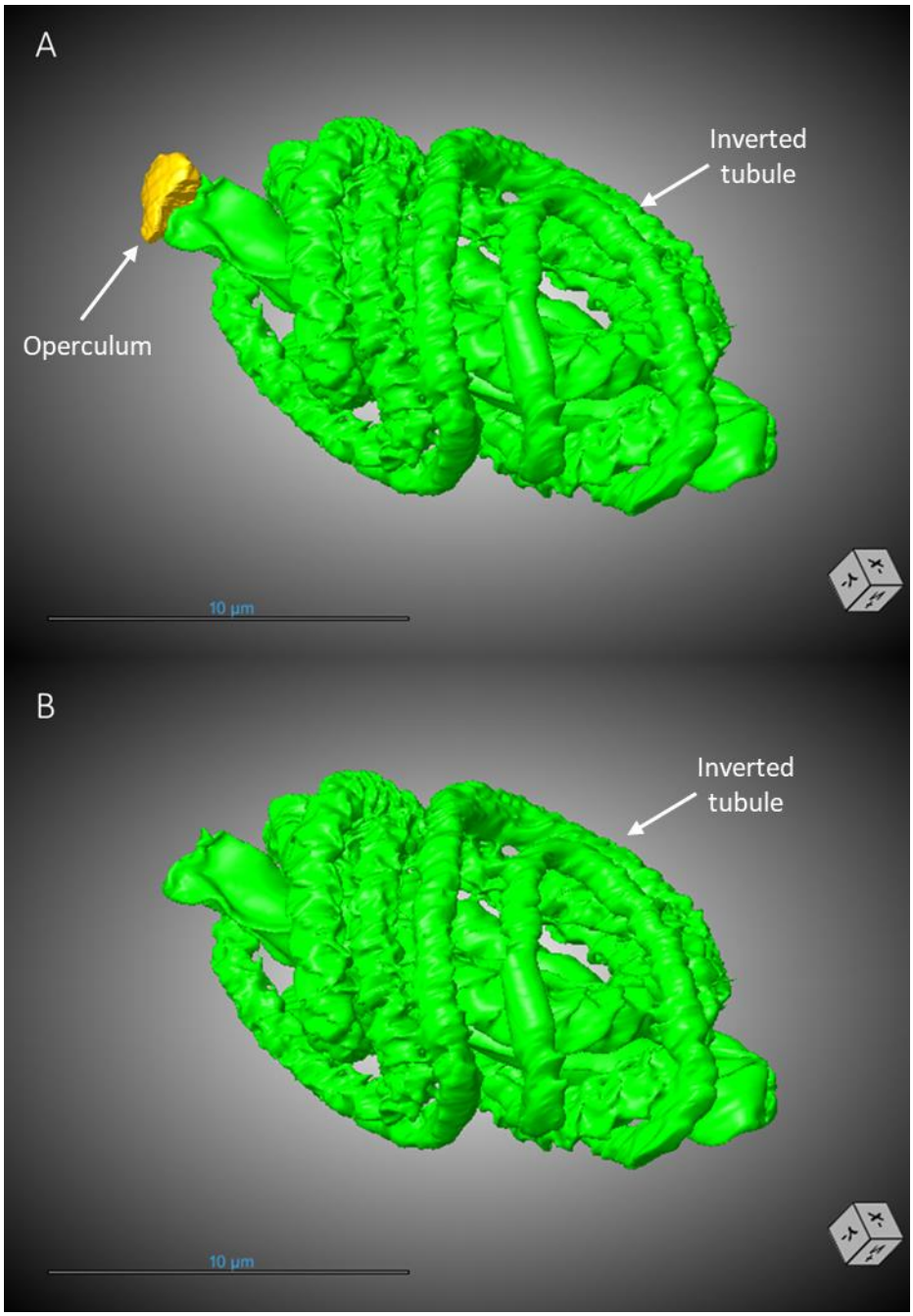

Figure 7.5: 3D model of an undischarged Tumitele nematocyst from the tentacles of an adult Carukia barnesi jellyfish. The capsule has been omitted to reveal the structure of the inverted tubule/shaft (green) coiled within. The relative positioning of the operculum (yellow) is evidenced both present (A) and absent (B) at the end of the shaft (green).

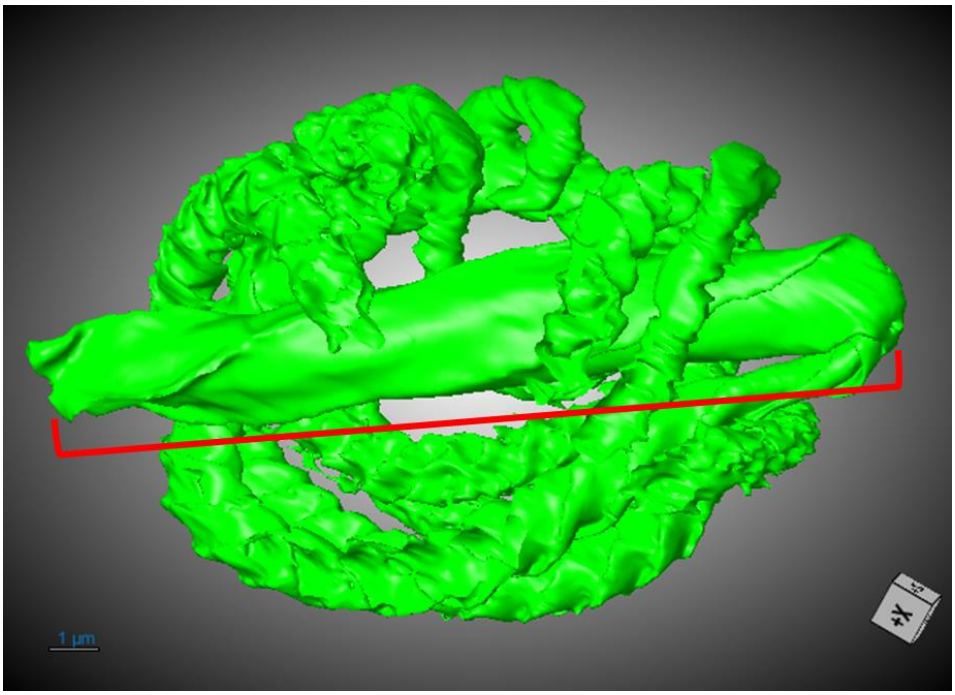

Figure 7.6: 3D model of an undischarged Tumitele nematocyst from the tentacles of an adult Carukia barnesi jellyfish, with the capsule omitted from view. The pane has been clipped to remove some tubules from view to facilitate better viewing to the centre of the model. The inverted shaft spans the length of the nematocyst, highlighted in red.

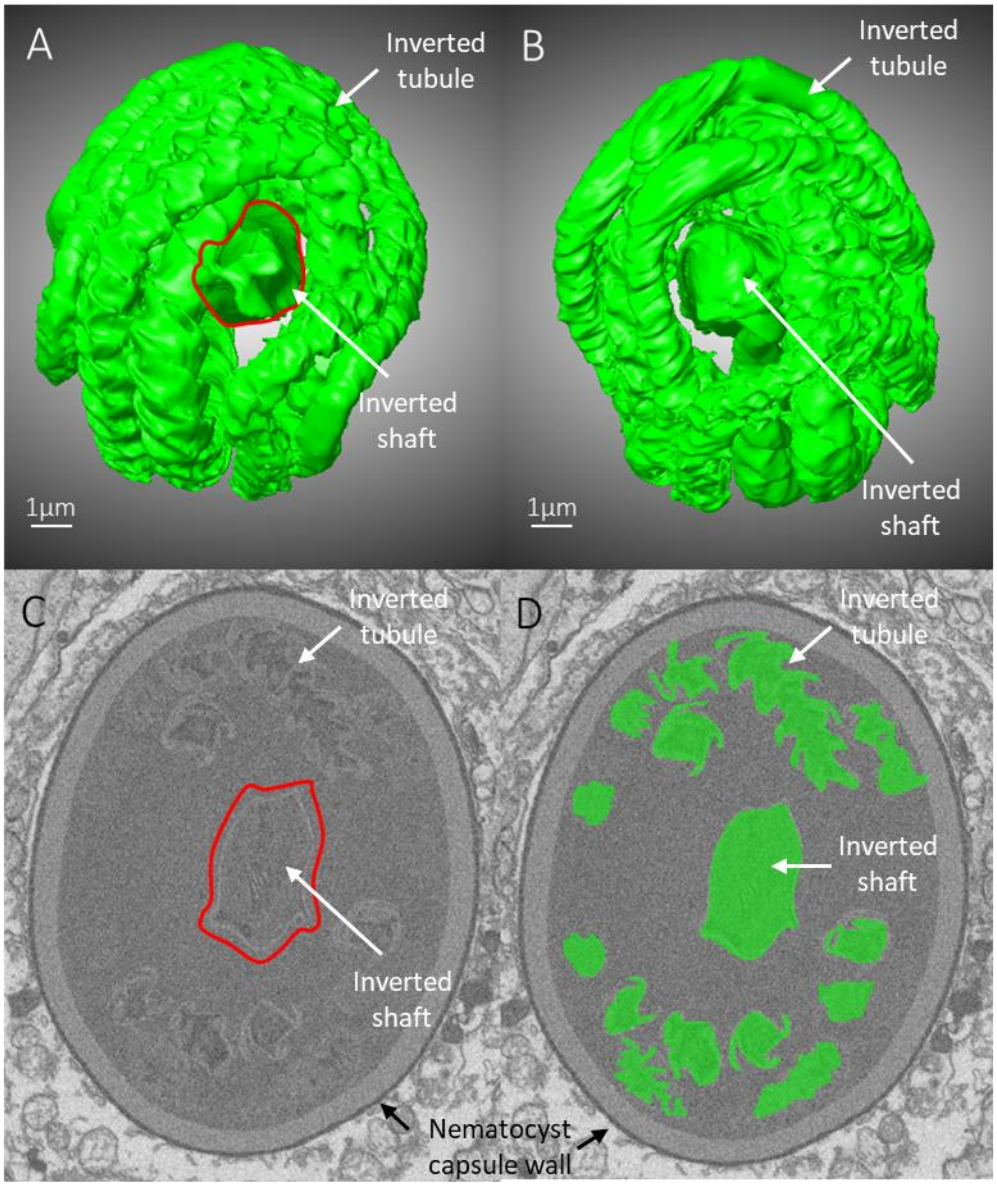

Figure 7.7: 3D model of an undischarged Tumitele nematocyst from the tentacles of an adult Carukia barnesi jellyfish, with the capsule omitted from view. The inverted shaft (red highlight in A) spans the length of the nematocyst, positioned centrally, surrounded by the coiled inverted tubules. Transverse plane view shows the shafts central positioning A: the shaft pole which would be connected to the capsule tip/operculum, B: the shaft pole continually connected to the coiled tubule. C/D: SBF-SEM slice through the nematocyst, both with (C) and without (D) the segmented regions of interest (green/red highlight as in A).

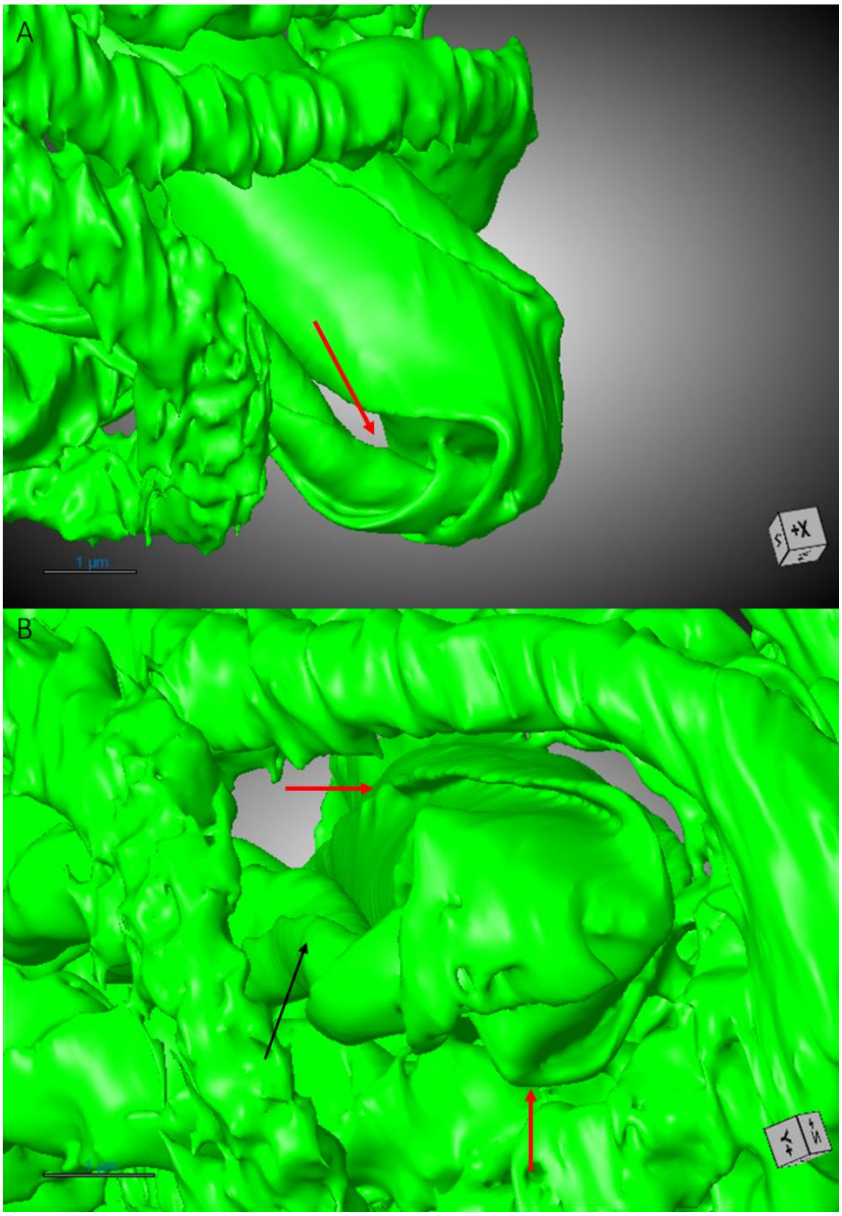

Figure 7.8: 3D model of an undischarged Tumitele nematocyst from the tentacles of an adult Carukia barnesi jellyfish, with the capsule omitted from view. Close up view of the inverted shaft posterior pole end connected to the inverted tubule. A: The point of transition between the long straight inverted shaft to the remaining tubule is almost fully doubled back on itself in angle (red arrow). B: The inverted shaft possesses much looser helices (red arrows) in comparison to the much more tightly coiled helices of the remaining inverted tubule (black arrows).

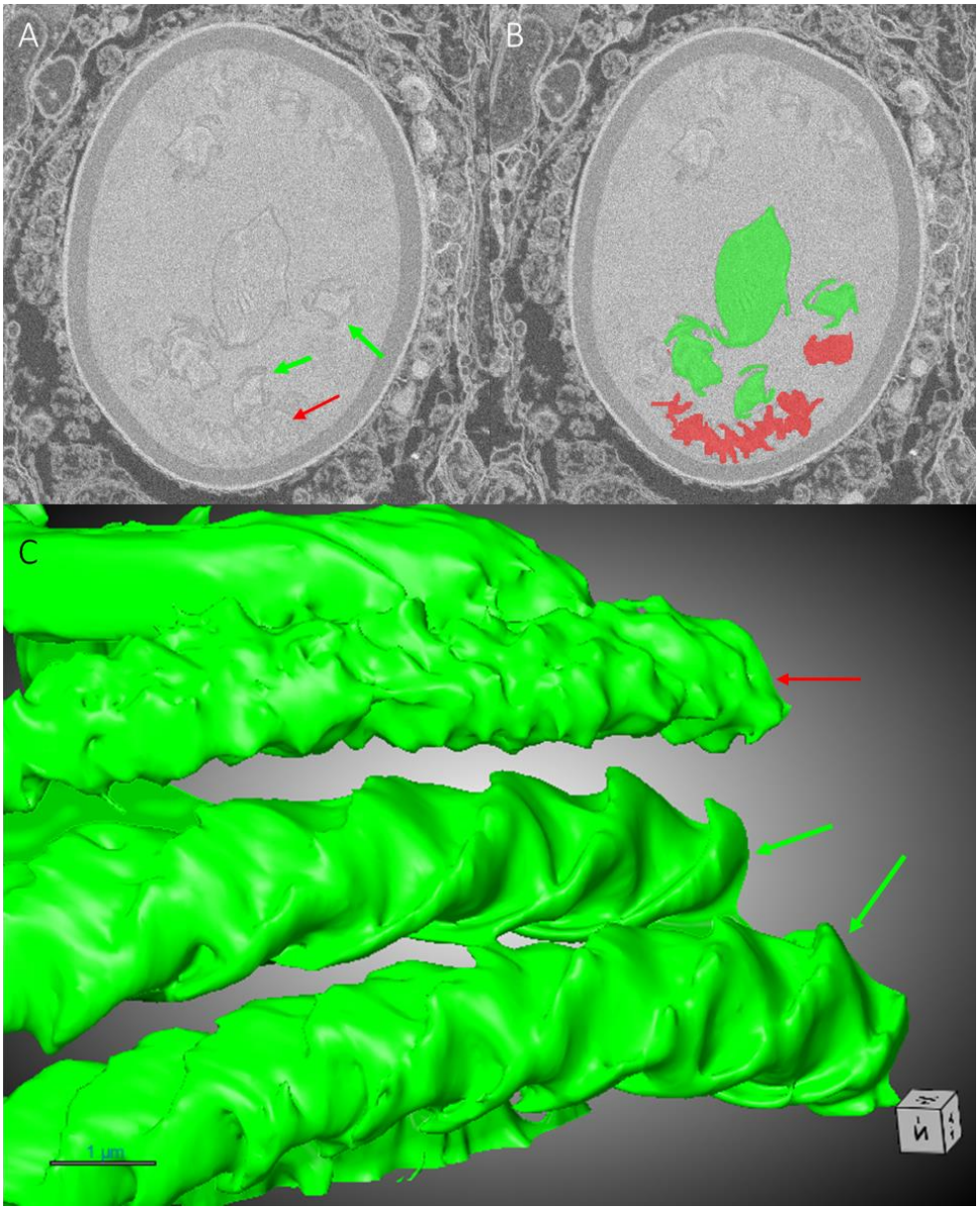

Figure 7.9: Partial 3D model of an undischarged Tumitele nematocyst from the tentacles of an adult Carukia barnesi jellyfish. Anisotropic datasets present differences in the details of ultrastructure. A: Differences in observable details between inverted tubules in the same SBF-SEM scan, due to the angle of the tubule. High resolution detail – green arrows, lower resolution detail – red arrow. B: Respective segmented models as in A. C: Differing rending quality of tubule ultrastructural details, high resolution detail – green arrows, lower resolution detail – red arrow, resulting from anisotropic data.

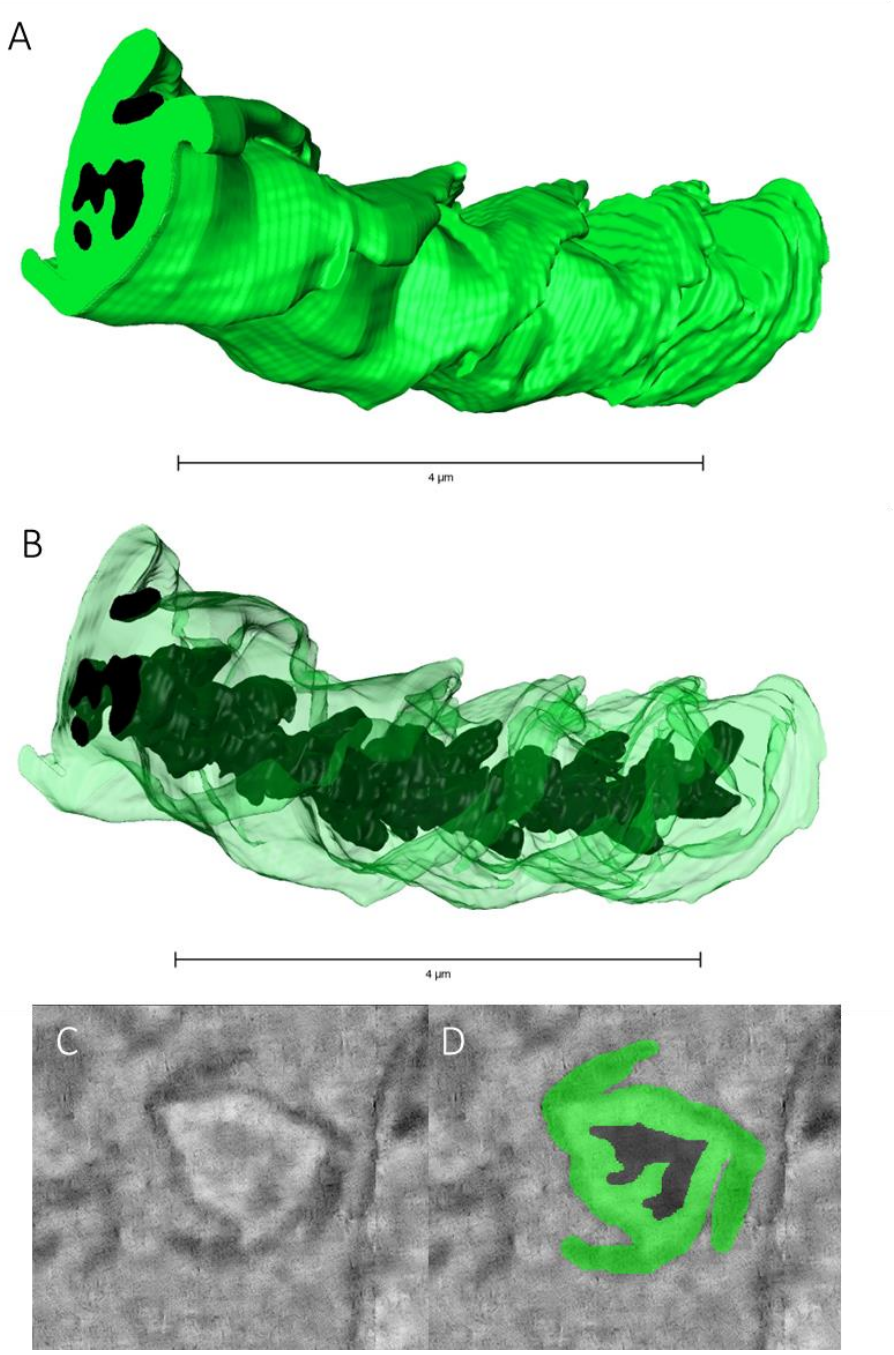

Figure 7.10: A cropped section of the inverted tubule of an undischarged Tumitele nematocyst from the tentacles of an adult Carukia barnesi jellyfish. A: An opaque rendering visualises the coiled springlike ultrastructure of the inverted tubule (green). B: The model as in A, with the opacity of the tubule (green) reduced to visualise the spines (black) lining the centre of the inverted tubule. C/D: SBF-SEM slice through the cropped tubule region within the nematocyst, both with (C) and without (D) the segmented regions of interest (green/black as in B).

7.4.3 Discharged Tumitele – full nematocyst

An ellipsoid, almost lemon shaped capsule (purple) approximately 20 µm in length with a discharged tripartite operculum (yellow) is shown in figure 7.11A. The everted tubule (green) consists of the shaft region located at the base of the tubule, with large triangular shaft spines stacked in triple helices. These large spines are pointed in the anterior direction, possibly a result of the artificial discharge method used during sample preparation. The remaining everted tubule continuing from the shaft region is lined with smaller spines, also triangular in shape, lining the tubule in triple helices. Consistent with SEM analysis (chapter six), these smaller spines all point in the posterior direction. The everted tubule has some level of flexibility, as evidenced in figure 7.11, as it appears to have not discharged in a completely straight line. In figure 7.11B the large shaft spines have been omitted from view to visualise the shape of this shaft region. The defining characteristic of a Tumitele nematocyst (discussed at length in chapter six) is the single median dilation of the shaft and is highlighted in red). All the nematocysts presented in this chapter posses a very thin outer capsule layer, however due to technical difficulties rendering, animating and 3D printing such a thin layer of ultrastructure, it has only been visualised in this single rendering. Figure 7.12 shows both this outer (purple) and inner (yellow) capsule layer visible in the raw SBF-SEM data and the corresponding example of segmented models, along with an accurate 3D rendering of the capsule with the outer layer (purple) partially clipped to reveal the inner capsule layer (yellow, reduced opacity). The thin outer layer may be represented marginally thicker than is biologically correct due to difficulties with segmenting such a thin structure. Figure 7.13 shows partial 3D models of the everted tubule, where a slight helical shape is evident along the discharged tubule itself (green), with the exterior lined with small triangular shaped spines (black) pointing in the posterior direction in triple helices. The complete, undischarged Tumitele can be viewed from all angles and in closer detail in video 3 (and 4), in which the relative positioning of all structures is evident, along with a simulation of the approximate discharge path of ejected venom. Video 4 shows the relative positioning of the model in the raw SBF-SEM slices.

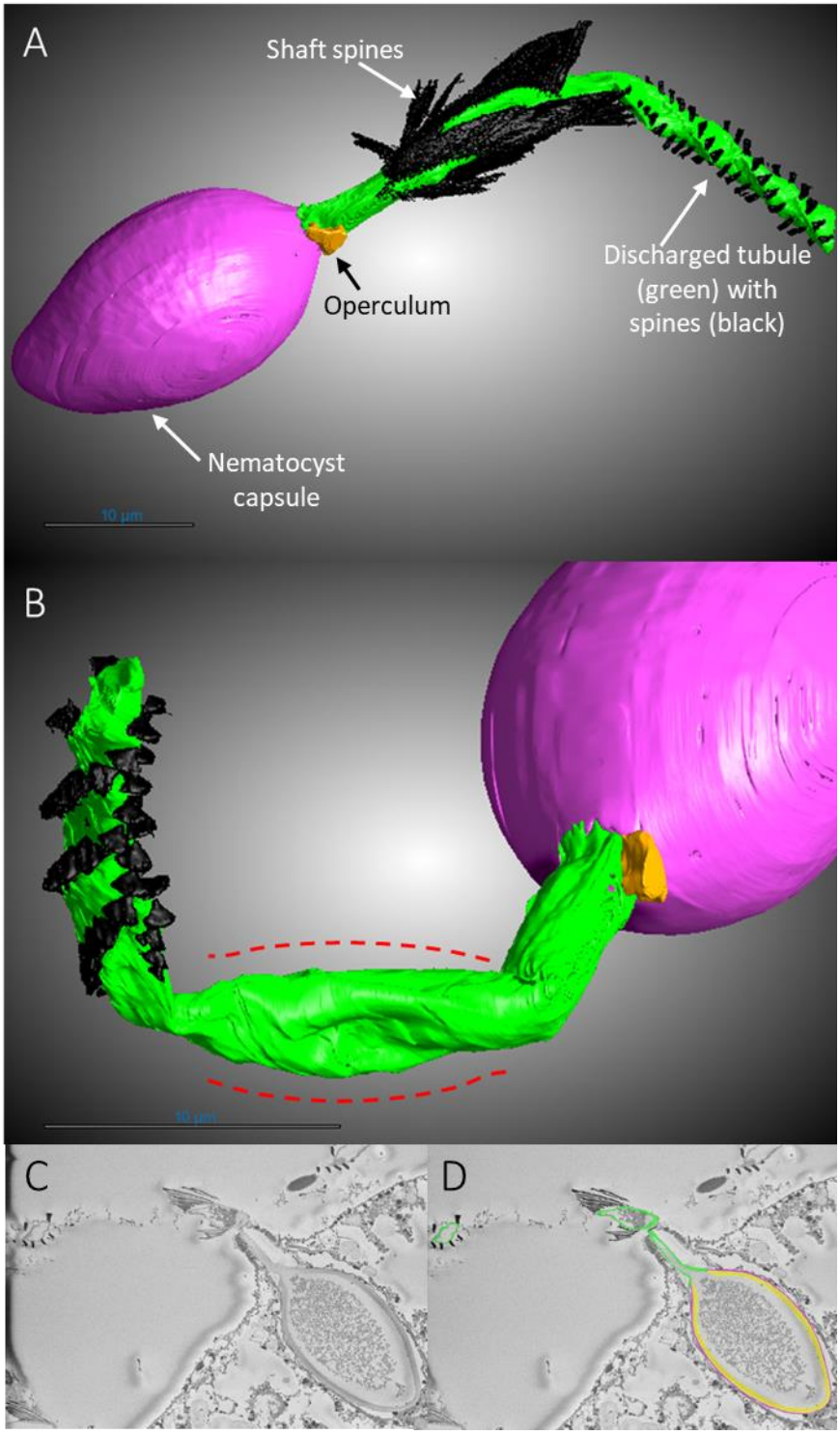

Figure 7.11: 3D model of a discharged Tumitele nematocyst from the tentacles of an adult Carukia barnesi jellyfish. A: Capsule (purple), everted tubule (green), operculum (yellow), large shaft spines and smaller tubules spines (black). B: Model as in A but with large shaft spines omitted. A slight dilation of the shaft, characteristic of Tumiteles, can be observed (red highlight).C/D: SBF-SEM slice through the nematocyst, both with (C) and without (D) the segmented regions of interest, colours as per A/B and fig 7.12.

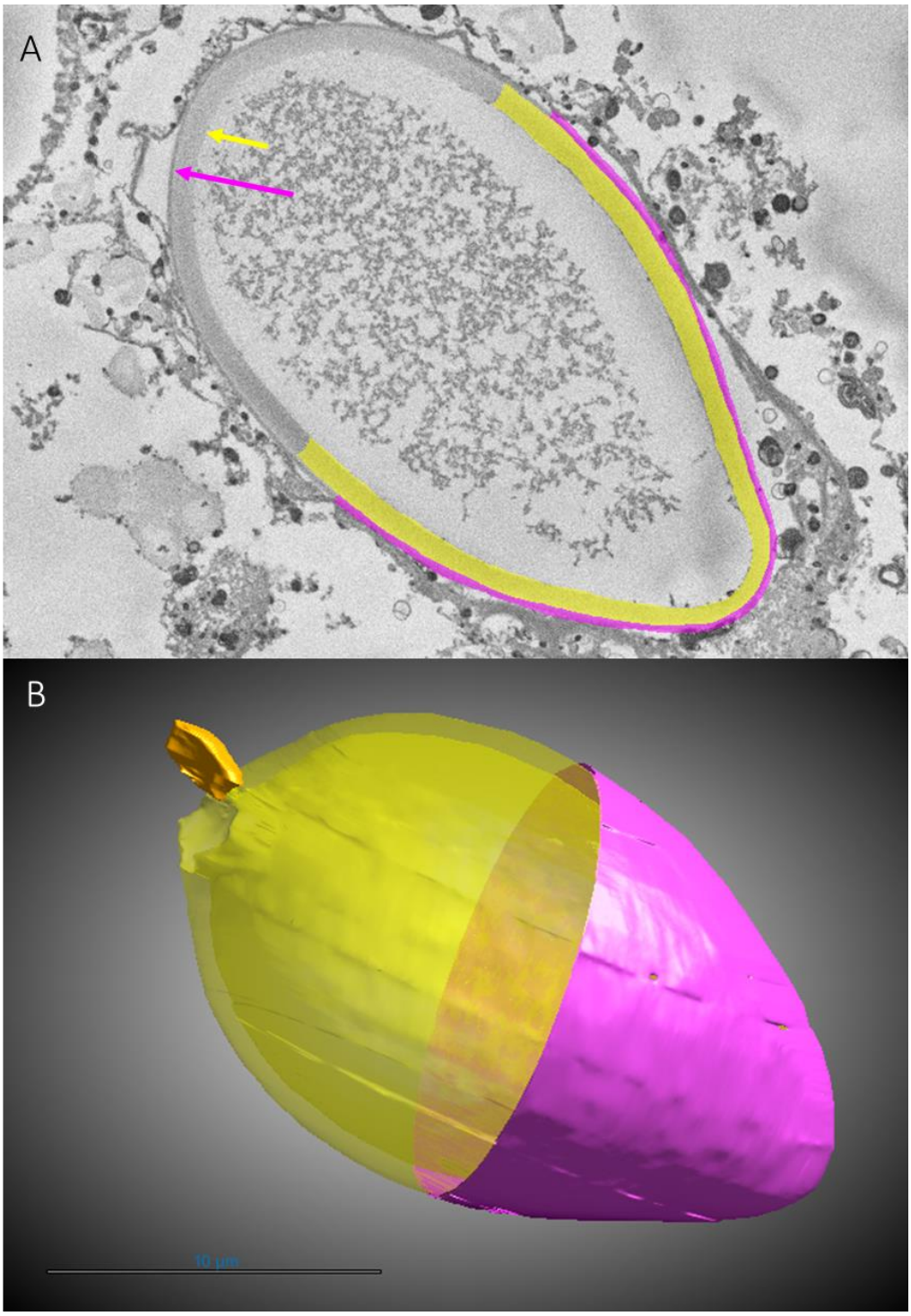

Figure 7.12: Partial 3D model of the capsule and operculum of a discharged Tumitele nematocyst from the tentacles of an adult Carukia barnesi jellyfish, tubule and spines omitted here. A: SBF-SEM slice through capsule, with examples of associated model segment (partial), capsule wall (yellow), outer capsule layer (purple). B: 3D rendering of the capsule with the outer layer (purple) partially clipped to reveal the capsule wall (yellow, reduced opacity) within.

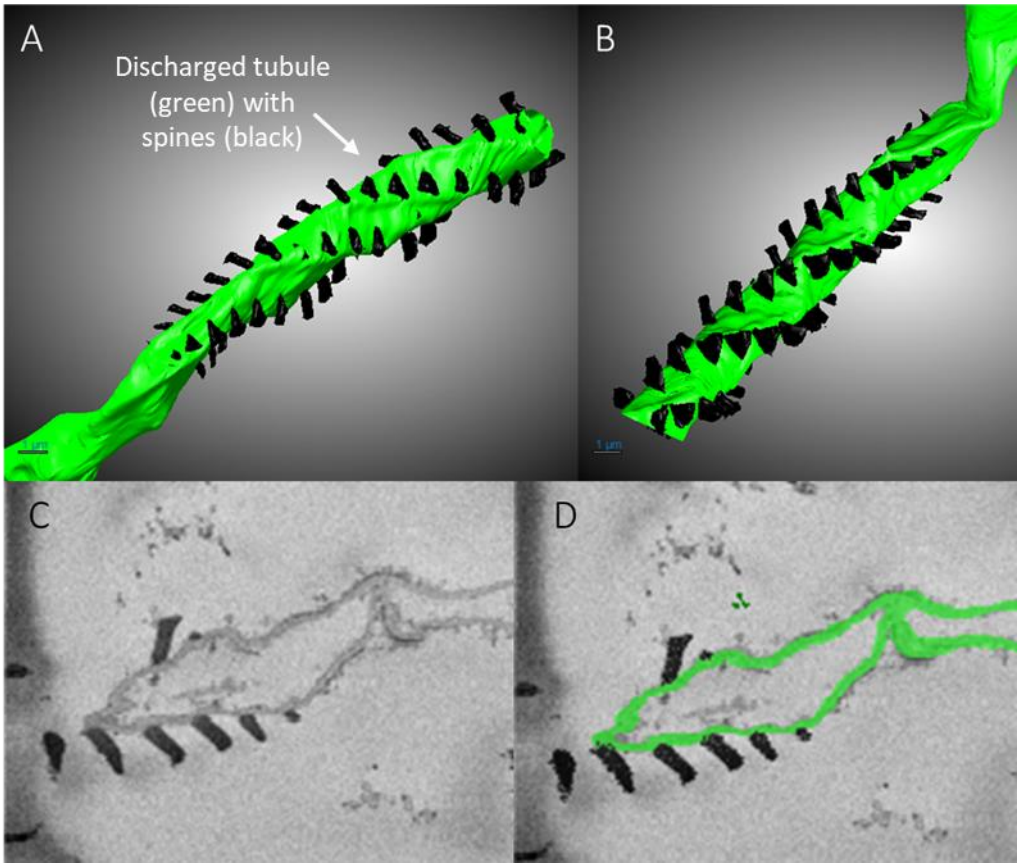

Figure 7.13: Partial 3D model of the everted tubule of a discharged Tumitele nematocyst from the tentacles of an adult Carukia barnesi jellyfish. A helical shape is evident along the discharged tubule (green), small triangular shaped spines (black) are present as three helical spirals along the discharged tubule. C/D: SBF-SEM slice through the nematocyst, both with (C) and without (D) the segmented regions of interest.

7.4.4 Undischarged Mastigophore – full nematocyst

A 3D model of an undischarged Mastigophore is shown as a long, cigar shaped capsule (purple) approximately 50 µm in length with a tripartite occluding operculum (yellow) is illustrated in figure 7.14A. In figure 14B the same model view is presented but with reduced opacity of the capsule (purple), showing the inner components of the capsule and the relative positioning and shape of the inverted tubule (green) coiled within. Figure 7.15 presents the capsule now fully absent from view to reveal the structure of the inverted tubule/shaft (green) coiled within. The relative positioning of the tripartite occluding operculum (yellow) is shown both present (A,C) and absent (B.D), situated at the anterior end of the shaft (green). The shaft runs from the anterior capsule tip to the posterior tip, , displaying a very loose, helical shaped coil i. Unlike in the Tumitele, the shaft occupies a different positioning relative to the remaining coiled tubule. Here, if we describe the relative positioning as seen in figure 7.14B & 7.15A, the shaft is positioned at the dorsal edge of the capsule, along the frontal plane, with the remaining inverted tubules wound into distinct coils beneath the shaft. The tubule does not coil transversally (as seen in the Tumitele fig 7.7) but rather the coiling pattern appears to loop in the frontal plane, from posterior to anterior tip (fig 7.16). Whilst the anterior pole of the shaft is connected to the operculum/capsule opening (figs 7.14 and 7.15), the posterior end is continuously connected to the remaining inverted tubule, with the remaining inverted tubule almost entirely doubling back on itself (figure 7.16). The differences in scan/render resolution of the tubule due to an anisotropic dataset are evident in figure 7.17. The full undischarged mastigophore can be viewed from all angles and in closer detail in video 5, in which the relative positioning of all structures are evident, tubule regions of high and low render detail can also be seen.

7.4.5 Undischarged Mastigophore – cropped tubule section

A smaller region of inverted tubule was rendered (figure 7.18 and video 6). Here the small internal spines are visible in helices within the inverted tubule. The presence of these internal inverted spines confirms that the discharged tubule will be lined with small spines, an ultrastructural detail that was previously unclear from the SEM images of this nematocysts presented in Chapter six.

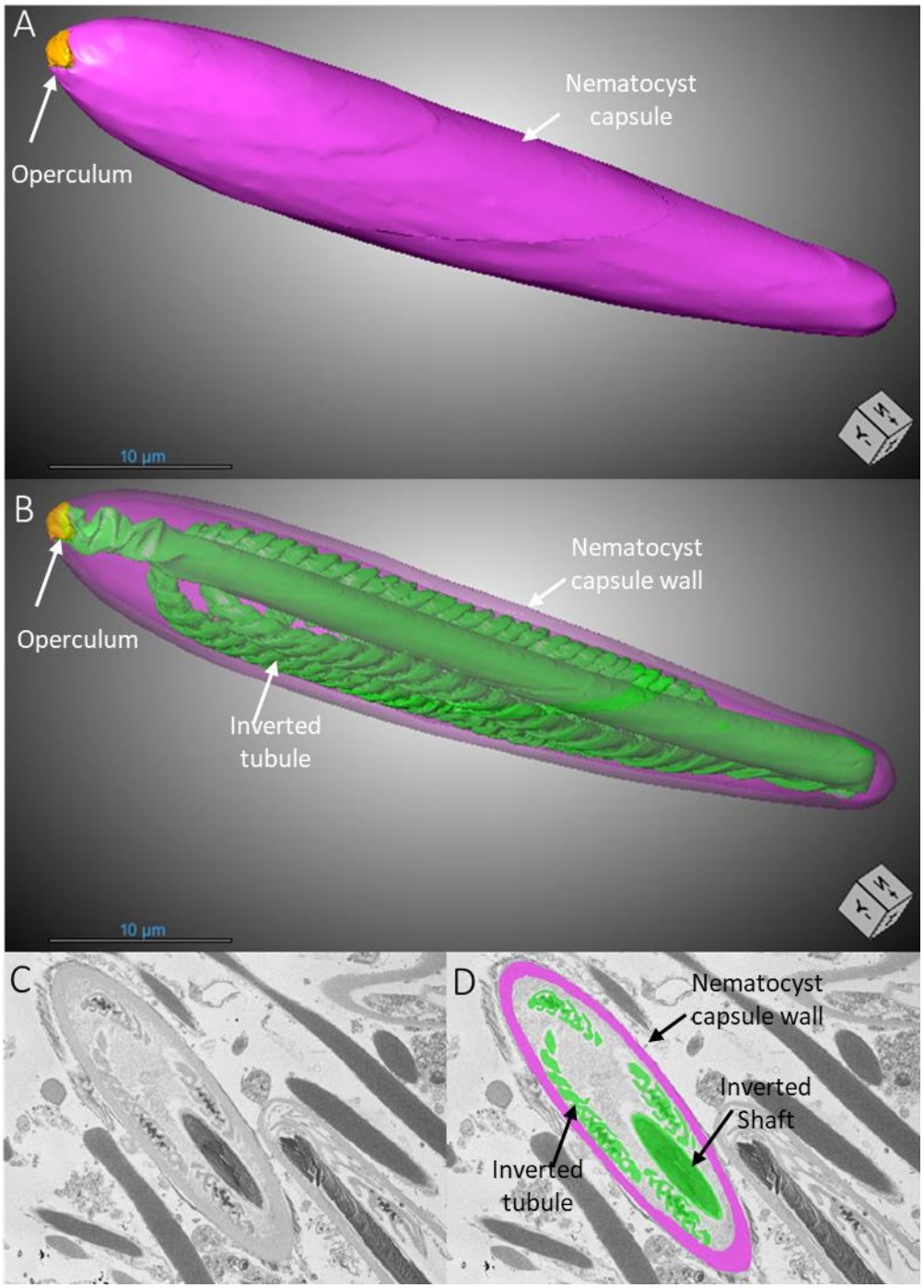

Figure 7.14: 3D model of an undischarged Mastigophore nematocyst from the tentacles of an adult Carukia barnesi jellyfish. A: A long, cigar shaped capsule (purple) with an occluding tripartite operculum (yellow). B: The same model as in A, but here with the capsule opacity reduced to reveal the relative positioning of the inverted tubule/shaft (green) coiled within. C/D: SBF-SEM slice through the nematocyst, both with (C) and without (D) the segmented regions of interest.

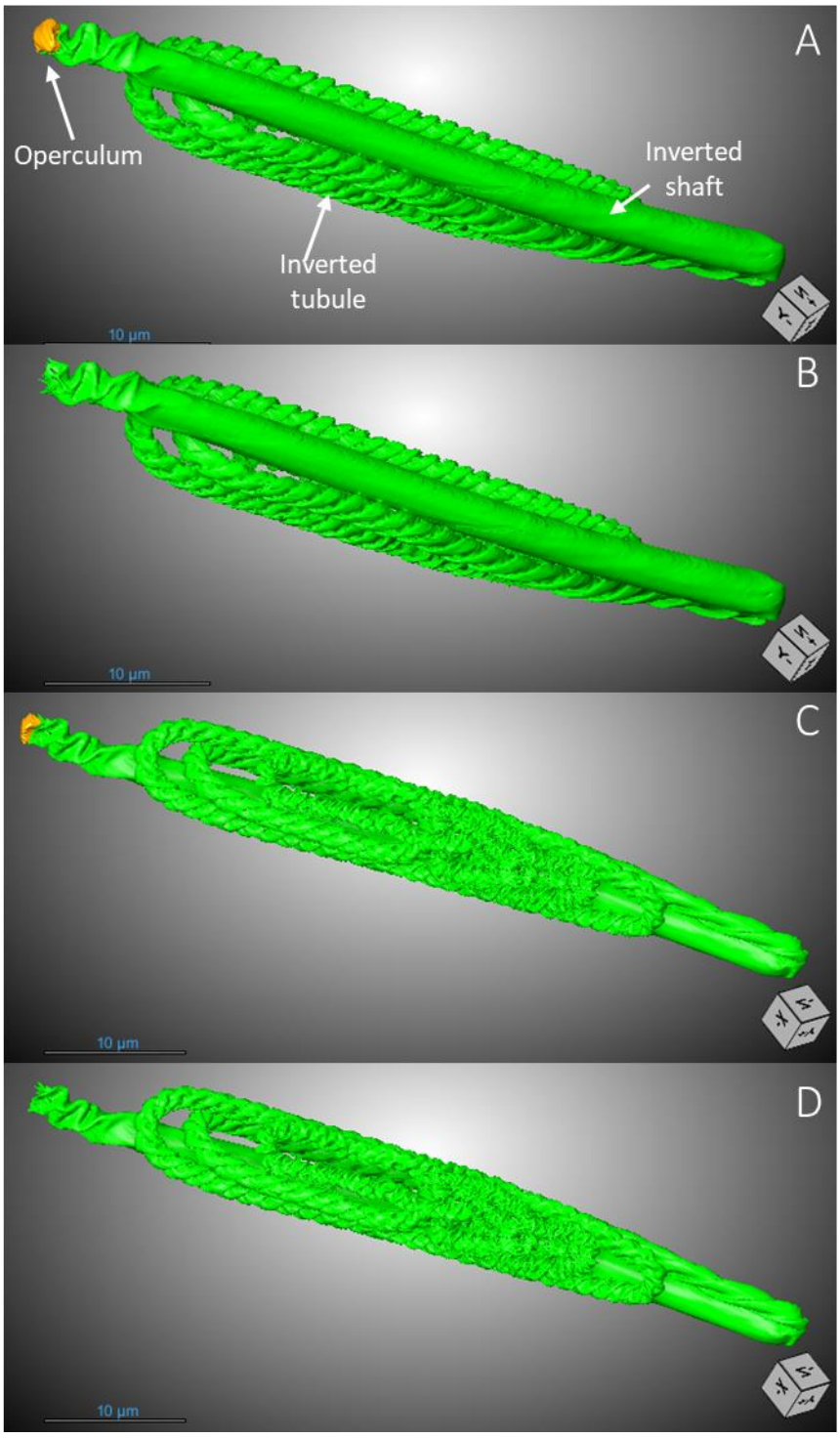

Figure 7.15: 3D model of an undischarged Mastigophore nematocyst from the tentacles of an adult Carukia barnesi jellyfish. The capsule has been omitted to reveal the structure of the inverted tubule/shaft (green) coiled within. The relative positioning of the operculum (yellow) is evident as present (A,C) and absent (B,D) at the end of the shaft. Two differing viewpoints (A/B and C/D) visualize the coiling pattern in space of the inverted tubule.

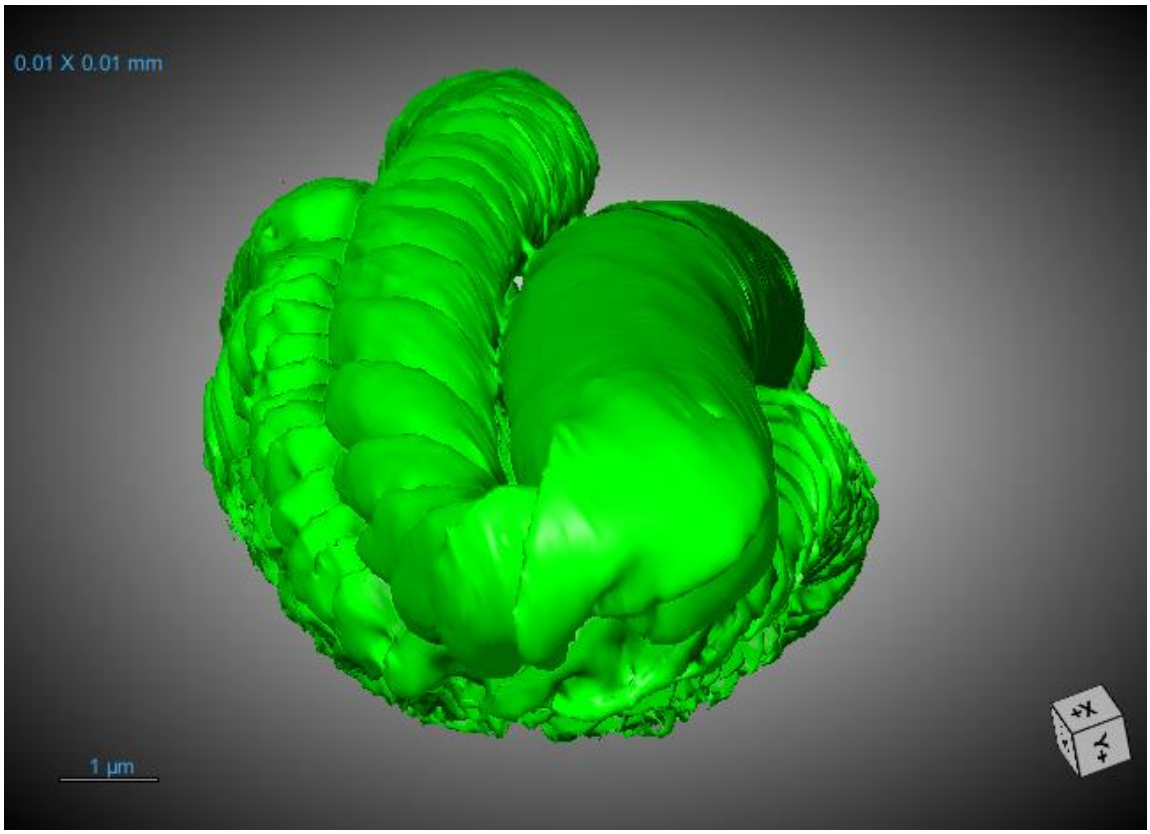

Figure 7.16: 3D model of an undischarged Mastigophore nematocyst from the tentacles of an adult Carukia barnesi jellyfish, with the capsule omitted from view. The inverted shaft spans the length of the nematocyst, positioned to one side of the coils of the inverted tubule. The inverted shaft pole continually connects to the inverted tubule. Note the diameter of the inverted tubule is smaller than the associated inverted tubule even at its thickest part.

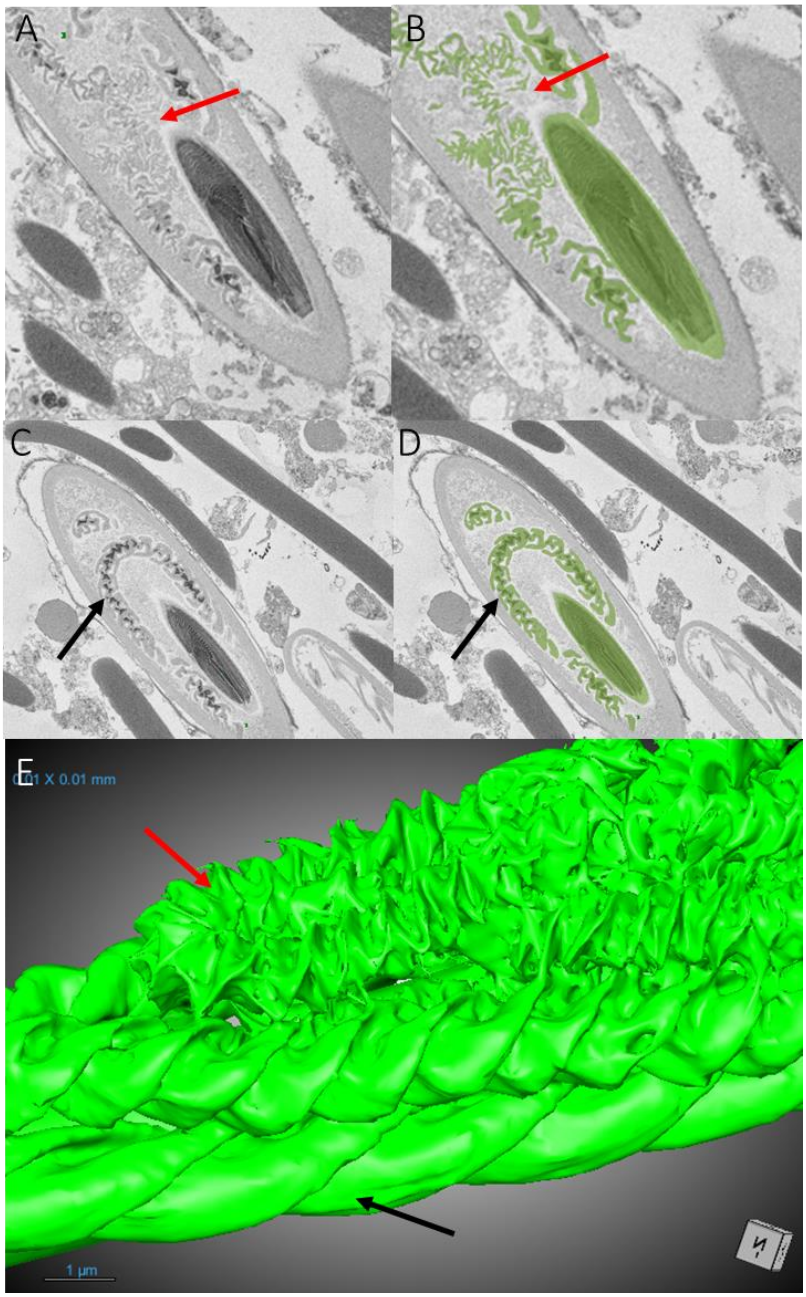

Figure 7.17: Partial 3D model of an undischarged Tumitele nematocyst from the tentacles of an adult Carukia barnesi jellyfish. Anisotropic datasets present differences in the details of ultrastructure. Differences in observable details between inverted tubules in the same SBF-SEM scan, due to the angle of the tubule. Lower resolution detail – red arrows (A,B), high resolution detail – black arrows (C,D). B/D: Respective segmented models as in A/C. E: Differing rending quality of tubule ultrastructural details, high resolution detail – black arrows, lower resolution detail – red arrow, resulting from anisotropic data.

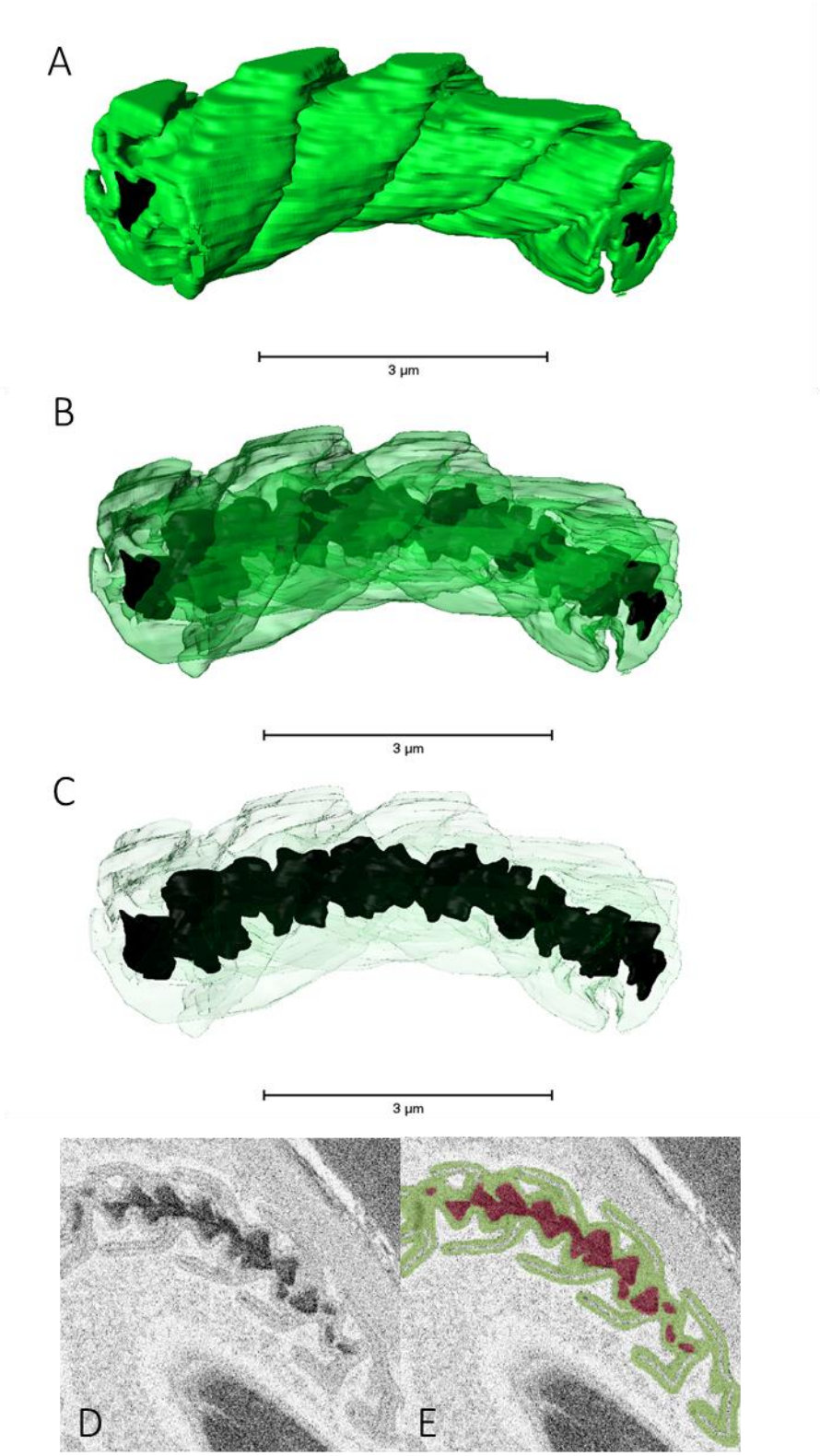

Figure 7.18: A cropped section of the inverted tubule of an undischarged Mastigophore nematocyst from the tentacles of an adult Carukia barnesi jellyfish. A: An opaque rendering visualises the coiled springlike ultrastructure of the inverted tubule (green). B/C: The model as in A, with the opacity of the tubule (green) reduced to visualise the spines (black) lining the centre

of the inverted tubule. D/E: SBF-SEM slice through the nematocyst with (D) and without (E) the segmented regions of interest.

7.4.6 3D printed models

3D models were printed via stereolithography to best capture the intricate details of the volumes. The discharged nematocyst was printed whole, whereas the undischarged capsules were printed in sections to create pull-apart models, whereby interaction with the models I.e., opening the capsule in half, allows interactive visualisation of the internal tubules. The interactive nature is intended to better facilitate outreach and education activities. Physical models have been painted, where possible, in the same colour scheme as the virtual models.

Figure 7.19: 3D printed and painted model of an undischarged Tumitele nematocyst from Carukia barnesi tentacles, shown from varying angles. Capsule (pink/purple) is printed in two halves as an interactive pull apart model. Coiled inverted tubule (green) fits within the capsule.

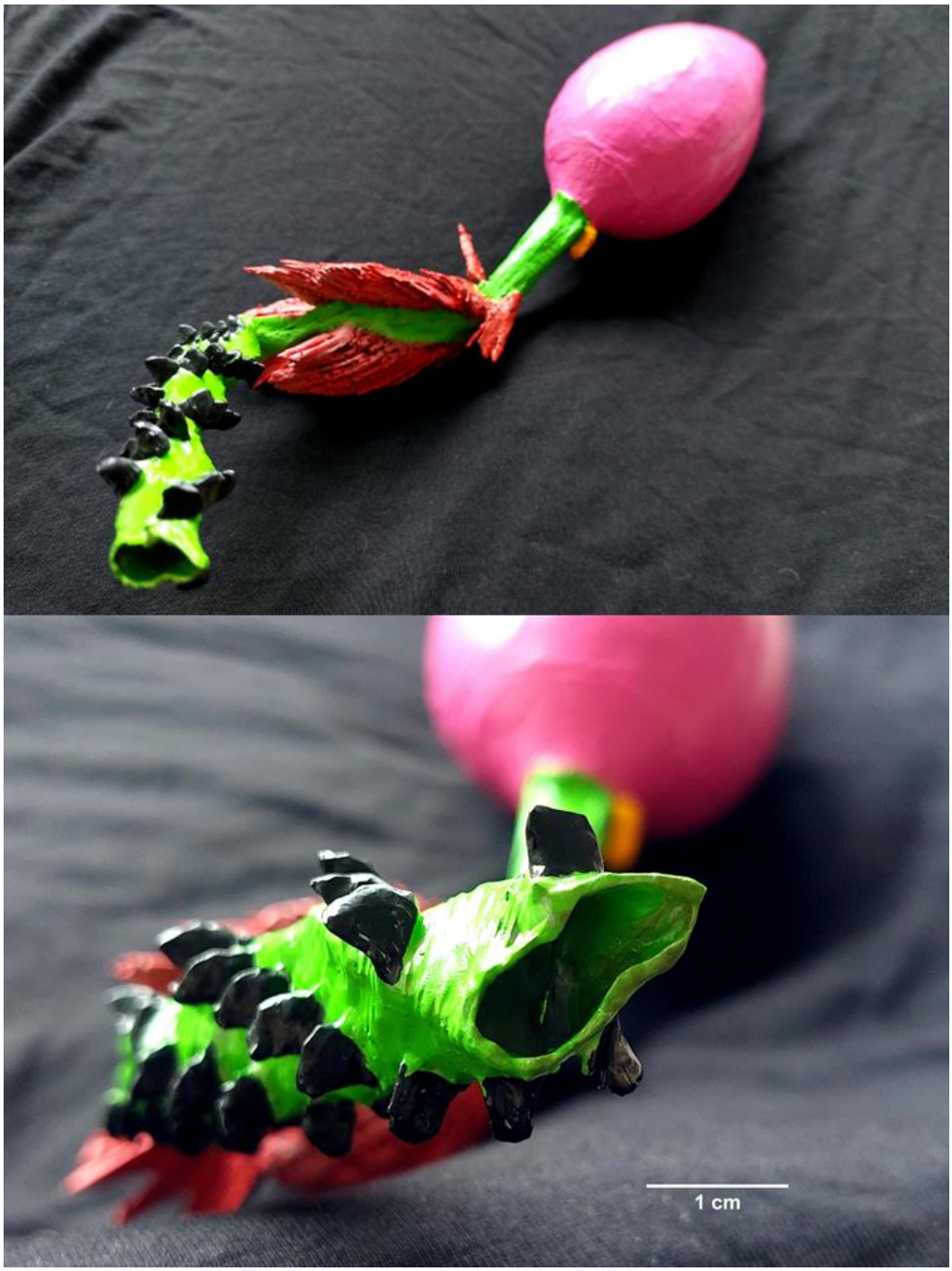

Figure 7.20: 3D printed and painted model of a discharged Tumitele nematocyst from Carukia barnesi tentacles, shown from varying angles. Capsule (pink/purple) and discharged tubule (green) are hollow as biologically accurate. Operculum (yellow) remains attached to nematocysts capsule after discharge. Shaft spines (red) and tubule spines (black) arranged helically along tubule. Unlike in the virtual models, the large shaft spines here are painted red, to better visual the surface details on the physical model.

Figure 7.21: 3D printed and painted model of an undischarged Tumitele nematocyst from Carukia barnesi tentacles, shown from varying angles. Capsule (pink/purple) is printed in two halves as an interactive pull apart model. Coiled inverted tubule (green) fits within the capsule.

7.5 Discussion

Serial Block Face Scanning Electron Microscopy (SBF-SEM) was successfully utilized to scan and reconstruct 3D volumes of two nematocyst types found within the tentacles of the Irukandji jellyfish *C. barnesi*. Previously undescribed ultrastructural details of both discharged and undischarged nematocysts derived from cubozoan jellyfish were observed. This work presents possibilities for further ecological insights and potential quantitative analysis, while this paper focusses on presenting the first biologically accurate nematocyst models from this highly venomous, medically important jellyfish.

7.5.1 Methodology

Serial Block Face Scanning Electron Microscopy was chosen for nematocyst data acquisition in the current study. To our knowledge, there are only two other instances in which 3D volumes have been rendered for nematocysts (or nematocyst-like organelles), both of which employed differing acquisition methods: FIB-SEM (Focussed Ion Beam-Scanning Electron microscopy) (Gavelis et al., 2017) and STEM (Scanning Transmission Electron Microscopy)(Karabulut et al., 2022). Harpoon-like secretory organelles within dinoflagellate protists, hypothesized to be homologous to cnidarian nematocysts were 3D imaged using FIB-SEM by (Gavelis et al., 2017) with great success. FIB-SEM uses the same basic principle as SBF-SEM, but instead of cutting through a sample with a diamond knife (as in SBF-SEM) FIB-SEM uses a focused ion beam to sputter the sample, essentially milling away each serial slice before imaging. Whilst advantageous in materials science for hard samples like metals, which can be resistant to diamond knife cutting, a downside to FIB-SEM is a slow sputtering speed (Haruta, n.d.). We opted to use SBF-SEM over FIB-SEM in the current study as some our nematocysts were much larger than those of Gavelis et al. (2017) and SBF-SEM typically has a wider cutting field than FIB-SEM. Along with the larger specimen sizes, in order to visualise the ultrastructural details of the cropped tubule sections and the internal and external spines on the tubules (both in- and e-verted) we deduced from optimization trials that a maximum slice interval of 50 nm was needed. The time required to image large samples at these intervals using FIB-SEM (due to the slow sputtering speed) would be logistically unfeasible, whereas the samples imaged by Gavelis et al. (2017) required only 250 nm thick slices to suitably visualise details. A typical advantage of FIB-SEM is the lack of complex fixing and heavy metal sample staining protocols as required with SBF-SEM. However, well characterized fixation protocols and chemicals, such as those used in conventional TEM, are also appropriate for SBF-SEM fixation and cnidarian nematocysts have been successfully stained and imaged for TEM frequently within the literature (Garm et al., 2007). Thus SBF-SEM was chosen for the current study. Similar work in which nematocyst volumes were created from the model

sea anemone *Nematostella vectensis* by Karabulut et al. (2022) has also been acquired using STEM. STEM acquisition is very similar to SBF-SEM; however, instead of serial slices being imaged directly throughout a sample block, slices are cut first and then individually imaged. Possibly the only advantage of SBF-SEM to STEM is that the imaged slices remain in alignment and do not need post processing to align the image stack prior to model segmentation. The current study is novel in regards to the utilization of SBF-SEM to achieve superior ultrastructural resolution, allowing us to describe in detail multiple nematocysts from highly venomous and poorly studied cubozoans.

The datasets acquired for our nematocysts were anisotropic, meaning the voxel size is not cubic. We acquired 10 nm in the X plane, 10 nm in the Y plane and 50 nm in the Z plane, meaning a higher image resolution was captured in the X and Y, and less in the Z plane. This meant that for samples such as the undischarged Mastigophore where SBF-SEM acquisition descended through the frontal plane, as the inverted tubule predominantly loops along the frontal plane, an unprecedented level of detailed was able to be captured allowing us to visualise nearly every individual smaller coil along the tubule. In contrast, the undischarged Tumitele volume shows increased areas of lower resolution along the inverted tubule. This is due to the tubule looping primarily in the transverse plane, but also back and forth along the frontal and median planes, essentially occupying all possible angles. This meant that, due to the anisotropic voxels, there was no single plane in which acquisition could have proceeded to preserve the best details. The undischarged Tumitele is also significantly smaller in size than the undischarged Mastigophore, meaning some loss of resolution is expected. Segmentation examples of regions of higher and lower resolution along the tubules are displayed in figures 7.9 and 7.17. It is these areas of higher resolution that allowed us to map and render both the finer coiling pattern and internal spines of cropped sections of the inverted tubules.

It is important to note that the tubule of the discharged Tumitele does not represent its full biological length. All microscopy techniques for volume imaging are restricted by their field of view/image acquisition window. In this particular case, the tubule actually extends more than 350 µm further in length, which is beyond the scope of the microscope to capture. From prior SEM imaging of these nematocysts in chapter six we have shown the external spines continue in the same triple helix pattern along the tubule, with roughly the same diameter at least to the midpoint. We can also infer from the 3D volumes of the undischarged nematocyst that the tubule diameter does get smaller as its length continues, and we have the ability to extract the exact measurements from this dataset. With this combined data, it may be possible in future studies to copy the rendered area of the existing discharged tubule and extrapolate it to its full biological

length, including taking into account diameter changes, to produce a full scale model of the discharged nematocysts. In the current study we found that the possibility of imaging transverse sections of a discharged nematocyst, where theoretically the entire length of the discharged tubule may be captured, was problematic. When imaged through the transverse plan, the tubule extended beyond the heavily stained tentacle tissue and was surrounded only by resin, resulting in problematic charging and imaging difficulties. Future studies may be required to determine the most effective way to image the full length of the discharged tubule with any suitable resolution.

Carukia barnesi is known to possess multiple types of nematocysts, dispersed between the bell and tentacle tissue, differing with ontogenetic stage (chapter six). We aimed to produce 3D volumes of the discharged and undischarged states of a Tumitele nematocyst only, as this is the sole type usually present in adult animal tentacles, and is the type typically associated with prey capture and human envenomation events. An undischarged Mastigophore was also presented and was an unexpected, but welcome addition, to this dataset. As discussed more in chapter six, these larger Mastigophore nematocysts are incredibly rare in *C. barnesi* and are only found in older and/or larger specimens. The nature of SBF-SEM means it is not possible to distinguish between nematocyst types until the sample is exposed during acquisition. Hence, we have been fortunate to image a rare specimen of *C. barnesi*. As the finding was unexpected, only the undischarged state of the Mastigophore is modelled.

7.5.2 Ecological/biological insights

The construction of the Mastigophore model, along with the SEM data described in chapter six, has provided a novel insight into the ecology of *C. barnesi*. Previously it had been suggested that older and rarer specimens of this animal do possess these larger Mastigophores as part of their cnidome (Pereira et al., 2010), but no direct evidence was ever presented. We provide the first definitive confirmation of Mastigophores as part of the cnidome of *C. barnesi*. From the SEM detail of the discharged Mastigophore in chapter six it was inconclusive as to if these discharged tubules were spined after the initial larger shaft spines. The resolution captured in the current data set and subsequent 3D models of the cropped section of the undischarged tubule (fig. 7.18) clearly demonstrate the presence of spines within the inverted tubule. This would translate to the spines lining the externals of the tubule when discharged. We know *C. barnesi* experiences a prey shift as it matures (Underwood & Seymour, 2007) and the addition of this newer, larger penetrative nematocyst suggests its ecology must again change at this older/larger life stage.

Examination of the ultrastructure of the two nematocyst types revealed clear and obvious differences, many of which have potential ecological implications. As previously discussed, the two nematocyst types in their undischarged state have completely different coiling patterns within their inverted tubules. The smaller Tumitele coils predominantly along the transverse plane around a central shaft, loop back and forth along the frontal and median planes, whilst the larger Mastigophore tubule coils completely separately to the side of the shaft, backwards and forwards in the frontal plane only. These different coiling patterns possibly impact the ejection mechanics of the nematocyst, explaining why they may be formed into such uniquely different structures. It has also been suggested that the twisted tubules store and transfer energy by acting as a spring (Karabulut et al., 2022) and, whilst the specific calculations are beyond the scope of the current study, the force of this "spring" power could be calculated for each nematocyst type. To calculate the force of a spring requires the counting of coils within a distance, which from the ultrastructure presented in our cropped tubule models (figs 7.10 and 7.18) can now easily be achieved, and would allow comparisons of the relative penetrative forces of each nematocyst type.

3D models allow the visualization and examination of nematocyst ultrastructure in novel ways, allowing for new observations as well as confirmation of established hypotheses. The discharged Tumitele nematocyst (fig. 7.11) clearly shows the discharge of the tubule has either not occurred in a straight trajectory, or did so and has since bent sideways prior to sample fixation. This allows us to confirm that the tubule is flexible, consistent with the ecological need of the structure to move and not snap when attaching to live motile prey. Additionally, a key feature of this discharged tubule is the presence of the single median shaft dilation identifying it as a Tumitele. This dilation has previously been contended within the literature and is discussed in depth in chapter six. Evident here is that with the large shaft spines omitted from view, the shaft dilation (fig. 7.11B) is less pronounced than might be expected given the significant dilation shape previously observed in light microscopy images (chapter six). One possible reason for this is no doubt attributable to the inferior resolving power of light microscopes with the large shaft spines, affixed to the shaft, perhaps contributing to the overall appearance of that dilations' shape when viewed with light microscopy. Once those spines are omitted from view in our model (fig 7.11B), the shaft dilation is still evident, however to a lesser extent than expected.

Visualising these completed structures in such a physical way also affords the opportunity to reflect upon and further improve ongoing method development. In this case, the large triangular shaft spines evident on the discharged Tumitele all point in the anterior direction way from the capsule towards the tubule tip. Whilst the physical structures of these spines are indeed

biologically accurate, the direction in which they point may be less so. During sample preparation 100% ethanol was topically added to the tentacles, which artificially induced discharge in the nematocysts. In doing so, we do not fully represent the natural discharged state (which would be mechanical/biological stimulation by prey or predator). SEM analysis of discharged tubules (unpublished work by the author) has certainly observed nematocysts discharged by ethanol when the tubule is fixed mid-eversion. This is in contrast to the SEM images of the discharged Tumitele shaft spines presented in chapter six, where the shaft spines in various stages were observed pointing all anteriorly, all posteriorly, or a combination of both. Ultimately, the direction the spines point might be an artefact arising from artificial discharge, or they might be a true reflection of the spines ability to point in all directions. This is sometimes used as a diagnostic feature in nematocyst identification; however, the models presented here provide evidence this may not be an accurate identifying feature.

7.5.3 Conclusion

Here we have presented the first biologically accurate nematocyst models from the highly venomous, medically important jellyfish, *C. barnesi*. This work offers the foundational volumes that can now facilitate a range of further ecological insights and future quantitative analysis. *C. barnesi* is one of the few jellyfish species known to possess nematocysts in both the bell and tentacles. We have conducted a thorough examination of the tentacular nematocysts from the adult medusa life stage. Future work should aim to capture the ultrastructure of the bell nematocysts in similar detail, to fully elucidate the stinging mechanisms of *C. barnesi.*

7.6 References

Australian Microscopy and Microanalysis Society, Volume Imaging Australia. (n.d.). Retrieved July 6, 2024, from https://microscopy.org.au/volume-imaging-australia/

Barnes, J. H. (1964). Cause and Effect in Irukandji Stingings. *The Medical Journal of Australia*, *1*(24), 897–904. https://doi.org/10.5694/j.1326-5377.1964.tb114424.x

Deerinck, T. J., Bushong, E. a., Thor, a., & Ellisman, M. H. (2010). NCMIR methods for 3D EM: A new protocol for preparation of biological specimens for serial block face scanning electron microscopy. *Microscopy*, 6–8. http://scholar.google.com/scholar?start=320&q=Mark+Ellisman&hl=en&as_sdt=0,5#0

Garm, A., Poussart, Y., Parkefelt, L., Ekström, P., & Nilsson, D. E. (2007). The ring nerve of the box jellyfish Tripedalia cystophora. *Cell and Tissue Research*, *329*(1), 147–157. https://doi.org/10.1007/s00441-007-0393-7

Gavelis, G. S., Wakeman, K. C., Tillmann, U., Ripken, C., Mitarai, S., Herranz, M., Özbek, S., Holstein, T., Keeling, P. J., & Leander, B. S. (2017). Microbial arms race: Ballistic "nematocysts" in dinoflagellates represent a new extreme in organelle complexity. *Science Advances*, *3*(3). https://doi.org/10.1126/sciadv.1602552

Haruta, T. (n.d.). *Comparison of 3D Imaging Methods in Electron Microscopy for Biomaterials*. JEOL NEWS Vol.53 No.8. Retrieved May 24, 2024, from https://www.jeol.com/solutions/applications/details/1695.php

Karabulut, A., McClain, M., Rubinstein, B., Sabin, K. Z., McKinney, S. A., & Gibson, M. C. (2022). The architecture and operating mechanism of a cnidarian stinging organelle. *Nature Communications*, *13*(1), 1–12. https://doi.org/10.1038/s41467-022-31090-0

Karolinska Institute, Volume Imaging. (n.d.). Retrieved July 6, 2024, from https://ki.se/en/research/research-infrastructure-and-environments/core-facilities-for-research/3d-em-core-facility/volume-imaging

McClounan, S., & Seymour, J. (2012). Venom and cnidome ontogeny of the cubomedusae *Chironex fleckeri*. *Toxicon*, *60*(8), 1335–1341. https://doi.org/10.1016/j.toxicon.2012.08.020

Pereira, P., Barry, J., Corkeron, M., Keir, P., Little, M., & Seymour, J. (2010). Intracerebral hemorrhage and death after envenoming by the jellyfish *Carukia barnesi*. *Clinical Toxicology*, *48*, 390–392. https://doi.org/10.3109/15563651003662675

Southcott, R. V. (1967). Revision of some Carybdeidae (scyphozoa: cubomedusae), including a description of the jellyfish responsible for the “irukandji syndrome.” *Australian Journal Of Zoology*, *15*, 651–671. https://www.mendeley.com/viewer/?fileId=2fa0eb3f-b65a-d78b-0aab-8d1da93fdb17&documentId=f0d95e7c-a226-37e1-ba96-636d97beaa71

Underwood, A. H., & Seymour, J. E. (2007). Venom ontogeny, diet and morphology in *Carukia barnesi*, a species of Australian box jellyfish that causes Irukandji syndrome. *Toxicon*, *49*(8), 1073–1082. https://doi.org/10.1016/j.toxicon.2007.01.014

Underwood, A. H., Straehler-Pohl, I., Carrette, T. J., Sleeman, J., & Seymour, J. E. (2018). Early life history and metamorphosis in Malo maxima Gershwin, 2005 (Carukiidae, Cubozoa, Cnidaria). *Plankton and Benthos Research*, *13*(4), 143–153. https://doi.org/10.3800/PBR.13.143

Chapter 8 . Too hot, too cold or just right? The influence of environmental temperature on the venom of the Irukandji jellyfish *Carukia barnesi.*

8.1 Abstract

Venom ecology is a relatively new area of research not well explored within cnidarians, although some venom shifts with environmental temperature, life stage and geography have been documented in a limited number of species. Here I take the highly venomous Irukandji jellyfish *Carukia barnesi* and use Ultra High Performance Liquid Chromatography Mass Spectrometry to asses the venom for compositional differences across three environmental temperatures: 27°C, 29°C and 31°C, and two life stages: polyp and newly detached medusa. Here we find molecular venom variations with both temperature and life stage, suggesting the animals venom is directly linked to those ecological factors. Possible impacts of these venom variations may include sting severity shifts with global warming, major ecological shifts between life stages and potential links to the known variations in symptom onset from Irukandji syndrome.

8.2 Introduction

8.2.1 Carukia barnesi

Jellyfish possess microscopic stinging organelles called nematocysts, which inject venom into the tissue of prey or human skin upon contact. Irukandji syndrome is the complex and excruciatingly painful condition that results from a sting from a range of small, almost invisible box jellyfish species. The most common and often documented species of Irukandji jellyfish from Northern Queensland, *Carukia barnesi,* is known to cause a range of symptoms from extreme muscle pains, nausea and vomiting, to instances which induce intracerebral haemorrhage and death (Barnes, 1964; Fenner & Hadok, 2002). However, it is not known what causes these variations in sting symptoms as differences in venom potency, geographic locations, temperature and sting source (bell versus tentacle) remain poorly understood.

8.2.2 Venom variation

The influence of temperature on cnidarian venoms is a severely understudied area and remains poorly understood, with very little dedicated research undertaken (O'Hara et al., 2021). Venom variation in cubozoans has been shown with ontogeny documented in adult *C. barnesi* (Underwood & Seymour, 2007) and with geographic location and season in *Chironex fleckeri* (Winter et al., 2010), demonstrating the capability of these venoms to alter with environmental parameters. Whilst venom composition has never been analysed in relation to temperature before in this species, the thermal tolerance of *C. barnesi* polyps has been explored (Boco et al., 2019; Courtney, Browning, Northfield, et al., 2016; Rowley et al., 2023), albeit from short-term temperature experiments. Respiration rates were found to vary with temperature (Boco et al., 2019; Rowley et al., 2023) and reproduction rate also significantly changes with temperature (Boco et al., 2019; Courtney, Browning, Northfield, et al., 2016). This shows the physiology of these animals is directly influenced by temperature. Within cnidarians, compositional differences in toxin gene expression with temperature have been documented twice before. Both long-term (O'Hara et al., 2018) and short-term (Sachkova et al., 2020) environmental temperature changes can cause variation in the expression sea anemone toxins, providing evidence cnidarian venom/toxins can be influenced by temperature.

8.2.3 Changing environmental temperature

Global sea surface temperatures are changing with global warming, with the detrimental effects of increased temperature on cnidarians, corals in particular, publicised both throughout the global media and scientific communities (e.g Chimienti et al., 2021; Goulet & Goulet, 2021; Hoegh-Guldberg, 1999; Sammarco & Strychar, 2009; Weis, 2008). Jellyfish blooms are increasing

with increasing temperatures and Irukandji stinger season is lengthening (Carrette & Seymour, 2013). Figure 8.1 visualises the increasing annual sea surface temperature anomalies recorded for the Coral Sea, the region inhabited by *C. barnesi*, showing their habitat has previously been, and will likely continue to be, subject to increasing environmental temperatures.

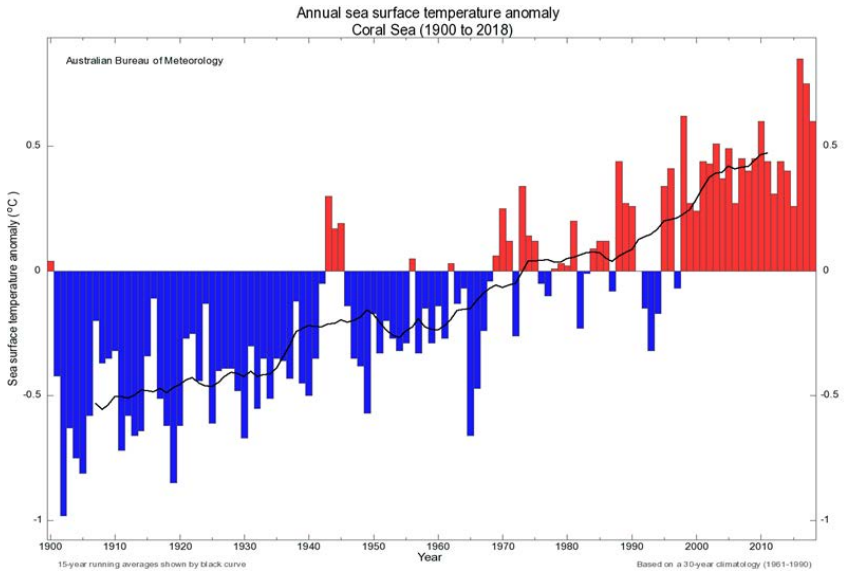

Figure 8.1*:* Sea surface temperature time series for the Coral Sea region of Australia, presented as anomalies/departures from the current international standard period for the calculation of climate averages 1961-1990. Date and graph production sourced from Bureau of Meteorology: Australian Government (2019).

Marine Heat Waves (MHWs) are also environmental anomalies which can cause extreme and sudden thermal changes to water temperature, which cause severe changes the animal's environmental temperature in the short-term. Evidence shows the global average of MHW frequency and duration has increased over the last century, and suggests these will continue to increase with global warming (Oliver et al., 2018). This increase in MHWs was also recently noted specifically around the Queensland region of Australia (Heidemann & Ribbe, 2019), and Irukandji from the sampled area of K'gari (Fraser Island) have been documented to occur at unusual high latitude clusters during or following a MHW (Walker 2013, as cited Gershwin & Hannay, 2014). Irukandji jellyfish are known to be distributed along the Great Barrier Reef and adjacent coastline, from Lizard Island to as far south as Hervey Bay and K'gari, with the latter known to encounter sporadic and ever increasing MHWs (Heidemann & Ribbe, 2019)).

8.2.4 The current study

The effect of environmental temperature on *C. barnesi*, or indeed any cubozoan, remains unknown. Any future changes in *C. barnesi* venom would severely exacerbate the current lack of understanding of Irukandji venom. These animals will experience future environmental temperature changes under current global warming forecasts and the resulting consequence of any change in venom composition has the potential to affect both medical sting severity and the feeding ecology of the animals. The current study sought to pre-emptively elucidate any potential compositional changes in the venom across two major life stages. Through ex-situ experimental temperature trials and venom analysis, the following hypothesis will be explored:

H_{0a}: The venom composition of *C. barnesi* polyps does not change with environmental temperature.

H_{0b}: The venom composition of *C. barnesi* newly detached medusa does not change with environmental temperature.

8.3 Methods

8.3.1 Experimental setup

C. barnesi polyps were available in culture at the James Cook University Aquarium, Cairns, housed long-term at 27°C (Courtney, Browning, & Seymour, 2016). Three individual polyps were taken from this stock and cultured into three separate clonal populations to be used as biological (clonal) replicates (A, B and C) throughout this work. Polyp clones were cultured in 450 mL tissue culture flasks at 27°C, water-changed and fed equal amounts of live 24-hour *Artemia sp*. nauplii every two days to promote the production of budding and swimming polyps (Courtney, Browning, & Seymour, 2016). Swimming polyps were harvested once a week and transferred into the final experimental set up. Polyps were housed in spherical 30 L BiOrb tanks in which they readily attached and matured to the tank walls and coral sand substrate. The tanks had a gravel filtration system driven by a central air pump which also oxygenated the water and provided water flow (Fig 8.2A). Method optimisation trials in polyp temperature acclimation showed the polyps could not survive long term at temperatures greater than 31°C. Three tanks per clonal replicate were set up (nine tanks total) and all maintained in constant temperature cabinets at 27 °C until a sufficient mature polyp population was reached (approximately >5000 per BiOrb). Upon population saturation, tanks were slowly acclimatised to their final experimental temperatures of 27°C, 29°C and 31°C at a rate of +0.5°C per week, providing an A, B and C clonal replicate per final temperature (Fig 8.2B). Polyp tanks were maintained at temperature for a minimum of eight months (see supplementary information 1) and fed ~300 mL of live 24-hour *Artemia sp*. nauplii

per tank approximately weekly, with water changes maintained to ensure a constant salinity of 35-36 PSU. Feeding of the polyps over an extended timeframe also ensured older nematocysts developed at the original environmental temperature would be readily expelled and replaced post-feeding by new nematocysts developed at the experimental environmental temperatures. Polyps were kept in complete darkness except for feeding/water exchange times to prevent algae build up and competition on tank walls. Care was taken to ensure all environmental variables (except for environmental temperature) remained constant across all polyp populations.

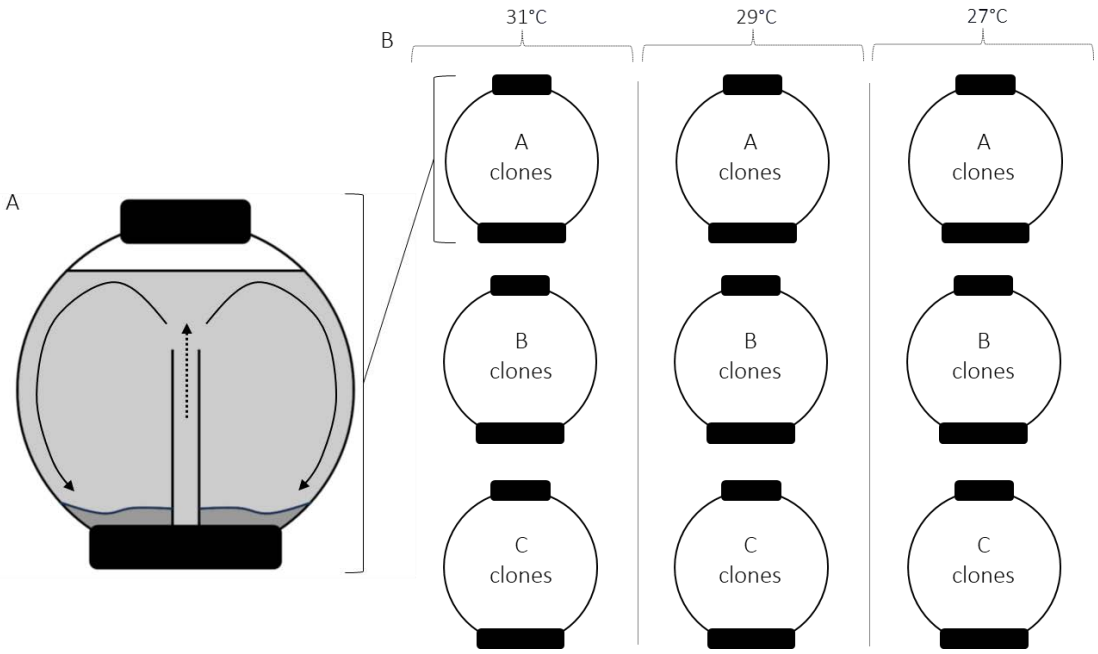

Figure 8.2: Experimental setup. A: 30 L spherical BiOrb aquarium tank used to house polyps. Coral sand substrate lies atop a gravel filtration system, driven by a central air pump which also oxygenates the water (dashed arrow) and provides water flow (solid arrow). Tanks stand on a solid base and have a circular apical opening for access which is covered to negate water evaporation. B: Set up of clonal replicates over three environmental temperatures. Replicates of A, B and C clones were raised at 31°C, 29°C and 27°C respectively.

8.3.2 Sample collection

A minimum of 400 polyps were collected by pipette from each clonal replicate. Less were trialed in method optimization, but venom analyses were not successful on lower sample sizes. B clones were all slightly smaller than A and C clones, thus a greater numbers of B polyps were used to make up to the equivalent mass of 400 A/C polyps. Polyps were added to a 1 M sodium citrate solution (and thus euthanized) and left at their respective environmental temperatures for 1-2 days to induce nematocyst expulsion from tentacles. Sodium citrate was used instead of the standard 3-7 days seawater and refrigeration technique (Bloom et al., 1998; T. Carrette &

Seymour, 2004) because, unlike the adult medusa, it was found during method optimization that the much smaller polyps and newly detached medusa do not readily degrade in seawater, remaining stable for upwards of a month and retaining their nematocysts within their tissue.

The remaining polyps continuing in the BiOrb cultures were then induced to metamorphose into medusa using iodine as per O'Hara & Seymour (2022). 40 drops of Lugol's solution (aqueous iodine) were added to each 30 L BiOrb (equivalent concentration = 3 µM iodine).

Medusa were collected the day they detached and became free swimming because 1: *C. barnesi* medusa have not successfully been raised *ex situ* in aquaria long term and their health/fitness declines rapidly after the first week post-detachment, 2: standardizing collection to the day of detachment negated that nematocysts would be discharged, detached and replaced during the collection time either through mechanical stimulation within the tank or through inadvertent feeding, and 3: day 0 as a collection time ensured age was consistent across all samples and could not contribute as a variable. All ensuing venom extraction should have occurred solely on nematocysts developed during metamorphosis at the polyp's respective environmental temperature and any minor nematocyst discharge would not have been replaced with new organelles within the collection time parameters. All metamorphosing medusa detached within 2-3 days of the first detachment occurrence, and every effort was made to collect the entirety of detached medusa. A minimum of 3000 medusa per BiOrb (clonal replicate) were collected, although as exact counts were not logistically possible, sample sizes varied slightly. Varying samples sizes of <500 medusa were trialed in method optimisation but venom analysis was not successful on lower sample sizes. In the same procedure as polyp collection, collected medusa were immediately added to a 1 M sodium citrate solution (and thus euthanized) and left at their respective environmental temperatures for 1-2 days to induce nematocyst expulsion.

8.3.3 Venom extraction

Venom was extracted from both polyps and medusa in the same manner. The nematocysts were present in solution following sodium citrate exposure. The samples were filtered through a 70 µm Biologix cell strainer to remove polyp/medusa tissue and centrifuged twice at 12500 g for four minutes to produce a nematocyst pellet. The supernatant was checked with microscopy to confirm no remaining nematocysts were present in solution and was discarded. For polyp samples (equal mass among replicates), a total of 50 µL of MiliQ (ultrapure) water was added to each clonal replicate. For medusa samples (slightly unequal sample size between replicates), MiliQ water was added to a level just covering each pellet (≤50 µL) to maintain equal nematocyst/liquid ratios between replicates. Samples were briefly vortexed and pipetted up and down to resuspend

the nematocyst pellet and the solution checked with microscopy to ensure nematocyst suspension and confirm the nematocysts remained in their undischarged state. Samples were refrigerated overnight at 4°C prior to further processing. A further 40 µL MiliQ water was added to each sample, along with 0.5 mm BioSpec Products glass beads and nematocysts were ruptured similar to Carrette & Seymour (2004). Briefly, samples were loaded into an Omni International™ Bead Ruptor Elite™ Bead Mill Homogenizer at 4°C and processed at a speed of 6 m/s for 2 x 5 minutes. The solution was then extracted from the glass beads using a micropipette and checked with microscopy to ensure 100% nematocyst discharge, then centrifuged on a mini benchtop unit (non-variable speed) for approximately 2-3 minutes to form a pellet. Microscopy analysis confirmed the pellet was composed of broken nematocyst capsule debris and no capsule debris was present in the supernatant indicating a pure venom extraction. The supernatant (venom) was extracted into fresh Eppendorf tubes and refrigerated at 4°C (method optimization showed freeze/thawing caused venom components to precipitate out of solution) until further analysis.

8.3.4 Mass spectrometry venom analysis

Venom samples were shipped cold and anaysled externally at the Institute for Molecular Bioscience Mass Spectrometry Facility at the University of Queensland, Australia, using Ultra High Performance Liquid Chromatography Mass Spectrometry (uHPLC-MS). The venom samples were analysed on a Shimadzu Nexera uHPLC, LC30 (Japan) coupled to a Triple Tof 5600 mass spectrometer (ABSCIEX, Canada) equipped with a duo electrospray ion source. Each extract (5 µL) was injected onto a 2 mm x 150 mm Gemini C4 3 µm column (Phenomenex) at 250 µL/min. Linear gradients of 1% solvent B for 0.5 minute, 1-80% solvent B over 20 min, followed by 80-98% over 2 min. Solvent B was held at 98% for 3 min for washing the column and returned to 1% solvent B for equilibration prior to the next sample injection. Solvent A consisted of 0.1% formic acid (aq) and solvent B contained acetonitrile/ 0.1% formic acid (aq). The ionspray voltage was set to 5500V, declustering potential (DP) 100V, curtain gas flow 25, nebuliser gas 1 (GS1) 50, GS2 to 60, interface heater at 150°C and the turbo heater to 500°C. The mass spectrometer acquired 250 ms full scan TOF-MS data with a scan range of *m/z* 400-2200 for mass profile analysis The data was acquired and processed using Analyst TF 1.6 software (ABSCIEX, Canada).

8.3.5 Data analysis

Data was returned to the author for analysis and both Total Ion Chromatograms (TICs) and their associated mass spectra were analysed with PeakView software (SCIEX). Similarities and differences in venom composition between the experimental temperatures were determined by the presence/absence and/or varying relative intensity of TIC and Mass Spectra peaks. The charge

state of the molecular ions was calculated by identifying the difference in *m/z* value between the mass spectra isotopic peaks, equivalent to 1/*z*: $[M+H]^+$ ions have a difference between peaks of 1, $[M+2H]^{2+}$ ions have a difference of 0.5, $[M+3H]^{3+}$ ions have a difference of 0.33, $[M+4H]^{4+}$ ions have a difference of 0.25, etc. Ion series identified in this study were reconstructed to the parent mass using the BioTools plugin in the PeakView software. All singly charged ions ($[M+H]^+$) identified within this study had the exact mass of molecules calculated from the mass spectra as follows:

$$exact\ mass\ (Daltons) = monoistopic\ ion\ (m/z) - 1.00728$$

C. barnesi venom was extracted and analysed using liquid chromatography mass spectrometry from two life stages (polyp and newly detached medusa) to look for compositional differences between three environmental temperatures (31°C, 29°C and 28°C), presented here as TICs and associated mass spectra. From the polyp venom, three clonal replicates are presented for each of the three temperatures; however, due to unforeseen differences in metamorphosis success between clonal cultures at different temperatures, only two clonal replicates are presented from the 31°C treatment, and a single clonal replicate each for the 29°C and 27°C treatments the medusa venom. These biological (clonal) replicates occasionally showed very minor variation in retention time of the TIC peaks (fig 8.3A) but the molecular ions/masses were consistent across runs (fig 8.3B/C).

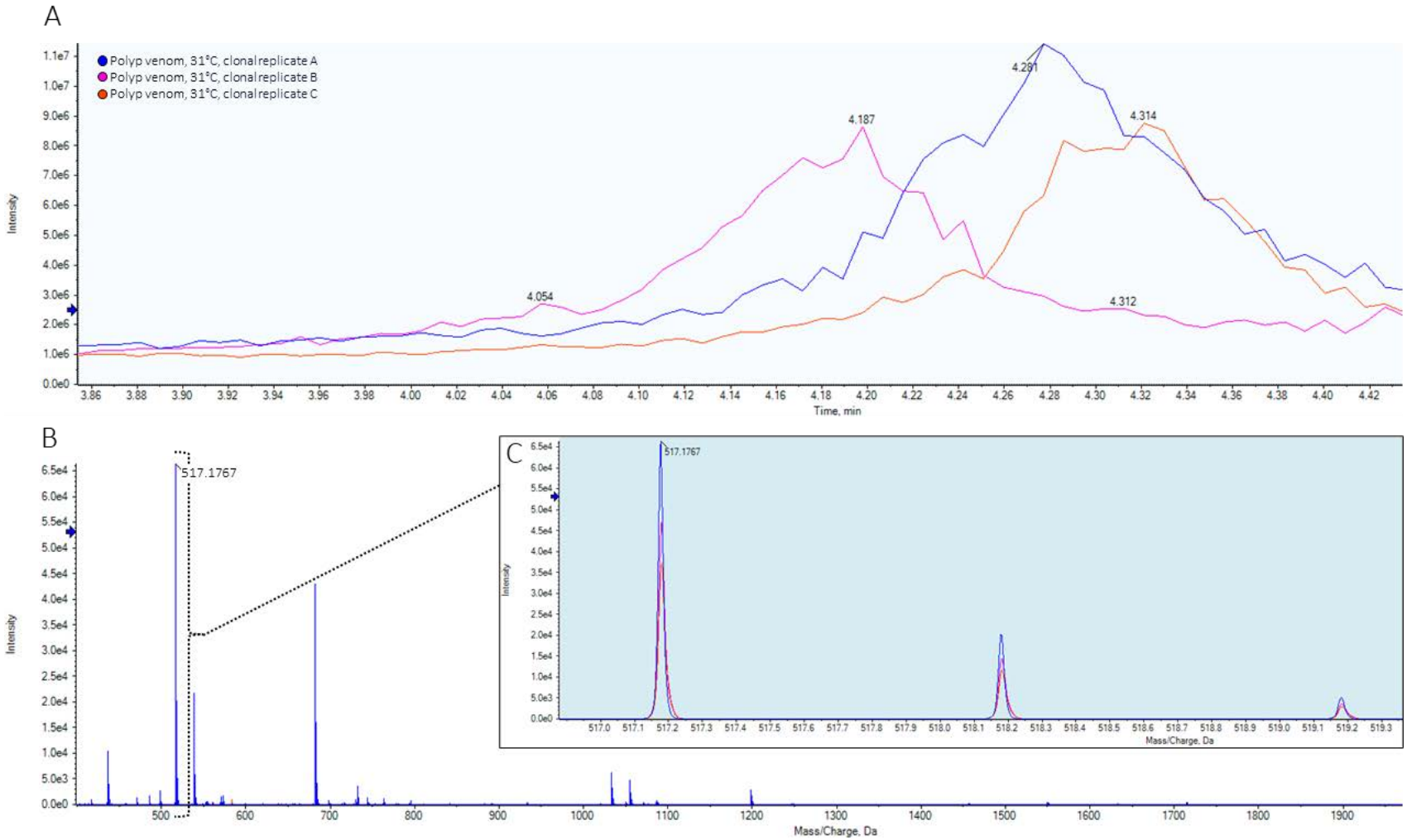

Figure 8.3: A: Zoomed region of TIC for polyp venom of *Carukia barnesi* raised at 31°C exemplifying minor differences in recorded retention times between peaks of biological (clonal) replicates. B: The mass spectra of molecules within the latter (3A) peaks. C: A zoomed region of mass spectrum for one specific molecular ion (517.1767) exemplifying the same monoisotopic masses of the replicates, despite the minor variation in retention times seen in 3A.

8.4 Results

8.4.1 Polyp v medusa

Compositional differences were evident between the polyp and newly detached medusa venom. from the total ion chromatograms (figure 8.4). Discounting the void volume prior to three minutes, obvious peaks can be seen between three and five minutes retention time in all polyp replicates, whilst none are present in the corresponding regions of the medusa venom. The medusa venom has large peaks at approximately six and 24 minutes, not seen in the polyp venom. The polyp venom also has peaks present around 15 minutes not present in the medusa venom. These large differences in TIC peaks suggest large compositional differences in venom between the two life stages.

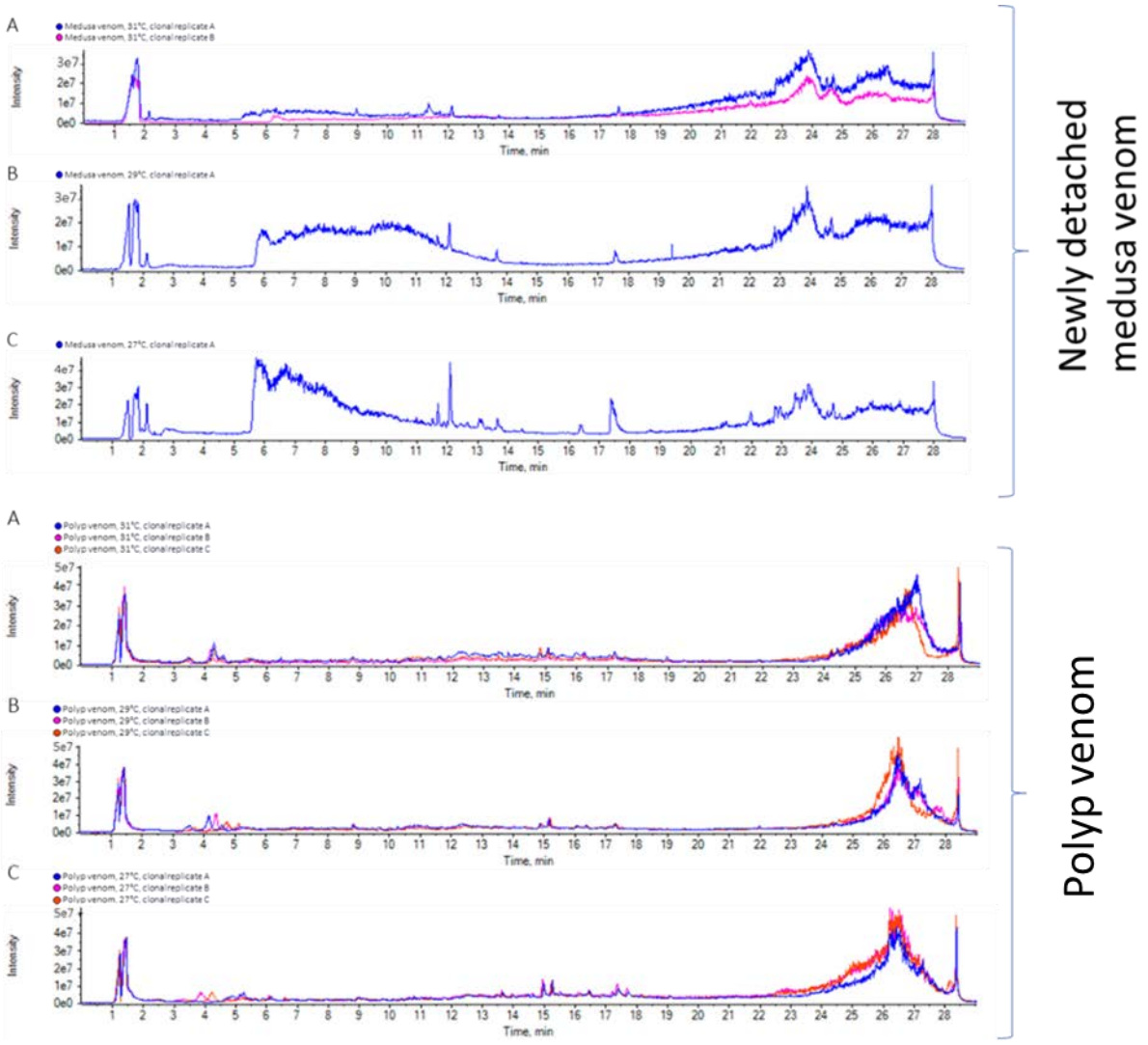

Figure 8.4:Total Ion Chromatograms for polyp and newly detached medusa *Carukia barnesi* venom, with replicates over three environmental temperatures A:31C, B:29C, C:27C. Differences in peaks represent compositional differences in the venom profiles.

8.4.2 Polyp venom

TICs of the polyp venom provide an overcall comparison of the venom composition between the three temperature treatments (fig 8.5). The initial peaks present with retention times between 0 and 2 minutes are the void volume, typically containing salts and highly polar compounds within the sample extract, and do not represent the majority of the venom composition. The polyp venom TICs showed most peaks are consistent between all temperature treatments, suggesting a mostly homogeneous venom composition between temperatures; however, some notable differences were evident. Peaks at ~6.5 min (fig 8.5 black arrows) and ~19 min (fig 8.5 red arrows) are present in the 31°C and 27°C treatments, but absent and/or much less intense in the 29°C treatment. Upon closer examination of the mass spectra of the absent peak at ~6.5 mins from 29°C, this region was found to contain the same composition of molecules (at similar intensities) as peaks noted in the 31°C and 27°C treatments (fig 8.5 black arrows). Molecular differences were evident between temperature treatments from the present/absent peaks at ~19 min (fig 8.5 red arrows). Examination of the associated mass spectra from these peaks/regions was conducted and exact masses were calculated for all major (distinct from background noise) peaks, presented in Table 8.1. Roughly 50% of these molecules were present across all temperature treatments at similar (<1000 difference) intensities, however the remaining 50% of molecules showed distinct differences (>1000) in intensities and/or a complete absence between temperatures (Table 8. 1 bold text). The two most significant molecular differences (Table 8.1 * and **) are further explored.

Figure 8.6 presents a zoomed segment of the overall TIC and the associated mass spectra at ~19 min and shows the presence/absence of peaks in this region. The series of peaks present in the mass spectra of the 31°C and 27°C treatments (fig 8.6 red arrows) are characteristic of an ion series. Protein reconstruction was conducted on this ion series using Peakview software and calculated a mass of 12059 Da (31°C: 12059.8 Da, 29°C: 12059.5 Da, 27°C: 12059.7 Da) (fig 8.7). The intensity of this molecule (likely a protein) in the polyp venom between temperatures is vastly different (Table 8.1). Whilst no peak is obviously visible within the TIC trace (fig 8.5) at 27°C, upon closer examination of the mass spectra this molecule is present at very relatively low intensities at 29°C, slightly higher intensities at 31°C, and much higher relative intensities (>7000) at 27°C (Table 8.1). In the same TIC peak at ~19 min, two molecular ion peaks are present in the mass spectra at 31°C and 29°C at high intensities (fig 8.6 black arrows) but is almost absent from 27°C. Zoomed views of the mass spectra (fig 8.8) show the individual isotopic peaks of this molecule, the patterning of which is characteristic of a brominated or chlorinated molecule. The mass calculated for this molecule is 715 Da (31°C: 715.21972 Da, 29°C:715.18752), with large differences in the relative intensities between temperatures (Table 8. 1) and present in the highest amounts at 29°C, lower intensities at 31°C and completely absent from 27°C.

Whilst the entirety of the molecules within the mass spectra were not analysed, two singly charged molecular ions $[M+H]^+$ of note were also identified from the polyp venom; one with a mass of 516 Da and the other with an exact mass of 1032.3427 Da, both suspected to be forms of cyclic γ-carboxyglutamic acid.

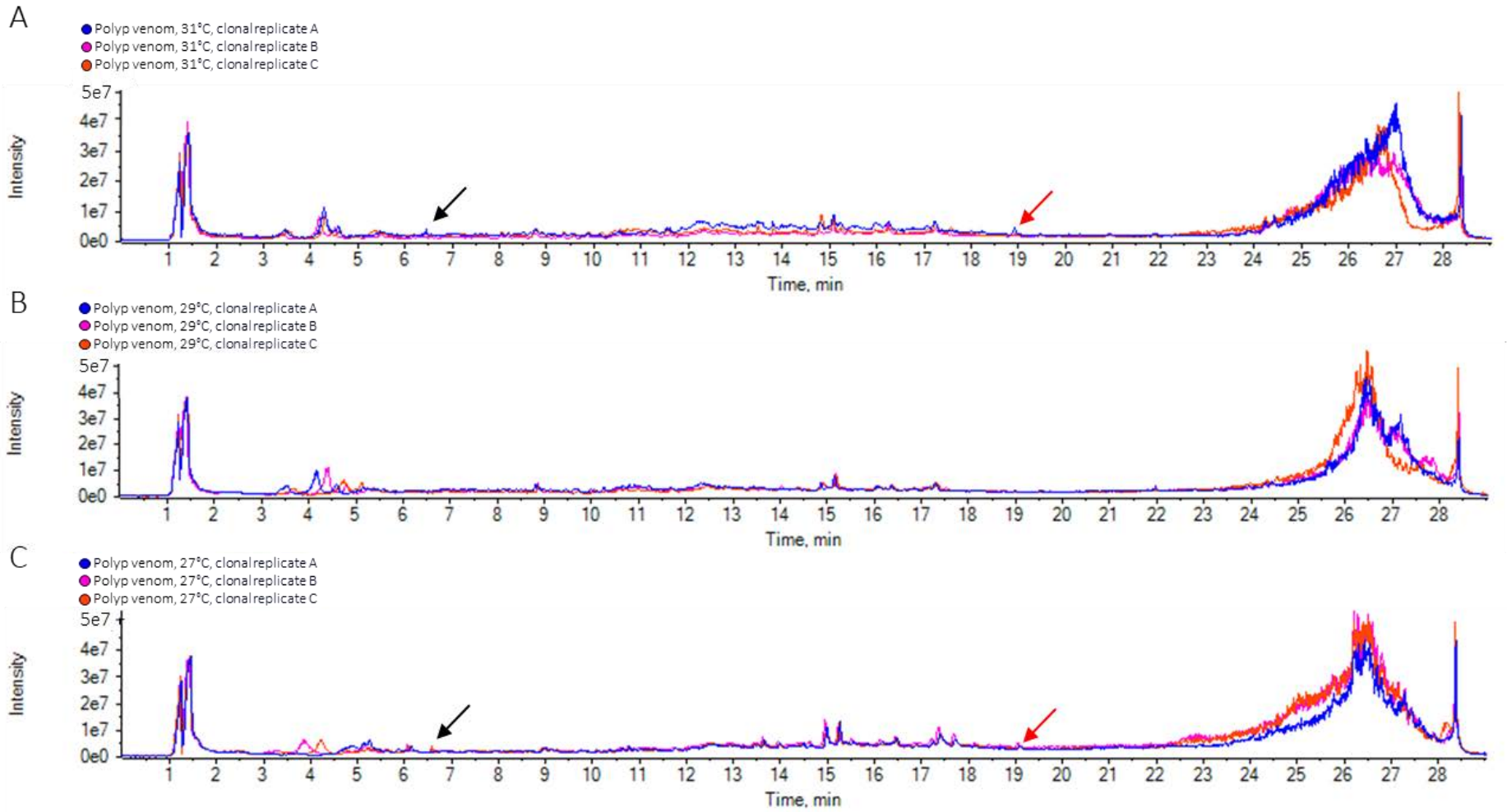

Figure 8.5: Total Ion Chromatograms (TICs) for polyp venom of *Carukia barnesi* raised at A: 31°C, B;29°C, C: 27°C. Differing venom composition is highlighted between temperatures by the presence /absence of peaks at ~6.5min (black arrows) and ~19 mins (red arrows).

Table 8.1:Exact masses and approximate peak intensities for molecules in the polyp venom of *Carukia barnesi* raised at 31°C, 29°C and 27°C corresponding to the peaks/region at ~19 min (indicated by red arrows in figure 7.5). The approximate peak intensity (counts per second) is that of the monoisotopic peak. **Bold** text indicates molecules that differ in intensity >1000 between temperature treatments. X indicates molecules absence from the particular temperature treatment. Molecules of significant interest that are further analysed in text and/or figures are indicated by * or **.

31°C		29°C		27°C	
Approx. peak intensity (cps)	Exact mass (Da)	Approx. peak intensity (cps)	Exact mass (Da)	Approx. peak intensity (cps)	Exact mass (Da)
2250	**435.43**	**700**	**435.43**	**300**	**435.43**
2250	452.344	2700	452.339	2700	452.343
2500	**465.33**	**325**	**465.32**	**2400**	**465.33**
500	474.321	500	474.32	500	474.325
250	481.357	200	482.359	400	481.326
300	495.374	160	495.373	650	495.377
450	**507.37**	**1000**	**507.37**	**2500**	**507.38**
200	516.177	160	516.174	130	516.179
350	521.391	160	521.39	1000	521.395
550	**531.38**	**550**	**531.37**	**4000**	**531.38**
300	637.309	160	637.308	250	637.307
250	**642.26**	**80**	**642.26**	**2600**	**642.52**
	X	550	658.519	650	658.518
300*	**715.21972[5]***	**1200***	**715.18752[5]***	**<40**	**715.2021[5]***
50	831.325	100	831.314	70	831.314
6000**	**12059.8****	**600****	**12059.5****	**13000****	**12059.7****

[5] Evidence suggests this molecule is halogenated (most likely bromine) and thus the exact mass presented here represents that of the initial isotope series only. It is described as 715/717 Da throughout the remainder of this work to represent both isotopic versions of this molecule

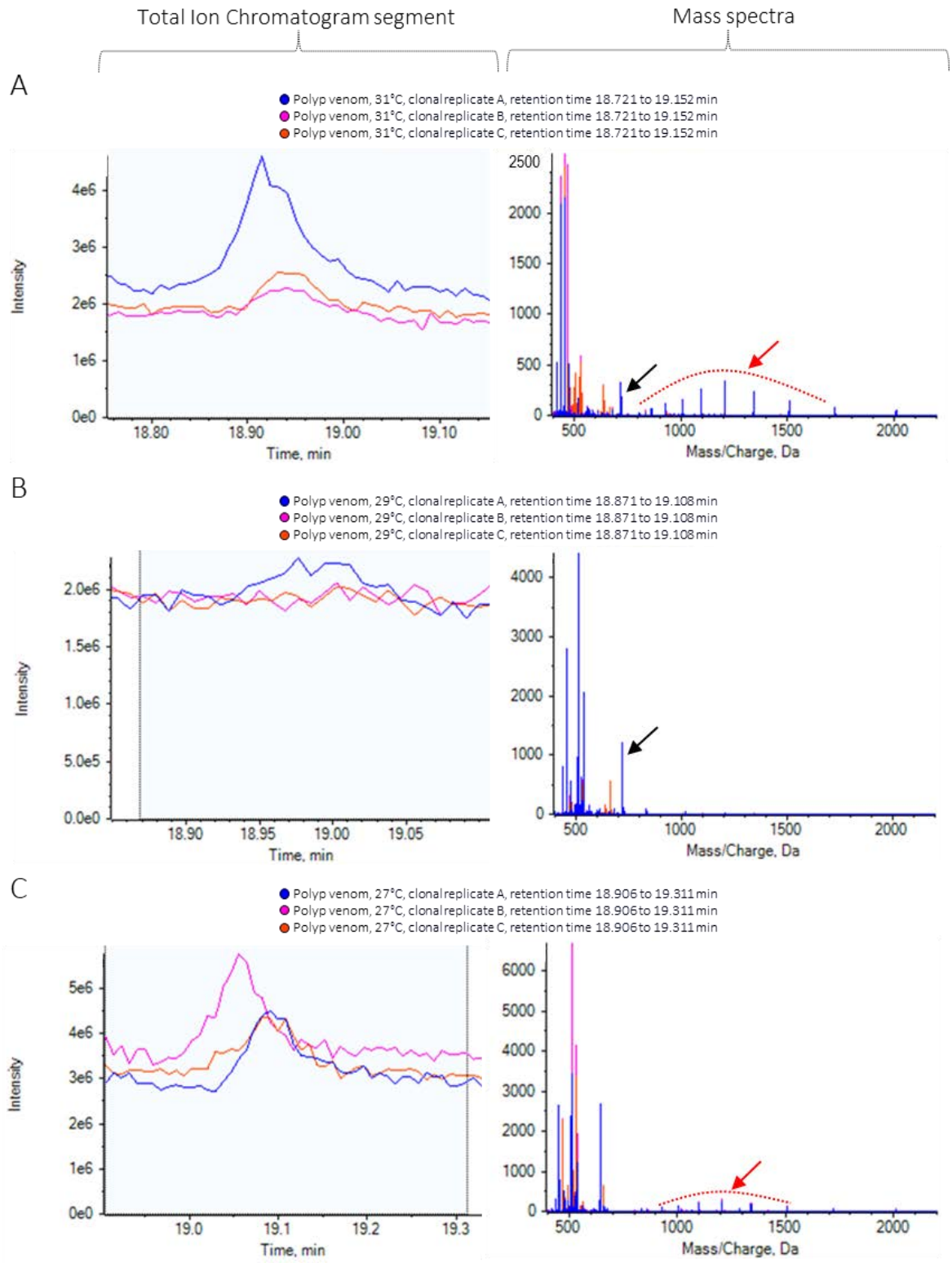

Figure 8.6: Zoom of mass spectra from the TICs at ~19 min for polyp venom of *Carukia barnesi* raised at 31°C, 29°C and 27°C and their associated mass spectra. Differences in venom composition between temperatures are highlighted by the presence/absence of peaks at ~715 *m/z* (black arrows) and peaks of an ion series at ~800-1500 *m/z*, the shape of which is highlighted by dashed red lines (red arrows).

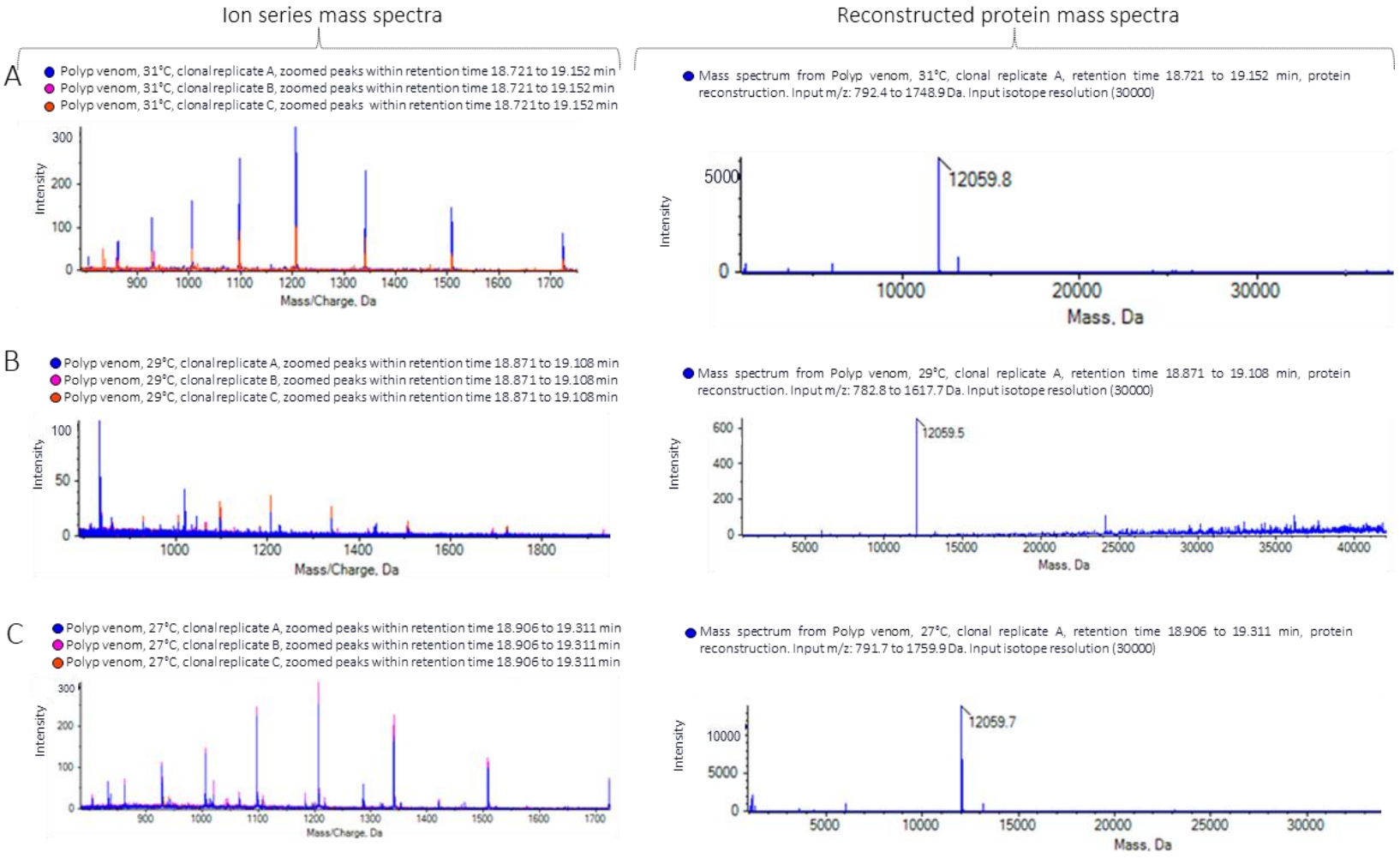

Figure 8.7: Zoom of mass spectra from polyp venom of *Carukia barnesi* raised at 31°C, 29°C and 27°C, showing an ion series at ~19 min retention time and the associated mass spectra of the reconstructed protein calculated in PeakView. The molecule is present at differing intensities between temperature treatments.

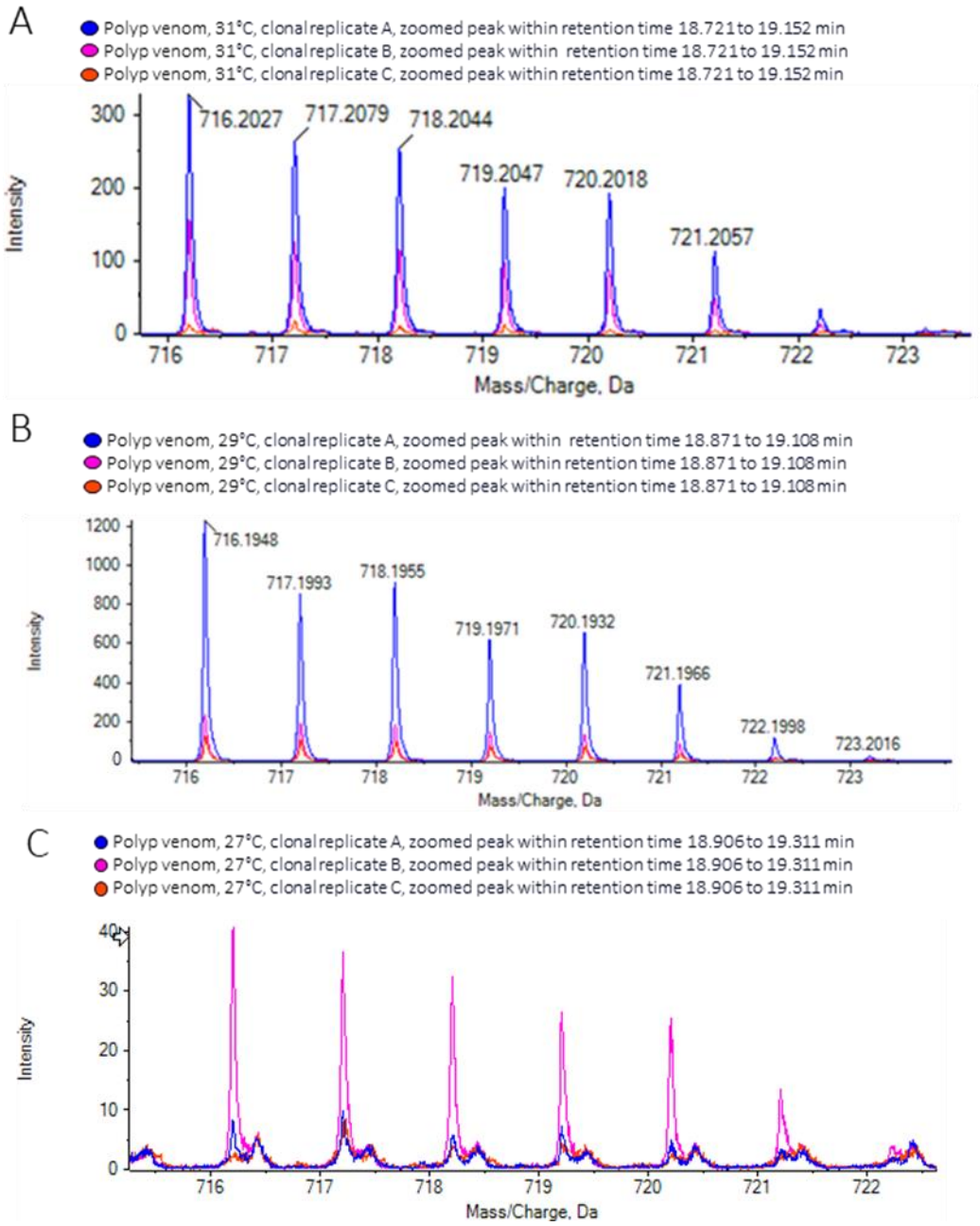

Figure 8.8: Zoom of mass spectra from polyp venom of *Carukia barnesi* raised at 31°C, 29°C and 27°C, showing the relative intensities of a molecule at ~19 min retention time with a monoisotopic ion of ~716 *m/z*. The isotope pattern is characteristic of a halogenated (e.g., bromine or chlorine) molecule. The molecule is present at differing intensities between all temperature treatments with very little presence/almost absence at 27°C.

8.4.3. Medusa venom

TICs of the newly detached medusa venom provided an overall comparison of the venom composition between the three temperature treatments (fig 8.9). The initial peaks present between 0 and 2 min are the void volume and do not represent the venom composition. The medusa venom TICs show most peaks are consistent between all temperature treatments, suggesting a mostly homogeneous venom composition between temperatures; however, some notable differences are evident. Peaks at ~16.5 min are present at 27 °C but absent at 31°C and 29°C (fig 8.9 red arrows) and a peak at ~19.5 min is evident only in the 29°C treatment (fig 8.9 *). Upon closer examination, this latter peak at ~19.5 min appears to be an anomaly in the spectra as this region was found to contain the same composition of molecules (at similar intensities) as peaks noted in the 31°C and 27°C treatments, given the sharpness of the peak it is most likely noise in the spectrum.

The peak at ~16.5 min present in the 27 °C medusa samples presents significant molecular differences to the corresponding regions at 29°C and 31°C treatments (Table 8.2). A downward trend in intensity is evident for a majority of molecules present within this peak, being highest at 31°C, less at 29°C and least and/or absent at 27°C (table 8.2), with the most significant differences (ion peak intensity >1000) highlighted in bold in Table 8.2. The most obvious exception is indicated in Table 8.2 with *, in which we see the only instance of a molecule in this peak at significantly higher intensity at 27°C and is further examined in Fig 8.10. The mass calculated for this molecule is 529 Da (31°C: 529.34962 Da, 29°C: 259.25152 Da, 27°C: 529.25242 Da), with large differences in the relative intensities between temperatures (Table 8.2), it is present in highest amounts at 27°C, and significantly (>28,000) lower intensities at 31°C and lower again at 29°C, an opposite trend to most other molecules in this peak.

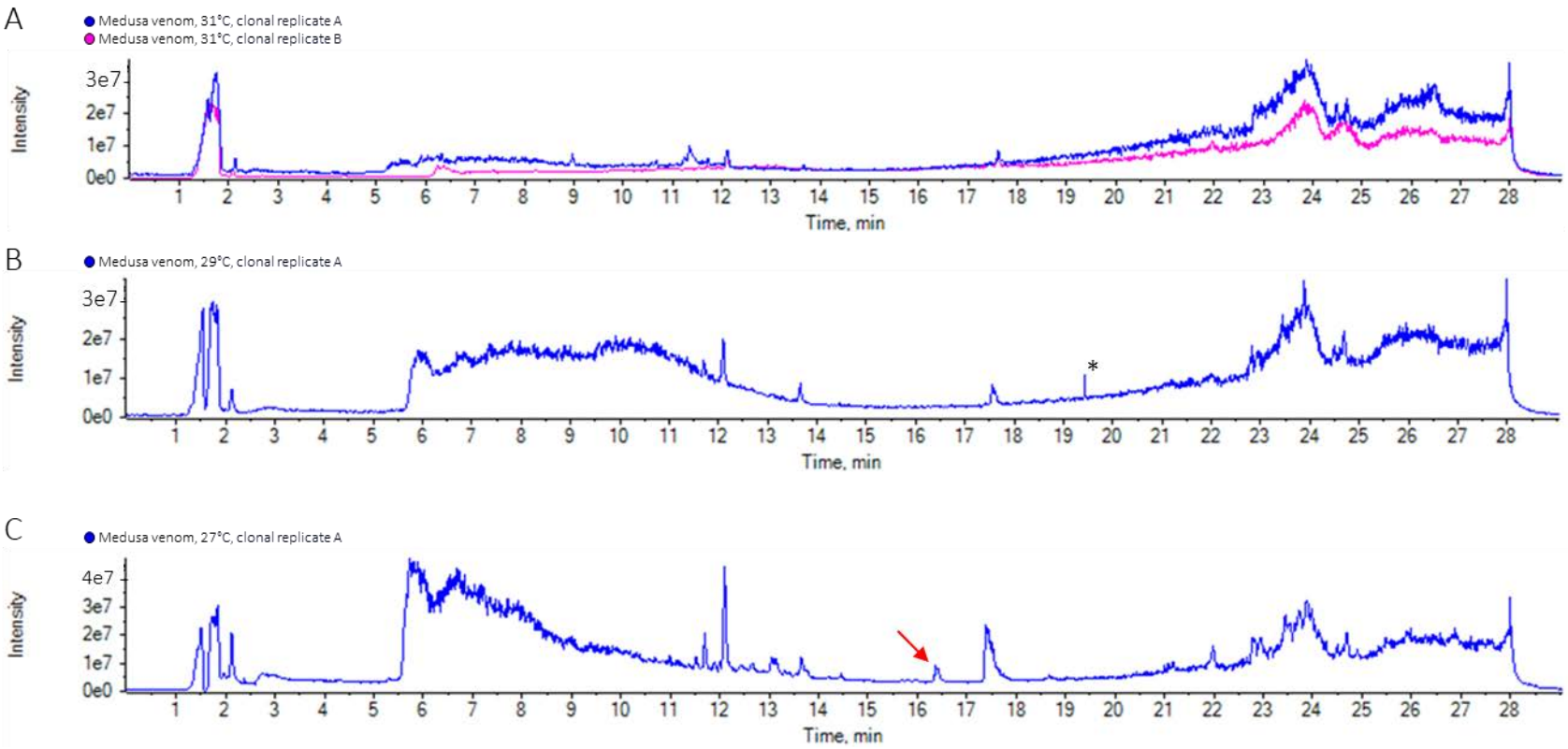

Figure 8.9: Total Ion Chromatograms (TICs) for newly detached medusa venom of *Carukia barnesi* raised at A: 31°C, B;29°C, C: 27°C. Differing venom composition is highlighted between temperatures by the presence /absence of peaks at ~16.5 min (red arrows) and ~19 min (*).

Table 8.2:Exact masses and approximate peak intensities for molecules in the newly detached medusa venom of *Carukia barnesi* raised at 31°C, 29°C and 27°C corresponding to the peaks/region at ~16.5 min (indicated by red arrows in figure 8.9]). The approximate peak intensity (counts per second) is provided for the monoisotopic peaks in the mass spectra. **Bold** text indicates molecules that differ in ion peak intensity >1000 between temperature treatments. X indicates a molecules absence from that temperature treatment. Molecules of significant interest that are further analysed in text and/or figures are indicated by *.

31°C		29°C		27°C	
Approx. peak intensity (cps)	Exact mass (Da)	Approx. peak intensity (cps)	Exact mass (Da)	Approx. peak intensity (cps)	Exact mass (Da)
14000	435.4177	5700	435.4227	3500	435.4217
1000	452.3292	850	452.3336	650	452.3337
1300	481.3074	650	481.3127	850	481.3131
24000	**507.3688**	**1150**	**507.3664**	**2000**	**507.3666**
1100	517.4771	60	517.4847	x	
4000*	**529.34962***	**1300***	**529.25152***	**32000***	529.25242****
27000	**642.5037**	**2100**	**642.5113**	**700**	**642.5107**
25000	**656.5173**	**3000**	**656.5283**	**1200**	**656.527**

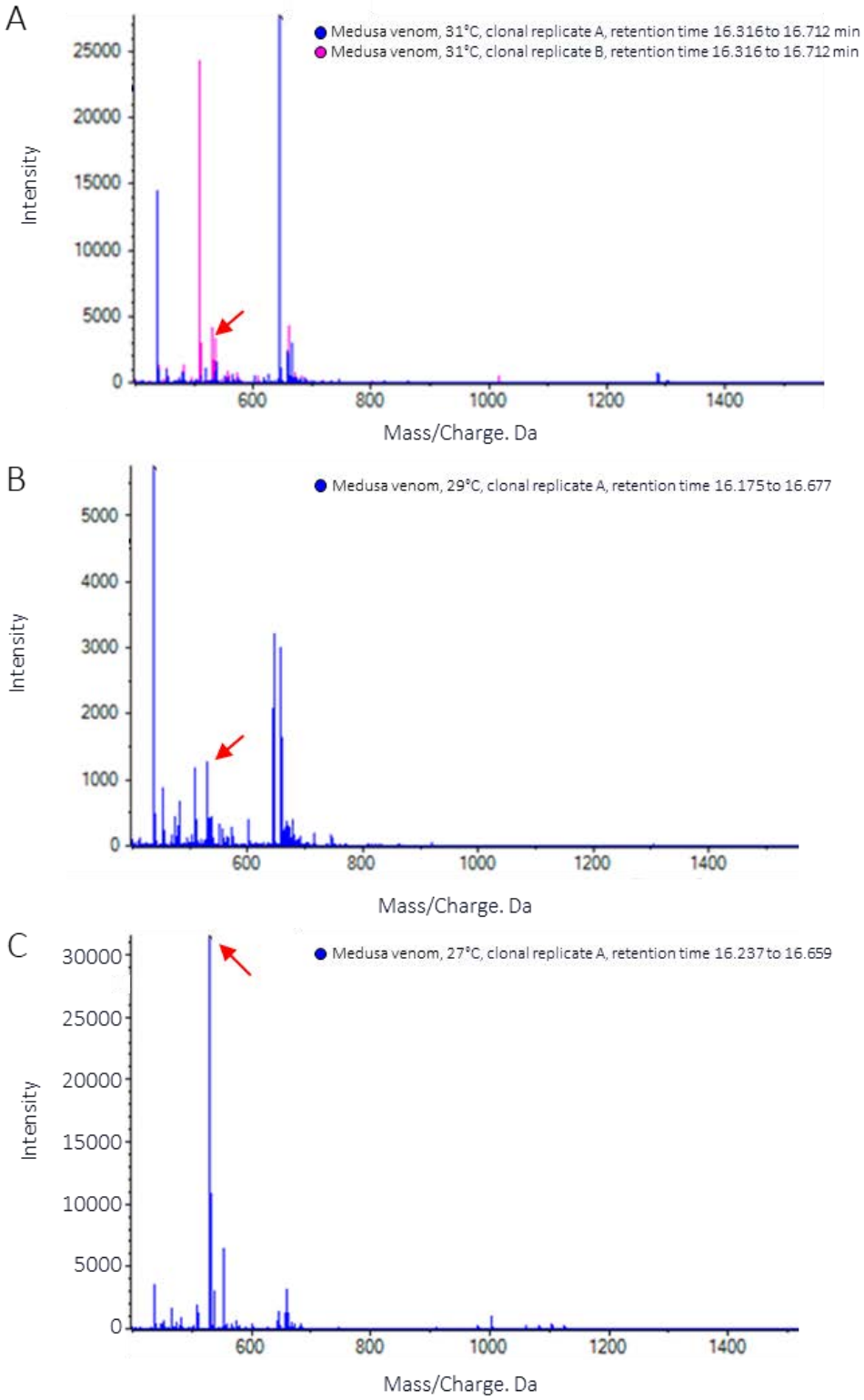

Figure 8.10: Mass spectra from the TIC peak at ~16.5 min from newly detached medusa venom of *Carukia barnesi* raised at 31°C, 29°C and 27°C, showing significant difference in intensities of a molecular ion at ~529 *M/z* (red arrows) between the three temperatures.

8.5 Discussion

Here we present for the first time, the venom composition of both the polyp and newly detached medusa life stages of the Irukandji jellyfish *Carukia barnesi* can alter with environmental temperature. Whilst both TICs show most peaks are consistent between all temperature treatments, which would suggest a mostly homogeneous venom composition between temperatures, upon closer examination of the mass spectra within the differing TIC peaks, significant molecular differences are evident between temperatures. Multiple molecular differences are recorded in tables 8.1 and 8.2, with three of the more significantly differing molecules to be discussed further.

8.5.1 Polyp v medusa venom

Polyp venom is significantly different compositionally than the newly detached medusa venom, as evident from the Total Ion Chromatograms in (fig 8.4) which show very different peaks between the two life stages. This differing venom composition was wholly expected for two reasons. 1) As evidenced in chapter six, we know the newly detached medusa have an entirely new nematocyst type in addition to the single type found in the polyp, thus it is logical this new nematocyst will contain a different venom. 2) The literature shows C*. barnesi* venom changes from juvenile to adult medusa, even when nematocysts remain consistent (Underwood & Seymour, 2007). The change from polyp to medusa is arguably more significant morphologically and therefor ecologically, thus it would be expected to have different venom compositions to align with different lifestyles

8.5.2 Polyp venom

12,059 Da molecule:

A molecule with a mass of 12,059 Da was identified from an ion series present in the polyp venom. This was initially only visible in the 31°C and 27°C treatments, but closer examination and "protein reconstruction" software also showed its presence at 29°C, albeit at a much lower relative intensity. It was found to present at the lowest relative intensities at 29°C, slightly higher intensities at 31°C and much (>7000) higher relative intensities at 27°C (Table 8.1). Whilst no further molecular characterisation was conducted in the current study, this size of this molecule is consistent with that of Phospholipase A_2 (PLA_2), of which several secretory forms ($sPLA_2$) comprise low-molecular weight proteins (13–15 kDA) (Liscovitch, 2004) and those derived from snake venom are

typically single chain polypeptides also with a molecular mass of 13–15 kDa (Harris & Scott-Davey, 2013). PLA_2s are a chemical family well documented in snake venom (Xiao et al., 2017) and PLA_2 *activity* has been documented in numerous cnidarians including adult *C. barnesi* medusa

(Nevalainen et al., 2004). The presence of PLA_2 activity in adult *C. barnesi* (Nevalainen et al., 2004), albeit from tissue homegenates and not pure venom extracts, would support a hypothesis that the 12,059 Da molecule found in the present study (in the younger ontogenetic stage of the polyp) has the potential to be a PLA_2. Geographic variation has been shown in both PLA_2 activity and lethality in the giant jellyfish *Nemopilema nomurai* (Yu et al., 2021) and, whilst geographic variation is a broad, difficult-to-interpret metric (as it does not solely encompass a single environmental factor), the authors do postulate the observed PLA_2 variation is likely due to climate change (temperature), ontogeny and/or species abundance associated to geography. This may further corroborate the idea that our 12,059 Da molecule may be a PLA_2 as we have shown this molecule directly varies with environmental temperature, as postulated/shown by Yu et al., (2021). If true, it could also be expected to see these variations in the 12,059 Da molecule effecting the venom lethality of *C. barnesi* as demonstrated by Yu et al. (2021). Ultimately, whilst this is a distinct possibility, the exact nature of this molecule would require further corroboration outside the scope of the current study.

516 Da and 1032.3427 Da molecules

Two singly charged molecular ions of note were identified from the polyp venom, one with a mass of 516 Da and the other with an exact mass of 1032.3427 Da, though not within any of the varying TIC peaks. However, the 516 Da molecule is of note as the size is consistent with tetracyclic γ-carboxyglutamic acids found in other cubozoan and Irukandji species venom (Reinicke et al., 2020). The 1032.3427 Da molecule is likely an eight membered ring cyclic γ-carboxyglutamic acid. It has been theorised the tetracyclic γ-carboxyglutamic acids do not act in a toxic role, but as a function in nematocyst discharge.

715/717 Da molecule:

A molecule with a mass of 715, and overlapping with a second molecule of mass 717 Da, was identified from peaks in the polyp venom at 31°C and 29°C (fig 8.6 black arrows) but was almost absent from 27°C, displaying large differences in the relative intensity present in the highest amounts at 29°C, lower intensities (>1000 difference) at 31°C and almost completely absent from 27°C. The isotope peak pattern of the molecular ion isotope peaks of the mass spectra are consistent with those of a brominated or chlorinated molecule (fig 8.11). The molecular ion peak isotope pattern is due to the presence of two versions of the same molecule containing the two naturally occurring bromine isotopes in *approximate* equal relative abundance, or the two naturally chlorine isotopes occurring at an *approximate* 3:1 relative abundance (e.g., two bromine isotopes ^{79}Br and ^{81}Br, or two chlorine isotopes ^{35}Cl and ^{37}Cl). There is a large presence of chlorine

and bromine in the marine environment, allowing for the frequent chlorination and bromination of many organic compounds found in marine organisms (Chen et al., 2023), particularly as post-translational modifications of peptides and shown to provide stability to marine antimicrobial peptides (e.g., to protect from proteases in the marine environment (Ponnappan et al., 2015; Shinnar et al., 2003)).

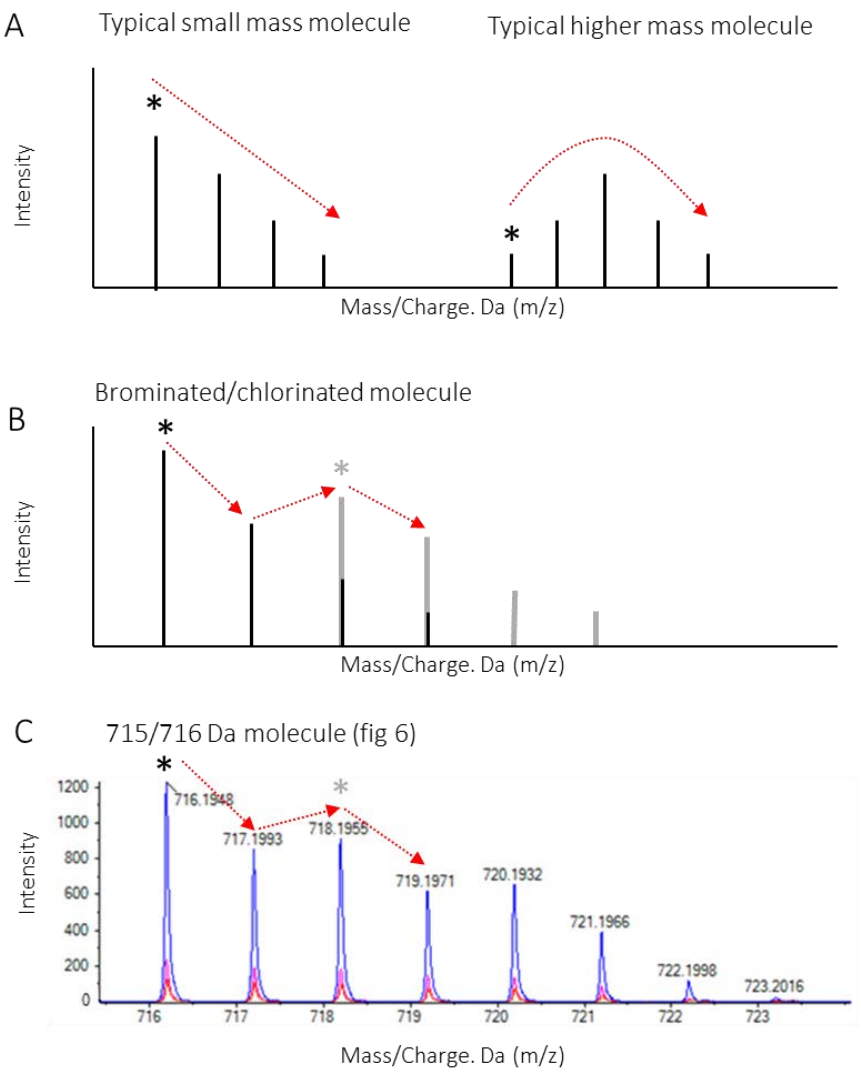

Figure 8.11: Molecular ion isotope peak patterns within mass spectra (ms) of small molecules/peptides/proteins. * indicates monoisotopic ions. A: The ms peaks of a typical small mass molecule show a downwards trend (red arrow) from the first (monoisotopic) peak, a higher mass molecule appears as a curve from the monoisotopic ion, peaking around the middle of the isotope distribution. B: A brominated or chlorinated molecule presents as two overlapping isotope series (black and grey lines) representing two versions of the same molecule just with different isotopes (e.g., two bromine isotopes ^{79}Br and ^{81}Br, or two chlorine isotopes ^{35}Cl and ^{37}Cl). This is due to the two bromine isotopes occurring naturally in *approximately* equal relative abundances, and chlorine isotopes occurring at an *approximate* 3:1 relative abundance. Overall, the resulting ms appears to show an almost up/down pattern (red arrows) from the first monoisotopic peak, which in actuality is just the two overlapping spectra. C: 715/717 Da molecule described in the current study (fig 8.8), presenting ms peaks consistent with the molecular ion isotope pattern of a brominated or chlorinated molecule (red arrows).

8.5.3 Medusa venom

529 Da molecule:

The medusa venom was more difficult to ensure equal venom sample concentrations between replicates than the polyp venom, due to slightly different samples sizes of collected medusa. Although every effort was made to ensure even concentrations by standardising nematocyst mass and miliQ water dilution proportions. Most of the molecular differences seen in table 8.2 show an obvious trend with highest intensities at 31°C, less at 29°C and lowest at 27°C and, whilst this could indeed be the accurate intensity trends, we are unable to rule out the possibility of it resulting from sample concentration. However, because of this, it can confidently be deemed that the one molecule where a different intensity trend is seen, is a true reflection of the effect of temperature. A 529 Da molecule identified at ~16.5 min with large differences in the relative intensities between temperatures (Table 8.2) it is present in highest amounts at 27°C, and significantly (>28,000) lower intensities at 31°C and lower again at 29°C.

8.5.4 General discussion

For the first time we show environmental temperature can influence the venom composition of the Irukandji jellyfish *C. barnesi*. This provides the foundational knowledge that the venom *can* change and, whilst we highlight the molecules (and their associated exact masses) that displayed the most significant changes with temperature, the exact molecular characterisation of those changes will be a path for future work. Not all molecules in a venom will be toxins (e.g., the cyclic γ-carboxyglutamic acid found in some cubozoan venoms is thought to function in nematocyst discharge (Reinicke et al., 2020)) and it cannot be assumed every molecular difference presented between the temperatures studied would reflect a difference in toxicity. However, as cnidarian venoms can contain large quantities of toxic molecules (e.g., the venom of the rhizostome jellyfish *Stomolophus meleagris* (now *Nemopilema nomurai*) has been shown to contain over 200 different toxins (Li et al., 2014)), it is likely that at least some of the identified molecules in this study will be toxins, such as the 12,059 Da molecule whose size is consistent with that of venom PLA_2s. This presents the possibility that the compositional differences found in *C. barnesi* venom across environmental temperatures could pose a plausible explanation for some of the differences in sting severity documented in human envenomations. Although the changes in venom were observed in this study of two of the younger life stage of *C. barnesi,* there is every reason to assume the venom of the adult medusa will also be subject to compositional changes driven by environmental temperature. We know from climate change predictions these animals

will ultimately be exposed to long-term environmental temperatures changes, with the current study showing how their venom composition could change along with temperature.

There appears to be a distinct lack of proteins/larger mass molecules present with both the polyp and newly detached medusa venom. Adult C. *barnesi* venom is known to contain numerous large proteins (Underwood & Seymour, 2007: pg1077 fig 2), so it was expected the younger life stages would also present some larger mass molecules. There are number of possibilities here. Whilst the adult venom does contain proteins, *C. barnesi* venom composition does change with ontogeny (Underwood & Seymour, 2007) and as this is the first instance of analysing the polyp and newly detached medusa venom, it may be that these life stages are simply composed of smaller mass molecules. Alternatively, it may be a limitation of the analysis process resulting from instability of the proteins at low pH/in organic solvent, or jellyfish proteins are seemingly often glycosylated, which can reduce the signal intensity, and/or they may be rather quite hydrophobic and stick to the chromatography column. The most likely explanation is instability at low pH, such as in the solvents used for LCMS. Ideally, these earlier life stage venom samples would also have been analysed with gel electrophoresis, whereby the samples are run pure without any additional solvents to impact sample integrity. However, this would require significantly larger sample volumes and/or higher concentrations than was logistically possible to collect from these small organisms. Here the difficulties ultimately lie less in optimising the method, but more with the current available technology. The occasional large mass molecule was visible, such as the 12,059 Da molecule discussed above and demonstrating some larger molecules/proteins are present/visible. However, the question remains if the lack of proteins in the study samples was a product of technical capabilities or a true reflection of ontogenetic variation in these earlier life stages. Future work would need to focus on rearing these animals in even higher numbers than the current study for gel analysis. For example, to increase the yield/concentration by ten from the current work would require >8,0000 polyps and >30,000 newly detached medusa per sample.

Significant compositional differences were found between the polyp and newly detached venom, which was not unexpected. *C. barnesi* is known to undergo venom ontogeny as its medusa stage ages, however this is the first time venom ontogeny has been evidenced between polyp and medusa stages. As shown in chapter six, their nematocysts change between polyp and medusa, thus a venom change would be expected. These compositional differences suggest the animals have two different ecologies, with different venoms needed in line with different predatory and defensive needs -as expected when shifting from a sedentary to a free-swimming lifestyle. The effect of environmental temperature on venom composition was a compete unknown prior to

this study and we evidence here for the first time that venom composition can be directly influenced by environmental temperature. The differing venom compositions are varied an non-linear over the three temperatures, both between molecules and life stages. The unpredictable nature of the compositional changes makes it challenging to attribute the changes to one specific temperature driven role, as no single correlation or trend was evident in molecular increase or decrease with temperature. The significance of this work is its foundational nature, we have now evidenced temperature *can* influence venom composition, future work should focus on the precise molecular characterisation of those changes and the associated impact on venom activity.

8.6 References

Barnes, J. H. (1964). Cause and Effect in Irukandji Stingings. *The Medical Journal of Australia*, *1*(24), 897–904. https://doi.org/10.5694/j.1326-5377.1964.tb114424.x

Bloom, D. A., Burnett, J. W., & Alderslade, P. (1998). Partial purification of box jellyfish (Chironex fleckeri) nematocyst venom isolated at the beachside. *Toxicon*, *36*(8), 1075–1085. https://doi.org/10.1016/S0041-0101(98)00096-8

Boco, S. R., Pitt, K. A., & Melvin, S. D. (2019). Extreme, but not moderate climate scenarios, impart sublethal effects on polyps of the Irukandji jellyfish, Carukia barnesi. *Science of the Total Environment*, *685*, 471–479. https://doi.org/10.1016/j.scitotenv.2019.05.451

Carrette, T. J., & Seymour, J. E. (2013). Long-term analysis of Irukandji stings in Far North Queensland. *Diving and Hyperbaric Medicine*, *43*(1), 9–15.

Carrette, T., & Seymour, J. (2004). A rapid and repeatable method for venom extraction from Cubozoan nematocysts. *Toxicon*, *44*(2), 135–139. https://doi.org/10.1016/J.TOXICON.2004.04.008

Chen, P., Ye, T., Li, C., Praveen, P., Hu, Z., Li, W., & Shang, C. (2023). Embracing the era of antimicrobial peptides with marine organisms. *Natural Product Reports*, *41*(3), 331–346. https://doi.org/10.1039/d3np00031a

Chimienti, G., De Padova, D., Adamo, M., Mossa, M., Bottalico, A., Lisco, A., Ungaro, N., & Mastrototaro, F. (2021). Effects of global warming on Mediterranean coral forests. *Scientific Reports*, *11*(1), 1–14. https://doi.org/10.1038/s41598-021-00162-4

Courtney, R., Browning, S., Northfield, T., & Seymour, J. (2016). Thermal and osmotic tolerance of "Irukandji" Polyps: Cubozoa; Carukia barnesi. *PLoS ONE*, *11*(7), 10–16. https://doi.org/10.1371/journal.pone.0159380

Courtney, R., Browning, S., & Seymour, J. (2016). Early life history of the "irukandji" jellyfish *Carukia barnesi*. *PLoS ONE*, *11*(3). https://doi.org/10.1371/journal.pone.0151197

Fenner, P., & Hadok, J. (2002). Fatal envenomation by jellyfish causing Irukandji syndrome. *Medical Journal of Australia*, *177*(7), 362–363.

Gershwin, L.-A., & Hannay, P. (2014). An anomalous cluster of Irukandji jelly stings (Cnidaria:

Cubozoa: Carybdeida) at Ningaloo Reef. *Records of the Western Australian Museum*, *29*(1), 78. https://doi.org/10.18195/issn.0312-3162.29(1).2014.078-081

Goulet, T. L., & Goulet, D. (2021). Climate Change Leads to a Reduction in Symbiotic Derived Cnidarian Biodiversity on Coral Reefs. *Frontiers in Ecology and Evolution*, *9*(March), 1–7. https://doi.org/10.3389/fevo.2021.636279

Harris, J. B., & Scott-Davey, T. (2013). Secreted phospholipases A2 of snake venoms: Effects on the peripheral neuromuscular system with comments on the role of phospholipases A2 in disorders of the CNS and their uses in industry. *Toxins*, *5*(12), 2533–2571. https://doi.org/10.3390/toxins5122533

Heidemann, H., & Ribbe, J. (2019). Marine heat waves and the influence of El Niño off southeast Queensland, Australia. *Frontiers in Marine Science*, *6*(FEB), 1–15. https://doi.org/10.3389/fmars.2019.00056

Hoegh-Guldberg, O. (1999). Climate change, coral bleaching and the future of the world's coral reefs. *Marine and Freshwater Research*, *50*(8), 839–866. https://doi.org/10.1071/MF99078

Li, R., Yu, H., Xue, W., Yue, Y., Liu, S., Xing, R., & Li, P. (2014). Jellyfish venomics and venom gland transcriptomics analysis of Stomolophus meleagris to reveal the toxins associated with sting. *Journal of Proteomics*, *106*, 17–29. https://doi.org/10.1016/j.jprot.2014.04.011

Liscovitch, M. (2004). Receptor-Regulated Phospholipases. In *Encyclopedia of Endocrine Diseases* (pp. 167–173).

Nevalainen, T. J., Peuravuori, H. J., Quinn, R. J., Llewellyn, L. E., Benzie, J. A. H., Fenner, P. J., & Winkel, K. D. (2004). Phospholipase A2 in Cnidaria. *Comparative Biochemistry and Physiology - B Biochemistry and Molecular Biology*, *139*(4), 731–735. https://doi.org/10.1016/j.cbpc.2004.09.006

O'Hara, E. P., Caldwell, G. S., & Bythell, J. (2018). Equistatin and equinatoxin gene expression is influenced by environmental temperature in the sea anemone Actinia equina. *Toxicon*, *153*, 12–16. https://doi.org/10.1016/j.toxicon.2018.08.004

O'Hara, E. P., Wilson, D., & Seymour, J. E. (2021). The influence of ecological factors on cnidarian venoms. *Toxicon: X*, *9–10*, 100067. https://doi.org/10.1016/j.toxcx.2021.100067

O'Hara, E., & Seymour, J. (2022). Inducing metamorphosis in the irukandji jellyfish Carukia

barnesi. *Scientific Reports 2022 12:1*, *12*(1), 1–12. https://doi.org/10.1038/s41598-022-12812-2

Oliver, E. C. J., Donat, M. G., Burrows, M. T., Moore, P. J., Smale, D. A., Alexander, L. V., Benthuysen, J. A., Feng, M., Sen Gupta, A., Hobday, A. J., Holbrook, N. J., Perkins-Kirkpatrick, S. E., Scannell, H. A., Straub, S. C., & Wernberg, T. (2018). Longer and more frequent marine heatwaves over the past century. *Nature Communications*, *9*(1), 1–12. https://doi.org/10.1038/s41467-018-03732-9

Ponnappan, N., Budagavi, D. P., Yadav, B. K., & Chugh, A. (2015). Membrane-Active Peptides from Marine Organisms—Antimicrobials, Cell-Penetrating Peptides and Peptide Toxins: Applications and Prospects. *Probiotics and Antimicrobial Proteins*, *7*(1), 75–89. https://doi.org/10.1007/s12602-014-9182-2

Reinicke, J., Kitatani, R., Masoud, S. S., Galbraith, K. K., Yoshida, W., Igarashi, A., Nagasawa, K., Berger, G., Yanagihara, A., Nagai, H., & David Horgen, F. (2020). Isolation, structure determination, and synthesis of cyclic tetraglutamic acids from box jellyfish species alatina alata and chironex yamaguchii. *Molecules*, *25*(4). https://doi.org/10.3390/molecules25040883

Rowley, O. C., Courtney, R. L., Northfield, T. D., & Seymour, J. E. (2023). Physiological and morphological responses of 'Irukandji' polyps to thermal and osmotic conditions: consequences for niche profiling. *Hydrobiologia*, *850*(5), 1207–1216. https://doi.org/10.1007/s10750-023-05162-1

Sachkova, M. Y., Macrander, J., Surm, J. M., Aharoni, R., Menard-Harvey, S. S., Klock, A., Leach, W. B., Reitzel, A. M., & Moran, Y. (2020). Some like it hot: Population-specific adaptations in venom production to abiotic stressors in a widely distributed cnidarian. *BMC Biology*, *18*(1), 121. https://doi.org/10.1186/s12915-020-00855-8

Sammarco, & Strychar. (2009). Effects of Climate Change/Global Warming on Coral Reefs: Adaptation/Exaptation in Corals, Evolution in Zooxanthellae, and Biogeographic Shifts. *Environmental Bioindicators*, *4*(1), 9–45. https://doi.org/https://doi.org/10.1080/15555270902905377

Shinnar, A. E., Butler, K. L., & Park, H. J. (2003). Cathelicidin family of antimicrobial peptides: Proteolytic processing and protease resistance. *Bioorganic Chemistry*, *31*(6), 425–436.

https://doi.org/10.1016/S0045-2068(03)00080-4

Underwood, A. H., & Seymour, J. E. (2007). Venom ontogeny, diet and morphology in *Carukia barnesi*, a species of Australian box jellyfish that causes Irukandji syndrome. *Toxicon*, *49*(8), 1073–1082. https://doi.org/10.1016/j.toxicon.2007.01.014

Weis, V. M. (2008). Cellular mechanisms of Cnidarian bleaching: Stress causes the collapse of symbiosis. *Journal of Experimental Biology*, *211*(19), 3059–3066. https://doi.org/10.1242/jeb.009597

Winter, K. L., Isbister, G. K., McGowan, S., Konstantakopoulos, N., Seymour, J. E., & Hodgson, W. C. (2010). A pharmacological and biochemical examination of the geographical variation of Chironex fleckeri venom. *Toxicology Letters*, *192*(3), 419–424. https://doi.org/10.1016/j.toxlet.2009.11.019

Xiao, H., Pan, H., Liao, K., Yang, M., & Huang, C. (2017). Snake Venom PLA2, a Promising Target for Broad-Spectrum Antivenom Drug Development. *BioMed Research International*, *2017*. https://doi.org/10.1155/2017/6592820

Yu, C., Yue, Y., Yin, X., Li, R., Yu, H., & Li, P. (2021). Identifying and revealing the geographical variation in Nemopilema nomurai venom metalloprotease and phospholipase A2 activities. *Chemosphere*, *266*(7), 129164. https://doi.org/10.1016/j.chemosphere.2020.129164

Chapter 9 . General discussion

9.1 Research overview

The Irukandji jellyfish *Carukia barnesi*, has been the focus of research into the pharmacological and toxicological aspects of its highly toxic venom (Little et al., 2020; Pereira et al., 2010; Pereira & Seymour, 2013; Ramasamy et al., 2005; Seymour et al., 2020; Winkel et al., 2005) but little is still understood about its venom ecology. Indeed, only one study has focused on the venom ecology of *C. barnesi,* elucidating that the venom, (but not the nematocysts) changes with ontogenetic stage (Underwood & Seymour, 2007). The core goal of this thesis was to further elucidate the venom ecology of *C. barnesi.* The need to conduct venom studies on Irukandji jellyfish has previously been highlighted by medical professionals, in the hope of developing preventive strategies and more effective treatments (Fenner & Hadok, 2002). The work presented in this thesissuggests that venom studies alone will not be sufficient for full characterisation demonstrated by the fact that that nematocysts of *C. barnesi*, and/or the venom they contain, significantly change over three key life stages and with environmental temperature. This suggests that the venom is not a single fixed attribute of the species , a fact rarely considered in medical venom studies. An ecological and toxicological approach to venom and anunderstanding of how a venom changes with ecology must be carefully considered, as medical treatments cannot advance if we do not acknowledge the two are inherently linked. Indeed, the effects of *C. barnesi*'s sting are a "syndrome", a range of varying symptoms, not one single fixed envenomation symptom, thus the notion of venom variability in this animal should not be surprising. From the comprehensive literature review presented in chapter two, the ability of cnidarian venoms to change with ecological factors is startlingly evident, yet there I highlight a distinct lack of research into the field. The work presented in this thesis is foundational research to begin to fill this knowledge gap, with a general discussion of the data chapters (chapters three – seven) discussed below.

9.2 Preliminary research

9.2.1 Creating a supply of medusa

To effectively analyse the venom ecology of *C. barnesi*, I had to first develop a method to generate a sufficient supply of the organisms to facilitate these experiments. Whilst C*. barnesi* polyps have never been found in the wild, artificially fertilised polyps from wild caught adults were available for use in the James Cook University aquarium, Cairns (Courtney et al., 2016). There has been only one published occurrence of these polyps metamorphosing into their next life stage as a

newly detached medusa, an event that appears both random and sporadic throughout the entire population (Courtney et al., 2016). Despite previous efforts to induce polyp metamorphosis through natural triggers such as environmental temperature and salinity changes, the metamorphosis event in these polyps had not ever successfully been reliably repeated (Courtney, 2016). For the sake of this research, to the main requirement was to develop a method to reliably induce metamorphosis on demand to facilitate experiments, and not to elucidate the natural trigger, therefore I chose to explore artificial induction methods. Indoles have been successfully used to induce metamorphosis in a small number of cubozoan species by adding them exogenously to the polyps (Helm & Dunn, 2017; Yamamori et al., 2017); however they were attributed with concentration-dependent deformities and inconsistent metamorphosis (Helm & Dunn, 2017). Whilst I chose to trial these same chemicals, ultimately unfit and/or deformed medusa would not be useful for my subsequent experiments, as such I placed an emphasis on quantifying both the total of detached medusas *and* the further subset of those that were healthy, fully formed and actively mobile, as that was the most useful metric to enable subsequent rearing of the medusae to adults. Initial tests using the indoles at the concentrations documented for other cubopolyps from the literature (Helm & Dunn, 2017; Yamamori et al., 2017), caused the *C. barnesi* polyps to die and/or encyst within a only a few days. Thus, it was assumed that the chemical concentration was the major limiting factor to the survival of *C. barnesi* polyps with these same chemicals. Therefore, for the main body of experiments I significantly dropped the experimental concentration range from those used in the literature 5-50 µM (Helm & Dunn, 2017; Yamamori et al., 2017) to 0.05-5 µM in my own research. Even then, with my most successful chemical 5-Methoxy-2-methylindole, low metamorphosis and health metrics were evident. The time parameter was then considered as causative agent in fatality, so I chose to optimise the use of 5-Methoxy-2-methylindole by experimenting with exposure times. This led to the development ofan optimized method that would reliably induce metamorphosis in *C. barnesi* polyps, producing fit and healthy medusa at a roughly 90% success rate. Thus, here I built upon previous experimental work in the literature with other cubozoans and refined an applicable method for use in my target species. Whilst the results from this chapter (chapter three) were ultimately focused on the indole compounds, while the use of iodine (lugols solution) was also somewhat successful.

Although it was not considered for further optimization due to poor yield and sample replication rate, one major advantage of iodine over the trialed indole compounds was that 100% of the medusa that were created were fit and healthy (albeit in very low and/or unpredictable numbers). Thus, in what may initially seem a backwards choice given the clear favoring of 5-Methoxy-2-

methylindole from these results, both 5-Methoxy-2-methylindole *and* iodine were used to induce metamorphosis in *C. barnesi* polyps in subsequent chapters. The optimized 5-Methoxy-2-methylindole method was used in all subsequent work aside from the final chapter in which polyps were grown *en mass* at differing environmental temperatures. In this instance, iodine was chosen as the metamorphic inducer for logistical reasons. Three separate polyp clonal replicate cultures were raised in temperature controlled cabinets, each in 30L BiOrb tanks (fig 9.1) and with the indole method, the indole is added to the polyp water, then 100% of the water was replaced after 24 hours with fresh seawater, the logistics of doing this within the temperature cabinets was challenging; 1) even if the replacement water was brought to temperature prior to addition, it was feared the open temperature doors and water changes would result in unwanted temperature changes from the experimental requirements; and 2) the BiOrb tanks have coral sand substrate, to which thousands of polyps were adhered – a full 30L water change would have inevitably disturbed thousands of these polyps, introducing a new stress factor to the experiment.

Despite the poor yields evidenced from iodine in chapter three, it was assumed that the large numbers of polyps being cultured for the experiments would negate this.

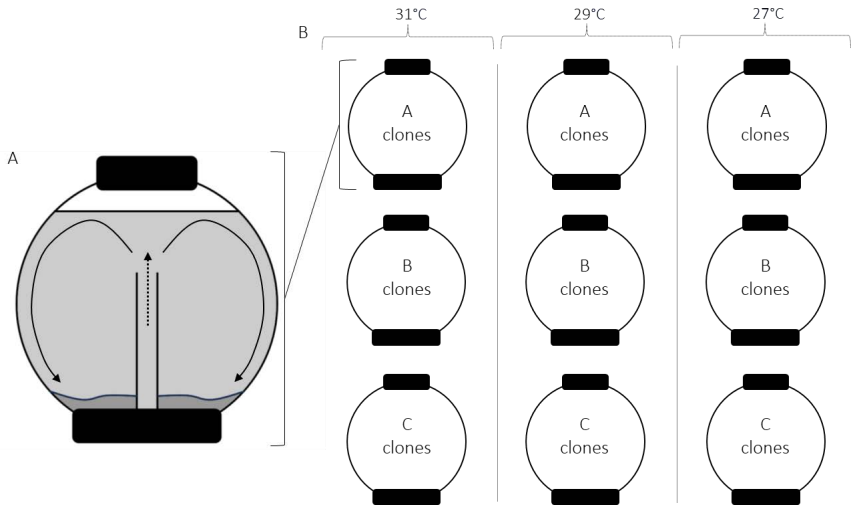

Figure 9.1: Polyp culture experimental setup (as in chapter eight).
A: 30 L spherical BiOrb aquarium tank used to house polyps. Coral sand substrate lies atop a gravel filtration system, driven by a central air pump which also oxygenates the water (dashed arrow) and provides water flow (solid arrow). Tanks stand on a solid base and have a circular apical opening for access which is covered to negate water evaporation. B: Set up of clonal replicates over three environmental temperatures. Replicates of A, B and C clones were raised at each of 31°C, 29°C and 27°C.

The impact of this particular research is twofold; 1) I successfully developed a method that I could employ throughout all subsequent chapters of my thesis in order to facilitate a supply of *C. barnesi* medusa for all ensuing research in this thesis; and 2) As this work is published, it has contributed new knowledge to the field of cubozoan research as a successful protocol for all future researchers wishing to work on *C. barnesi* newly detached medusa, which prior to this work was an unattainable life stage.

9.2.2 Promoting feeding

The second hurdle in in this preliminary research was that no carybdeid or indeed any cubozoan had successfully been reared in aquaria to adulthood, with newly detached medusa typically surviving weeks to months at best, a fact documented across multiple species; *Carybdea morandinii* (Straehler-Pohl & Jarms, 2011; Straehler-Pohl & Toshino, 2016), *Malo maxima* (Underwood et al., 2018), *Copula sivickisi* (Toshino et al., 2014) *Tripedalia cystophora* and *Alatina moseri* (Gurska & Garm, 2014) *Carybdea brevipedalia* (Toshino et al., 2018) *Alatina* cf. *moseri* (Carrette et al., 2014), *Carybdea marsupialis* (Acevedo et al., 2013). My newly detached *C. barnesi* medusa appeared to behave similarly; they would initially feed on a range of offered food (including but not limited to: live 24-hour *Artemia sp*. nauplii, fresh and frozen algae species, fish eggs, lobster eggs, aquaria coral food, live and frozen copepods) for around one week, stop eating, then ultimately die of starvation after approximately two to four weeks. Thus, I chose to explore ways to promote feeding in the newly detached medusa, aiming to extend the life span of the medusa in aquaria and to enable subsequent experiments to run for longer with healthy animals. There were three key reasons to explore light and visual ecology.Firstly, the newly detached medusa of *C. barnesi* have spots/warts on their bell, which are yellow gold in colour, in line with the typical coloration of symbiotic zooxanthellae. Initially observations also suggested the medusa seemed to feed more in direct sunlight. If this was the case, light would act as a direct food source via symbiotic zooxanthellae. Secondly,light has been shown to control the discharge of cnidarian nematocysts (Jindrich, 2012; Plachetzki et al., 2012), thus directly impacting predation and feeding; and thirdly,all cubozoa, including *C. barnesi* medusa typically have excellent vision with highly developed eyes (rhopalia) which are intrinsically associated with their ecology.

The first reason was ultimately discredited but will be discussed further here. *Carybdea morandinii* is the only cubozoan documented to possess zooxanthellae (photosymbiotic algal cells) (Straehler-Pohl & Jarms, 2011; Straehler-Pohl & Toshino, 2016), both in the polyp stage and the bell warts of the newly detached medusa. My newly detached *C. barnesi* medusa have

pigments in their bell visually similar to those of *C. morandinii* (figure 9.2), thus crediting the idea that *C. barnesi* may possess zooxanthellae.

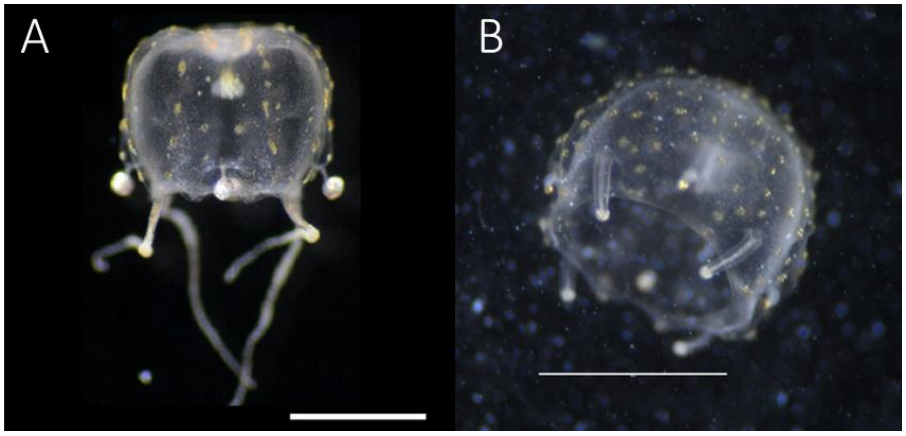

Figure 9.2: *Carybdea morandinii* and *Carukia barnesi* young medusa.
A: 1 day old *Carybdea morandinii* medusa (figure sourced from Straehler-Pohl and Toshino 2016). Colouration of bell spots were attributed to the presence of zooxanthellae by the authors (Straehler-Pohl & Toshino, 2016); B: <7 day old *Carukia barnesi* medusa, current study. Yellow spots present on bell – unidentified cause. Scale bars are 1mm (A and B)

Like *C. morandinii,* the pigments in *C. barnesi* are irregularly shaped when viewed under the microscope, however upon consultation with a symbiodinium expert these pigments were deemed too irregularly shaped (fig 9.3) and likely too small to be zooxanthellae. Less than 4 um in diameter (as in the *C. barnesi* pigmentation, Figure 9.3), is typically too small for algaeand closer to the range for cyanobacteria, though again the irregularity of the shape suggests that the particles are neither. A more conclusive test would be to determine the presence or absence of autofluorescence (personal communication April 2020, Professor Simon K. Davy, Victoria University of Wellington, President of the International Symbiosis Society) as zooxanthellae contain chlorophyl which fluoresces when excited by UV, blue and/or green light and emits strongly in the red (Donaldson, 2020). Microscopic examination of autofluorescence of *C. barnesi* pigments was thus conducted with a Zeiss Axioimager. No fluorescence was detected, thus it was conclusively determined these pigments were not zooxanthellae, and as such would not facilitate direct feeding via photosynthesis[6]. Thus, this initial exploration into the jellyfish pigments was considered too tangential to detail in the feeding experiments of Chapter four, but warranted further discussion and explanation here. The similar pigments found in *C. morandinii* (Straehler-

[6] It is possible that *C. barnesi* may indeed require zooxanthellae, but in this ex situ setting there is none available to uptake from the water. However, this is highly unlikely as the aquaria they were maintained in uses frequently replaced natural seawater, and multiple other zooxanthellate species thrive in the system with their required zooxanthellae.

Pohl & Jarms, 2011; Straehler-Pohl & Toshino, 2016) were not tested for autofluorescence, nor presented with size/scale so direct comparisons *to C. barnesi* and confirmation of their algal nature were unable to be made, however due to similarities with the current work this author suggests those pigments identified a zooxanthellae in *C. morandinii* may potentially also not be zooxanthellae. However, in line with observations that *C. barnesi* medusa did appear to initially (prior to experimental analysis) feed more in natural sunlight, and the observation by Straehler-Pohl and Jarms (2011) that the "zooxanthellae" of *C. morandinii* are more abundant in medusa cultured in natural sunlight, there is a strong possibility that whilst these are not photosynthetic zooxanthellae, they might be some form of light sensitive and/or photo-pigment. Thus providing further reason to explore the effect of light on the animals feeding ecology and behaviour.

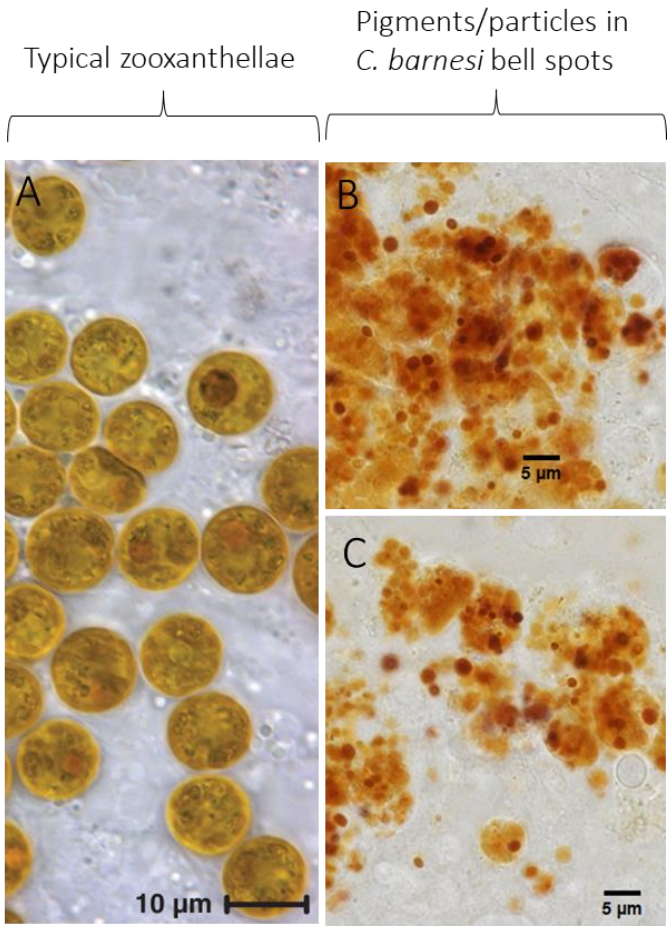

Figure 9.3: Comparison of typical zooxanthellae and the pigments/particles in *C. barnesi* bell spots.

A: Typical zooxanthellae (figure sourced from LaJeunesse 2020), note larger size and regular spherical shapes. B: The pigments/particles in *C. barnesi* bell spots, with similar golden colours as in A, but note smaller size and irregular shapes.

The light experiments conducted in chapter four evidenced that the newly detached medusa feed more in the dark than in the lights. This was not wholly unexpected as we know C. barnesi is a jellyfish with high visual acuity (Seymour & O'Hara, 2020) thus light should enable better vision in the animal and to an extent does aid in the chapters ultimate goal – to promote feeding. What was unexpected was that for all light colour and/or dark treatments, there no linear relationship between pulse rate and feeding, which we assumed would be evident as adult cubozoans often stop/reduce pulsing as they transfer prey from their tentacles to their mouths. Additionally, here it was evinced that the pulse rate of the newly detached medusa speed up in the dark, whereas previous work has shown the adult medusa slow down their pulse rate in the dark (Courtney, 2016)evidencing completely opposite reactions to darkness between ontogenetic stages. Future work should aim to compare and contrast the differing ecologies with ontogeny, a feat that can now be achieved with the younger medusa using the metamorphosis method developed in chapter three of this thesis, a life stage which was previously unattainable in sufficient numbers for research.

The light trials run in chapter four were the first of its kind, both in subjecting the jellyfish to individual light colours and in doing so to newly detached *C. barnesi* medusa. Thus resulting in a lot more questions than answers, which is often the case with novel exploratory research. We saw some evidence the animals were red colour blind like other cubozoans, but also evidence they were reacting to red light, as such the findings remained inconclusive. The ability of the animals to react to multiple light colours again poses more questions than answers, with one possibility being they may possess colour vision – however this is currently unheard of in jellyfish. The ultimate significance of this work lies in the experimental novelty, the results of which suggest the animals respond markedly and differently to individual light colours and darkness, with non-linear changes in pulse rate and feeding also apparent. Future work should focus on elucidating the specific causes and interactions alluded to in these results, specifically which and how many opsins are present in the rhopalia, which will confirm or disprove the notion of colour vision in C. barnesi at this life stage, which should further be compared to the adult life stage.

9.2.3 Divergent research- cubozoan vision

Chapter five is included in this thesis as a piece of work divergent (but still relevant) to the core research aims. This work supplements the vision-based feeding experiments conducted in chapter four, by demonstrating that visual acuity in some cubozoans, including the jellyfish of interest *C. barnesi*, can be attributed to their prey capture ecology.

Poor vision has previously been linked to feeding ecology in the nocturnal box jellyfish *Copula sivickisi*, which possesses underfocused eyes with very low temporal resolution (Garm et al., 2016) allowing it to visualise the bioluminescence of its dinoflagellate prey but not individual prey items. In the current research we observed the opposite in diurnal cubozoans, whereby heightened vision was linked to prey capture in visually complex environments, necessitating the ability to perceive individual prey items within complex backgrounds. *Carukia barnesi* showed the greatest visual acuity with the rate of pupil constriction fastest and final constriction greatest, attributed to the need to identify small larval prey fish in structurally complex coral reef environments, *Chironex fleckeri* possessed the next fastest pupil and final construction, again linked to its need to identify larger prey fish in complex mangrove habitats, with *Chiropsella bronzie* showing the slowest and least final pupil constriction, suggesting the lowest visual acuity, attributed to its comparably less complex but more turbid hunting environments of shallow sandy beaches, where its food source of small shrimps is highly aggregated and less mobile.

As a published research piece this contributes new knowledge to the field and provides peer reviewed evidence to supplement the ideas explored in chapter four. Here we confirmed a link between feeding ecology and vision in the adult medusa of. *barnesi*, supplementing the notion that that same vision-feeding link could be present in the younger medusa – which chapter four attempted to explore and exploit.

9.3 Core research

Cnidarians are unique in that their venom is produced, contained and stored in thousands to millions of nematocysts dispersed throughout their tentacles (and often other body parts), unlike most venomous animals where venom is usually contained to a single venom gland or originating organ. This means that cnidarian venom ecology can be researched both indirectly, via analysis of the nematocysts (as in chapter six and seven), or directly, via the venom they contain (as in chapter eight).

9.3.1 Venom ecology - nematocysts

I will first further discuss the exploration of *C. barnesi*'s venom ecology in this thesis, conducted through indirect analysis – via the nematocysts. I identified and quantitatively analysed all nematocyst types found across three key life stages: the polyp, newly detached medusa and adult medusa, with some additional analysis conducted on one rarer older specimen. Which ultimately yielded two key contributions, 1) coalesced and rectified inconsistencies in the current literature regarding *C. barnesi* nematocyst identifications; 2) elucidated how the nematocyst types and sizes

(and therefore venom type and potential volume) changes over ontogenetic stages in *C. barnesi*, thus revealing novel insights into their venom ecology.

1) It is difficult as readers to trust published nematocyst identifications when often no evidence is provided to support the given identifications. Indeed, most of the previous literature (Ávila-Soria, 2009; Courtney et al., 2016; Underwood & Seymour, 2007) which documents *C. barnesi* nematocyst identification, presents only the final identification by name, with no descriptions of the identifying features of the classification, nor images and/or illustrations of the nematocysts themselves. Additionally, all available literature identifying *C. barnesi* nematocysts documents very inconsistent identification and nomenclature (Ávila-Soria, 2009; Courtney et al., 2016; Gershwin, 2006; Southcott, 1967; Underwood & Seymour, 2007). The current study therefore strives to conduct a rigorous examination into the cnidome of *C. barnesi* over numerous major life stages, presenting thorough evidence for each classification and identification, which will serve as a strong foundation for future inquiries into the nematocysts of this dangerous jellyfish. Here I have initially assessed the literature surrounding the nematocysts of *C. barnesi* and found inconsistencies, and ultimately created a solid, informative article of research on these nematocysts. It is difficult to develop a thorough understanding of the venom and sting mechanisms of *C. barnesi* without first developing a thorough accurate understanding of the nematocysts on which to build future research. It hoped that the nematocyst identifications included in this research can contribute this much needed knowledge to future research in this field.

2) Throughout chapter six three confirmed types of nematocyst are identified across *C. barnesi*'s life stages as well as the strong likelihood of two more types, though further research and/or replicates would be needed to confirm the latter. One particular nematocyst proved particularly challenging to identify. In 1967, Southcott first introduced the nematocyst identity of "Tumitele" as a new classification category within the nematocysts to better encompass the characteristics of nematocysts found in carybdeidae. As the carybdeidae is a relatively specialised branch of cnidarians, common nematocyst classification systems (Östman, 2000; Weill, 1934) typically do not describe the Tumitele, which makes identification challenging. The identification process of some *C. barnesi* nematocysts as Tumiteles was discussed at length in chapter six, however a caveat to this must be acknowledged. In the adult medusa particularly, some of the nematocyst shaft dilations (an identifying feature of Tumiteles) were sometimes difficult to see over differing focal planes, and it is understood that some Tumiteles (especially within the wild caught adults) do appear less dilated than others. One possible explanation may be that we know cubozoan venom can change potency between seasons (ie. successive medusa populations each year)

(Winter et al., 2010). This suggests that perhaps we are simply looking at the evolution of different populations/seasons. If the nematocyst ultrastructure/type is changing slightly each season, as they are the organelles producing the animals venom, logically the venom could be changing with them. The polyps and baby medusa used in this thesis were bred in the lab all from one originating population cultured in 2014/2015 (Courtney et al., 2016), whereas the adults analysed were wild caught at the time of writing, so would be years ahead regarding genetic divergence and/or drift. For example, the Tumiteles from my wild caught adult medusa, whilst possessing the same dilation positioning as those originally photographed by (Southcott, 1967), displayed slight visible differences . E.g in the breadth of the shaft and dilation length (fig 9.4). Whilst this could be due to the resolution of the imaging methods, it could potentially be a reflection of ~56 years of genetic divergence and/or drift between the two studies. Or, it may simply be that the adults are exposed to a whole range of environmental and biological variables in the wild population. We know nematocyst types and/or proportion can change rapidly when influenced by external factors such as prey, predation and environmental chemistry in other cnidarians (Gochfeld, 2004; Koch, 2014). Perhaps this slight change in Tumitele morphology is a reflection of one or more of the above. This brings to light new aspects of *C. barnesi*'s nematocyst ecology not previously analysed: potential change with genetic drift and/or divergence between seasonal populations. The possibility of influencing external factors is also a valid reason, aligning nicely with the later research in this thesis which finds the external factor of temperature does contribute to venom changes.

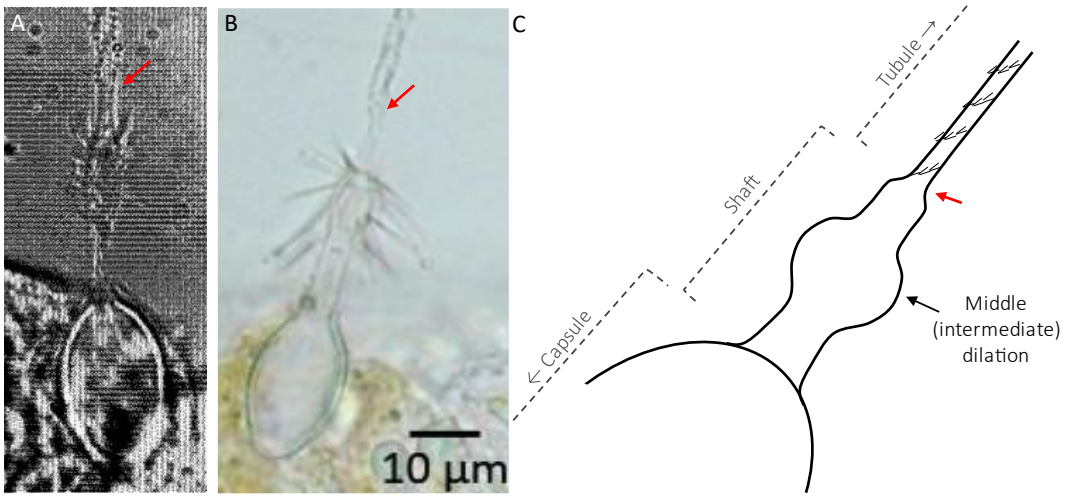

Figure 9.4: Tumitele nematocysts: original versus current comparison (as presented in chapter six).

A: Figure from Southcott 1967, the original nematocyst identified in *Carukia barnesi* tentacles, for which the new terminology "Tumitele" was developed. B: Figure from the current study, nematocyst from adult *Carukia barnesi* tentacles, identified as a Tumitele. C: Illustration of the identifying features of a "Tumitele", notably the dilation in the middle of the shaft. See figure 6.3 for comparative distal and proximal dilations. Large spines on the shaft dilation have been omitted for diagram clarity. Diagram was created by the current author (EO) based on Southcott's original description and in reference to Östman's (2000) nematocyst classification system.

From the qualitative analysis conducted on the nematocysts of *C. barnesi*, major differences between the life stages are evident, suggesting equivalent changes in the animals venom ecology. To some extend this was known/assumed in this species (Courtney et al., 2016; Underwood & Seymour, 2007), but contrasting identifications, as well as novel insights into potentially unidentified nematocysts and new nematocysts found in older life stages are elucidated for the first time here. The nematocyst work presented in chapter six focusses mostly on discussing the identification work itself, whereas the associated venom ecology is discussed in more detail here.

Nematocysts from *C. barnesi*'s polyp stage have only been described once, when the early life history was first elucidated (Courtney et al., 2016) and described as possessing both Tumiteles and isorhizas. Here, using higher resolution scanning electron microscopy and testing for differences in nematocyst maturity using fluorescent staining, I evidenced the polyp stage contains only one type of mature nematocyst – Tumiteles. From metamorphosis into a medusa, I found the newly detached medusa possess two types, Tumiteles and Isorizas in their bell, and a

single type – Tumiteles, in their tentacles. Later in the adult medusa this is reduced to a single type in each the bell and tentacles; Tumiteles in the tentacles and Isorhizas in the bell. In one older, rarer adult Mastigophores were also additionally identified in the tentacle. I will first discuss the first three ontogenetic stages, which between them contain Tumiteles and isorhizas (fig 9.5).

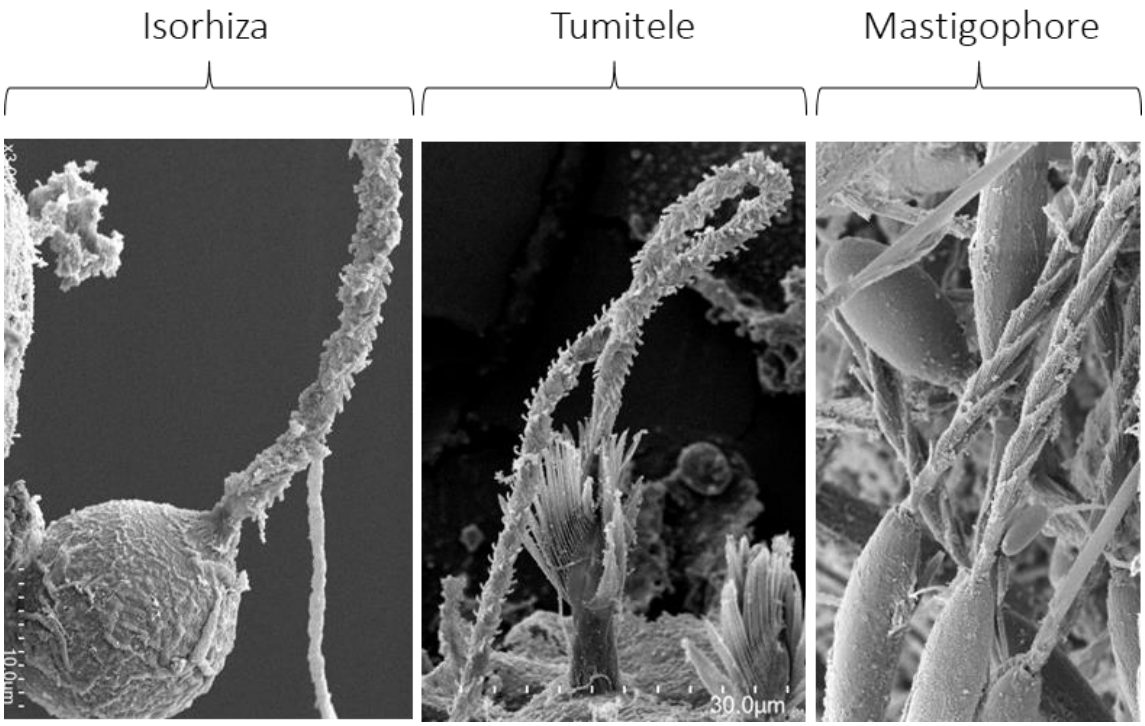

Figure 9.5: Three confirmed nematocysts types in *Carukia barnesi* (as in chapter six).

Tumiteles are a subcategory of the rhopaloids, which are a subcategory of the Heteronemes. Whilst under the umbrella term of Stomocnidae, which are *mainly* penetrants (Östman, 2000), both Heteroneme and Haplonemes nematocysts serve both penetrant and entangling functions (Damian-Serrano et al., 2021), meaning the Tumitele (as a type of Heteroneme) should function in both penetration and entanglement. As the Tumitele nematocyst is the sole mature nematocyst type present in the polyp stage, this dual function serves to both ensnare and envenomate prey with a single nematocyst type.

Isorhizas do not possess a distinct shaft at the base of its tubule. Categorisation is further split based on the everted tubule; Holotrichous - meaning spines on the tubule or Atrichous – unspined tubule. Atrichous isorhizas present in the cubozoan *Chironex fleckeri* have been attributed to function solely in entangling prey, due to the lack of penetrative spines along the tubule. However, its possible that due to the microscopic size of the tubule and the powerful everting force of the discharging nematocysts, that atrichous nematocysts could still function in a

penetrative role, as, similarly to isorhizas, the tubules are open at the tip suggesting a penetrative injecting function. Discussion of the function of *holo*trichous isorhizas in cubozoans is lacking in the literature, although their function in a hydrozoan (phylum cnidaria) has been elucidated. *Holo*trichous isorhizas were shown to fire exclusively when simulated by animals which are not normally consumed by *Hydra* and evoke no feeding reaction. The holotrichous isorhizas also do not discharge during locomotion (hydra can use nematocysts to "walk") nor any other stimulation, only exclusively to non-food animals, thus they are suggested to function exclusively in defence (Ewer & Fox, 1947). This same defensive function would function in all the medusa life stages of *C. barnesi*. As the medusa is a free-swimming organism it much more susceptible to dangers and predation, literally from all angles, whereas the polyp Is relatively safer attached to the substate and is a much smaller target – especially compared to the adult medusa, thus would explain the presence of defensive holotrichous isorhizas in the medusa but not the polyp stage. The holotrichous isorhizas are also located exclusively in the medusa bell, thus a defensive role would be consistent with this location as the bell is the main "body" of the jellyfish which needs protecting, tentacles can regrow whilst the contents of the bell are less able to do so. Future research to conclusively elucidate their functional role should follow the example of Ewer and Fox (1947), measuring the discharge response of the nematocysts to differing ecological stimuli.

The newly detached medusa are the only life stage to have both Tumiteles and the assumed defensive isorhizas in there bell. This may be due to the relatively short length of the Tumitele wielding tentacles at this age, necessitating the bell to aid in prey capture. Thisuggests the newly detached medusa can employ two nematocysts types in the same tissue for different functions. Indeed, some cnidarians demonstrate remarkable control of their nematocyst discharge, some *hyrda* can "walk" along the side of a tank discharging its atrichous isorhizas only to facilitate locomotion, and during feeding only discharge its stenoteles and desmonemes, all of which are located in the same tissues and receive the same stimulation all at once (Ewer & Fox, 1947). This same control may be employed by newly detached *C. barnesi*, potentially explaining the ability to possess both defensive and predatory nematocysts together in its bell. Although no visual observations were seen of *C. barnesi* exhibiting this in the current study using their bells for prey capture, that does not mean they are not capable of it, and would explain the presence of predatory nematocysts on their bell.

The adult *C. barnesi* medusa reduce down to only the presumed defensive holotrichous isorhizas on their bell. As their tentacles can reach close to 1m in length at maturity, where their predatory nematocyst (Tumiteles) are located, the sheer length of predatory tentacles would outweigh the need for any reliance on the competitively small bell for prey capture.

This study was fortunate enough to capture one single, rarer older specimen of *C. barnesi* in which the presence of a new additional nematocyst type in the tentacles was confirmed, a mastigophore (fig 9.5). The Mastigophores are another type of Heteroneme (Östman, 2000), which again are mainly venomous penetrants but can also entangle. The presence of Mastigophores in older *C. barnesi* has previously been alluded to in the literature but no visual evidence has ever previously been confirmed, and the Mastigophores have been linked to a rare fatal case of Irukandji syndrome (Pereira et al., 2010). The notion of the Mastigophores as a more toxic addition to *C. barnesi* would be consistent with the known ecology of the younger life stages – *C. barnesi* venom changes between juvenile to adult medusa as shifts its prey from invertebrates to vertebrates (Underwood & Seymour, 2007). Therefore, it is logically capable of further prey (and thus venom) shifts as It continues to age. Additionally, in the highly venomous cubozoan *Chironex fleckeri*, it has been shown that the Mastigophores contain the highest proportion of the vertebrate toxin within animals venom (McClounan & Seymour, 2012), thus it would be reasonable to expect this in the *C. barnesi* Mastigophores. Further replicates of *C. barnesi* containing these rarer Mastigophores and venom activity testing from this single type is required to confirm this. The fact that the Mastigophores are an addition to the pre-existing Tumiteles in the older *C. barnesi* tentacles, and not a full replacement, suggest that the mastigophore venom may be designed to work synergistically with the Tumitele venom, and not on its own.

Two potential nematocyst types were also described for *C. barnesi* in chapter six though full confirmation of their identity as nematocysts was outside the scope of this work. In both light microscopy and SEM analysis, we found evidence for an additional (to the holotrichous isorhizas) nematocyst type in the bells of adult medusa – atrichous isorhizas (unspined isorhizas). Atrichous isorhizas are have been documented in the cubozoan *Chironex fleckeri* attributed to function solely in entangling prey, but they are classed within the stomoncidae– a class of mainly penetrative nematocysts (Östman, 2000) suggesting they should have some penetrative function. If these are truly atrichous isorhizas, they appear to replace the Tumiteles in the bell of the newly detached medusa. This could be an effort to reduce the cost of producing metabolically expensive venom in predatory bell nematocysts at a life stage when predation is now contained to the tentacles, but also still aid in entangling any prey. Additionally, in the rare older medusa, what appear to be very small very small nematocysts, possibly small Mastigophores or elongate Haplonemess are present. The lack of replication in this older sample makes identification challenging and should be explored in future research.

Ultimately, the major variation in nematocysts types with ontogeny in *C. barnesi* not only evidences major changes in ecological functions, but these nematocyst changes may contribute to the known variations in sting severity seen in human envenomations.

Quantitative analysis of the confirmed nematocysts identified significant differences in the sizes of same nematocysts types between ontogenetic stage and body part (fig 9.6). Tumiteles in the polyps stage had the largest volumes, lower volumes in adult medusa and lowest in the newly detached medusa. The Tumiteles are the single nematocyst type present in the polyps, and why they are the largest size here (and thus assumed venom content and penetrating power) is unclear but could potentially be attributed to available surface area. Potentially, the polyp tentacle tips (where the nematocysts are) have a significantly smaller diameter than the adult medusa (fig 9.7) thus the larger nematocysts may make them more potent in a smaller surface area, similarly the polyps tentacles are also smaller than the newly detached medusa but to a lesser extent (fig 9.7). Likely, this smaller available area in addition to the sole reliance on a single nematocyst type compared to other life stages, may explain the larger size of the polyp nematocysts. That the Tumiteles are larger in the adult medusa than the newly detached medusa is ecologically relevant, the animal is much larger and thus can/needs to capture larger prey items. This change in size may also contribute to the known variations in sting symptoms in human envenomations. Tumiteles are consistently the typically nematocysts identified from skin scrapings from Irukandji stings attributed t o *C. barnesi* (Huynh et al., 2003). Jellyfish with longer nematocysts have been associated with more painful human stings (Kitatani et al., 2015), thus the larger nematocyst in the adults compared to the newly detached medusa may be contributing to differences in sting severity.

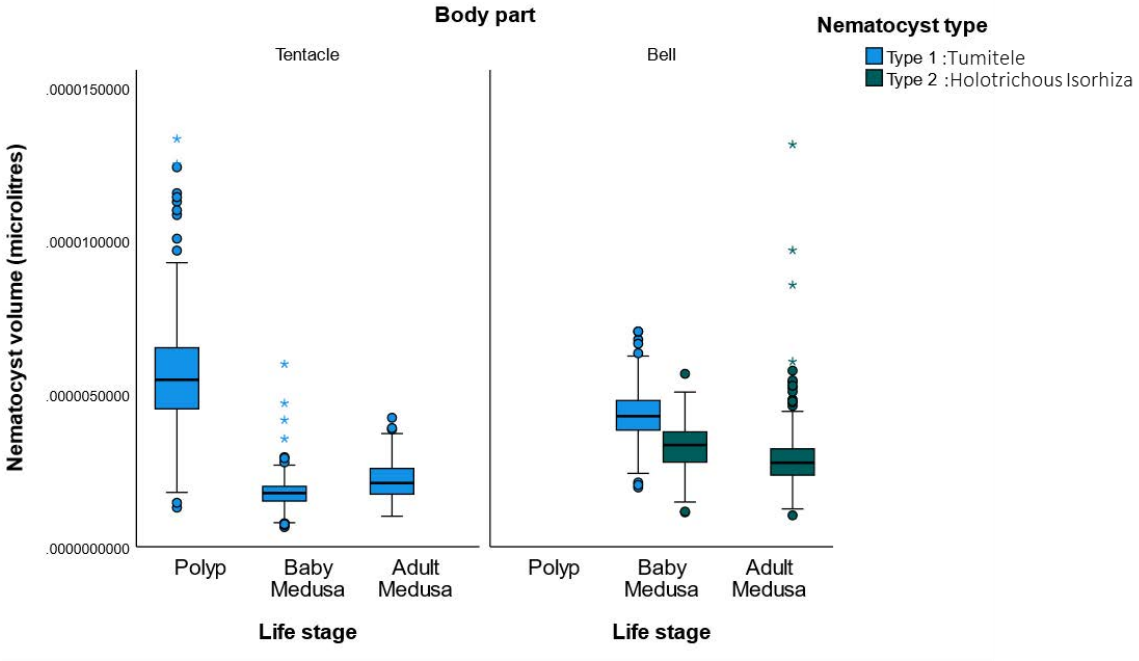

Figure 9.6: Box and whisker plot (95% CIs) depicting the volume (µL) of the different types of nematocysts in *Carukia barnesi* (as in chapter six).

Results are displayed per variable: body part the nematocysts originate in (horizontal panels), further split by life stage the life stage of the jellyfish (x axis). Note the polyp stage does not have a bell so no data is presented here.

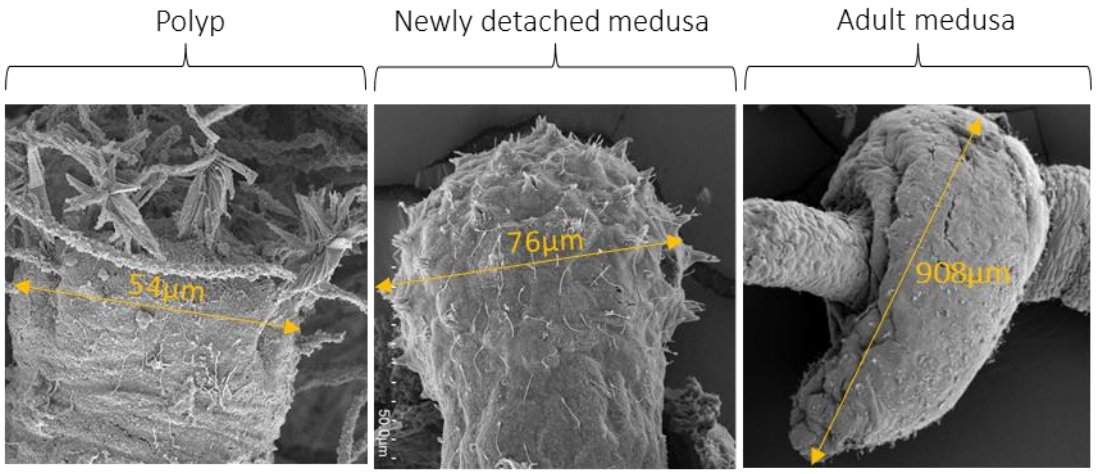

Figure 9.7: Nematocyst bearing tentacle tips of *C. barnesi* polyp and newly detached medusa tentacles, and nematocyst bearing "neckerchiefs" on the tentacles of adult medusa, with example diameters.

Tumiteles from the bells of newly detached medusa were significantly larger than the Tumiteles present in the tentacles. Which as discussed previously, may be a reflection of the animal placing less reliance on tentacular prey capture whilst the tentacles are so short at this young age. Although, this is unclear as prey capture using their bell has never been documented in this species at this age, and was not observed over the course of this research. It is unknown if *C. barnesi* is toxic to humans at this very young age, so the effect of human sting potency regarding these nematocyst size changes requires further elucidation.

Additionally, holotrichous isorhizas are larger in the bells of the newly detached medusa than in the bells of the adult medusa. We know that *C. barnesi* shift between invertebrate to vertebrate prey from a juvenile stage to the adults, we may be seeing an extension of that shift herein the newly detached medusa. Alternatively, as holotrichous isorhizas are theorized to function in defense, it could be that they need to be bigger to deliver more venom in the newly detached medusa as this is really their soles means of defense. In the adult medusa, the long tentacles are full of nematocysts that have venom powerful enough to incapacitate a human, thus they should be more than capable of acting also in defense of the jellyfish, thus less defense would be needed proportionally from the bell.

Ultimately, all the observed size changes mean differences in the maximum venom volume the nematocysts can contain, and potentially their penetrating power. Thus, changing nematocyst sizes reflect changing ecological functions. I have discussed here the logical reasoning behind the observed changes in regards to the jellyfishes ecology, however dedicated research to uncovering these roles would be the next continuation from this research which showcases these changes exist.

9.3.2 Tangential research – nematocyst ultrastructure and 3D modelling

Serial Block Face Scanning Electron Microscopy (SBF-SEM) was successfully utilized to scan and reconstruct 3D volumes of two nematocyst types found within the tentacles of the Irukandji jellyfish *C. barnesi*. Previously undescribed ultrastructural details of both discharged and undischarged nematocysts were observed, creating the foundational work for future research build upon with huge potential for future quantitative analysis. Here I have created the first biologically accurate nematocyst models from the highly venomous, medically important jellyfish, *C. barnesi.* This is a highly novel contribution to existing research, which 1) is very limited, only twice before have 3D models been created for nematocysts or nematocyst-like organelles (Gavelis et al., 2017; Karabulut et al., 2022); 2) has never been examined in a highly venomous, medically important species.

The significance of this work lies in the generation of novel foundational data – the method optimizing alone took over three years to complete, and the catch rate of adult *C. barnesi* is so unpredictable that the samples themselves are very rare. So much so that our research team (Seymour Lab, James Cook University, Cairns) is one of only teams worldwide that can facilitate field collection of *C. barnesi.* Together making this a very rare, difficult to attain dataset. From the 3D models produced in this thesis, a whole range of future analytical work could be conducted to further elucidate the venom ecology of *C. barnesi,* including but not limited too:

The ejecting force and/or penetrating power of the everting tubule. Whilst the stored energy of the capsule will of course influence this, other contributing factors could be calculated from this data; 1) the length and diameter of the coiled tubules; 2) the differing overall coiling patterns within the capsule must play some role in discharge mechanics which would explain why they may be formed into such uniquely different structures; and 3) It has been suggested that the twisted tubules themselves store and transfer energy by acting as a spring (Karabulut et al., 2022), the force of this "spring" power could be calculated by counting of coils within a known distance. Whilst the specific calculations are beyond the scope of the current study, we can elucidate a rough comparison here; from figure 9.8 we see that for approximately the same distance of inverted tubule, both the Tumitele and Mastigophore show the same number of coils, suggesting similar spring forces. This was highly unexpected given the massive size differences between the two capsules, it was assumed the large mastigophore would possess an obviously higher force.

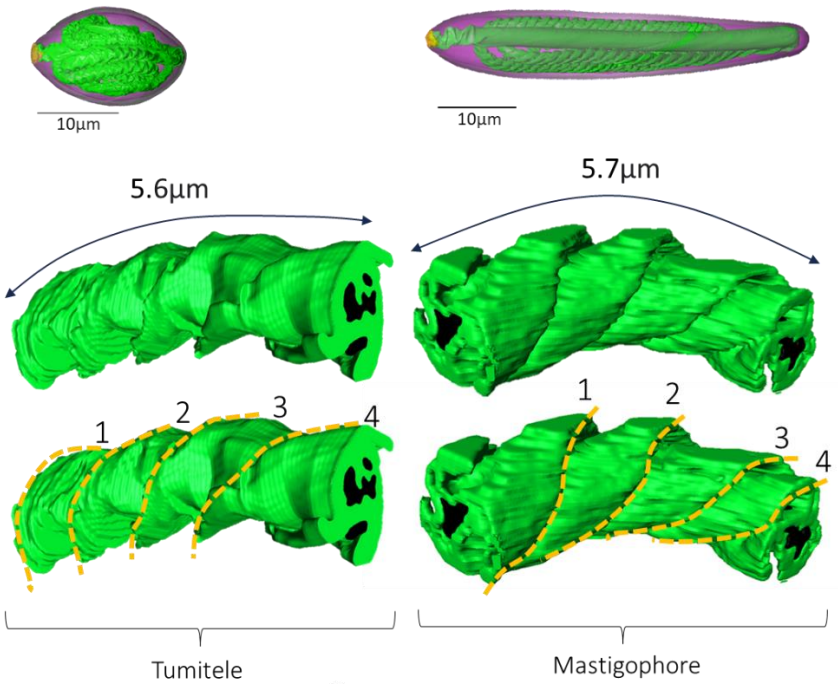

Figure 9.8: Tubule coiling characteristics of the Tumitele and Mastigophore of *C. barnesi.*

Research shows shared mechanics underlie the diversity of biological puncture across multiple venomous organisms (Anderson 2018) and both the size and speed of an apparatus contribute to the exact puncture mechanics (Anderson, Lacosse, and Pankow 2016). Metrics such as this can be elucidated as the structure of the penetrating apparatus is known, thus it is my hope that the ultrastructures, as presented in this thesis, will contribute to future research to understand the biological puncture/injection mechanisms of *C. barnesi* nematocysts to further understand the animals venom ecology. The possibility may even exist to use my physical 3D models in ballistics gel experiments as has been used previously to detail the puncture mechanics of arrows tips (Anderson, Lacosse, and Pankow 2016). From a solely venom minded aspect, future quantitative work could also calculate the exact quantities of venom present in each capsule, by subtracting quantifying the empty space between the internal capsule and the inverted tubule. Such analysis has never been possible prior to the 3D modelling. Ultimately, the production of 3D models elucidating the nematocysts ultrastructure generated in this thesis provides the foundational models for a range of further analysis.

The models produced in this work, initially generated virtually, were then also formatted for physical 3D printing. This will further facilitate scientific outreach engagement and display models. Whole capsules were printed in sections to create pull-apart models, whereby interaction with the model I.e., opening the capsule in half allows interactive visualization of the internal tubules. These are the first and only (to our knowledge) biologically accurate physical models ever created of nematocysts.

Overall, the significance of this work lies in the generation of novel foundational data. Contributing new knowledge to understanding the ecology of this animal by visualizing nematocyst ultrastructure, future research can now use these models to quantitatively analyse the venom ecology/ injection mechanism in a variety of novel ways. Due to the length of time needed to optimise the methods for these novel samples, only nematocysts from the tentacles of *C. barnesi* were imaged. Future work should aim to conduct this same volume imaging on bell nematocysts also.

9.3.3 Venom ecology – environmental temperature

In my final data chapter (chapter eight) the venom ecology of *C. barnesi* was explored via direct venom analysis, with the aims to determine 1) how/if the venom changes between the polyp and medusa; and 2) how/if the venom changes with environmental temperature. The experimental set up of this research was integral to producing accurate results, ensuring environmental temperature would be the sole variable *C. barnesi* was exposed to. Clonal cultures of the polyps

were set up as three biological (true) replicates (fig 9.1) over the three temperatures. All the venom analysis of *C. barnesi* to date has been conducted on venom extracted from pooled specimens of wild caught juvenile-adult medusa (Pereira & Seymour, 2013; Ramasamy et al., 2005; Seymour et al., 2020; Underwood & Seymour, 2007; Winkel et al., 2005) as pooling multiple medusa is the only way to extract sufficient quantities of venom for analysis. The polyp venom has never been studied before, but consistent with adult venom extraction, pooling of specimens would be even more necessary here as the polyps are significantly smaller – thus contain less nematocysts/venom – so even more would be required to pool to extract sufficient quantities. In my research, we ultimately pooled a minimum of 400 polyps per replicate, however did not want to use 400 genetically different individuals as this would introduce >400 sources of variables per replicate. This was not a concern in previous literature as the pooled venom was used for things like venom activity and toxicology studies (Pereira & Seymour, 2013; Ramasamy et al., 2005; Seymour et al., 2020; Underwood & Seymour, 2007; Winkel et al., 2005), whereas here I needed a controlled environmental set up to ensure the sole variable would be the temperature the polyps were raised at. To this end I created cloned polyp cultures, which would also transition into medusa of those same clones, ensuring a fully replicated venom analysis from genetically identical samples (fig 9.1).

Venom from both the polyp and newly detached medusa stages grown at varying environmental temperatures was analysed. Prior to the work of this thesis, both life stages would not have been possible, but the successful development of a method to induce polyps to metamorphose into medusa in chapter three served to facilitate this work. Ideally, the newly detached medusae could have been raised through to juvenile and adults also for these experiments. However, despite all efforts to promote feeding (chapter four), this was ultimately unattainable in this thesis. The alternative of using wild caught adults here was unfavorable due to variables such as age, previous environmental temperatures, salinities, water chemistry and diet; meaning any venom changes with my experimental temperatures we may find could not conclusively be linked to temperature alone. Additionally, the wild caught adults perform even worse in aquaria than the newly detached medusa, typically surviving less than a week before death introducing deteriorating health as another variable to the results. If future research could find a successful method of rearing these animals in aquaria, it would enable a vast amount of experimental research currently not possible. However, the use of both the polyp and newly detached medusa life stages here are both completely novel, as neither of their venoms have ever been analysed before and were sufficient to evidence both venom changes between life stage and environmental temperature.

Firstly, the polyp venom is significantly different compositionally than the newly detached medusa venom, as evident from the Total Ion Chromatograms in chapter eight which show very different peaks between the two life stages. This differing venom composition was wholly expected for two reasons. 1) As evidenced in chapter six, we know the newly detached medusa have an entirely new nematocyst type in addition to the single type found in the polyp, thus it is logical this new nematocyst will contain a different venom. 2) The literature shows *C. barnesi* venom changes from juvenile to adult medusa, even when nematocysts remain consistent (Underwood & Seymour, 2007). The change from polyp to medusa is arguably more significant morphologically and therefor ecologically, thus it would be expected to have different venom compositions to align with different lifestyles.

Secondly, the venom composition of both the polyp and newly detached medusa life stages of the Irukandji jellyfish *Carukia barnesi* can alter with environmental temperature. Whilst both TICs show most peaks are consistent between all temperature treatments, which would suggest a mostly homogeneous venom composition between temperatures, upon closer examination of the mass spectra within the differing TIC peaks, molecular differences are significantly evident between temperatures. Cnidarians venom composition has not previously been analsyed in relation to environmental temperature. Only, twice before has venom/toxins have been studied regarding temperature, with the studies suggesting long-term (O'Hara et al., 2018) and short-term (Sachkova et al., 2020) environmental temperature changes may cause variation in the *gene expression* of sea anemone toxins. One limiting factor to these previous studies was that the changes documented were toxin gene expression, and not direct venom composition changes. Changes in gene expression can be difficult to interpret, , the increased expression of a toxin gene may reflect 1) an actual increase in the translated toxin in the venom; or 2) an increase in gene expression to compensate for a lack of the translated toxin in the venom. Thus it can be stated that there are changes, but interpreting those changes compositionally is challenging. In contrast, the direct analysis of venom components using Mass Spectroscopy on extracted venom, as employed in this thesis, results in direct observations of compositional changes. Here we evidence, for the first time, that environmental temperature can influence the venom composition of the Irukandji jellyfish *Carukia barnesi*. This provides important knowledge that the venom *can* change and whilst I highlight the molecules (and their associated exact masses) that displayed the most significant changes with temperature, the exact molecular characterisation of those changes will be focus of future work, along with determining any effect these changes have on venom activity. These animals will experience future environmental temperature changes under current global warming forecasts and the resulting consequence of these evidenced

changes in venom composition have the potential to affect both medical sting severity and the animals' feeding ecology.

9.4 Conclusion

The core research of this thesis aimed to show if nematocysts and their contained venom changed with ecological factors, and results suggest this occurs due to life stage and environmental temperature changes. The preliminary work conducted to facilitate the later venom ecology experiments has also significantly added to the field with the development of a method to induce metamorphosis between life stages, which has now made a previously inaccessible life stage accessible to all researchers.

C. barnesi is one of the smallest, yet most venomous jellyfish in the world, and as such garners a lot of medical attention. However, the value of ecology is largely overlooked in medical research, but as evidenced here ecology has the ability to drastically influence the nematocysts and/or venom of *C. barnesi*. The need to conduct venom studies on Irukandji jellyfish in order to develop preventive strategies and effective treatments has previously been highlighted in medical research (Fenner & Hadok, 2002). However, venom studies alone will not be sufficient. Data from ecology and toxicology studies must be considered in combination, as medical treatments cannot advance if we do not acknowledge the two are inherently linked. The two fields need to coalesce, as working separately has led to drastic gaps in our understanding, leaving us unprepared to predict how a changing environment and biological factors will affect the severity of human envenomations by dangerous cnidarians. The effects of *C. barnesi*'s sting are a "syndrome", a range of varying symptoms, not one single fixed envenomation symptom, thus the notion of venom variability in this animal is not surprising – but is understudied – and the evidenced changes presented in this thesis may even be contributing to the known variation in sting severity.

This thesis demonstrates convincingly that the venom and nematocysts of *C. barnesi* can change over a range of ecological factors, the next steps will be to understand the effects of those changes. Given the very visual nature of the data within this thesis- especially the electron microscopy and volume imaging data- the work within this thesis can/will be utilised to inform the public and/or medical health professionals. The nematocyst classification data over the three ontogenetic stages, will be published, thus giving medical professionals a clear, in-depth, visual classification system to assist with identifying the causative organism in Irukandji sting victims. A task which is currently difficult to conclusively diagnose as the ~20 minute delay between sting and symptom onset means the causative organism is never usually sighted. This work, once

published, should significantly aid with species identification from an Irukandji sting. The volume imaging data and 3D nematocysts models hold massive potential to aid in outreach and public education. The video simulation of the models allows for presentation to large audiences, creating a walk through each component that is engaging, and the physical models allow for hands on learning. Broad gaps still remain, especially regarding the 3D modelling. The methodology was extremely difficult to optimise, with the nematocysts difficult to isolate for data analysis, thus only the tentacle nematocysts were imaged in this thesis. To fully understand the nematocyst structure, function and ecology of *C. barnesi*, volume imaging of the bell nematocysts should also be conducted, something this author hopes to realise in future work.

In the broader umbrella of venom research, there is often considered to be valuable knowledge to be gained from comparing venoms between animals, e.g. comparing jellyfish venom with snake or spider venom. However, from the work of this thesis, I would emphasise the importance of truly studying venom variation not only at the species level, but below that. Here we evidence that within a clonal population of the same organism, environmental factors such as external temperature can influence venom composition/variation. Akin to humans exploring space before we fully understand our own planet, we can't truly hope to make true comparisons between venom across animals, when there are so many factors, still unknown to us, that effect venom at the organismal level.

9.5 References

Acevedo, M. J., Fuentes, V. L., Olariaga, A., Canepa, A., Belmar, M. B., Bordehore, C., & Calbet, A. (2013). Maintenance, feeding and growth of Carybdea marsupialis (Cnidaria: Cubozoa) in the laboratory. *Journal of Experimental Marine Biology and Ecology*, *439*, 84–91. https://doi.org/10.1016/j.jembe.2012.10.007

Anderson, P. S. L. (2018). Making a point: Shared mechanics underlying the diversity of biological puncture. *Journal of Experimental Biology*, *221*(22). https://doi.org/10.1242/jeb.187294

Anderson, P. S. L., Lacosse, J., & Pankow, M. (2016). Point of impact: The effect of size and speed on puncture mechanics. *Interface Focus*, *6*(3). https://doi.org/10.1098/rsfs.2015.0111

Ávila-Soria, G. (2009). *Molecular characterization of Carukia barnesi and Malo kingi, Cnidaria; Cubozoa; Carybdeidae.* James Cook University.

Carrette, T., Straehler-Pohl, I., & Seymour, J. (2014). Early Life History of Alatina cf. moseri Populations from Australia and Hawaii with Implications for Taxonomy (Cubozoa: Carybdeida, Alatinidae). *PLOS ONE*, *9*(1), e84377. https://doi.org/10.1371/JOURNAL.PONE.0084377

Courtney, R. (2016). Life cycle, prey capture ecology, and physiological tolerances of Medusae and polyps of the "Irukandji" jellyfish: Carukia barnesi. In *PhD Thesis, James Cook University*. https://researchonline.jcu.edu.au/49935/

Courtney, R., Browning, S., & Seymour, J. (2016). Early life history of the "irukandji" jellyfish *Carukia barnesi*. *PLoS ONE*, *11*(3). https://doi.org/10.1371/journal.pone.0151197

Damian-Serrano, A., Haddock, S. H. D., & Dunn, C. W. (2021). The Evolutionary History of Siphonophore Tentilla: Novelties, Convergence, and Integration. *Integrative Organismal Biology*, *3*(1). https://doi.org/10.1093/iob/obab019

Donaldson, L. (2020). Autofluorescence in plants. *Current Biology*, *25*(10). https://doi.org/10.3390/molecules25102393

Ewer, R. F., & Fox, H. M. (1947). On the Functions and Mode of Action of the Nematocysts of Hydra. *Proceedings of the Zoological Society of London*, *117*(2–3), 365–376. https://doi.org/https://doi.org/10.1111/j.1096-3642.1947.tb00524.x

Fenner, P., & Hadok, J. (2002). Fatal envenomation by jellyfish causing Irukandji syndrome. *Medical Journal of Australia*, *177*(7), 362–363.

Garm, A., Bielecki, J., Petie, R., & Nilsson, D. E. (2016). Hunting in bioluminescent light: Vision in the nocturnal box jellyfish Copula sivickisi. *Frontiers in Physiology*, *7*(MAR), 1–9. https://doi.org/10.3389/fphys.2016.00099

Gavelis, G. S., Wakeman, K. C., Tillmann, U., Ripken, C., Mitarai, S., Herranz, M., Özbek, S., Holstein, T., Keeling, P. J., & Leander, B. S. (2017). Microbial arms race: Ballistic "nematocysts" in dinoflagellates represent a new extreme in organelle complexity. *Science Advances*, *3*(3). https://doi.org/10.1126/sciadv.1602552

Gershwin, L. A. (2006). Nematocysts of the Cubozoa. *Zootaxa*, *57*(1232), 1–57. https://doi.org/10.11646/zootaxa.1232.1.1

Gochfeld, D. J. (2004). Predation-induced morphological and behavioral defenses in a hard coral: Implications for foraging behavior of coral-feeding butterflyfishes. *Marine Ecology Progress Series*, *267*(Harvell 1990), 145–158. https://doi.org/10.3354/meps267145

Gurska, D., & Garm, A. (2014). Cell proliferation in cubozoan jellyfish tripedalia cystophora and alatina moseri. *PLoS ONE*, *9*(7). https://doi.org/10.1371/journal.pone.0102628

Helm, R. R., & Dunn, C. W. (2017). Indoles induce metamorphosis in a broad diversity of jellyfish, but not in a crown jelly (Coronatae). *PLoS ONE*, *12*(12), 1–13. https://doi.org/10.1371/journal.pone.0188601

Huynh, T. T., Seymour, J., Pereira, P., Mulcahy, R., Cullen, P., Carrette, T., & Little, M. (2003). Severity of Irukandji syndrome and nematocyst identification from skin scrapings. *Medical Journal of Australia*, *178*(1), 38–41. https://doi.org/10.5694/J.1326-5377.2003.TB05041.X

Jindrich, K. (2012). *Light influence on nematocyst firing in the sea anemone Haliplanella luciae*. Lund University.

Karabulut, A., McClain, M., Rubinstein, B., Sabin, K. Z., McKinney, S. A., & Gibson, M. C. (2022). The architecture and operating mechanism of a cnidarian stinging organelle. *Nature Communications*, *13*(1), 1–12. https://doi.org/10.1038/s41467-022-31090-0

Kitatani, R., Yamada, M., Kamio, M., & Nagai, H. (2015). Length is associated with pain: Jellyfish with painful sting have longer nematocyst tubules than harmless jellyfish. *PLoS ONE*, *10*(8), 1–13. https://doi.org/10.1371/journal.pone.0135015

Koch, J. C. (2014). *Effects of increased pCO 2 levels on the nematocyst densities in the symbiotic sea anemone Anthopleura elegantissima*.

LaJeunesse, T. C. (2020). Zooxanthellae. *Current Biology*, *30*(19), R1110–R1113. https://doi.org/10.1016/j.cub.2020.03.058

Little, M., Pereira, P., & Seymour, J. (2020). Differences in Cardiac Effects of Venoms from Tentacles and the Bell of Live Carukia barnesi: Using Non-Invasive Pulse Wave Doppler. *Toxins 2021, Vol. 13, Page 19*, *13*(1), 19. https://doi.org/10.3390/TOXINS13010019

McClounan, S., & Seymour, J. (2012). Venom and cnidome ontogeny of the cubomedusae *Chironex fleckeri*. *Toxicon*, *60*(8), 1335–1341. https://doi.org/10.1016/j.toxicon.2012.08.020

O'Hara, E. P., Caldwell, G. S., & Bythell, J. (2018). Equistatin and equinatoxin gene expression is influenced by environmental temperature in the sea anemone Actinia equina. *Toxicon*, *153*, 12–16. https://doi.org/10.1016/j.toxicon.2018.08.004

Östman, C. (2000). A guideline to nematocyst nomenclature and classification, and some notes on the systematic value of nematocysts. *Scientia Marina*, *64*(SUPPLEMENT 1), 31–46. https://doi.org/10.3989/scimar.2000.64s131

Pereira, P., Barry, J., Corkeron, M., Keir, P., Little, M., & Seymour, J. (2010). Intracerebral hemorrhage and death after envenoming by the jellyfish *Carukia barnesi*. *Clinical Toxicology*, *48*, 390–392. https://doi.org/10.3109/15563651003662675

Pereira, P., & Seymour, J. E. (2013). In vitro effects on human heart and skeletal cells of the venom from two cubozoans, Chironex fleckeri and Carukia barnesi. *Toxicon*, *76*, 310–315. https://doi.org/10.1016/j.toxicon.2013.10.023

Plachetzki, D. C., Fong, C. R., & Oakley, T. H. (2012). Cnidocyte discharge is regulated by light and opsin-mediated phototransduction. *BMC Biology*, *10*(March). https://doi.org/10.1186/1741-7007-10-17

Ramasamy, S., Isbister, G. K., Seymour, J. E., & Hodgson, W. C. (2005). The in vivo cardiovascular effects of the Irukandji jellyfish (Carukia barnesi) nematocyst venom and a tentacle extract in rats. *Toxicology Letters*, *155*(1), 135–141. https://doi.org/10.1016/j.toxlet.2004.09.004

Sachkova, M. Y., Macrander, J., Surm, J. M., Aharoni, R., Menard-Harvey, S. S., Klock, A., Leach, W. B., Reitzel, A. M., & Moran, Y. (2020). Some like it hot: Population-specific adaptations in venom production to abiotic stressors in a widely distributed cnidarian. *BMC Biology*, *18*(1), 121. https://doi.org/10.1186/s12915-020-00855-8

Seymour, J., Saggiomo, S., Lam, W., Pereira, P., & Little, M. (2020). Non-invasive assessment of

the cardiac effects of Chironex fleckeri and Carukia barnesi venoms in mice, using pulse wave doppler. *Toxicon*, *185*(April), 15–25. https://doi.org/10.1016/j.toxicon.2020.06.018

Southcott, R. V. (1967). Revision of some Carybdeidae (scyphozoa: cubomedusae), including a description of the jellyfish responsible for the "irukandji syndrome." *Australian Journal Of Zoology*, *15*, 651–671. https://www.mendeley.com/viewer/?fileId=2fa0eb3f-b65a-d78b-0aab-8d1da93fdb17&documentId=f0d95e7c-a226-37e1-ba96-636d97beaa71

Straehler-Pohl, I., & Jarms, G. (2011). Morphology and life cycle of Carybdea morandinii, sp. nov. (Cnidaria), a cubo-zoan with zooxanthellae and peculiar polyp anatomy. *Zootaxa*, *2755*, 36–56. https://doi.org/10.11646/zootaxa.2755.1.2

Straehler-Pohl, I., & Toshino, S. (2016). Carybdea morandinii—new investigations on its life cycle reveal its true genus: Carybdea Morandinii straehler-pohl & jarms, 2011 becomes Alatina Morandinii (Straehler-Pohl & jarms, 2011). *Plankton and Benthos Research*, *10*(4), 167–177. https://doi.org/10.3800/pbr.10.167

Toshino, S., Miyake, H., & Haruka, S. (2018). Development of Carybdea brevipedalia Kishinouye, 1891 (Cnidaria: Cubozoa: Carybdeida: Carybdeidae) collected from northern Japan. *Plankton and Benthos Research*, *13*(3), 116–128.

Toshino, S., Miyake, H., & Iwanaga, S. (2014). Development of Copula sivickisi (Stiasny, 1926) (Cnidaria: Cubozoa: Carybdeidae: Tripedaliidae) collected from the Ryukyu Archipelago, southern Japan. *Plankton and Benthos Research*, *9*(1), 32–41. https://doi.org/10.3800/pbr.9.32

Underwood, A. H., & Seymour, J. E. (2007). Venom ontogeny, diet and morphology in *Carukia barnesi*, a species of Australian box jellyfish that causes Irukandji syndrome. *Toxicon*, *49*(8), 1073–1082. https://doi.org/10.1016/j.toxicon.2007.01.014

Underwood, A. H., Straehler-Pohl, I., Carrette, T. J., Sleeman, J., & Seymour, J. E. (2018). Early life history and metamorphosis in Malo maxima Gershwin, 2005 (Carukiidae, Cubozoa, Cnidaria). *Plankton and Benthos Research*, *13*(4), 143–153. https://doi.org/10.3800/PBR.13.143

Weill, R. (1934). Contribution à l'étude des cnidaires et de leurs nématocystes. *Laboratoire d'évolution Des Êtres Organisés.*

Winkel, K. D., Tibballs, J., Molenaar, P., Lambert, G., Coles, P., Ross-Smith, M., Wiltshire, C., Fenner, P. J., Gershwin, L. A., Hawdon, G. M., Wright, C. E., & Angus, J. A. (2005).

Cardiovascular actions of the venom from the Irukandji (*Carukia barnesi*) jellyfish: Effects in human, rat and guinea-pig tissues in vitro and in pigs in vivo. *Clinical and Experimental Pharmacology and Physiology*, *32*(9), 777–788. https://doi.org/10.1111/j.1440-1681.2005.04258.x

Winter, K. L., Isbister, G. K., McGowan, S., Konstantakopoulos, N., Seymour, J. E., & Hodgson, W. C. (2010). A pharmacological and biochemical examination of the geographical variation of Chironex fleckeri venom. *Toxicology Letters*, *192*(3), 419–424. https://doi.org/10.1016/j.toxlet.2009.11.019

Yamamori, L., Okuizumi, K., Sato, C., Ikeda, S., & Toyohara, H. (2017). Comparison of the Inducing Effect of Indole Compounds on Medusa Formation in Different Classes of Medusozoa. *Zoological Science*, *34*(3), 173–178. https://doi.org/10.2108/zs160161

Appendix A

Three published journal articles are attached to this appendix (in the PhD version of this thesis only), from chapters in this thesis.

Paper 1 / Chapter 2:

O'Hara, E. P., Wilson, D., & Seymour, J. E. (2021). The influence of ecological factors on cnidarian venoms. *Toxicon: X*, *9*, 100067

Paper 2/ Chapter 3:

E., & Seymour, J. (2022). Inducing metamorphosis in the irukandji jellyfish *Carukia barnesi*. *Scientific Reports*, *12*(1), 9052

Paper 3/ Chapter 5:

Seymour, J. E., & O'Hara, E. P. (2020). Pupillary response to light in three species of Cubozoa (box jellyfish). *Plankton and Benthos Research*, *15*(2), 73-77.